GENETIC DIVERSITY AND ENVIRONMENTAL STRUCTURING OF FUNGAL AND ALGAL SYMBIONTS IN THE LICHEN *UMBILICARIA PUSTULATA*

Dissertation
zur Erlangung des Doktorgrades
der Naturwissenschaften

vorgelegt beim Fachbereich Biowissenschaften
der Johann Wolfgang Goethe-Universität
in Frankfurt am Main

von

Anna Dominika Sadowska-Deś
aus Jelenia Góra, Polen

Frankfurt am Main, 2019
(D30)
vom Fachbereich 15 (Biowissenschaften)
der Johann Wolfgang Goethe-Universität
Frankfurt am Main als Dissertation angenommen.

Dekan:

Prof. Dr. Sven Klimpel
Goethe-Universität Frankfurt am Main
Max-von-Laue-Str. 13, D-60438 Frankfurt am Main

Gutachter:

Prof. Dr. Imke Schmitt
Senckenberg Biodiversität und Klimaforschung Zentrum (SBiK-F)
Senckenberganlage 25, D-60325 Frankfurt am Main
und
Goethe-Universität, Fachbereich 15 Biowissenschaften
Institut für Ökologie, Evolution und Diversität
Max-von-Laue-Str. 13, D-60438 Frankfurt am Main

Prof. Dr. Georg Zizka
Senckenberg Forschungsinstitut
Senckenberganlage 25, D-60325 Frankfurt am Main
und
Goethe-Universität, Fachbereich 15 Biowissenschaften
Institut für Ökologie, Evolution und Diversität
Max-von-Laue-Str. 13, D-60438 Frankfurt am Main

Datum der Disputation: 24. 01. 2020

To my beloved Parents

Jadwiga and Zbigniew Sadowscy

TABLE OF CONTENTS

1. ABBREVIATIONS

a.s.l.	Above sea level
ABGD	Automatic Barcode Gap Discovery
ATP	Synthase-subunit 6
BAPS	Bayesian Analysis of Population Structure
BP&P	Bayesian Phylogenetics and Phylogeography
COX2	Cytochrome oxidase
DISSECT	Division of Individuals into Species using Sequences and Epsilon-Collapsed Trees
DNA	Deoxyribonucleic Acid
EF1	Elongation factor alpha
GBiF	The global biodiversity information facility
GMYC	General Mixed Yule Coalescent
GPD	Glyceraldehyde 3-phosphate dehydrogenase
ITS	Internal transcribed spacer
IGS	Nuclear ribosomal DNA intergenic spacer
LSU	Large subunit of ribosomal RNA
MCM7	Minichromosome Maintenance Complex Component 7
NGS	Next Generation Sequencing
OTU	Operational taxonomic units
PCR	DNA Polymerase Chain Reaction
psbJ-L	Intergenic spacer region
rbcL	Ribulose-bisphosphate carboxylase
RPB1	RNA polymerase II largest subunit coding gene
RPB2	RNA polymerase II second largest subunit coding gene
SNPs	Single nucleotide polymorphisms
spedeSTEM	Species delimitation using species trees
SSU	Small subunit
STEM	Species Tree Estimation using Maximum Likelihood
TSR1	Ribosome biogenesis protein
*tuf*A	Plastid encoded elongation factor
UV	Ultraviolet

2. ABSTRACT

The existence of all living organisms depends on their multidimensional adjustment to the conditions of the environment in which they live. Organisms must constantly deal with not only abiotic stress factors (such as water availability or extreme temperatures), but also with various biotic interactions (the competition between different organisms, both intraspecific and interspecies). When there is a consensus between an organism and the environment it means that this organism is well adjusted and increases its probability of survival.

Symbiotic organisms possess the ability to establish an intimate interaction with another species (symbiont) that provides benefits for survival. Organisms that are involved in obligate symbiosis may adapt to a new environment by switching to another symbiotic partner that is locally better adapted; or by reshuffling symbiont communities present in the holobiont. This ability potentially gives them the opportunity to flexibly react to changing environmental conditions.

In this thesis I studied the genetic diversity and geographic distribution of symbiont lineages in a lichen symbiosis to better understand environmental adaptation in symbiotic systems. Lichens are symbiotic associations of photobionts (one or several green-algal species or cyanobacteria), filamentous mycobionts (lichen-forming fungi) and co-inhabiting symbiotic microorganisms (lichen-associated bacteria, endolichenic fungi, and basidiomycete yeast). The coccoid green algae of the genus *Trebouxia* are the most common and the most studied lichen photobionts. However, the lack of formal *Trebouxia* taxonomy impedes our understanding of this photobiont diversity.

Different species of mycobionts may share the same photobionts and a single species of mycobiont may associate with multiple, genetically different photobionts. Interactions among symbionts are not random and are constrained by evolutionary and environmental processes. The ability to associate with specific symbiotic partner is considered as a lichen strategy to facilitate adaptation to the constantly changing environments.

The objectives of this thesis were to 1. Elucidate the intraspecific diversity of fungal and algal symbionts in the lichen *Umbilicaria pustulata*, given a range-wide (Europe-wide) sampling; 2. Evaluate species delimitation in trebouxioid

photobionts based on molecular data, and 3. Quantify the climatic niches of photobiont lineages within *U. pustulata*, to establish whether the association with particular photobionts may modify the range and ecological niche of this lichen.

The main findings of this thesis are:

1. The genetic diversity within trebouxoid photobiont of *U. pustulata* is higher than within the mycobiont. The most variable photobiont loci are nrITS rDNA, *psbJ-L, and COX2*. *RbcL* is the least variable photobiont locus. The most variable mycobiont loci are *MCM7* and *TSR1*. This study shows a lack of genetic variability in the mycobiont loci *EF1*, nrITS rDNA, *RPB1*, and *RPB2*.

2. *U. pustulata* shows a low level of selectivity and is associated with numerous (most likely six) putative algal species. All photobiont haplotypes found in *U. pustulata* are shared between other lichen-forming fungi species, showing different patterns of species-to-species and species-to-community interactions.

3. The geographic distribution of *U. pustulata* symbionts associations is strongly connected to changes in the climatic niches. The mycobiont-photobiont interactions change along latitudinal temperature gradients (cold-adapted hotspot) and in Mediterranean climate zones (warm-adapted hotspot). *U. pustulata* broadens its distribution range by switching between photobionts that posses specific environmental preferences.

Overall, this thesis contributes to the understanding of the symbiont diversity, fungal-algal association patterns and local adaptation linked to symbiont-mediated niche expansion in lichens. While identifying intraspecific diversity of both lichen symbionts is a key predisposition to understand symbiont interactions, population dynamics or co-evolution, my comparative study of the sequence-based molecular markers is relevant to reveal cryptic diversity in other lichen-forming fungi and their photobionts.

The determination of species boundaries in lichen symbionts is essential for the study of selectivity and specificity, co-distribution, and co-evolution. Whereas

the phylogenetic relationships of Trebouxiophyceae are poorly understood, the application of a novel multifaceted approach based on phylogenetic relationships, coalescence methods and morphological traits presented in this thesis is a promising tool to address species boundaries within this heterogeneous genus.

This thesis provides evidence for symbiont-mediated niche expansion in lichens and highlights the preferential photobiont association from a niche-modeling perspective. My results shed light on symbiont polymorphism and partner switching as potential mechanisms of environmental adaptation in the lichen symbiosis. The spatial genetic pattern found in *U. pustulata* symbionts supports the concept of ecological fitting and is consistent with patterns found in other lichen studies. Results presented here relate also to findings in different symbiotic systems, like reef-building corals, where different latitudinal patterns and symbiont switching has been reported as an adaptive response to severe bleaching events. Furthermore, this study is timely in light of global warming, because the identification of interaction hotspots among symbionts helps to understand how lichens or other symbiotic organisms adjust to the ongoing climate change. This knowledge will, in turn, facilitate the proper conservation of the most vulnerable lichen populations. My doctoral thesis provides a conceptual framework for analyzing symbiont diversity, interaction patterns, and symbiont-mediated niche expansion that could be applied to other types of lichen species as well as other organisms involved in facultative or obligate symbiosis.

3. ZUSAMMENFASSUNG

Alle Organismen sind an ihre Umwelt angepasst. Sie müssen mit abiotischen Bedingungen (wie Wasser- und Lichtverfügbarkeit), sowie biotischen Interaktionen (z. B. Konkurrenz) zurechtkommen. Diese Umweltbedingungen und Wechselwirkungen beeinflussen die Dimension der ökologischen Nische, in denen ein Organismus bestehen kann. Eine Art wird nicht ihre gesamte fundamentale Nische besetzen, sondern nur den Raum, in dem sie im Wettbewerb bestehen kann (realisierte Nische). Antagonistische Assoziationen, z.B. Parasiten oder Pathogene, können die realisierte Nische einschränken. Im Gegensatz zu antagonistischen Interaktionen kann eine durch Gegenseitigkeit vermittelte Beziehung die Toleranz einer Art gegenüber der Umwelt erweitern und die realisierte Nische vergrößern oder verschieben. Diese Möglichkeit besteht bei mutualistischen Symbiosen. Das mutualistische Nischenkonzept definiert einen potenziell geeigneten Raum, in dem Organismen, die in einer engen Beziehung zueinander stehen, existieren können. Die mutualistische Nische der assoziierten Organismen kann größer sein als die Nische der Wirtsspezies allein. In der vorliegenden Arbeit teste ich die Hypothese, dass spezifische Partnerkombinationen die mutualistische Nische einer obligaten mutualistischen Symbiose, der Flechtensymbiose, beeinflussen.

Einige symbiotische Lebensgemeinschaften können ihre Umweltverträglichkeit erhöhen, indem sie einen Teil ihrer Symbionten durch lokal besser angepasste Partner austauschen. Der Austausch kann entweder durch die Aufnahme eines neuen kompatiblen Symbionten aus der Umwelt, oder durch eine Umstrukturierung bereits im Holobionten vorhandener symbiotischer Stämme erreicht werden. Dadurch erweitert der Holobiontseine ökologische Reichweite und geographische Verbreitung. Es wurde gezeigt, dass solche Veränderung in der Kombination und Verbreitung von Symbionten bei riffbildenden Korallen und ihren fotosynthetischen Endosymbionten ein Mechanismus sein können, der die Auswirkungen des anthropogenen Klimawandels (z. B. Korallenbleiche) zu einem gewissen Grad abpuffern kann. In vielen anderen mutualistischen Systemen sind solche Anpassungsprozesse bislang nicht der Form nachgewiesen.

Flechten sind symbiotische Assoziationen von primären Pilzpartnern (= Mykobionten) und primären Fotosynthesepartnern (eine oder mehrere Grünalgenarten oder Cyanobakterien, = Photobionten). Zusätzlich können weitere Artengemeinschaften von Pilzen, Algen und Bakterien mit dem Flechtenholobionten assoziiert sein. Obwohl die einzelligen Grünalgen der Gattung *Trebouxia* die häufigsten Flechtenphotobionten sind, ist die Kenntnis der Diversität und der symbiotischen Interaktionen derzeit noch eingeschränkt. Insbesondere die Artabgrenzung, die molekulare Phylogenie und die geografische Verbreitung sind nur unzureichend bekannt.

DIE MODELLSPEZIES

Umbilicaria pustulata, die Pustel-Nabelflechte, ist eine foliose, gesteinsbewohnende Art, die zur Familie der Umbilicariaceae gehört. *U. pustulata* hat verschiedene Fortpflanzungsstrategien, ist aber überwiegend asexuell. Sie verfügt über eine europaweite Verbreitung und kommt zwischen 0-1800 m ü.d.M vor. Das große Areal und die breite Höhenverteilung deuten darauf hin, dass diese Art an verschiedene Umweltbedingungen und Klimazonen angepasst ist. Daher ist *U. pustulata* eine ideale Modellart, um die genetische Diversität der Pilz- und Algenpartner, deren geografische Verbreitung und spezifische Assoziation, sowie das Konzept der mutualistischen Nischenerweiterung zu untersuchen.

ZIELSETZUNG

Diese Dissertation hatte folgende Ziele: 1. Aufklärung der intraspezifischen Vielfalt von Pilz- und Algensymbionten in der Flechte *U. pustulata* anhand einer arealweiten (europaweiten) Aufsammlung; 2. Beurteilung der Artabgrenzung der trebouxioiden Photobionen von *U. pustulata* anhand molekularer Daten und 3. Quantifizierung der klimatischen Nische von Photobiontlinien innerhalb von *U. pustulata,* um festzustellen, ob die Assoziation mit bestimmten Photobionten das Areal und die ökologische Nische dieser Flechte erweitern kann. Um diese Ziele zu erreichen, habe ich zunächst den am besten geeigneten Satz von Sequenzmarkern zum Nachweis der intraspezifischen Variabilität innerhalb von Photobionten und Mykobionten *U. pustulata* identifiziert. Dann habe ich die Photobiontenarten unter Verwendung eines neuen Ansatzes, der die Koaleszenz, phylogenetische Analysen und morphologische Merkmale vereint, abgegrenzt.

Abschießend untersuchte ich, welche klimatischen Faktoren die Symbiontenverteilung beeinflussen und wie Wechselwirkungen zwischen Pilz- und Algengenotyp zur Nischenexpansion bei dieser Flechtenart beitragen.

KAPITEL 1. GENETISCHE VIELFALT BEI *UMBILICARIA PUSTULATA*.

Im ersten Teil dieser Arbeit untersuchte ich die intraspezifische genetische Vielfalt in beiden Symbionten der Flechte *U. pustulata*. Ich verwendete ribosomale, Protein-kodierende Gene sowie intergene Spacer-Marker. Beim Testen von Photobionten habe ich auch Loci aus dem nuklearen, mitochondrialen Genom und zusätzlich aus dem Chloroplastengenom einbezogen. Meine Ergebnisse zeigen, dass die genetische Vielfalt des Photobionten von *U. pustulata* höher ist als die des Mykobionten. Von den getesteten Markern war beim Photobionten nrITS-rDNA am variabelsten, gefolgt von *COX2* und *psbJ-L.* Der *rbcL*-Marker hatte die geringste genetische Variabilität. Die variabelsten Mykobiont-Loci waren *MCM7* und *TSR1*. Unzureichende innerartliche Variabilität gab es bei *EF1,* nrITS rDNA, *RPB1* und *RPB2*.

KAPITEL 2. ARTABGRENZUNG VON *TREBOUXIA* PHOTOBIONTEN.

In diesem Teil meiner Arbeit habe ich Artengrenzen innerhalb der trebouxioiden Photobionen des flechtenbildenden Pilzes *U. pustulata* untersucht. Ich habe einen neuen Ansatz verwendet, der Koaleszenz, phylogenetische Analysen und morphologische Merkmale kombiniert. Ich habe einen Datensatz basierend auf vier genetischen Markern angewendet: nrITS rDNA, *psbJ*-L, *COX2* und *rbcL*. Darüber hinaus charakterisierte ich die Morphologie von kultivierten Algenzellen mutmaßlicher Arten, um Phänotypvariabilität zu finden, die die molekulare Abgrenzung unterstützen könnte. Ich wollte auch Muster von Spezies-zu-Spezies- und Spezies-zu-Gemeinschaft-Interaktion von Photobiont-Kandidaten untersuchen und herausfinden, ob sie mit anderen flechtenbildenden Pilzen assoziiert sind. Ich verglich nrITS-rDNA-*Trebouxia*-Haplotypen mit ähnlichen Sequenzen, die in GenBank verfügbar sind. Verschiedene in meiner Studie verwendete Abgrenzungsmethoden ergaben kongruente Ergebnisse und zeigten, dass *U. pustulata* mit mindestens fünf mutmaßlichen Algenarten assoziiert ist. Trotz der Tatsache, dass die Gattung *Trebouxia* in phänotypischen Merkmalen

wenig Plastizität aufweist, unterschieden sich zwei der untersuchten mutmaßlichen Photobionten-Arten in der Morphologie der Chloroplasten, was die Unterscheidung dieser Abstammungslinien in verschiedene Arten unterstützt. Alle in *U. pustulata* gefundenen Photobiont-Haplotypen werden von anderen flechtenbildenden Pilzarten geteilt und zeigen unterschiedliche Muster der Spezies-zu-Spezies- und Spezies-zu-Gemeinschaft-Interaktionen.

KAPITEL 3. UMWELTSTRUKTURIERUNG IN EINER FLECHTENSYMBIOSE.

In dem letzten Teil meiner Arbeit habe ich einzelne Nischenbeiträge genetisch differenzierter symbiotischer Algen und flechtenbildender Pilze in *U. pustulata* über das gesamte Areal der Flechte quantifiziert. Ich verwendete nrITS rDNA (für Photobiont) und *MCM7* (für Mykobiont) Sequenzmarker, die die höchste Auflösung innerhalb der Population zeigten. Ich wendete zwei Artenabgrenzungsansätze an - die hierarchische Zusammenfassung paarweiser genetischer Abstände und die ABGD-Abgrenzungsmethode - die beide ähnliche Ergebnisse erbrachten. Durch Modellierung der Artenverteilung und Rekonstruktion der klimatischen Hypervolumina einzelner Linien habe ich geschätzt, welche klimatischen Faktoren die geografische Verteilung spezifischer Mykobiont-Photobiont-Assoziationen beeinflussen können. Die räumliche Verteilung der genetischen Variabilität zeigte eine starke Umweltstrukturierung. Die geografische Verteilung der Vereinigungen von *U. pustulata* Symbionten ist stark mit Veränderungen in den klimatischen Nischen verbunden. Die Wechselwirkungen zwischen Mykobionten und Photobionten ändern sich auf Artenebene entlang von Temperaturgradienten in Breitenrichtung und in mediterranen Klimazonen. Insbesondere konnte ich zeigen, dass es unter den fünf identifizierten Algenlinien eine wärmeliebende und eine kälteliebende Linie gibt. Die drei übrigen Algenlinien haben keine spezifische Klimanische. *U. pustulata* erweitert ihr Verbreitungsgebiet durch die spezifische Assoziation mit Photobiont-Partnern unterschiedlicher Umweltpräferenzen.

Diese Arbeit trägt zum Verständnis der Symbiontenvielfalt, der Assoziationsmuster zwischen Pilzen und Algen und ihrer lokalen Anpassung bei, die mit der symbiontenbedingten Nischenexpansion in Flechten verbunden ist. Der

hier gezeigte Vergleich von sequenz-basierten molekularen Markern ist wichtig, um die verborgene Vielfalt in vielen flechtenbildende Pilzen und ihren Photobionten aufzuzeigen. Die Bestimmung der Artengrenzen in Flechtensymbionten ist für die Untersuchung von Selektivität und Spezifität, Ko-Verteilung und Ko-Evolution von wesentlicher Bedeutung. Meine Untersuchung zur Abgrenzung von *Trebouxia*-Arten gehört zu den ersten, die die auf Koaleszenz basierenden Ansätze zur Abgrenzung von Arten zur Identifizierung von Symbionten aus grünen Algenflechten einsetzt haben. Diese Ergebnisse zeigen, dass die geringe Selektivität von *U. pustulata* ermöglicht, sich mit einer Reihe von Photobiont-Stämmen zu assoziieren. Während die phylogenetischen Zusammenhänge von Trebouxiophyceae nur unzureichend erforscht sind, ist die Anwendung eines neuartigen, vielfältigen Ansatzes, der auf den in dieser Arbeit vorgestellten phylogenetischen Zusammenhängen, Koaleszenzmethoden und morphologischen Merkmalen basiert, ein vielversprechendes Instrument, um Artengrenzen innerhalb dieser heterogenen Gattung anzugehen. Meine Ergebnisse verbesserten die bestehenden Beschreibungen der Vielfalt in Trebouxia. Die Quantifizierung der räumlich-genetischen Struktur und des Aufbaus der klimatischen Nische beider symbiotischer Partner in *U. pustulata* lieferte die Beweise für eine symbiontenvermittelte Nischenexpansion in Flechten und unterstützten die Hypothese von Photobionten-Schaltern als eine adaptive Strategie für einen generalistischen flechtenbildenden Pilz, um sein Areal zu erweitern. Dies ist die erste Studie, die sich aus einer Nischenmodellierungsperspektive mit der Frage der bevorzugten Photobiontenassoziation in Flechten befasst. Präsentiert wird in dieser Studien, dass die Identifizierung von Interaktions-Hotspots zwischen Flechten-Symbionten-Partnern helfen kann zu verstehen, wie verschiedene Flechtenarten mit sich verändernden klimatischen Selektionsregimen und der ökologischen Expansion von Symbionten umgehen können.

Meine Doktorarbeit bietet einen konzeptionellen Rahmen für die Analyse der Symbiontenvielfalt, der Interaktionsmuster und der symbiontenvermittelten Nischenexpansion bei Flechten, die theoretische Ansätze in der Symbioseforschung vorantreiben können, z.B. das Konzept der mutualistischen Nische.

4. INTRODUCTION

4.1 SYMBIOTIC ORGANISMS AND THEIR ADAPTATION TO ENVIRONMENT

The survival, reproductive success and general fitness of all living organisms depend on the multidimensional adjustment to the conditions of the environment in which these organisms live. The environment constitutes the sum of all factors that are present in given space (Pianka, 2011; Poisot *et al.*, 2011). Organisms need to constantly cope not only with the abiotic conditions (such as water availability, temperature regulation, sunlight access) but also with numerous different biotic interactions (e.g. competition between different organisms). When there is a consensus between an organism and the environment it means that organism is well adapted (Futuyma, 2013). Adaptation is defined as dynamic evolutionary process by which organisms acquire physiological, behavioral, and ecological features that improve their evolutionary success (Williams, 2008; Futuyma, 2013). In order to survive an organism needs to be well adjusted at every developmental stage, which is why adaptive traits may be structural (e.g. body shape), behavioral (e.g. instinct) or physiological (e.g. homeostasis) (Williams, 2008).

Adaptation to the environment is achieved by the interplay of neutral genetic processes (e.g. genetic drift) that are selectively neutral as well as selective processes (i.e. natural selection) that influence the organism fitness and level of adaptation (Holderegger *et al.*, 2006). Natural selection is the process by which organisms gain adaptation to their environment where they are able to survive and produce more offspring than organisms less adapted (Darwin, 1859). Symbiotic organisms possess additional options to adapt to their environment. One possibility is to incorporate foreign genes directly into a recipient genome (Moran, 2007). Uptake of the new gene facilitates the acquisition of new adaptive capabilities and increases viability in the environment. Another option is to establish an intimate interaction with another species that will provide some survival benefits (Dimijian, 2000). Those close relationships may be achieved by facultative uptake of symbionts. For instance, plants maintain ancient facultative associations with endophytic fungi, which support the resistance to habitat stress like soil pH, salinity or temperatures (Rodriguez *et al.*, 2008). These mutualist-carrying organisms benefit by gaining environmental tolerances that result in

opportunities for geographic range expansions, and ecological niche broadening (Rodriguez-Cabal *et al.*, 2012; Afkhami *et al.*, 2014).

Systems that are involved in obligate symbiosis may adapt to the environment by switching to another symbiotic partner that is locally better adapted. This can be done by the acquisition of a new compatible symbiont or by reshuffling symbiotic strains that are already present. For instance, the mountain pine beetle *Dendroctonus ponderosae* is permanently associated with two co-occurring ophiostomatoid fungi that are differently adapted to extreme temperatures. This strategy significantly improves the environmental flexibility of the hosts (Hussa & Goodrich-Blair, 2013). Another and one of the most striking examples of multipartite mutualistic organisms is the obligate symbiosis between reef-building corals and endosymbiotic algae (LaJeunesse *et al.*, 2010). Reef ecosystems are highly sensitive to climate-related stressors such as high water temperatures. In recent decades due to increasing water temperatures fragile corals lose their photosynthetic algae – zooxanthellae (*Symbiodinium*) in a process called 'bleaching' (Rowan, 2004). However, it was shown that corals, except dominant symbiotic algae, may also associate with background symbionts better adapted to different temperatures (Byler *et al.*, 2013). In the case of adverse environmental conditions, some of the coral species can shift their photobiont composition and establish more favorable symbiosis. The flexibility in symbiont acquisition seems to be one of the most important mechanisms of a relatively quick response to environmental stress (Hussa & Goodrich-Blair, 2013).

4.2 The lichen symbiosis

Lichens represent a symbiotic association of photobionts (one or several green-algal species or cyanobacteria) and filamentous mycobionts (a lichen-forming fungus) (Ahmadjian, 1967, 1993). Together they form a symbiotic unit – the holobiont, that can involve partners from three kingdoms (Grube *et al.*, 2009; Bates *et al.*, 2011; Spribille *et al.*, 2016). Recently, the concept of a lichen has been expanded to also include other co-inhabiting symbiotic microorganisms such as lichen-associated bacteria, endolichenic fungi and basidiomycete yeasts (Grube *et al*., 2009; Bates *et al*., 2011; U'Ren *et al*., 2012; Aschenbrenner *et al*., 2016; Duarte *et al*. 2016; Spribille *et al*., 2016). The lichen-forming fungus

expresses its characteristic phenotype (e.g. thallus features or physiology) only when associated with a compatible symbiotic photobiont. Axenically cultured mycobionts have different morphologies (Ahmadjian, 1993; Büdel & Scheidegger, 2008). In the lichen association, the mycobiont benefits through gaining photosynthetic products from the photobiont, whereas the benefits for the algal partner are not as obvious. Some authors suggest a parasitic relationship between lichenized fungi and algal partners due to the presence of haustoria in some species (Honegger, 1986), and the fact that the fungus controls algal growth and suppresses algal sexuality (Ahmadjian, 1993). Furthermore, algae that act as lichen photobionts can also occur free living, whereas most lichenized fungi cannot (Friedl & Büdel, 1996; Honegger, 1998). On the other hand, the mycobiont provides habitat, which allows the photobiont to occur in ecological niches it could not persist in on its own. For example, many mycobionts grow on exposed rocks in intense sunlight and experience frequently changing hydration cycles or longer periods of drought. These conditions are unfavorable for free-living green algae, however, inside the lichen thallus the algae are protected from too much UV radiation by cortical pigments synthesized by the mycobiont (Gauslaa & Solhaug, 2001) and experience more stable hydrological conditions (Scheidegger *et al.*, 1995; Schlensog *et al.*, 2000). Given these interdependencies, the lichen symbiosis is most often regarded as a mutualistic relationship (Aanen & Bisseling, 2014).

Lichens evolved approx. 415 million years ago (Honegger *et al.*, 2013). More than 18 000 lichen-forming fungi are known to date (Nash, 2008), but still many geographic regions are poorly examined. Lichens exhibit enormous morphological variation. They vary in color, growth form, thallus size (from less than a 1 mm to more than 2 m), thallus structure or live span. Some species are estimated to survive over 1000 years (Nash, 2008). Lichens provide nitrogen to the ecosystem, store moisture and serve as pioneer vegetation. As poikilohydric organisms, they are very sensitive to sulfur dioxide and play a significant role as indicator organisms in air pollution, forest age, and climate changes (McCune, 2000; Conti & Cecchetti, 2001; Will-Wolf *et al.*, 2015).

Ecology and distribution of lichen-forming fungi

Lichens can be found in almost all terrestrial habitats. In many polar ecosystems lichens are the dominant autotrophs (Longton, 1988). Temperate and tropical forests also host an enormous diversity of lichen species (Cáceres, 2007; Lücking, 2008). Many lichenized fungi are broadly distributed through numerous climatic zones or continents (e.g. Widmer *et al.,* 2012; Printzen *et al.,* 2013; Sork & Werth, 2014). Although many lichens can be found in ecologically divers habitats (such us *Umbilicaria pustulata*), some lichen species are restricted only to the ecosystems with similar climatic conditions (like cosmopolitan *Protoparmelia badia* found in an arctic/alpine habitats). There are lichen species with a distribution restricted to the northern hemisphere or tropical/subtropical regions (Litterski, 1999). In the 'bipolar' model, lichens are distributed in both polar regions (e.g. Printzen *et al.,* 2013). Species with this distribution pattern can also be found at higher elevations in warmer temperate zones (Galloway & Aptroot, 1995). Another distribution pattern describes species that occur in different regions with a Mediterranean climate (Barreno, 1991; Crespo & Pérez-Ortega, 2009).

Lichen-forming fungi, thanks to physiological mechanisms can tolerate environmental limitations, such as low nutrient supply, extremes in temperatures, light intensities or air humidity. For instance, when the water content of the thallus drops below 5 %, the lichen physiological activity approaches zero (Beckett *et al.,* 2008). Because of their poikilohydric nature lichen holobionts can thrive in climates of Antarctic Dry Valleys or the Atacama Desert (Domaschke *et al.,* 2012; Pérez-Ortega *et al.,* 2012). In an experiment conducted by de Vera *et al.* (2014) the species *Pleopsidium chlorophanum* survived more than 30 days in a Mars Simulation Chamber including high UV fluxes, low temperatures, low humidity, high CO2 concentrations, and an atmospheric pressure of about 800 Pa. After 30 days the lichen started to modify its physiology by increasing photosynthetic activity (de Vera *et al.,* 2014; Brandt *et al.,* 2015).

It has been shown that climate may influence specific fungal-algal interactions (Fernández-Mendoza *et al.,* 2011; Werth & Sork, 2014). For instance, in the genus *Protoparmelia* association with multiple symbionts is more frequent in the arctic-temperate regions, while in warmer climate (Mediterranean or tropical

regions) partner specificity increases (Singh *et al*. 2017). Moreover, association with locally adapted photobionts may broaden the geographic distribution and promote ecological niche expansion of the holobiont (Muggia *et al.,* 2014b, Rolshausen *et al*., 2018). Understanding the environmental preferences of symbiont partners in different lichen species or lichen communities may be particularly helpful in the context of shifting lichen distribution range in response to ongoing anthropogenic climate change.

Ecological gradients strongly influence the distribution of photobionts (Dal Grande *et al*., 2018). Climatic conditions like humidity, temperature or exposure to sunlight are the most significant environmental factors that affect photosynthesis and clearly control algal distributions (Beckett *et al*., 2008; Peksa & Škaloud, 2011). Also altitudinal clines exhibit steep ecological transitions over short distances (Körner, 2007, Keller *et al*., 2013), and therefore have been used to investigate how climate affects species diversity (e.g. in plants elevational belts, Mayor *et al*., 2017). Altitudinal transects have also been used to investigate ecological differentiation of lichen symbionts (e.g. Vargas Castillo & Beck 2012; Dal Grande *et al*., 2017; 2018). In a study on *Caloplaca* communities along an ecological gradient, Vargas Castillo and Beck (2012) have found that environmental factors like precipitation shape the composition of photobiont species and significantly influence the range of possible symbiotic associations. Recently, Dal Grande *et al*. (2018) examined effects of altitude and lichen host preferences (*Umbilicaria pustulata* and *U. hispanica*) in shaping photobiont communities along the altitudinal gradient. The authors found that some *Trebouxia* lineages exhibit clear altitudinal preferences, while others were common along the whole transect. The reported local-scale pattern, where warm adapted algae replace the generalist photobiont, was consistent also with the broad-scale latitudinal pattern described in this thesis (Rolshausen *et al*., 2018).

Lichen photobionts

The diversity of lichen photobionts is poorly understood. About 100 photobiont species belonging to 40 genera were reported to establish symbiotic associations with lichen-forming fungi (Tschermak-Woess, 1988). The most frequent lichen photobionts are green algae from the genera *Trebouxia* and

Trentepohlia, and cyanobacteria from the genera *Nostoc* and *Scytonema* (Ahmadjian, 1967; Friedl & Büdel, 1996). Although most of photobionts studies have focused mainly on the *Trebouxia* group, some studies also investigate other photobionts from the Trebouxiophyceae class e.g. *Dictyochloropsis* (Dal Grande *et al.*, 2014b), *Diplosphaera* (Fontaine *et al.*, 2012; Voytsekhovich & Beck, 2016), *Coccomyxa* and *Pseudococcomyxa* (Zoller & Lutzoni, 2003; Muggia *et al.*, 2011).

Green algae from the genus *Trebouxia* de Pulmaly are involved in symbiosis with more than half of all lichenized fungi (Friedl & Büdel, 1996; Blaha *et al.*, 2006). The coccoid, single cells of *Trebouxia* contain a central pyrenoid and differently shaped chloroplast (e.g. lobed or crenulate) that may be used as a morphological marker (Škaloud *et al.*, 2015; Muggia *et al.*, 2018). *Trebouxia* reproduces by autospores that are non-motile spores and are produced inside its parent cell (Ahmadjian, 1967). Algae involved in the lichen symbiosis usually do not display stages of sexual reproduction (Casano *et al*., 2011). Nevertheless, studies on photobiont populations reveal a high genetic diversity and recombinant population structure (Beck *et al.*, 1998; Blaha *et al.*, 2006; Dal Grande *et al.*, 2013; Werth & Sork, 2014).

The geographic range of *Trebouxia* is still not completely known, but several species are truly cosmopolitan and are the most widespread photobionts worldwide. For example, lichens associated with *T. simplex* were found in Antarctica, Europe, and North America (Beck, 2002; Romeike *et al.*, 2002; Blaha *et al.*, 2006). Despite *Trebouxia* having a wide ecological amplitude (Kroken & Taylor, 2000; Yahr *et al.*, 2006; Werth & Sork, 2010), some species exhibit a preferential occurrence in specific environmental conditions such as tropics (Cordeiro *et al.*, 2005) or cold climates and high altitudes (Ohmura *et al.*, 2006; Nelsen & Gargas, 2009).

Trebouxia is the most studied photobiont genus (Friedl & Rokitta, 1997), nevertheless, molecular phylogeny is still troublesome (Muggia *et al.*, 2014b; Voytsekhovich & Beck, 2016). Currently, the genus *Trebouxia* contains 28 described species (Guiry & Guiry, 2017), but identification and description of these species are difficult due to the presence of morphospecies (Kroken & Taylor, 2000; Blaha *et al.*, 2006; Leavitt *et al.*, 2015a). Some green algal photobionts have been found as free-living populations on different substrates (Ahmadjian, 1993;

Mukhtar *et al.*, 1994; Friedl & Büdel, 1996; Casano *et al*. 2011). *Trebouxia* as well is not an obligate lichen photobiont and can exist in a free-living state (Mukhart *et al*., 1994; Ettl & Gärtner 1995). However, small colonies that have been found outside the lichen thallus (Tschermak-Woess, 1988; Handa *et al.*, 2007; Hallmann *et. al.,* 2013; Yung *et al.,* 2014) could be the effect of photobiont escape from damaged thalli under humid conditions and probably are not able to exist as free-living for a long time (Bubrick *et al.*, 1984; Sanders, 2005).

The traditional description of a lichen symbiosis assumed that single mycobiont associate only with a single photobiont strain. Recent studies, however, have shown that some lichen species harbor more than one algal genotype within individual thalli, e.g. *Ramalina farinacea* (Casano *et al.*, 2011; Del Campo *et al.*, 2013); *R. fraxinea*, *Protoparmeliopsis muralis* (Guzow-Krzemińska, 2006); *Protoparmelia tinctorum* (Mansournia *et al*., 2012); *Tephromela* sp. (Muggia *et al.*, 2014a); *Circinaria* sp. (Molins *et al*., 2018), *Xanthoria parietina* (Dal Grande *et al*., 2014a), and this phenomenon may be relatively common in lichen symbiosis. Authors of those investigations speculate that fungi that possess multiple photobiont strains may respond by favoring one of them and use this to create more beneficial symbiosis (Piercey-Normore, 2006; Leavitt *et al.*, 2015a; Dal Grande *et al.*, 2018). Although a multiplicity of photobionts may facilitate lichen distribution across a wider range of habitats (Casano *et al.*, 2011; Werth & Sork, 2014; Muggia *et al.*, 2014b; Moya *et al.*, 2017) those associations are still far from being understood.

Reproduction modes and symbiont transmission in lichens

The reproduction mode strongly influences the genetic structure in symbiotic organisms. Two dispersal mechanisms can be distinguished: vertical (or co-dependent) transmission, i.e. symbiont dispersal from parent to offspring; and horizontal (or independent) transmission, i.e. symbiont uptake from an environmental source in each new generation (Bright & Bulgheresi, 2010). Both vertical and horizontal transmissions are possible in lichen-forming fungi and their photosynthetic symbionts.

In sexually reproducing lichens, the mycobiont produces meiospores (ascospores or basidiospores), which are dispersed independently of the

photobiont (horizontal transmission). The mycobiont may also disperse by producing mitospores – vegetative thalloconidia (Vobis & Hawksworth, 1981). The sexual or asexual fungal spores germinate and associate with a new photobiont strain available in the environment in a process called relichenization (Beck *et al.*, 1998; Sanders, 2010). Some mycobionts may change photobionts during their lifetime, suggesting that sub-optimal or incompatible algae can be replaced by well-matched photobionts at later stages in thallus development (Ott, 1987; Wedin *et al.*, 2016).

Many lichens form unique morphological structures – e.g. soredia, isidia - that aid simultaneous vegetative dispersal of both symbionts in vertical transmission (Büdel & Scheidegger, 2008; Cassie & Piercey-Normore, 2008; Dal Grande *et al.*, 2012). Co-dispersal of symbionts avoids the complex process of relichenization, but the disadvantage is a lack of genetic recombination that results in clonality of lineages (Piercey-Normore, 2005). Asexual reproduction may lead to congruent genetic structures of mycobiont and photobiont at the population level (Widmer *et al.*, 2012). However, a growing body of literature suggests that maintenance of the association of specific partners in asexually reproducing lichens from generation to generation is an option rather than an obligate event (Wornik & Grube, 2010; Casano *et al.*, 2011). Many vegetatively reproducing mycobiont (morpho)species associate with more than one algal strain e.g. *Parmotrema tinctorum* (Ohmura *et al.*, 2006), *Rinodina atrocinerea* (Helms *et al.*, 2001)*, Thamnolia vermicularis* (Nelsen & Gargas, 2009)*, Cladonia perforata* (Yahr *et al.*, 2004), *Cetraria aculeata* (Domaschke *et al.*, 2012), *Umbilicaria pustulata* (Sadowska-Deś *et al.*, 2014). These lichen species are able to produce conidia - mitotic fungal spores (Vobis & Hawksworth, 1981), which may relichenize with free-living algal cells (Sanders, 2005) or may capture photobionts from other lichen thalli (Friedl, 1987). The other possibilities of high genetic variation in co-dispersing lichens may be the fusion of two genetically different individuals (Asta & Letrouit-Galinou, 1995) or long-distance dispersal of propagules distributed by vectors such as wind or birds (Romeike *et al.*, 2002; Opanowicz & Grube, 2004). Those events may occur at several stages in the lichen life cycle and may explain the polyphyly of photobionts in vegetatively reproducing lichens (Beck *et al.*, 1998; Nelsen & Gargas, 2009). The ability to switch symbiotic partners may be a

substitution for genetic recombination, which facilitates local adaptation and persistence in a new environment (Nelsen & Gargas, 2008).

4.3 SELECTIVITY AND SPECIFICITY IN THE LICHEN SYMBIOSIS

Symbiotic interactions can be described in terms of selectivity and specificity. Selectivity is defined as the "preferential interaction between organisms" (Galun & Bubrick, 1984), which means that a host will interact with one biont selected from the pool of available symbionts. Specificity is described as "cell–cell interaction with absolute exclusivity" (Galun & Bubrick, 1984), where two symbionts associate only with one another without any other potential combination. The degree of selectivity is high for specialists, moderate for intermediates, and low for generalists (Beck *et al.*, 2002; Yahr *et al.*, 2004). In lichen studies, the term selectivity was attributed mainly to mycobiont partners. However, to cover the whole range of possible symbiotic interactions, Beck *et al.* (2002) proposed that selectivity should be understood as ‘interaction between organisms viewed from the perspective of one biont only', which can be a mycobiont or a photobiont. Lichen-forming fungi can form an association with more than one species of algae (low/moderate selectivity); and single algal species or strains may be incorporated into symbiosis with different lichenized fungi (Beck *et al.*, 1998; Kroken & Taylor, 2000; Piercey-Normore, 2006). Specificity depends on selectivity and describes whole symbiotic interactions. If both symbionts exhibit a high degree of selectivity, then the symbiotic association is specific (Rambold *et al.*, 1998; DePriest, 2004).

Fungal-algal association patterns in lichens are not random, and the interactions between the symbionts are constrained by evolutionary and environmental processes (Leavitt *et al.*, 2015a). The symbiosis, even in the widely distributed lichens, is fine-tuned to space and a given environment (Rambold *et al.*, 1998; Peksa & Škaloud, 2011). Low specificity and selectivity are considered as a strategy to facilitate the process of relichenization and help symbionts to survive in constantly changing environments (Romeike *et al.*, 2002; Wirtz *et al.*, 2003; Vargas Castillo & Beck, 2012; Muggia *et al.*, 2014b; Leavitt *et al.*, 2015a). Fungi that can select their photobionts from a set of potential algal strains may be ecologically more successful (Blaha *et al.*, 2006; Guzow-Krzemińska, 2006; Muggia *et al.*, 2013).

Environmental factors may influence the degree of partner selectivity, and fungal-algal association patterns correlate with geographic distribution and ecological conditions (Fernández-Mendoza *et al.*, 2011; Peksa & Škaloud, 2011; Muggia *et al.*, 2014b; Singh *et al.*, 2017). In this case, both compatible symbiotic partners may have similar ecological requirements thus they can meet in adequate habitats (Beck *et al.*, 2002). Extreme climatic conditions are factors that may decrease algal diversity in severe habitats (Wirtz *et al*., 2003; Muggia *et al*., 2008; Pérez-Ortega *et al*., 2012). Lichens-forming fungi with the low level of selectivity may associate with the photobionts available in those harsh environments and by this colonize habitats that are not available for other more selective mycobionts (Romeike *et al*., 2002). A recent investigation at the ecogeographic scale revealed that not the ecology and environmental conditions, but fungal specificity and selectivity are the strongest forces that determine the composition of lichen photobionts (Leavitt *et al.*, 2015a).

In lichens with a predominantly sexual mode of reproduction, where fungal spores require relichenization with an adequate photobiont partner, the symbiotic association seems to be less specific and those lichens have higher chances to associate with various algal lineages. On the contrary, vegetatively reproducing lichens seem to be more specific due to propagation via vegetative propagules already containing appropriate photobiont cells (Ohmura *et al.*, 2006; Dal Grande *et al.*, 2012).

The structure of the lichen thalli and substrate may also influence the level of specificity. Leavitt *et al.* (2015a) demonstrated that some foliose lichens growing on rocks (e.g. *Montanelia, Protoparmeliopsis,* and *Xanthoparmelia*) exhibit lower specificity towards photobiont compared to epiphytic fruticose lichens (e.g. *Letharia* and *Oropogon*). The reason may be that the three-dimensional fruticose forms require highly specialized photobionts that are adapted to increased exposure (McEvoy *et al.*, 2007). The correlation between specificity level and the thallus growth form was found only in some lichen species, therefore it may not be valid for all lichens (Leavitt *et al.*, 2015a).

4.4 GENETIC DIVERSITY OF FUNGAL AND ALGAL SYMBIONTS

Selection of molecular markers

Genetic diversity hidden within a (morpho)species affects the interpretation of species boundaries, cryptic speciation events, symbiont specificity, and adaptation mechanisms. However, finding an appropriate sequence-based DNA marker that reveals sufficient genetic diversity at the population level can be challenging in fungi (Werth, 2010). Ideal are loci that produce high-quality (unambiguous) alignments with sufficient variability. The application of inadequate sequence markers or relying only on a single locus may result in a misrepresentation of genetic diversity (Arnaud-Haond *et al.*, 2005; Dupuis *et al.*, 2012). Therefore, it is important to test highly variable markers from several independently inherited loci (i.e. those from different organelles), with different evolutionary dynamics and various mutational rates (Parker *et al.*, 1998; Zhang & Hewitt, 2003).

A variety of molecular markers have been used in fungal phylogenetics and population genetics. The first markers that were available were ribosomal DNAs, such as nuclear small subunit nrSSU, nuclear large subunit nrLSU (Vilgalys & Hester, 1990; Gargas & Taylor, 1992) and internal transcribed spacer nrITS rDNA (Niu & Wei, 1993). Additionally, the mitochondrial mtSSU and mtLSU were used (Zoller *et al.*, 1999; Printzen, 2002). Protein-coding genes that have been commonly employed include RNA polymerase II largest subunit *RPB1* (Stiller & Hall, 1997; Matheny *et al.*, 2002), and second largest subunit *RPB2* (Liu & Hall, 2004), elongation factor alpha *EF1* (Rehner, 2001), ribosome biogenesis protein *TSR1* and Minichromosome Maintenance Complex Component 7 *MCM7* (Schmitt *et al.*, 2009a), mitochondrial ATP synthase–subunit 6 (Sung *et al.*, 2007), β-tubulin (Glass & Donaldson, 1995), alpha-actin (Carbone & Kohn, 1999) and glyceraldehyde 3-phosphate dehydrogenase GPD (Myllys *et al.*, 2002).

Fungal sequence markers that are variable enough to be used at the level of subspecies include *MCM7*, *RPB1*, *RPB2*, *TSR1* or *GPD* (Fernández-Mendoza *et al.*, 2011; Leavitt *et al.*, 2011b; Wirtz *et al.*, 2012; Sadowska-Deś *et al.*, 2013). All of those markers show different resolution at the subspecies level. For example *RPB1* and *RPB2* show very little variability (Buschbom & Mueller, 2006; Wirtz *et al.*, 2012; Sadowska-Deś *et al.*, 2013), while *MCM7* and *TSR1* show an

acceptable level of intraspecific polymorphism (Spribille *et al.*, 2011; Leavitt *et al.*, 2011b; Sadowska-Deś *et al.*, 2013). nrITS rDNA is considered as highly variable (Lindblom & Ekman, 2006; Del-Prado *et al.*, 2011; Wirtz *et al.*, 2012), but for some species exhibit low genetic variation at population level (Ivanova *et al.*, 1999; Martín *et al.*, 2000; Sadowska-Deś *et al.*, 2014). nrITS rDNA, due to high variability at the inter-species level has been widely used as a universal DNA barcode marker for fungi (Schoch *et al.* 2012). Another locus from the nuclear ribosomal cistron IGS rDNA shows a similarity to the nrITS rDNA variability level and was also successfully used in numerous lichen studies (e.g. Printzen *et al.*, 2003; Lindblom & Ekman, 2006; Leavitt *et al.*, 2011b; Wirtz *et al.*, 2012).

Fewer molecular markers are available for lichen photobionts than mycobionts. The marker that is the most commonly used to identify symbiotic green algae in lichens is the nrITS rDNA (Kroken & Taylor, 2000), however, the phylogenetic resolution of this locus may be insufficient when testing closely related lineages, like *Trebouxia glomerata* and *T. irregularis* (Škaloud & Peksa, 2010). Although an official barcode for algae has not yet been assigned, some authors suggest that nrITS locus could be suitable bar code to estimate genetic species diversity in *Trebouxia* (Leavitt *et al*., 2015; Moya *et al*., 2017; Muggia *et al*., 2018). Additionally other markers were applied to discover genetic variation: nuclear SSU (Weisburg *et al.*, 1991; Turner *et al.*, 1999), nuclear LSU (Piercey-Normore & DePriest, 2001), chloroplast ribulose-bis-phosphate carboxylase *rbcL* (Rudi *et al.*, 1998; O'Brien *et al.*, 2005), nuclear actin (Kroken & Taylor, 2000), chloroplast intergenic spacer *psbJ-L* (Werth & Sork, 2010), mitochondrial cytochrome C oxidase II *COX2* (Fernández-Mendoza *et al.*, 2011) and plastid encoded elongation factor *tuf*A (Famà *et al.*, 2002). More recently chloroplast LSU has been proposed for phylogenetic analysis of lichen photobionts (Del Campo *et al.*, 2010a; Moya *et al.*, 2015, 2018).

Cryptic diversity

Cryptic species are morphologically indistinguishable species, which are phylogenetically distinct and reproductively isolated (Bickford *et al.*, 2007). The progress in molecular phylogenetics and population genetics showed that a lot of genetic variability is present in species, which are morphologically and chemically hardly distinguishable, or these differences are either not obvious or simply overlooked (Victor 2015; Hebert *et al*., 2004). Cryptic species have been found in different organism groups and in every type of habitat across all biogeographic regions (Vrijenhoek *et al.*, 1994; Pfenninger & Schwenk, 2007). Morphologically similar but phylogenetically different lineages often occur sympatrically (Crespo *et al.*, 2002) and the exact number of cryptic species in different ecosystems is unknown. Some studies reveal a high number of previously unrecognized species in extreme environments (Grundt *et al.*, 2006; Lefébure *et al.*, 2006) while others argue that cryptic species are evenly distributed among all biogeographic regions (Pfenninger & Schwenk, 2007). Revealing hidden species diversity has significant implications for understanding the distribution of genetic diversity, and predicting losses in genetic diversity caused by the effects of global climate change (Bálint *et al.*, 2011).

The application of molecular data revealed that cryptic diversity is a common phenomenon also in lichen-forming fungi (Crespo & Pérez-Ortega, 2009; Crespo & Lumbsch, 2010; Lumbsch & Leavitt, 2011; Altermann *et al.*, 2014; Lücking *et al.*, 2014; Singh *et al.*, 2015). Lichens were traditionally described by phenotype, that often led to overestimation or underestimation of species number (Purvis, 1997; Leavitt *et al.*, 2011a). Many lichen species were considered to have wide geographical distributions (e.g. cosmopolitan or pantropical species). However, molecular investigations demonstrated that these lineages are in fact cryptic entities, differentiated because of their evolutionary history and biogeographic mechanisms, or because of local adaptation (Vondrák *et al.*, 2009; Crespo & Lumbsch, 2010; Fernández-Mendoza *et al.*, 2011).

In taxa with lower morphological complexity, as unicellular green algae, cryptic species can be found even more often (Van Oppen *et al.*, 1996; Verbruggen, 2014; Leliaert *et al.*, 2014). Many algal species exhibit intraspecific phenotype variation as a result of genetic or environmental plasticity (Logares *et*

al., 2007). Subtle morphological or chemical features may not correlate with the extensive genetic diversity of photobionts (Pino-Bodas *et al.*, 2012; Payo *et al.*, 2013; Dal Grande *et al.*, 2014b; Magain *et al.*, 2016).

4.5 Species concept and assessment of species boundaries in algae

'Species' represents a fundamental unit in every subfield of biology and helps to organize and evaluate biological theories and principles (Darwin, 1859; Leavitt *et al.*, 2015b). Despite the obvious advantages of accurate species description, the species concept remains incoherent (Mayden, 1997; Taylor *et al.*, 2000; Leavitt *et al.*, 2015b). Many species concepts have been proposed (reviewed in De Queiroz, 2007) and all of them are based on different biological assumptions and delimitation criteria such as morphology, biogeography, ecological niches, reproductive isolation, etc. Some of the species recognitions are considered as theoretical concepts and other serves as operational criteria for taxa recognition (De Queiroz, 2007).

Species delimitation in algae has always been a problematic issue due to the scarcity of features that could be useful to describe species. Phycologists applied numerous species concepts to facilitate algal delineation (Manhart & McCourt, 1992; Mayden, 1997; De Queiroz, 2007) with no exception for lichen photobionts (Beck *et al.*, 1998; Rambold *et al.*, 1998; Helms, 2003; Dal Grande *et al.*, 2014b; Leavitt *et al.*, 2015b; Škaloud *et al.*, 2015; Muggia *et al*., 2018). One of the first concepts, the biological species concept, made 'species' the fundamental unit of biology (Dobzhansky, 1935; Wright, 1940), however, application to algae became challenging. This concept explains species as interbreeding and reproductively isolated populations that occupy a specific niche (Mayr, 1982). The presence of hybridization between different lineages and asexual reproduction mode of algae are the main constraints that make the biological concept faulty (McCourt & Hoshaw, 1990). That is why this concept was considered only as a "species recognition" that does not present the real phylogenetic relationship of species units (Taylor *et al.*, 2000).

Traditionally algae were defined mainly based on phenotypic characters. However, morphological traits are not always conclusive when delimiting recently diverged, morphologically simple groups such as many algal species. Moreover,

some morphological characters can be lost and gained multiple times during evolution and may be present in genetically unrelated taxa (Hafellner, 1984; Leavitt *et al.*, 2011b). Additional difficulties may arise when the examined algae are in the lichenized stage and show few morphological characters that those from axenic culture (Helms, 2003; Beck *et al.*, 1998; Škaloud *et al.*, 2015; Zahradníková *et al.*, 2017). The morphological approach often overlooks intraspecific variation and indicates a false phylogenetic relationship (Leavitt *et al.*, 2011b). That is why today the morphological species concept is not regarded as 'true' species concept, but rather technique working hypothesis, which should be complemented by other approaches, such as the phylogenetic species concept based on molecular data (Leavitt *et al.*, 2015b).

In the last decade, the dramatically increased availability of genetic data, innovative analytical methods, bioinformatical and computational capability gave the opportunity to explore species' boundaries and their phylogenetic relations in a way that had not been previously possible (Carstens *et al.*, 2013). The phylogenetic species concept (Hennig, 1966; Ridley, 1989), that is based on the systematic analysis of homologous traits, assumes species as a group of entities arising from a common ancestor and forming a supported monophyletic clade on the phylogenetic tree (Taylor *et al.*, 2000). The phylogenetic species concept has been promoted also in lichen photobionts and has become the predominant approach for assessing algal diversity (Krienitz *et al.*, 2012; Fucíková *et al.*, 2013; Škaloud *et al.*, 2015, Muggia *et. al.,* 2018). Thanks to this approach numerous phenotypically cryptic lineages were recognized in lichenized algae (Lewis & Flechtner, 2004; Fawley *et al.*, 2011; Demchenko *et al.*, 2012).

Coalescent theory (Kingman, 2000) has highly improved the objective testing of taxon boundaries (Fujita *et al.*, 2012) and has been successfully applied to delimit species in algae (e.g. Yang & Rannala, 2010; Payo *et al.*, 2013; Montecinos *et al.*, 2017). Coalescent-based species delimitation estimates the evolutionary independence of the species units by adjusting conflicts between gene trees, that are inferred from multiple independent loci (Liu *et al.*, 2009; Fujita *et al.*, 2012). Coalescent-based approaches assume there is recombination between genes, random mating, and that the analyzed loci are unlinked (Carstens & Dewey, 2010; Jones & Oxelman, 2014). Some coalescence-based species

delimitation approaches require a *priori* information i.e. assignment of putative species units or population definition e.g. BP&P (Yang & Rannala, 2010), STEM (Kubatko *et al.*, 2009), SpedeStem (Ence & Carstens, 2011), Brownie (O'Meara, 2010) or DISSECT (Jones & Oxelman, 2014). This type of validation approach often works for organisms that exhibit some characters that may help to assign different lineages or species (e.g. Carstens & Dewey, 2010). The other type, species discovery methods, does not require a *priori* information regarding species grouping (O'Meara, 2010). Among these methods are population assignment using Gaussian Clustering (Hausdorf & Hennig, 2010), BAPS (Corander *et al.*, 2008), STRUCTURE (Pritchard *et al.*, 2000; Falush *et al.*, 2003), Structurama (Huelsenbeck *et al.*, 2011) or the General Mixed Yule Coalescent model GMYC (Pons *et al.*, 2006) recently widely used in studies on algae (Tronholm *et al.*, 2012; Hoef-Emden, 2012; Payo *et al.*, 2013; Garrido-Benavent *et al.*, 2017).

The selection of molecular species delimitation approaches is large. The assessment of species boundaries based on single-locus data aims to separate intraspecific population variability from interspecific differences and is mostly based on genetic distances (Puillandre *et al.*, 2012) or tree-based approaches (Fujisawa & Barraclough, 2013; Zhang *et al.*, 2013) and has been applied in numerous algal investigations (Verbruggen *et al.*, 2007; Rybalka *et al.*, 2009). For instance, SPecies IDentity and Evolution Spider implemented in R (Brown *et al.*, 2012) or Automatic Barcode Gap Discovery ABGD (Puillandre *et al.*, 2012) are based on single-locus and are considered to be more effective for rapid and large-scale assessment of species diversity (Leliaert *et al.*, 2014). Despite the common application of single-locus delimitation methods, delineation that is based on concatenated multiple independent loci is a more reliable source of data and generates a robust hypothesis of species boundaries (Dupuis *et al.*, 2012; Leavitt *et al.*, 2013a,b; Del-Prado *et al.*, 2013).

None of the species delineation approaches is universal and may be not suitable for testing selected organisms or given data sets. All approaches have limitations and are applicable to different types of data. Carstens *et al.* (2013) have noticed that all available delimitation models simplify assumptions about the speciation process and suggested: "*it is better to fail to delimit species than it is to delimit falsely entities that do not represent actual evolutionary lineages*".

Awareness of the limitations and pitfalls of species delimitation approaches hopefully allows us to select the most fitting approach for our data, and as a result improve our knowledge on taxa diversity, symbiont interactions, ecological patterns, and appropriate species conservation practices (Beck, 1999; Bickford *et al.*, 2007; Pauls *et al.*, 2013; Leavitt *et al.*, 2015b).

4.6 MUTUALISTS AND THE ECOLOGICAL NICHE

One commonly used concept of the ecological niche describes the niche as multi-dimensional hypervolume of environmental conditions (such as ecological resources or climatic variables) in which an organism can persist (Hutchinson, 1957). Every species has different types and numbers of variables (dimensions) of environmental space (Peterson, 2011). A species will not occupy its entire potential niche i.e. fundamental niche, rather only the space where it can persist given competition, i.e. realized niche (Figure 1 A) (Hutchinson, 1957; Pulliam, 2000). The fundamental niche is defined as abiotic conditions, while realized niche is the outcome of the biotic interactions between organisms (Pulliam, 2000; Warren *et al.*, 2014). As a consequence of strong competition between organisms, the realized niche is narrower than fundamental niche, and different biotic interactions between species can change niche breadth (Pulliam, 2000). For instance, antagonistic associations, such as predators or pathogens, may constrain the realized niche, and contrary, mutualistic – mediated relationship may expand or even shift realized niche (Poisot *et al.*, 2011).

Symbiotic organisms may enhance the environmental tolerance of one partner, by taking up symbionts, and thus expand their ecological and geographic range (Palmer *et al.*, 2003; Moran, 2007; Poisot *et al.*, 2011; Afkhami *et al.*, 2014). The mutualist-mediated niche concept defines the potentially suitable space in which organisms involved in a close relationship may exist (Peay, 2016). The realized niche of the association can be larger than the fundamental niche of the host species alone (Figure 1 B) (Bruno *et al.*, 2003). Although some studies have documented how symbiotic interactions affect species distribution and ecological niche expansion (Joy, 2013; Afkhami *et al.*, 2014; Kazenel *et al.*, 2015; Pita *et al.*,

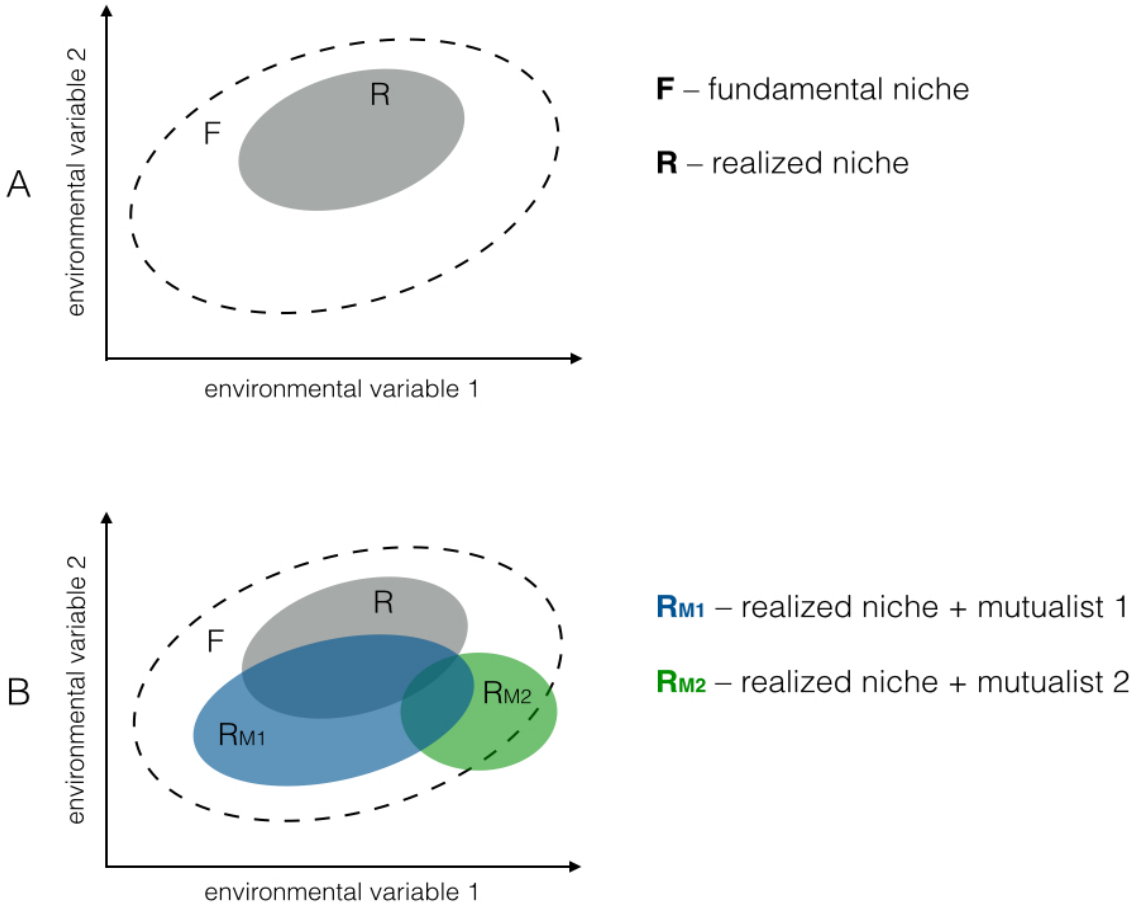

Figure 1. Ecological niche concept (A) and the expansion of the mutualistic niche (B). The dashed line depicts the fundamental niche (F) of the host species, the gray area the realized niche. Acquisition of mutualists may extend the realized niche of the host – depicted as blue (R_{M1}) and green (R_{M2}) areas (adapted from Poisot *et al.*, 2011).

2016), the role of mutualistic associations in shaping species niches is still not well understood.The current literature shows that mycobionts possess the ability to harbor multiple photobiont lineages (Romeike *et al.*, 2002; Blaha *et al.*, 2006; Muggia *et al.*, 2013; Del Campo *et al.*, 2013; Dal Grande *et al.*, 2014a; Muggia *et al.*, 2014b). All those papers speculate that lichen-forming fungi may broaden their range (realized niche) by interacting with a wide range of autotrophic algal ecotypes. So far, only the investigation by Casano *et. al.* (2011) has indicated that different photobiont strains (described as 'TR1' and 'TR9') within one thallus of *Ramalina farinacea* possesses different physiological properties. Mycobionts that associate with multiple strains of photobionts can potentially shuffle their symbiotic algae and thus respond to habitat changes (Piercey-Normore, 2006; Yahr *et al.*, 2006; Muggia *et al.*, 2008). The coexistence of multiple photobiont lineages is revealed mainly from phylogenetic analyses, and additional relevant investigations that could confirm the presence of algal ecotypes and algal niche expansion are missing. Stronger evidence for different photobiont ecotypes has been presented only in a few publications (e.g. Casano *et al.*, 2011; Fernández-Mendoza *et al.*, 2011; Peksa & Škaloud, 2011). As presented in this thesis, the association patterns in the lichen *Umbilicaria pustulata* provide evidence for symbiont-mediated niche expansion in lichens for the first time (Rolshausen *et al.*, 2018).

The mycobiont usually exhibit less genetic structure at the population level across different habitat (generalist strategy), compared to the high level of genetic variability within photobiont partner (Piercey-Normore, 2006; Yahr *et al.*, 2006; Dal Grande *et al.*, 2012; Sadowska-Deś *et al.*, 2013; Muggia *et al.*, 2014b). These observations could suggest that spatial distribution and niche breadth of lichen holobiont depend mainly on the photobiont ability to adapt to the local environmental conditions (Yahr *et al.*, 2006; Fernández-Mendoza *et al.*, 2011) or, alternatively, it may also mean that the fungal markers we use are just not variable enough to show this kind of differentiation.

4.7 THE MODEL SPECIES - *UMBILICARIA PUSTULATA* (SUBG. *LASALLIA*)

The lichen-forming fungus *Umbilicaria pustulata*, together with its trebouxioid photobiont, is a useful model species to explore symbiont diversity, and fungal-algal association patterns because of its morphology and reproduction mode, as well as its distribution and ecology. *U. pustulata* is a foliose macrolichen (Figure 2 A), which belongs to the family Umbilicariaceae. Until recently this lichen family was considered to be composed of two genera, *Umbilicaria* Hoffm., and *Lasallia* Mérat. (Poelt, 1962; Wei & Jiang, 1993). Initially, based on molecular traits and characteristic morphology, *Umbilicaria pustulata* was recognized as *Lasallia pustulata (Davydov et al., 2010)*. However, according to the most recent classification of the Umbilicariaceae (Davydov *et al*., 2017), *Lasallia* was reduced to synonymy with *Umbilicaria*. This helped to keep a consistent phylogeny of Umbilicariaceae that is based on monophyletic groups.

The size of *U. pustulata* thalli is typically 3-6 cm, but mature individuals can grow up to 40 cm in diameter. Thalli are brown to gray when dry, and dark green when water saturated (Fałtynowicz & Bylińska, 1999). Each thallus is attached to the substrate with an umbilicate central holdfast. The upper surface of the thallus is covered with conspicuous, convex pustules that gave the species its name (Figure 2 E). *U. pustulata* grows radially from the center of the thallus (Hestmark *et al.*, 1997). The photobiont of *U. pustulata* is a coccoid green alga of the genus *Trebouxia* (Figure 2 B).

Umbilicaria pustulata occurs on granite, slate, and sandstone, and prefers vertical, sunny outcrops that are often fertilized by birds. Populations are large and densely clustered, and often cover the rock surface entirely (Hestmark, 1992). Although individual populations may form spectacular ‘carpets’, the species’ occurrence in the landscape can be rather local, and restricted to smaller scattered rocks. Generally, *U. pustulata* populations are ideal for population-style sampling.

Umbilicaria pustulata has a mixed reproduction pattern but is predominantly asexual. In young thalli reproduction is achieved by asexual propagules: isidia (Figure 2 D). These coralloid or pin-like structures tend to grow on the marginal areas on the upper side of the thalli. Isidia are very brittle and break off the thallus

easily. Rainwater is thought to play the main role as a dispersal vector and carries the propagules downwards the slope (Hestmark, 1992). Due to the effective short distance dispersal of the isidia, young thalli can cover the whole available surface at a population site (Hestmark, 1992). *U. pustulata* contains also asexual conidia. Older thalli may sometimes form fruiting bodies (apothecia) on the upper surface (Figure 2 C), which produce sexual ascospores. Ascospores are actively discharged and efficiently dispersed by wind.

Umbilicaria pustulata has a Europe-wide range spanning from central Scandinavia to the Mediterranean, and from France to the European part of Russia (Figure 3). The southernmost confirmed records are from the Canary Islands. Specimens collected in North America or Asia are likely to represent different species (Brodo *et al.*, 2001; author observation). The altitudinal range of the species is between 0-1800 m a.s.l, but most populations occur between 400-800 m a.s.l. The wide geographic and elevational distribution indicates that the species has a broad ecological amplitude.

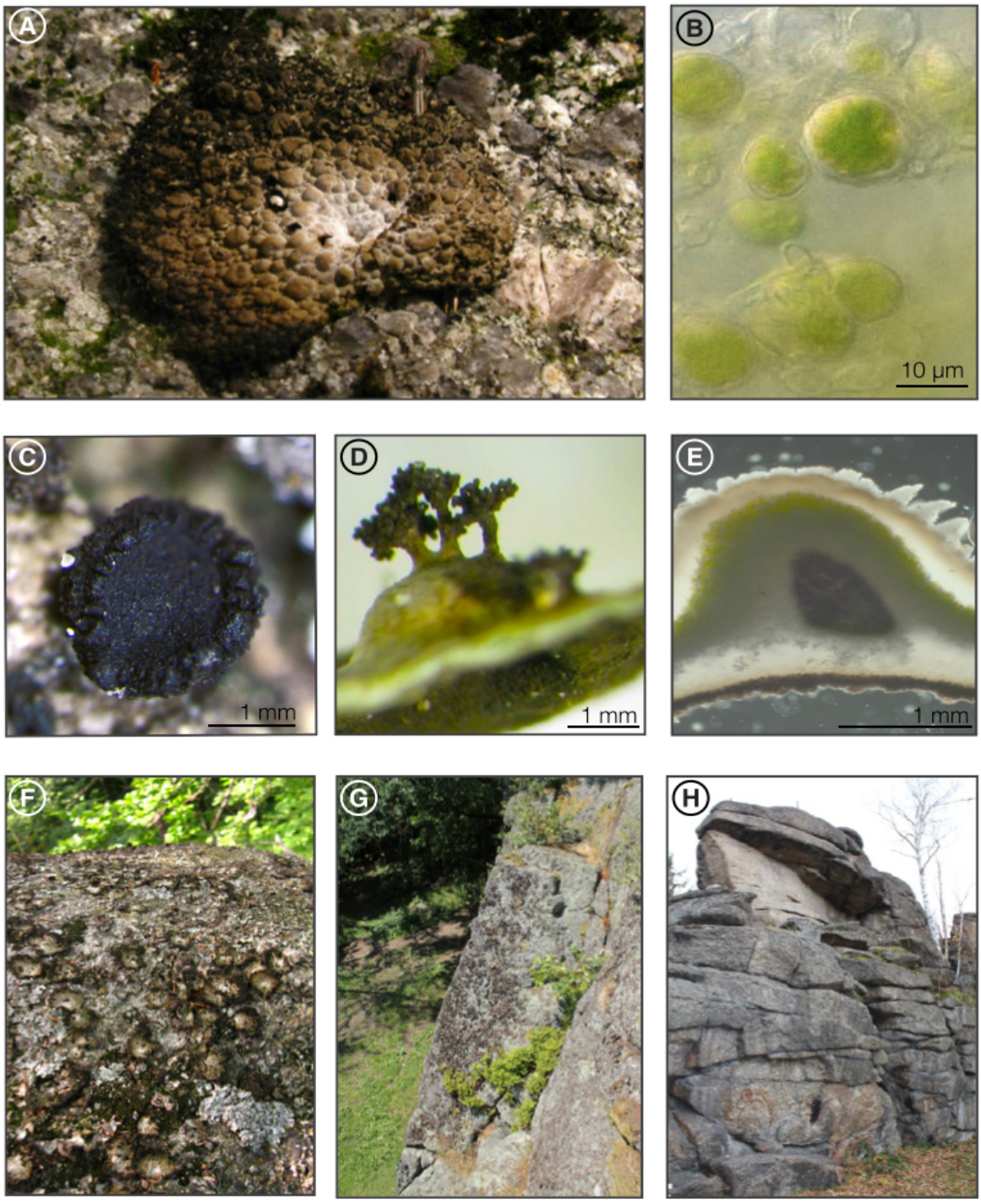

Figure 2. Thallus of *Umbilicaria pustulata* (A), photobiont: *Trebouxia* sp. (B), apothecium (C), branched isidia on the upper surface of the thallus (D), cross section through a young pustule (E), population on rock (F), typical steep rock covered with dense population (G), example of habitat (H).

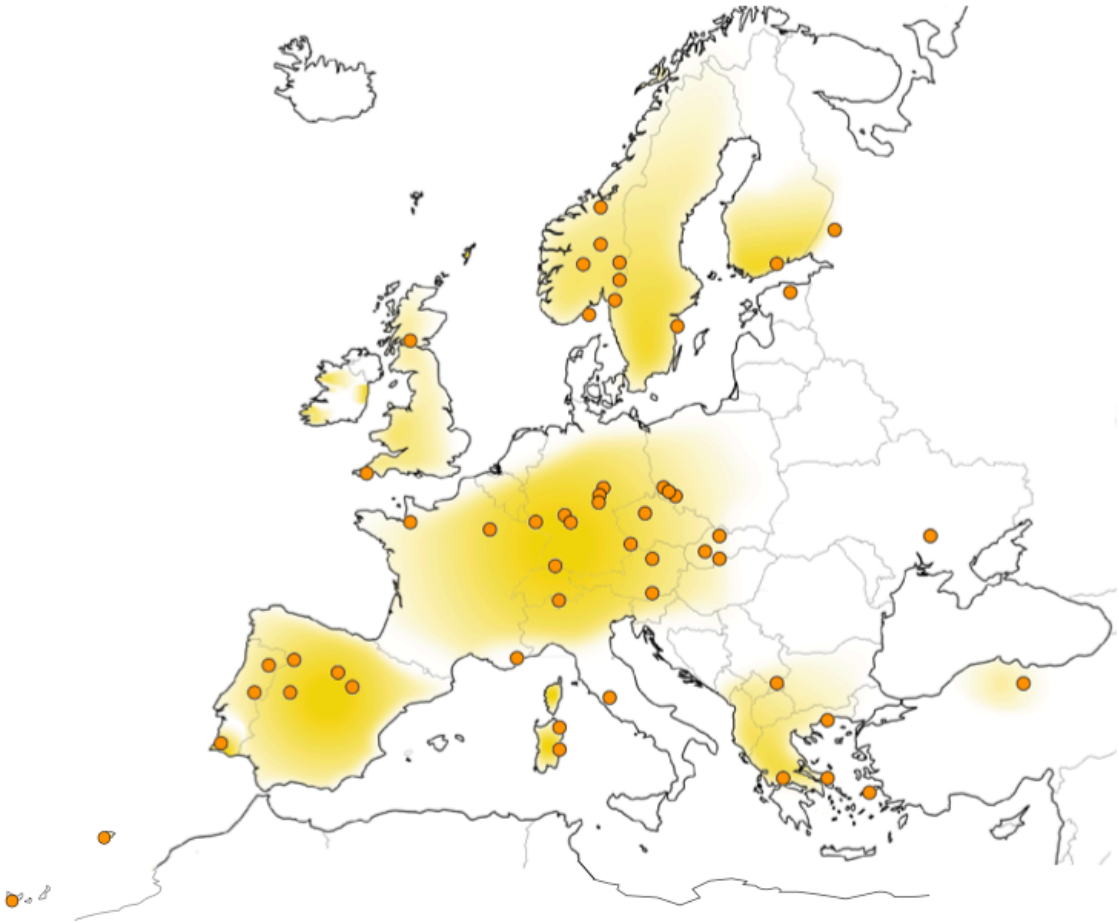

Figure 3. The geographic distribution of *Umbilicaria pustulata*. Dots indicate collection sites used in this study. Shaded areas indicate distribution reconstructed from the data available in the GBiF repository (GBIF, 2011).

5. RESEARCH QUESTIONS

Specifically, I aim to answer the following questions (Figure 4):

Q1 What is the intraspecific diversity of fungal and algal symbionts in the lichen Umbilicaria pustulata, given a range-wide sampling?

Analyzing intraspecific diversity of both lichen symbionts is a key predisposition to understand fungal-algal interactions, population dynamics and co-evolution. Numerous studies revealed cryptic diversity in lichen-forming fungi and their photobionts (e.g. Piercey-Normore, 2009; Crespo & Lumbsch, 2010; Pérez-Ortega *et al.*, 2012; Altermann *et al.*, 2014). It is particularly challenging to find sequence markers that show sufficient variability at the species and sub-species level in fungi. To identify the most suitable set of sequence markers and to detect intraspecific variability within *Umbilicaria pustulata* I aim to test all presently used molecular markers (nuclear and mitochondrial, ribosomal and protein-coding). Respectively for the algal partner, I tested all presently used molecular markers to determine the most suitable fragments to detect photobiont variability within a single lichen species.

Q2 How can we use molecular data to delimit species in trebouxioid photobionts?

The correct determination of species boundaries in lichens is crucial for the study of selectivity, specificity, co-distribution, and co-evolution of lichen symbionts. Because of the substantial number of cryptic species and lack of satisfactory species concept, I investigated species boundaries within the trebouxioid photobionts of the lichen-forming fungus *Umbilicaria pustulata*. The goal was to delimit algal species using a novel multifaceted approach based on phylogenetic relationships and coalescence methods (GMYC, STEM). I aimed at exploring patterns of species-to-species and species-to-community interaction of candidate photobiont species and whether they associate with other lichen-forming fungi.

Q3 How do fungal-algal association patterns in a lichen change along environmental gradients? Can association with particular photobiont lineages lead to niche expansion of the holobiont?

Lichen-forming fungi may broaden their ecological niche by using multiple, and ecologically differentiated photobiont lineages. This can be considered as a potential adaptive mechanism to expand the holobiont's range. To better understand the role of photobionts in environmental adaptation of lichen-forming fungi, we need to describe and quantify the ecological niches of different photobiont lineages. Here, I applied a spatial genetic approach to determine the ecological drivers that affect symbiotic associations. I investigated population genetic structure of fungal and algal partner in the lichen *Umbilicaria pustulata* throughout its range. By application of species distribution modeling and the reconstruction of Hutchinsonian climatic hypervolumes, I estimated which climatic factors may control the geographic distribution of specific mycobiont-photobiont associations. I hypothesize that lichens may cope with different environmental conditions by associating with alternative symbiotic partners.

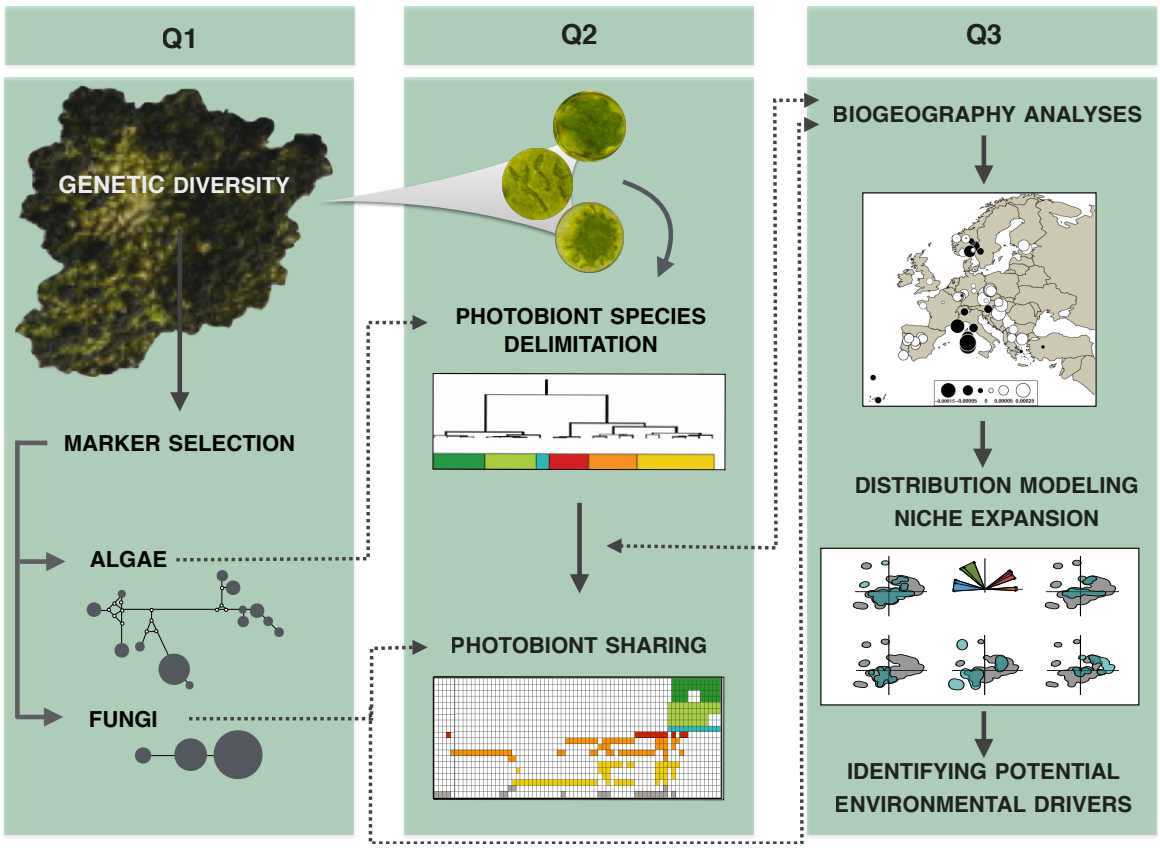

Figure 4. Overview of the structure and workflow of the present thesis. The first step of this study was to evaluate the genetic diversity of fungal and algal partner in the lichen *Umbilicaria pustulata*, covering the entire range of the species. The second step was to delimit species in the *U. pustulata* photobiont (*Trebouxia* sp.) by using phylogenetic and coalescent-based approaches. The third step was to find out which environmental factors favour the distribution of symbionts and whether interactions with specific photobiont strains influence environmental adaptation and niche expansion of the lichen holobiont (based on Sadowska-Deś *et al*., 2013, 2014; Rolshausen *et al*., 2018).

6. THESIS STRUCTURE

In this study I will discuss (a) intraspecific diversity of both, algal and fungal symbionts of the lichen species *Umbilicaria pustulata*. Then I will evaluate (b) species delimitation in the most common lichen photobiont *Trebouxia* that is associated with my model species *U. pustulata*. For the first time I am using a coalescent-based approach to delimit species in *Trebouxia*. Moreover, based on the data from environmental distribution of *U. pustulata* I try to (c) establish which climatic factors influence symbiont distribution and how fungal-algal genotype interactions contribute to niche expansion in lichens.

This thesis is based on three published articles (see Appendices). References and Supplementary data are presented with each appendix. The authors' contributions to the articles are given at the beginning of each appendix.

7. RESULTS AND DISCUSSION

7.1 GENETIC DIVERSITY IN *UMBILICARIA PUSTULATA*

Numerous studies attempt to develop molecular markers suitable for testing population structure in lichen-forming fungi and their photobionts (DePriest, 1993; Zoller *et al.*, 1999; Högberg *et al.*, 2002). However, an overall comparison of the molecular loci that are tested on single lichen species is still missing. My comparative study aims at facilitating the selection of molecular markers used for population studies. I investigated intraspecific genetic diversity in both symbionts of the lichen *Umbilicaria pustulata* (Appendix I). To increase the chances of finding the most variable loci for the population study, I conducted a comparison of molecular markers that are commonly used in mycobiont and photobiont investigations. I used ribosomal, protein-coding genes, as well as intergenic spacer markers. I also included loci from the nuclear, mitochondrial genome, and additionally from the chloroplast genome while testing photobiont (Table 1). All tested loci showed a similar evolutionary history.

The nuclear internal transcribed spacer region of the ribosomal operon nrITS rDNA is considered as a highly variable genetic marker. High levels of genetic diversity have been reported in numerous lichen species (e.g. *Cavernularia hultenii Printzen et al.*, 2003; *Xanthoria parietina* Lindblom & Ekman, 2006; *Parmelina tiliacea Núñez-Zapata et al.*, 2011; *Usnea* Wirtz *et al.*, 2012; *Cladonia rei* Osyczka *et al.*, 2014). However, the possibility of revealing intragenomic variations while using nrITS rDNA is a disadvantage in population study (Simon & Weiß, 2008). This marker serves more as a species identifier and may reveal cryptic diversity in lichen-forming fungi with unclear species boundaries (Núñez-Zapata *et al.*, 2011; Schoch *et al.*, 2012). My results show a lack of genetic variability in the nrITS rDNA region in *U. pustulata* mycobiont, which supports the aforementioned statement. Among the tested protein-coding gene markers (*GPD*, *EF1*, *MCM7*, *RPB1, RPB2*, *TSR1*) only *MCM7* shows an appropriate level of polymorphism.

Table 1. All loci used in this study.

	TYPE	LOCUS	GENOME	LOCUS NAME
PHOTOBIONT	Ribosomal	ITS rDNA	Nuclear	Internal transcribed spacer
		LSU rDNA	Chloroplast	Large subunit
	Intergenic spacer	*psbJ-L*	Chloroplast	Intergenic spacer region
	Protein coding	*COX2*	Mitochondrial	Cytochrome C oxidase II
		rbcL	Chloroplast	Ribulose-bis-phosphate carboxylase
		ACT	Nuclear	Actin
MYCOBIONT	Ribosomal	ITS rDNA	Nuclear	Internal transcribed spacer
		mtSSU rDNA	Mitochondrial	Small subunit
		mtLSU rDNA	Mitochondrial	Large subunit
	Protein coding	*TSR1*	Nuclear	Ribosome biogenesis protein
		MCM7	Nuclear	Minichromosome Maintenance Complex Component 7
		RPB1	Nuclear	RNA polymerase II largest subunit
		RPB2	Nuclear	RNA polymerase II 2nd largest subunit
		EF1	Nuclear	Elongation factor alpha
		GPD	Nuclear	Glyceraldehyde-3-phosphate dehydrogenase

TSR1 marker that was tested at the population level for the first time in this study was considered to be sufficient for resolving fine within-genus phylogenetic relationships (Schmitt *et al.*, 2009a). My results show that the genetic variation of *TSR1* was at a similar level as *MCM7*. mtSSU and mtLSU were the least variable loci. These mitochondrial markers were successfully used in other studies (Vargas *et al.*, 1999; Moon-van der Staay *et al.*, 2001). Recently mtSSU and mtLSU were considered to underestimate the genetic variations (Hall *et al.*, 2010; Piganeau *et al.*, 2011). My results show no sequence variability in *RPB1*, *RPB2*, and *GPD*, which is also consistent with similar studies on *Porpidia* sp. (Buschbom & Mueller, 2006) or *Usnea* sp. (Wirtz *et al.*, 2012).

The application of several molecular markers reveals high genetic diversity in photobiont of *U. pustulata*. Although *COX2* and *psbJ-L* revealed a high number of *Trebouxia* haplotypes, the nrITS rDNA was the most variable locus. Even though nrITS rDNA has slow coalescence (Hall *et al.*, 2010; Piganeau *et al.*, 2011) this marker provides the highest resolution in various algal groups (Lundholm *et al.*, 2006; Škaloud & Peksa, 2010; Pröschold *et al.*, 2011; Muggia *et al.*, 2013). Application of *rbcL* marker revealed the lowest genetic variability in *U. pustulata* photobiont.

Two median-joining haplotype networks based on nrITS rDNA and *COX2* showed two haplotype groups separated by a substantial number (23 and 37) of mutational steps (Sadowska-Deś *et al.*, 2013). I speculate that these divergent groups may constitute different species of *Trebouxia*. High genetic diversity of photobionts associated with one fungal species has been reported in numerous studies (e.g. Blaha *et al.*, 2006; Piercey-Normore, 2006; Nelsen & Gargas, 2009; Dal Grande *et al.*, 2013; Leavitt *et al.*, 2013b). These variations include haplotypes, lineages or even different species of symbiotic algae. High algal variability within a mainly asexual reproducing lichen-forming fungus is surprising, but high photobiont diversity was reported even in strictly asexual lichens (e.g. sterile *Cavernularia hultenii* Printzen *et al.,* 2003; or *Cetraria aculeata* Fernández-Mendoza *et al.,* 2011). This could be evidence for photobiont switch or uptake from free-living strains, as a response to environmental changes. It needs to be emphasized that even the very low rate of sexual reproduction could be an important factor in shaping the genetic structure and this phenomenon was

described in numerous studies (Wornik & Grube, 2010; Grube & Spribille, 2012; Dal Grande *et al.*, 2012).

It is generally difficult to find sequence markers with sufficient resolution at the intra-species level because the utility of certain markers is not the same for every species. Some genetic markers may work with a given species, while in other species it simply does not show any variability. *GAP* was successfully used in studies on *Cetraria aculeata* (Fernández-Mendoza *et al.*, 2011) but caused sequencing problems when analyzing the population of *Umbilicaria pustulata* (Sadowska-Deś *et al.*, 2013). I had similar difficulties with actin, that showed satisfactory results in other photobiont investigations (Grube & Muggia, 2010; Skaloud & Peksa, 2010) and with chloroplast LSU rDNA recommend to resolve variation in *Trebouxia* (Del Campo *et al.*, 2010b; Catalá *et al.*, 2016).

Studying highly clonal organisms, such as some species of lichenized fungi, requires genetic markers with high resolution. Although sequence-based markers are widely used in the study on symbiont diversity and selectivity, other studies often apply different types of markers like SNPs (Baird *et al.*, 2008) or single sequence repeats - microsatellites (Morgante & Olivieri, 1993). These new generation markers are especially valuable for high-resolution population studies in lichen-forming fungi (Magain *et al.*, 2010; Guzow-Krzemińska & Stocker-Wörgötter, 2013; Nadyeina *et al.*, 2014; Dal Grande *et al.* 2014a) and for some green algal photobionts (Dal Grande *et al.*, 2010; Mansournia *et al.*, 2012; Widmer *et al.*, 2012; Dal Grande *et al.*, 2013). However, the development of such markers typically requires axenic cultivation, which is time-consuming, often hampered by contaminations or not always feasible (Widmer *et al.*, 2010).

Application of conventional Sanger DNA-sequencing (Sanger *et al.*, 1977), which at once sequences only one individual specimen, may be problematic for complex environmental samples (Shokralla *et al.*, 2012), including lichens. Indeed, I was unable to obtain an unambiguous Sanger sequence of the photobiont from some individuals. This suggests the presence of multiple genetically different algal strains within some of the thalli. Recent studies targeting algal diversity in lichens using Next Generation Sequencing (NGS) confirmed the presence of many different photobionts within lichen individuals or populations (Moya *et al.*, 2017; Dal Grande *et al.*, 2018; Molins *et al.*, 2018; Onuț-Brännström *et al.*, 2018).

However, a direct comparison of the two methods, Sanger sequencing and NGS metabarcoding showed that a single most abundant photobiont is present in most individuals of *Umbilicaria pustulata* (Paul *et al* 2018). Sanger sequencing will persistently pick up the dominant photobiont lineage in an individual unless a second photobiont species is present and contributes at least 30% of the NGS reads. This shows that Sanger sequencing underestimates the real symbiont diversity (Voytsekhovich & Beck, 2016; Moya *et al.*, 2017; Paul *et al.*, 2018), but it consistently reveals the dominant, and thus ecologically relevant, lineages.

7.2 SPECIES DELIMITATION IN *TREBOUXIA* PHOTOBIONTS

The knowledge of diversity and symbiotic interactions between the most common photobiont *Trebouxia* and various lichen-forming fungi are at the moment constrained by inconsistency and uncertainty in *Trebouxia* taxonomy. Recent studies revealed lots of diversity within the genus *Trebouxia*, however, only a limited number of studies took up the challenge to delimit species-level lineages in *Trebouxia* (e.g. Kroken & Taylor, 2000; Blaha *et al.*, 2006; Leavitt *et al.*, 2015b). To partially fill this gap I aimed to delimit species in the trebouxioid photobiont in the species *Umbilicaria pustulata.* For the first time, I applied a novel multifaceted approach that incorporates coalescence and phylogenetic analyses (Appendix II). Different delimitation methods (GMYC, STEM, phylogenetic analyses and morphological features) used in my study yielded congruent results and showed that *U. pustulata* is associated with at least five putative algal species. This indicates that *U. pustulata* is not a highly selective lichen mycobiont and is able to take up different *Trebouxia* lineages. As presented in my study, high genetic variability within symbiotic algae is in concordance with other molecular investigations that revealed the high genetic diversity of *Trebouxia* in various lichen species (e.g. Ohmura *et al.*, 2006; Muggia *et al.*, 2014b; Leavitt *et al.*, 2015a).

Although a large body of literature shows a high diversity of algal lineages, most of these studies base their findings solely on a single-locus phylogeny (i.e. Blaha *et al*., 2006; Muggia *et al*., 2013; Ruprecht *et al*., 2012; Vargas Castillo & Beck, 2012). It has been shown, however, that species delimitation based on a single marker is often uncertain, because it will not reveal processes like

incomplete lineage sorting, trans-species polymorphism, hybridization, and introgression (Taylor *et al.*, 2000; Knowles & Carstens, 2007; Heled & Drummond, 2010). To facilitate species description Carstens *et al*., (2013) recommend using multiple DNA-based delimitation methods that are based on multilocus sampling. Following the above suggestion, in my investigation of *Trebouxia* boundaries I have applied dataset based on four concatenated genetic markers: nrITS rDNA, *psbJ-L*, *COX2,* and *rbcL*, which were congruent and could be combined.

The assessment of species strongly depends on the selection of adequate genetic markers. To find sequence differences that may indicate species boundaries, the interspecific variation of selected molecular marker should be higher than intraspecific variation (Leliaert *et al.,* 2014). Although a single base pair may be enough to delimit species (e.g. Brodie *et al.*, 1996), delimitation that is strongly supported requires genetic marker with the highest possible resolution. The variation of the genetic marker depends on evolutionary rate and length of the selected locus. The most common markers used in species delimitation in studies on green algae are nuclear SSU rDNA, LSU rDNA, rDNA ITS, plastid *tuf*A and *rbcL* (Saunders & Kucera, 2010; Leliaert *et al.*, 2014; Garrido-Benavent *et al.*, 2017) although their genetic variation depends on the model species. The selection of genetic markers used in *Trebouxia* species delimitation was based on the assessment of the markers resolution in the previous study on *Umbilicaria pustulata* symbionts (Sadowska-Deś *et al.*, 2013).

All existing species delimitation methods have some disadvantages and may give deviating results when applied to the same dataset (Camargo *et al.*, 2012; Miralles & Vences, 2013; Carstens *et al.*, 2013). For instance, one of the major disadvantages while using GMYC or STEM is that they both may overestimate species delimitation by increasing the number of branches in the species tree and decreasing the average number of lineages in each branch (Harrington & Near, 2012; Miralles & Vences, 2013). Moreover, GMYC is affected by the population size relative to the divergence times between them (Fujisawa & Barraclough, 2013; Talavera *et al.*, 2013). Some studies also suggest that GMYC may provide a higher estimation of operational taxonomic units (OTUs) than other species delimitation methods (Miralles & Vences, 2013; Talavera *et al.*, 2013; Hamilton *et al.*, 2014). A similar problem is present in STEM analyses. Although STEM is not

affected by the phylogenetic uncertainty in the species tree, the correctness of the method depends on the accuracy of the gene tree (Carstens & Dewey, 2010). Harrington and Near (2012) presented that STEM may increase the number of species tree branches and decrease the average number of lineages in each branch. Recently some promising methods such as Automatic Barcode Gap Discovery ABGD (Puillandre *et al.*, 2012), or Poisson tree processes PTP were suggested to be more accurate when using a single-locus approach (Puillandre *et al*., 2012; Zhang *et al*., 2013). ABGD method has been applied to assess candidate species-level based on nrITS rDNA marker in photobiont *Trebouxia* (Leavitt *et al.*, 2015b). Although a completely reliable method of species delimitation based on molecular data is still missing, the multifaceted delimitation methods presented in this thesis advance the current descriptions of diversity within *Trebouxia* photobionts.

While selecting an appropriate delimitation method, it is important to take care of an adequate sample number for analysis. A sampling at suitable ecological scale is always challenging (Jackson &Fahrig, 2014, 2015). Although the optimal sample size strongly depends on the model organism and type of selected analysis, the recommended sampling represents at least 10-20 individuals from all candidate lineages (Esselstyn *et al.* 2012; Carstens *et al.,* 2013, Bergsten *et al.,* 2012). This standard is not always feasible and using a lower sample number may influence the total amount of detected species. Presented in my study the low number of samples assigned to putative species 3, could possibly influence the final delimitation of *Trebouxia* photobionts in *U. pustulata*.

Many authors argue that pure DNA sequence information without other supporting evidence cannot be used by itself for species circumscription, similarly as morphological characters cannot stand for species delimitation alone (Desalle, 2006; Darienko *et al.*, 2015). Despite the broad usefulness of molecular data it is important to consider additional lines of evidence such as chemistry, geographical distribution, morphology and the behavior of the tested organism (Pröschold *et al.*, 2001; Fujita *et al.*, 2012; Leliaert *et al.*, 2014). Malavasi *et al*., (2016) pointed out that ecological characters have been successfully used for species delimitation in various organisms (Raxworthy *et al.*, 2007; Ruiz-Sanchez & Sosa, 2010) but have not received similar attention in studies on lichen symbiosis. Moreover, when

"*closely related lineages distinguishable by ecological preferences are well supported in molecular phylogenetic analyses, they should be recognized as different species regardless of ambiguities in other types of data*" (Malavasi *et al.*, 2016). Ecological features of microalgae are difficult to assess. However, some investigations managed to include ecological preferences (such as rain exposure and sunlight) that supported species delimitation based on diverse sources of evidence (Rindi & Guiry, 2002; Peksa & Škaloud, 2011). Such integrative methods may significantly contribute to statistical species delimitation. Although phenotype-based species delimitation is not sufficient to characterize species in *Trebouxia (Kroken & Taylor, 2000; Blaha et al.*, 2006) it may serve as an additional source of evidence (Muggia *et al.*, 2018). That is why I characterized the morphology of cultivated algal cells from putative species to find phenotype variability that may support molecular delineation. Despite the fact that the genus *Trebouxia* shows little plasticity in phenotypic characters, two of the examined putative photobiont species differed in chloroplast morphology (Figure 5), supporting the recognition of these lineages as species. Due to the lack of formal taxonomic names for *Trebouxia* lineages, previous phylogenetic studies typically assigned provisional names to lineages, consisting of letters and numbers (Kroken & Taylor, 2000; Leavitt *et al.*, 2013b; Sadowska-Deś *et al.*, 2014; Muggia *et al.*, 2014b; Leavitt *et al.*, 2015a; Catalá *et al.*, 2016; Leavitt *et al.*, 2016). As a consequence, the DNA databases are full of units that are classified neither into morphotypes nor species, and the names of the lineages are inconsistent across different phylogenetic studies. This strongly hampers the correct assignment of newly sequenced individuals, comparisons across studies, and communication about trebouxioid taxa (Desalle, 2006; Leliaert & De Clerck, 2017). The provisional naming system for *Trebouxia*, which was recently proposed by Leavitt *et al*. (2015a) is based on a broad sampled *Trebouxia* nrITS DNA sequences. The authors apply the ABGD species delimitation method and received the operational taxonomic units (OTUs) that were treated as candidate species and assigned to major *Trebouxia* clades (A, G, I, S) defined by Helms *et al*. (2001). The presented system could be a good starting point for a more consistent nomenclature of this complex genus and may facilitate communication in future studies. It has been already employed in some recent lichen investigation (Moya *et al*., 2017; Molins *et al*., 2018; Dal Grande *et*

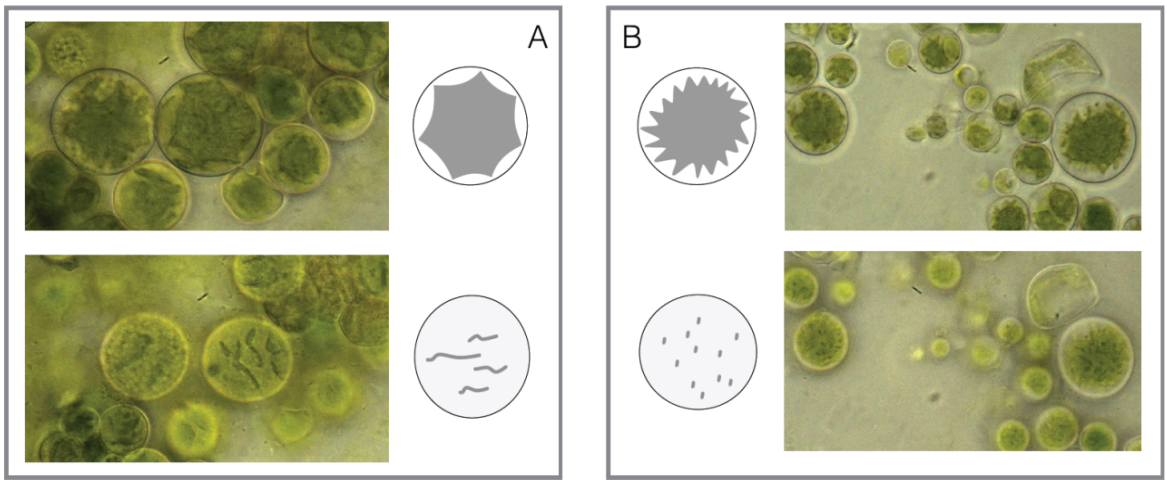

Figure 5. Different *Trebouxia* morphotypes. The chloroplast of the first algal strain (A) is characterized by deep incisions with long narrow ridges at the margin of the cell. The chloroplast of the second algal strain (B) is characterized by short and narrow ridges at the margin of the cell. The space between the cell wall and chloroplast is wider than in the first strain. Upper picture – optical section; lower picture – surface view (based on Sadowska-Deś *et al.*, 2014).

al., 2017), however, not all newly recognized *Trebouxia* lineages fitted into this novel naming system (Singh *et al.*, 2017). Additionally, in progress are taxonomic studies that will use all available *Trebouxia* nrITS rDNA sequences to facilitate species recognition (Muggia, personal communitcation). Still, the lack of a comprehensive and complete *Trebouxia* taxonomy based on molecular data hamper our progress in understanding species interactions, biogeographic patterns, ecology and diversity of symbiotic algae.

Photobiont sharing analyses

Lichen forming-fungi that are highly selective toward photobionts associate with a small number of (or even only one) compatible algal species (e.g. *Psoroglaena stigonemoides* associated with *Auxenochlorella protothecoides*, Nyati *et al.*, 2007). This unique symbiotic association is restricted to the narrow range of the compatible algal pool and is limited to the ecological niche where suitable

photobionts exist (Kroken & Taylor, 2000; Helms *et al.*, 2001; Beck, 2002; Rikkinen, 2003). Conversely, lichen-forming fungi that exhibit a low level of selectivity associate with a wide range of different photobiont partners (Cao *et al.*, 2015; Catalá *et al.*, 2016). Possibly, those mycobionts by the acquisition of various compatible algae with clear environmental preferences expand the ecological niche or increase the fitness of the holobiont (Yahr *et al.*, 2006; Nelsen & Gargas, 2008; Peksa & Škaloud, 2011).

Photobionts seem to be less selective than mycobionts and it has been shown that the same photobiont strain may be shared among various unrelated lichen species with similar ecological requirements (Beck, 1999; Piercey-Normore & DePriest, 2001; Romeike *et al.*, 2002; Wirtz *et al.*, 2003; Yahr *et al.*, 2004; O'Brien *et al.*, 2005; Peksa & Škaloud, 2011). The communities of lichens linked by sharing the same algal lineage and living in the same habitat are known as photobiont mediated lichen guilds (Rikkinen, 2003). A system of lichen guilds has been observed in green algal lichens e.g. *Umbilicaria*, *Lecidella* or *Xanthoria* associated with *Trebouxia* and *Lepraria* or in *Stereocaulon* associated with *Asterochloris;* as well as for cyanobacteria lichens (Beck *et al.*, 1998; Rikkinen, 2002; Peksa & Škaloud, 2011; Hestmark *et al.,* 2016). Recently, Hestmark *et al*. (2016) demonstrated an example of photobiont – mediated lichen guild *sensu* Rikkinen (2003) for two co-occurring lichens (the sexually reproducing *Umbilicaria spodochroa* and mainly vegetatively reproducing *Umbilicaria pustulata*). The authors speculate that *U. pustulata* may serve as a potential 'photobiont donor' for *U. spodochroa*. The latter species, in order to re-establish, would 'pirate' compatible photobiont cells from the symbiotic propagules (isidia) of *U. pustulata*. As it was shown for other lichens, the benefit of being a member of a lichen guild is the permanent availability of compatible photobionts that may be used for relichenization and support survival in a given environment (Piercey-Normore & DePriest, 2001; Piercey-Normore, 2006; O'Brien, 2013; Dal Grande *et al.*, 2014b).

Trebouxia is a generalist symbiont and is able to associate with a broad range of distantly related mycobiont species (Muggia *et al.,* 2017). To find out whether putative photobiont species found in *U. pustulata* are shared with other lichen-forming fungi, I compared nrITS rDNA *Trebouxia* haplotypes with similar sequences available in GenBank (98% identity threshold). Investigation revealed

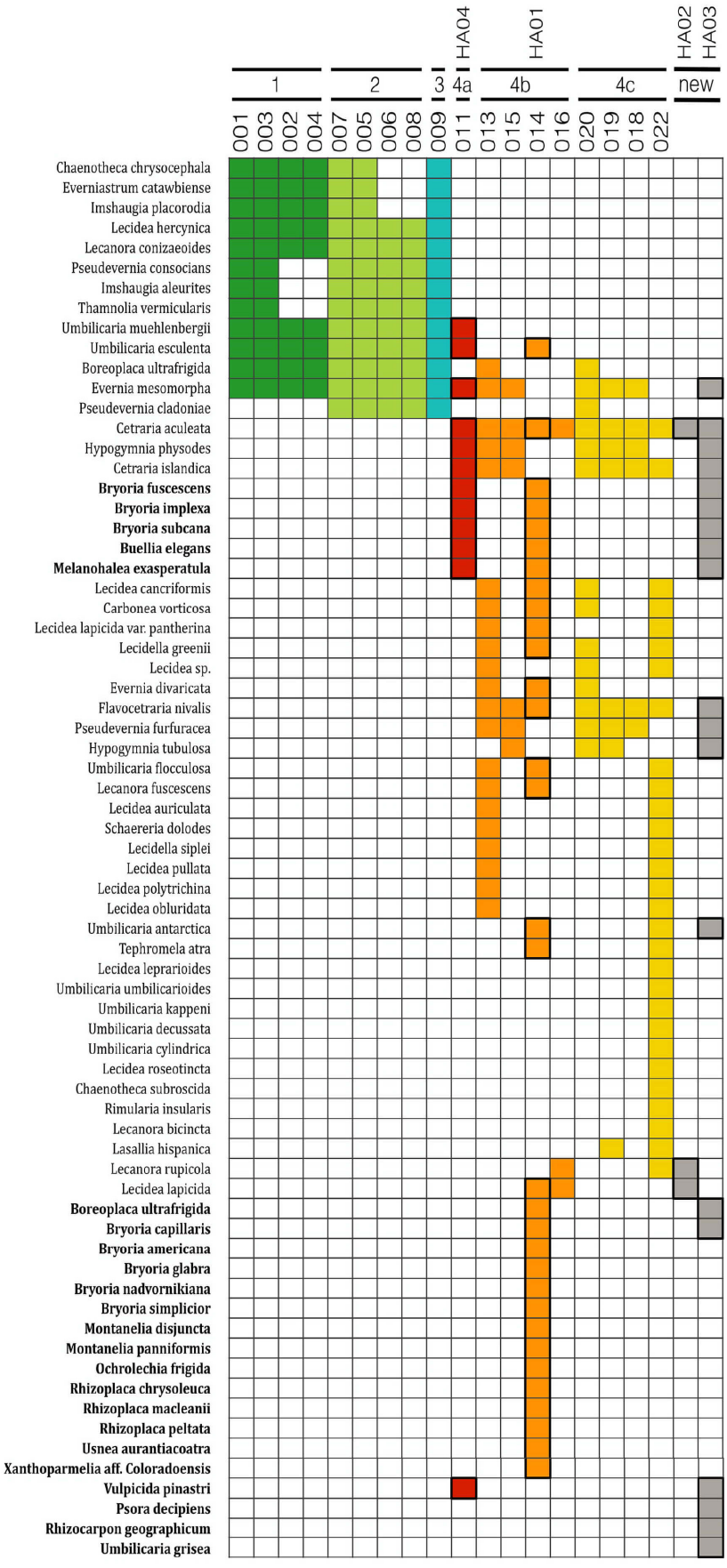

Figure 6. Heatmap showing sharing of photobiont lineages among different species of lichen-forming fungi. Based on 98% ITS rDNA identity. This is an updated analysis following Sadowska-Deś *et al.* (2014). Bold grids and bolded species names indicate additional hits found since the 2014 study. Colors indicate putative *Trebouxia* species. Gray haplotypes are not assigned to any putative species.

47 lichen-forming fungi that share the same photobiont haplotypes as associated with *U. pustulata* (Sadowska-Deś *et al*., 2014). After two years I have updated photobiont sharing analyses by including four nrITS rDNA *Trebouxia* haplotypes found in the altitudinal gradient study on *U. pustulata* (manuscript in preparation). The two haplotypes were new for the dataset. The newly generated heatmap (Figure 6) resulted in an additional 23 lichen species belonging to 10 genera that share at least one algal haplotype as found in *U. pustulata.* One of the putative photobiont species (4a) was initially considered to associate with *U. pustulata* exclusively, however, after heatmap revision, it has been found to associate with 12 other lichen-forming fungi from 8 genera. Different lichens species showed various association patterns, and mainly were divided into two groups of putative algal species, where the first group consists of putative species 1, 2 and 3, and the second group contains putative species 4a, 4b, 4c and possibly two new haplotypes. Only five species of lichen-forming fungi were associated with both groups of *Trebouxia* species. This pattern could be a result of biased sampling represented in GenBank, however, even species with large sample sizes (e.g. *Cetraria aculeata*) associate with specific *Trebouxia* haplotype groups. This, in turn, would suggest strong lichen preferences for the specific photobiont strains. The lichens that were found to associate with the same photobiont lineages as *U. pustulata* exhibit different ecological requirements, and are widely distributed. For instance samples of *Bryoria fuscescens (ncbi* KJ576648), *Melanohalea exasperatula (ncbi* KR914065) or *Tephromela atra* (*ncbi* KJ754231) that share the same haplotype (HA01) from the putative species 4b, come from Finland, Morocco, and New Zealand, respectively. The presented result shows that the low level of selectivity allows *U. pustulata* to associate with an array of photobiont strains and overlap with a range of other lichen-forming fungi.

7.3 Environmental structuring in a lichen symbiosis

Theory predicts that association with environmentally adapted mutualists may increase a holobiont's range and ecological niche (Poisot *et al*., 2011; Hussa & Goodrich-Blair, 2013; Peay, 2016). However, only very few studies exist which use empirical data to test this hypothesis. Those investigations show symbiotic fungi or bacteria that induce niche expansion in plants and invertebrates (Joy,

2013; Giauque & Hawkes, 2013; Afkhami *et al*., 2014; Kazenel *et al*., 2015; Chong & Moran, 2016; Maher *et al*., 2017) or photosynthetic algae that cause environmental zonation in corals and sea anemones (Iglesias-Prieto *et al*., 2004; Mieog *et al*., 2009; Bates *et al*., 2011; Bongaerts *et al*., 2015).

An analogous pattern has been hypothesized also for lichens, where a single lichen-forming fungus may associate with different ecotypes of photobionts across a broad eco-geographic range (Opanowicz & Grube, 2004; Yahr *et al*. 2006; Fernández-Mendoza *et al.*, 2011; Werth & Sork, 2014; Muggia *et al.*, 2014b). Although some studies attempted to explain the genetic variability of lichen symbionts in diverse habitats (Yahr *et al.*, 2006; Werth & Sork, 2010; Peksa & Škaloud, 2011; Singh *et al.*, 2017) or describe this variation based on environmental variables (Fernández-Mendoza *et al*., 2011; Marini *et al.*, 2011; Werth & Sork, 2014), the study presented here is the first that aimed to quantify the lichen symbiont-mediated niche breadth. I demonstrated that geographic distribution of mycobionts and photobionts is strongly connected with changes in the climatic niches. My results support the commonly observed pattern in the lichen symbiosis where generalistic mycobiont broaden its ecological niche by associating with ecologically diversified photobionts. Recently, Vančurová *et al*. (2018) have also focused their study on explaining the lichen climatic niches from the symbionts interaction perspective. Authors investigated the effects of different variables (climate, habitat/substrate and spatial distribution of mycobionts and photobionts) on the distribution of both symbiotic partners of the lichen Stereocaulon. From all tested variables the selection of symbiotic partner was the most significant and the width of the climatic niche of the mycobionts was positively correlated with a number of different symbiotic partners. Moreover, mycobionts found on substrates containing heavy metals associated with toxicity-tolerant photobionts and by this facilitated its persistence in this habitat. The mycobionts which are not highly specific, but which associate with different photobiont ecotypes, potentially expand their distribution range.

To shed light on the concept of mutualist-mediated niche expansion in lichens I quantified individual niche contributions of genetically differentiated symbiotic algae and lichen-forming fungi in the species *Umbilicaria pustulata* across its entire range. I used nrITS rDNA (for photobiont) and *MCM7* (for

mycobiont) sequence markers that revealed the highest intra-population resolution (Sadowska-Deś *et al.*, 2013). Application of two species delimitation approaches - hierarchical clustering of pair-wise genetic distances and ABGD delimitation method revealed similar results. The first approach grouped 42 algal nrITS rDNA haplotypes into 7 clusters. The alternative, ABGD delimitation method, revealed 6 algal OTUs. 11 *MCM7* mycobiont haplotypes were divided into 9 clusters and 7 OTUs. The spatial genetic variability among haplotypes of algal nrITS rDNA showed strong environmental structuring in photobionts. The strongest differentiation between algal haplotypes was found in central Europe, the Mediterranean region, the British Isles and south-eastern Europe. The mycobiont did not show strong spatial structure Reconstructions of the Hutchinsonian climatic niche space of algal OTU clusters indicated that two of the algal OTU clusters (4 and 5) occupied a unique section of the total algal niche space. Cluster 4 pushes the niche space toward the colder and wetter conditions, whereas cluster 5 expands the niche space into the warmer and drier conditions (Figure 7 A, B). Species distribution modeling of these clusters indicates that the potential distribution of members of cluster 4 is in the cooler areas of Europe, while the potential occurrence of members of cluster 5 is predominantly in the Mediterranean region (Figure 7 A, B). Contrarily, the other algal clusters, do not cover unique Hutchinsonian niche space and have a broad potential distribution across the entire range of *U. pustulata*, e.g. algal cluster 1 (Figure 7 C). I interpret this pattern as algal clusters 4 and 5 being specialists for cooler and hotter climatic zones, and the other algal clusters being generalists, inhabiting a variety of environments that are mostly between the climatic extremes favored by 4 and 5. Associating with all of these algal clusters thus allows the *U. pustulata* holobiont to occupy a broader environmental niche and a larger geographic area than associating with only an algal single lineage.

I hypothesize that algal switches occur along the whole distribution range of the generalistic mycobiont and the association with new photobiont ecotypes will take place in characteristic geographic regions i.e. hotspots. The overlap of species distribution models predictions for photobionts and mycobionts revealed a map of interaction hotspots: first hotspot for OTUalg1 – the broadly distributed generalist, second hotspot for OTUalg4 (cold-adapted) in cold regions or higher

altitudes, third hotspot for OTUalg5 (warm-adapted) in Mediterranean regions and in the Canary Islands. This broad-scale switching pattern from generalistic photobiont (OTUalga1) to the warm adapted photobiont (OTUalga5) has been recently detected also in the local-scale study on altitudinal gradient (Dal Grande *et al.*, 2018). The authors demonstrated that the distribution of *Trebouxia* photobionts is shaped by different environmental conditions along the cline.

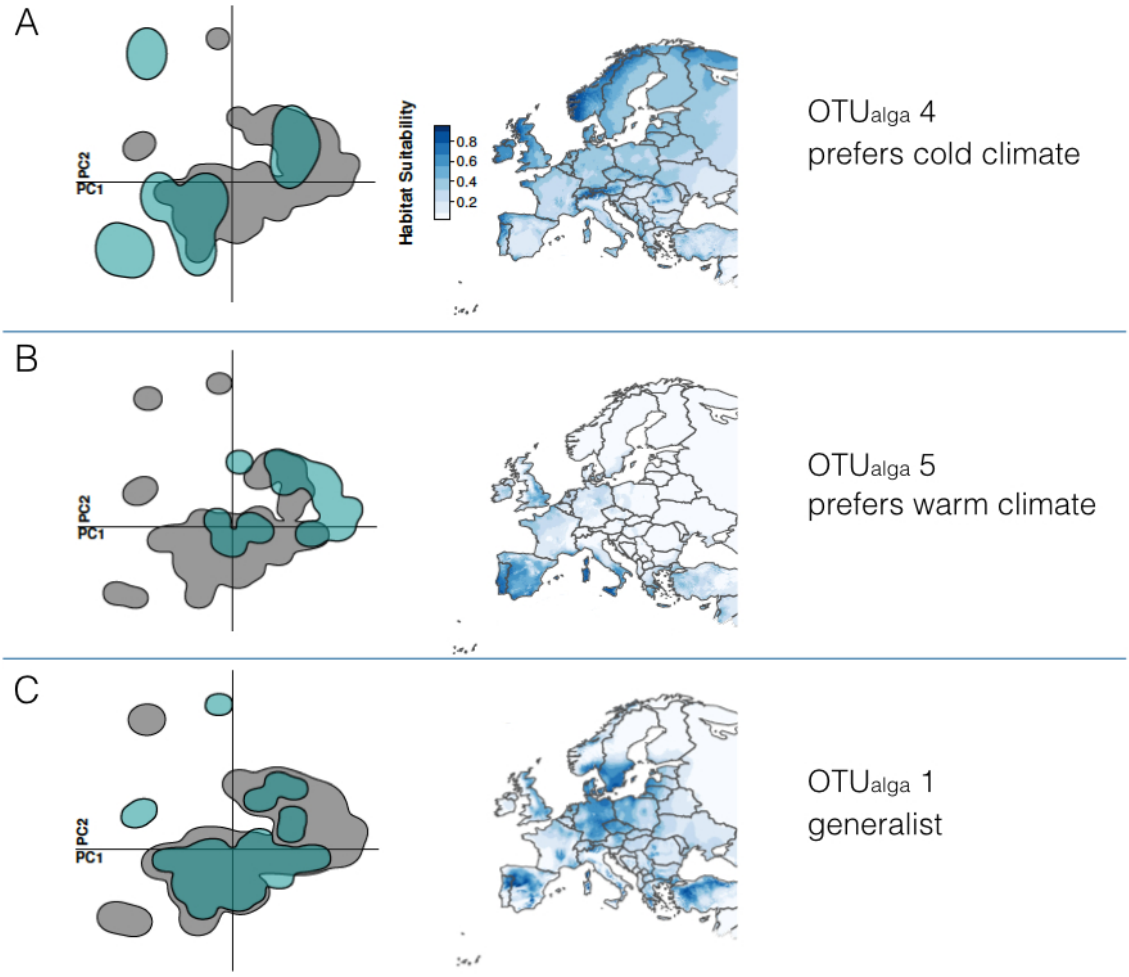

Figure 7. Niche hypervolumes and habitat suitability predictions for *selected Trebouxia* OTUs. Niche hypervolumes of particular algal OTUs (green) are exposed to the niche hypervolumes of all algal OTUs (gray). (A) $OUT_{algal}4$ – ecotype prefers cold, (B) $OTU_{algal}5$ – ecotype prefers warm, (C) $OUT_{algal}1$ – generalist ecotype (based on Rolshausen *et al.*, 2018).

The species distribution models show that photobiont OTUs significantly broaden the niche space of *U. pustulata* in the direction of the colder and warmer climate. The distribution of the lichen-forming fungus was narrower than that of *Trebouxia* alone. Photobiont samples from my dataset included only *Trebouxia* associated with *U. pustulata*. To fully understand the mechanism of local adaptation of lichens photobionts there is a need to examine whole lichen communities associated with same strains of photobionts as in *U. pustulata*. While *Trebouxia* has low specificity towards its mycobionts (Peksa & Škaloud, 2011) it is not possible to discover the entire mechanism without checking other co-occurring lichen species.

On the broad-scale phylogenetic level, the associations between symbionts in lichens are structured in the process of coevolution (DePriest, 2004; Yahr *et al.*, 2004; Miądlikowska *et al.*, 2006; Singh *et al.*, 2017). Two independently evolving species (i.e. lichen-forming fungus and photobiont) associate together and are dependent on each other in their lifestyle (Ahmadjian, 1987; DePriest, 2004). Coevolution involves reciprocal selection pressure in fitness functions between interacting species and leads to a geographic structure that is based on local genotype-by-genotype-by-environment interactions (Thompson, 1999; 2005). The alternative pattern – ecological fitting (Janzen, 1985) is the process of species interaction with a new environment (or host) that seems to indicate the process of coevolution. In fact, those interactions are the results of already existing in the organism relevant traits that evolved in a different environment (Agosta & Klemens, 2008). I suggest that the spatial genetic pattern found in *U. pustulata* confirms the concept of ecological fitting and is coherent with patterns found in other lichen studies at the level of sub-species or population (i.e. Miądlikowska *et al.* 2006; Muggia *et al.* 2014b).

Symbiont exchange in mutualistic associations is a mechanism that may mediate the impact of ongoing climate change. Understanding how symbiotic organisms can cope with stressful global climate change will facilitate our understanding how to protect potentially vulnerable populations (Klanderud & Totland, 2005; Ellis, 2012; Kivlin *et al.*, 2013; Allen & Lendemer, 2016).

Results of the present investigation show that *U. pustulata* broadens its distribution range by association with photobiont partners with specific

environmental preferences. To widen its ecological niche *U. pustulata* switches to different photosynthetic algae. This study facilitates the understanding of lichens adaptive strategies and symbiont-mediated niche expansion in mutualists.

8. SUMMARY

Integration of several methodological approaches, such as testing intraspecific diversity of both lichen symbionts, detecting species boundaries by using novel methods of species delimitation and finding patterns of species distribution along environmental gradients resulted in a comprehensive description of symbiotic interactions between the lichen-forming fungus *Umbilicaria pustulata* and its symbiotic photobiont *Trebouxia*.

This study presents the evaluation of commonly used sequence-based molecular markers that help to recognize unique fungal and algal haplotypes, as well as the number of unique symbiotic pairs (Sadowska-Deś *et al*., 2013; Appendix I). Through testing various loci I presented that the application of a molecular marker with sufficient variability at the species and the sub-species level is a prerequisite for studying symbiont associations, ecological preferences and adaptation mechanisms of lichenized fungi and their photobionts. The selection of genetic markers that provide the highest intra-population resolution facilitated my further investigation on species boundaries within the trebouxioid photobionts of *U. pustulata* (Sadowska-Deś *et al.,* 2014; Appendix II). While phylogenetic relationships of Trebouxiophyceae are poorly understood and the species delimitation of the heterogeneous *Trebouxia* group is not coherent, the broad application of innovative species delimitation methods presented in this study will help to resolve problems of hidden variability and help to unify the taxonomic status of photobionts. Furthermore, the correct assessment of photobiont genotypes is crucial for finding association patterns among unrelated lichen-forming fungi and evaluating patterns of species-to-species and species-to-community interactions. In the present study, the quantification of spatial genetic structure and construction of the climatic niche of both symbiotic partners in *U. pustulata* provided for the first time evidence for symbiont-mediated niche expansion in lichens and supported the hypothesis of photobiont switches as an adaptative strategy for a generalistic lichen-forming fungus to broaden its distributional range (Rolshausen *et al.,* 2018; Appendix III).

The key results of this work are:

1. Intraspecific diversity within both symbionts of *Umbilicaria pustulata* is high. However, the genetic variability of the trebouxioid photobiont is much higher than of the mycobiont (given the tested markers).

2. *U. pustulata* associates with numerous algal species. The application of multifaceted species delimitation approaches based on coalescence, phylogenetic analyses, and anatomical traits yielded congruent results.

3. The geographic distribution of *U. pustulata* – *Trebouxia* interactions pairs is strongly related to changes in the climatic niche. Switches of photobiont partners with specific environmental preferences broaden the range of *U. pustulata*.

9. ACKNOWLEDGEMENTS

I would like to express special thanks to my advisor Imke Schmitt for her superb guidance, scientific support and contribution of time. Thank you for your incredible patience and kindness throughout my doctoral studies.

I am very grateful to Christian Prinzten for his stimulating ideas, help with herbarium collections and for introducing me to the Senckenberg Choir, within which I had the privilege of singing for a couple of semesters. I am also indebted to Wiesław Fałtynowicz who introduced me to the wonderful world of lichens. Thank you for your friendship and for always encouraging me to discover new horizons.

I would like to especially thank Francesco Dal Grande for his motivating and contagious enthusiasm for research as well as his endless patience and amazing talent to pass on knowledge with stoic calm. Thank you for your friendship, help and support throughout my entire project… *Tante grazie!* I am also particularly thankful to Miklós Bálint for his brilliant advice and suggestions for my projects; introducing me to new computing methods, not to mention his friendship and time spent together since my first days in Frankfurt… *Köszönöm!*

Furthermore, I would like to thank Jürgen Otte for generating vast molecular datasets used in my research, for his advice and friendly atmosphere in the lab. I am grateful to Steffen Pauls for his scientific support and suggestions for my project. I am indebted to Andreas Beck for his scientific advice and stimulating conversations on lichen photobionts; also for his invaluable comments on this thesis and his time during my stay in Munich; Thorsten Lumbsch for the inspiring discussions on species delimitation of photobionts and support whilst writing the manuscript; Martin Kukwa for help with proofreading and valuable suggestions.

I would like to thank all my friends I have from the Senckenberg Biodiversity and Climate Research Centre, Frankfurt (BiK-F), especially Anjuli Calchera for her friendly support and comments on an earlier draft of this thesis; Gregor Rolshausen for his invaluable help in the third part of this work, Phillip-André Schmidt for his companionship and the great times that we had together in BiK-f,

and Garima Singh for her friendship and invitations to wonderful Indian dinners (with great Italian espresso – *grazie* Francesco!), at a time when it was really needed… *Dhanyawaad*!

I am grateful Eva-Maria Gerstner and Johan Liakka for their help with analyzing geographic data. I would like to thank Jano Nuñez-Zapata, Raquel Pino-Bodas, Pamela Rodriguez-Flakus and Kasia Szczepańska for the enjoyable time we spent together in Frankfurt. I thank Mercedes Vivas-Rebuelta for wonderful field trips in Spain. Furthermore, I thank Maria Albrecht, Kathrin Gattinger, Katharina Nikolai and Ricarda Prinz for their friendly help from the beginning of my stay in Germany, Jennifer Carrier-Dorman and Declan Delaney for improving the English language of this thesis.

I would also like to acknowledge Oleg Blum, Mahmet Candan, Evgeny Davydov, Pradeep K. Divakar, Eva Farkas, Fernando Fernández Mendoza, Tassilo Feuerer, Martin Grube, Anna Guttová, Volker John, Jiří Liška, László Lökös, Jesus Martinez, Helmut Mayrhofer, Lucia Muggia, Olga Nadyeina, Zdeněk Palice, Svetlana Popova, Tina Randle, Christoph Scheideger, Mohammad Sohrabi, Tobi Spribille, Ave Suija, Einar Timdal, Robert Vogt, Jan Vondrak and Mats Wedin for support in acquiring invaluable lichen material used in this thesis.
I want to thank all my friends from Munich, especially Dragana Bjelan for her permanent support. Special thanks to my best friends, Kasia Pietrzykowska-Urban for standing by me from the very beginning, and Agnieszka Pacyga- Łebek for constant motivation and encouragement.

I would also like to warmly thank my parents, Jadwiga and Zbigniew, for all their endless support and encouragement throughout the entire experience. Your determination to see me and my work succeed is what has sustained me thus far. Thank you for your involvement and time during our wonderful field trips. Especial thanks goes also to my brother Piotr for his encouragement and graphical support.
Most of all, I would like to thank my husband Marcin – thank you for your limitless patience during this (too) long process of completing this thesis. Without you this would simply not be possible! Finally, I would like to thank my children Beniamin and Aurelia for filling my life with new, wonderful energy and love beyond anything.

I am grateful to the Deutsche Bundesstiftung Umwelt (DBU) and the German Academic Exchange Service (DAAD) for the financial support. My PhD project was funded by the research-funding programme “LOEWE – Landes-Offensive zur Entwicklung Wissenschaftlich-ökonomischer Exzellenz” of Hesse’s Ministry of Higher Education, Research, and the Arts.

Thank you,
Dankeschön,
Dziękuję.

10. REFERENCES

Aanen DK, Bisseling T. 2014. The birth of cooperation. *Science* 345: 29–30.

Afkhami ME, McIntyre PJ, Strauss SY. 2014. Mutualist-mediated effects on species' range limits across large geographic scales. *Ecology Letters* 17: 1265–1273.

Agosta SJ, Klemens JA. 2008. Ecological fitting by phenotypically flexible genotypes: implications for species associations, community assembly and evolution. *Ecology Letters* 11: 1123–1134.

Ahmadjian V. 1967. A Guide to the Algae Occurring as Lichen Symbionts: Isolation, Culture, Cultural Physiology, and Identification. *Phycologia* 6: 127–160.

Ahmadjian V. 1987. Coevolution in Lichensa. *Annals of the New York Academy of Sciences* 503: 307–315.

Ahmadjian V. 1993. *The Lichen Symbiosis*. New York, USA: John Wiley & Sons.

Allen JL, Lendemer JC. 2016. Climate change impacts on endemic, high-elevation lichens in a biodiversity hotspot. *Biodiversity and Conservation* 25: 555–568.

Altermann S, Leavitt S, Goward T, Nelsen MP, Lumbsch HT. 2014. How do you solve a problem like *Letharia*? A new look at cryptic species in lichen-forming fungi using bayesian clustering and SNPs from multilocus sequence data. *PLoS ONE* 9: e97556.

Arnaud-Haond S, Alberto F, Teixeira S, Procaccini G, Serrão EA, Duarte CM. 2005. Assessing genetic diversity in clonal organisms: low diversity or low resolution? Combining power and cost efficiency in selecting markers. *The Journal of heredity* 96: 434–440.

Aschenbrenner IA, Cernava T, Berg G, Grube M. 2016. Understanding Microbial Multi-Species Symbioses. *Frontiers in Microbiology* 7.

Asta J, Letrouit-Galinou MA. 1995. Observations on the early growth of *Rhizocarpon geographicum*thalli. *Herzogia* 11: 239–252.

Baird NA, Etter PD, Atwood TS, Currey MC, Shiver AL, Lewis ZA, Selker EU, Cresko WA, Johnson EA. 2008. Rapid SNP discovery and genetic mapping using sequenced RAD markers. *PLoS ONE* 3: e3376.

Bálint M, Domisch S, Engelhardt CHM, Haase P, Lehrian S, Sauer J, Theissinger K, Pauls SU, Nowak C. 2011. Cryptic biodiversity loss linked to global climate change. *Nature Climate Change* 1: 313–318.

Barreno E. 1991. Phytogeography of terricolous lichens in the Iberian Peninsula and the Canary Islands. *Botanika Chronika* 10: 199–210.

Bates ST, Cropsey GWG, Caporaso JG, Knight R, Fierer N. 2011. Bacterial communities associated with the lichen symbiosis. *Applied and Environmental Microbiology* 77:

1309–1314.

Beck A. 1999. Photobiont inventory of a lichen community growing on heavy-metal-rich rock. *The Lichenologist* 31: 501–510.

Beck A. 2002. Photobionts: diversity and selectivity in lichen symbioses. *International lichenological newsletter*: 18–24.

Beck A, Friedl T, Rambold G. 1998. Selectivity of photobiont choice in a defined lichen community: inferences from cultural and molecular studies. *New Phytologist* 139: 709–720.

Beck A, Kasalicky T, Rambold G. 2002. Myco-photobiontal selection in a Mediterranean cryptogam community with *Fulgensia fulgida*. *New Phytologist* 153: 317–326.

Beckett PDRP, Kranner DIC, Minibayeva FV. 2008. Stress physiology and symbiosis. In: Lichen biology, 2nd edn. Cambridge: Cambridge University Press, 136–153.

Bergsten J, Bilton DT, Fujisawa T, Elliott M, Monaghan MT, Balke M, Hendrich L, Geijer J, Herrmann J, Foster GN, *et al.* 2012. The Effect of Geographical Scale of Sampling on DNA Barcoding. *Systematic Biology*: sys037.

Bickford D, Lohman DJ, Sodhi NS, Ng PKL, Meier R, Winker K, Ingram KK, Das I. 2007. Cryptic species as a window on diversity and conservation. *Trends in Ecology & Evolution* 22: 148–155.

Blaha J, Baloch E, Grube M. 2006. High photobiont diversity associated with the euryoecious lichen-forming ascomycete *Lecanora rupicola* (Lecanoraceae, Ascomycota). *Biological Journal of the Linnean Society* 88: 283–293.

Bongaerts P, Carmichael M, Hay KB, Tonk L, Frade PR, Hoegh-Guldberg O. 2015. Prevalent endosymbiont zonation shapes the depth distributions of scleractinian coral species. *Open Science* 2: 140297.

Brandt A, de Vera J-P, Onofri S, Ott S. 2015. Viability of the lichen *Xanthoria elegans* and its symbionts after 18 months of space exposure and simulated Mars conditions on the ISS. *International Journal of Astrobiology* 14: 411–425.

Bright M, Bulgheresi S. 2010. A complex journey: transmission of microbial symbionts. *Nature Reviews Microbiology* 8: 218–230.

Brodie J, Hayes PK, Barker GL, Irvine LM. 1996. Molecular and morphological characters distinguishing two *Porphyra species* (Rhodophyta: Bangiophycidae). *European Journal of Phycology* 31: 303–308.

Brodo IM, Sharnoff SD, Sharnoff S. 2001. *Lichens of North America*. Yale University Press.

Brown SDJ, Collins RA, Boyer S, Lefort M-C, Malumbres-Olarte J, Vink CJ, Cruickshank RH. 2012. Spider: An R package for the analysis of species identity and evolution,

with particular reference to DNA barcoding. *Molecular Ecology Resources* 12: 562–565.

Bruno JF, Stachowicz JJ, Bertness MD. 2003. Inclusion of facilitation into ecological theory. *Trends in Ecology & Evolution* 18: 119–125.

Bubrick P, Galun M, Frensdorff A. 1984. Observations on free-living *Trebouxia* De Puymaly and *Pseudotrebouxia archibald*, and evidence that both symbionts from *Xanthoria parietina* (l.) Th. Fr. can be found free-living in nature. *New Phytologist* 97: 455–462.

Büdel B, Scheidegger C. 2008. Thallus morphology and anatomy. In: Lichen biology, 2nd edn. Cambridge: Cambridge University Press, 40–68.

Buschbom J, Mueller GM. 2006. Testing 'species pair' hypotheses: Evolutionary Ppocesses in the lichen-forming species complex *Porpidia flavocoerulescens* and *Porpidia melinodes*. *Molecular Biology and Evolution* 23: 574–586.

Byler KA, Carmi-Veal M, Fine M, Goulet TL. 2013. Multiple symbiont acquisition strategies as an adaptive mechanism in the coral *Stylophora pistillata*. *PLoS ONE* 8: e59596.

Cáceres ME da S. 2007. *Corticolous crustose and microfoliose lichens of Northeastern Brazil*. IHW-Verlag.

Camargo A, Morando M, Avila LJ, Sites JW Jr. 2012. Species delimitation with ABC and other coalescent-based methods: a test of accuracy with simulations and an empirical example with lizards of the *Liolaemus darwinii* complex (Squamata: Liolaemidae). *Evolution; international journal of organic evolution* 66: 2834–2849.

Cao S, Zhang F, Liu C, Hao Z, Tian Y, Zhu L, Zhou Q. 2015. Distribution patterns of haplotypes for symbionts from *Umbilicaria esculenta* and *U. muehlenbergii* reflect the importance of reproductive strategy in shaping population genetic structure. *BMC Microbiology* 15: 212.

Carbone I, Kohn LM. 1999. A Method for Designing Primer Sets for Speciation Studies in Filamentous Ascomycetes. *Mycologia* 91: 553–556.

Carstens BC, Dewey TA. 2010. Species delimitation using a combined coalescent and information-theoretic approach: An example from North American Myotis bats. *Systematic Biology* 59: 400–414.

Carstens BC, Pelletier TA, Reid NM, Satler JD. 2013. How to fail at species delimitation. *Molecular Ecology* 22: 4369–4383.

Casano LM, del Campo EM, García-Breijo FJ, Reig-Armiñana J, Gasulla F, del Hoyo A, Guéra A, Barreno E. 2011. Two *Trebouxia* algae with different physiological performances are ever-present in lichen thalli of *Ramalina farinacea*. Coexistence versus competition? *Environmental Microbiology* 13: 806–818.

Cassie DM, Piercey-Normore MD. 2008. Dispersal in a sterile lichen-forming fungus, *Thamnolia subuliformis* (Ascomycotina: Icmadophilaceae). *Botany* 86: 751–762.

Catalá S, del Campo EM, Barreno E, García-Breijo FJ, Reig-Armiñana J, Casano LM. 2016. Coordinated ultrastructural and phylogenomic analyses shed light on the hidden phycobiont diversity of *Trebouxia microalgae* in *Ramalina fraxinea*. *Molecular Phylogenetics and Evolution* 94, Part B: 765–777.

Chong RA, Moran NA. 2016. Intraspecific genetic variation in hosts affects regulation of obligate heritable symbionts. *Proceedings of the National Academy of Sciences* 113: 13114–13119.

Conti ME, Cecchetti G. 2001. Biological monitoring: lichens as bioindicators of air pollution assessment — a review. *Environmental Pollution* 114: 471–492.

Corander J, Marttinen P, Sirén J, Tang J. 2008. Enhanced Bayesian modelling in BAPS software for learning genetic structures of populations. *BMC Bioinformatics* 9: 539.

Cordeiro LMC, Reis RA, Cruz LM, Stocker-Wörgötter E, Grube M, Iacomini M. 2005. Molecular studies of photobionts of selected lichens from the coastal vegetation of Brazil. *FEMS Microbiology Ecology* 54: 381–390.

Crespo A, Lumbsch HT. 2010. Cryptic species in lichen-forming fungi. *IMA Fungus : The Global Mycological Journal* 1: 167–170.

Crespo A, Molina MC, Blanco O, Schroeter B, Sancho LG, Hawksworth DL. 2002. rDNA ITS and β-tubulin gene sequence analyses reveal two monophyletic groups within the cosmopolitan lichen *Parmelia saxatilis*. *Mycological Research* 106: 788–795.

Crespo A, Pérez-Ortega S. 2009. Cryptic species and species pairs in lichens: A discussion on the relationship between molecular phylogenies and morphological characters. *Anales del Jardín Botánico de Madrid* 66.

Dal Grande F, Alors D, Divakar PK, Bálint M, Crespo A, Schmitt I. 2014a. Insights into intrathalline genetic diversity of the cosmopolitan lichen symbiotic green alga *Trebouxia decolorans* Ahmadjian using microsatellite markers. *Molecular Phylogenetics and Evolution* 72: 54–60.

Dal Grande F, Beck A, Cornejo C, Singh G, Cheenacharoen S, Nelsen MP, Scheidegger C. 2014b. Molecular phylogeny and symbiotic selectivity of the green algal genus *Dictyochloropsis* s.l. (Trebouxiophyceae): a polyphyletic and widespread group forming photobiont-mediated guilds in the lichen family Lobariaceae. *New Phytologist* 202: 455–470.

Dal Grande FD, Beck A, Singh G, Schmitt I. 2013. Microsatellite primers in the lichen symbiotic alga *Trebouxia decolorans* (Trebouxiophyceae). *Applications in Plant Sciences* 1: 1200400.

Dal Grande F, Rolshausen G, Divakar PK, Crespo A, Otte J, Schleuning M, Schmitt I. 2018. Environment and host identity structure communities of green algal symbionts in lichens. *New Phytologist* 217: 277–289.

Dal Grande F, Sharma R, Meiser A, Rolshausen G, Büdel B, Mishra B, Thines M, Otte J, Pfenninger M, Schmitt I. 2017. Adaptive differentiation coincides with local bioclimatic conditions along an elevational cline in populations of a lichen-forming fungus. *BMC Evolutionary Biology* 17: 93.

Dal Grande F, Widmer I, Beck A, Scheidegger C. 2010. Microsatellite markers for *Dictyochloropsis reticulata* (Trebouxiophyceae), the symbiotic alga of the lichen *Lobaria pulmonaria* (L.). *Conservation Genetics* 11: 1147–1149.

Dal Grande F, Widmer I, Wagner HH, Scheidegger C, Dal Grande F, Widmer I, Wagner HH, Scheidegger C. 2012. Vertical and horizontal photobiont transmission within populations of a lichen symbiosis. *Molecular Ecology*.

Darienko T, Gustavs L, Eggert A, Wolf W, Pröschold T. 2015. Evaluating the species boundaries of green microalgae (Coccomyxa, Trebouxiophyceae, Chlorophyta) using integrative taxonomy and DNA barcoding with further implications for the species identification in nevironmental samples. *PLoS ONE* 10.

Darwin C. 1859. *On the Origin of the Species by Natural Selection*. Murray.

Davydov EA, Peršoh D, Rambold G. 2010. The systematic position of *Umbilicaria caroliniana* (Tuck.) Davydov, Peršoh & Rambold comb. nova and considerations on the generic concept of *Umbilicaria* (Umbilicariaceae, Ascomycota). *Mycological Progress* 9: 261–266.

Davydov EA, Peršoh D, Rambold, G. 2017. Umbilicariaceae (lichenized Ascomycota) – Trait evolution and a new generic concept. *Taxon*, 66 (6), 1282-1303.

De Queiroz K. 2007. Species Concepts and Species Delimitation. *Systematic Biology* 56: 879–886.

Del Campo EM, Casano LM, Gasulla F, Barreno E. 2010a. Suitability of chloroplast LSU rDNA and its diverse group I introns for species recognition and phylogenetic analyses of lichen-forming *Trebouxia* algae. *Molecular Phylogenetics and Evolution* 54: 437–444.

Del Campo EM, Catalá S, Gimeno J, del Hoyo A, Martínez-Alberola F, Casano LM, Grube M, Barreno E. 2013. The genetic structure of the cosmopolitan three-partner lichen *Ramalina farinacea* evidences the concerted diversification of symbionts. *FEMS microbiology ecology* 83: 310–323.

Del Campo EM, Gimeno J, Casano LM, Gasulla F, García-Breijo F, Reig-Armiñana J, Gasulla F, Barreno E. 2010b. South European populations of *Ramalina farinacea* (L.)

Ach. share different *Trebouxia* algae. *Bibliotheca Lichenolgica* 105: 247–256.

Del-Prado R, Blanco O, Lumbsch HT, Divakar PK, Elix JA, Molina MC, Crespo A. 2013. Molecular phylogeny and historical biogeography of the lichen-forming fungal genus Flavoparmelia (Ascomycota: Parmeliaceae). *Taxon* 62: 928–939.

Del-Prado R, Divakar PK, Crespo A. 2011. Using genetic distances in addition to ITS molecular phylogeny to identify potential species in the *Parmotrema reticulatum* complex: a case study. *The Lichenologist* 43: 569–583.

Demchenko E, Mikhailyuk T, Coleman AW, Pröschold T. 2012. Generic and species concepts in *Microglena* (previously the *Chlamydomonas monadina* group) revised using an integrative approach. *European Journal of Phycology* 47: 264–290.

DePriest PT. 1993. Small subunit rDNA variation in a population of lichen fungi due to optional group-I introns. *Gene* 134: 67–74.

DePriest PT. 2004. Early molecular investigations of lichen-forming symbionts: 1986-2001. *Annual Review of Microbiology* 58: 273–301.

Desalle R. 2006. Species discovery versus species identification in DNA barcoding efforts: response to Rubinoff. *Conservation Biology: The Journal of the Society for Conservation Biology* 20: 1545–1547.

Dimijian GG. 2000. Evolving Together: The Biology of Symbiosis, Part 2. *Baylor University Medical Center Proceedings* 13: 381–390.

Dobzhansky T. 1935. A Critique of the Species Concept in Biology. *Philosophy of Science* 2: 344–355.

Doering M, Piercey-Normore MD. 2009. Genetically divergent algae Shape an epiphytic lichen community on Jack Pine in Manitoba. *The Lichenologist* 41: 69–80.

Domaschke S, Fernández-Mendoza F, A. García M, Martín MP, Printzen C. 2012. Low genetic diversity in Antarctic populations of the lichen-forming ascomycete *Cetraria aculeata* and its photobiont. *Polar Research* 31.

Duarte AWF, Passarini MRZ, Delforno TP, Pellizzari FM, Cipro CVZ, Montone RC, Petry MV, Putzke J, Rosa LH, Sette LD. 2016. Yeasts from macroalgae and lichens that inhabit the South Shetland Islands, Antarctica. *Environmental Microbiology Reports* 8: 874–885.

Dupuis JR, Roe AD, Sperling F a. H. 2012. Multi-locus species delimitation in closely related animals and fungi: one marker is not enough. *Molecular Ecology* 21: 4422–4436.

Ellis CJ. 2012. Lichen epiphyte diversity: A species, community and trait-based review. *Perspectives in Plant Ecology, Evolution and Systematics* 14: 131–152.

Ence DD, Carstens BC. 2011. SpedeSTEM: a rapid and accurate method for species

delimitation. *Molecular Ecology Resources* 11: 473–480.

Esselstyn JA, Evans BJ, Sedlock JL, Anwarali Khan FA, Heaney LR. 2012. Single-locus species delimitation: a test of the mixed Yule-coalescent model, with an empirical application to Philippine round-leaf bats. *Proceedings. Biological sciences / The Royal Society* 279: 3678–3686.

Ettl H, Gärtner G. 1995. *Syllabus der Boden-, Luft- und Flechtenalgen*. Springer-Verlag.

Fałtynowicz W, Bylińska E. 1999. *Lasallia pustulata* (L.) Merat. In: Atlas of the geographical distribution of lichens in Poland. Kraków: Instytut Botaniki PAN, 29–33.

Falush D, Stephens M, Pritchard JK. 2003. Inference of population structure using multilocus genotype data: Linked loci and correlated allele frequencies. *Genetics* 164: 1567–1587.

Famà P, Wysor B, Kooistra WHCF, Zuccarello GC. 2002. Molecular Phylogeny Of The Genus *Caulerpa* (Caulerpales,Chlorophyta) Inferred From Chloroplast tufA Gene1. *Journal of Phycology* 38: 1040–1050.

Fawley MW, Fawley KP, Hegewald E. 2011. Taxonomy of *Desmodesmus serratus* (Chlorophyceae, Chlorophyta) and related taxa on the basis of morphological and DNA sequence data. *Phycologia* 50: 23–56.

Fernández-Mendoza F, Domaschke S, Gracia MA, Jordan P, Martin MP, Printzen C. 2011. Population structure of mycobionts and photobionts of the widespread lichen *Cetraria aculeata*. *Molecular Ecology* 20: 1208–1232.

Fontaine KM, Beck A, Stocker-Wörgötter E, Piercey-Normore MD. 2012. Photobiont relationships and phylogenetic history of *Dermatocarpon luridum var. luridum* and related *Dermatocarpon* species. *Plants* 1: 39–60.

Friedl T. 1987. Thallus development and phycobionts of the parasitic lichen *Diploschistes muscorum*. *The Lichenologist* 19: 183–191.

Friedl T, Büdel B. 1996. Photobionts. *Lichen biology, 2nd edn.*: 8–23.

Friedl T, Rokitta C. 1997. Species relationships in the lichen alga *Trebouxia* (Chlorophyta, Trebouxiophyceae): molecular phylogenetic analyses of nuclear-encoded large subunit rRNA gene sequences. *Symbiosis, Philadelphia, Pa. (USA)*.

Fucíková K, Flechtner VR, Lewis LA. 2013. Revision of the genus *Bracteacoccus* Tereg (Chlorophyceae, Chlorophyta) based on a phylogenetic approach. *Nova Hedwigia* 96: 15–59.

Fujisawa T, Barraclough TG. 2013. Delimiting species using single-locus data and the Generalized Mixed Yule Coalescent approach: A revised method and evaluation on simulated data sets. *Systematic biology*.

Fujita MK, Leaché AD, Burbrink FT, McGuire JA, Moritz C. 2012. Coalescent-based

species delimitation in an integrative taxonomy. *Trends in Ecology & Evolution* 27: 480–488.

Futuyma D. 2013. *Evolution*. Sinauer Associates. Sunderland, MA.

Galloway DJ, Aptroot A. 1995. Bipolar lichens: a review. *Cryptogamic botany*: 184–191.

Galun M, Bubrick P. 1984. Physiological interactions between the partners of the lichen symbiosis. In: Linskens PDHF, Heslop-Harrison PDJ, eds. Encyclopedia of Plant Physiology. Cellular Interactions. Springer Berlin Heidelberg, 362–401.

Gargas A, Taylor JW. 1992. Polymerase Chain Reaction (PCR) primers for amplifying and sequencing nuclear 18s rDNA from lichenized fungi. *Mycologia* 84: 589–592.

Garrido-Benavent I, Pérez-Ortega S, de los Ríos A. 2017. From Alaska to Antarctica: Species boundaries and genetic diversity of *Prasiola* (Trebouxiophyceae), a foliose chlorophyte associated with the bipolar lichen-forming fungus *Mastodia tessellata*. *Molecular Phylogenetics and Evolution* 107: 117–131.

Gauslaa Y, Solhaug KA. 2001. Fungal melanins as a sun screen for symbiotic green algae in the lichen *Lobaria pulmonaria*. *Oecologia* 126: 462–471.

Glass NL, Donaldson GC. 1995. Development of primer sets designed for use with the PCR to amplify conserved genes from filamentous ascomycetes. *Appl. Environ. Microbiol.* 61: 1323–1330.

Giauque H, Hawkes CV. 2013. Climate affects symbiotic fungal endophyte diversity and performance. *American Journal of Botany* 100: 1435–1444.

Grube M, Cardinale M, de Castro JV, Müller H, Berg G. 2009. Species-specific structural and functional diversity of bacterial communities in lichen symbioses. *The ISME Journal* 3: 1105–1115.

Grube M, Muggia L. 2010. Identifying algal symbionts in lichen symbioses. In: EUT Edizioni Università di Trieste.

Grube M, Spribille T. 2012. Exploring symbiont management in lichens. *Molecular Ecology* 21: 3098–3099.

Grundt HH, Kjølner S, Borgen L, Rieseberg LH, Brochmann C. 2006. High biological species diversity in the arctic flora. *Proceedings of the National Academy of Sciences of the United States of America* 103: 972–975.

Guiry MD, Guiry GM, 2017. AlgaeBase. World-wide electronic publication, National University of Ireland, Galway. http://www.algaebase.org; searched on 20 February 2018.

Guzow-Krzemińska B. 2006. Photobiont flexibility in the lichen *Protoparmeliopsis muralis* as revealed by ITS rDNA analyses. *The Lichenologist* 38: 469–476.

Guzow-Krzemińska B, Stocker-Wörgötter E. 2013. Development of microsatellite markers

in *Protoparmeliopsis muralis* (lichenized Ascomycete) – a common lichen species. *The Lichenologist* 45: 791–798.

Hafellner J. 1984. Studien in Richtung einer natürlicheren Gliederung der Sammelfamilien Lecanoraceae und Lecideaceae. *Beihefte zur Nova Hedwigia*: 241–371.

Hall JD, Fucikova K, Lo C, Lewis LA, Karol KG. 2010. An assessment of proposed DNA barcodes in freshwater green algae. *Cryptogamie. Algologie* 31: 529–555.

Hallmann C, Stannek L, Fritzlar D, Hause-Reitner D, Friedl T, Hoppert M. 2013. Molecular diversity of phototrophic biofilms on building stone. FEMS Microbiol Ecol 84: 355–72.

Hamilton CA, Hendrixson BE, Brewer MS, Bond JE. 2014. An evaluation of sampling effects on multiple DNA barcoding methods leads to an integrative approach for delimiting species: A case study of the North American tarantula genus *phonopelma*A (Araneae, Mygalomorphae, Theraphosidae). *Molecular Phylogenetics and Evolution* 71: 79–93.

Handa S, Ohmura Y, Nakano T, Nakahara-Tsubota M. 2007. Airborne green microalgae (Chlorophyta) in snowfall. Hikobia, 15, 109-120. *Hikobia*: 109–120.

Harrington RC, Near TJ. 2012. Phylogenetic and coalescent strategies of species delimitation in snubnose darters (Percidae: *Etheostoma*). *Systematic biology* 61: 63–79.

Hausdorf B, Hennig C. 2010. Species delimitation using dominant and codominant multilocus markers. *Systematic biology* 59: 491–503.

Hebert PDN, Penton EH, Burns JM, Janzen DH, Hallwachs W. 2004. Ten species in one: DNA barcoding reveals cryptic species in the neotropical skipper butterfly Astraptes fulgerator. *Proceedings of the National Academy of Sciences of the United States of America* 101: 14812–14817.

Heled J, Drummond AJ. 2010. Bayesian inference of species trees from multilocus data. *Molecular Biology and Evolution* 27: 570–580.

Helms G. 2003. Taxonomy and symbiosis in associations of *Physciaceae* and *Trebouxia*.

Helms G, Friedl T, Rambold G, Mayrhofer H. 2001. Identification of Photobionts from the lichen family Physciaceae using algal-specific ITS rDNA sequencing. *The Lichenologist* 33: 73–86.

Hennig W. 1966. Phylogenetic systematics. University of Illinois Press, Urbana.

Hestmark G. 1992. Sex, size, competition and escape—strategies of reproduction and dispersal in *Lasallia pustulata* (Umbilicariaceae, Ascomycetes). *Oecologia* 92: 305–312.

Hestmark G, Lutzoni F, Miadlikowska J. 2016. Photobiont associations in co-occurring umbilicate lichens with contrasting modes of reproduction in coastal Norway. *The*

Lichenologist 48: 545–557.

Hestmark G, Schroeter B, Kappen L. 1997. Intrathalline and size-dependent patterns of activity in *Lasallia pustulata* and their possible consequences for competitive interactions. 11: 318–322.

Hoef-Emden K. 2012. Pitfalls of establishing DNA barcoding systems in Protists: The Cryptophyceae as a test case. *PLoS ONE* 7: e43652.

Högberg N, Kroken S, Thor G, Taylor JW. 2002. Reproductive mode and genetic variation suggest a North American origin of European *Letharia vulpina*. *Molecular Ecology* 11: 1191–1196.

Holderegger R, Kamm U, Gugerli F. 2006. Adaptive vs. neutral genetic diversity: implications for landscape genetics. *Landscape Ecology* 21: 797–807.

Honegger R. 1986. Ultrastructural studies in lichens. I. Haustorial types and their frequencies in a range of lichens with trebouxioid photobionts. *The New Phytologist* 103: 785–795.

Honegger R. 1998. The lichen symbiosis—what is so spectacular about it? *The Lichenologist* 30: 193–212.

Honegger R, Edwards D, Axe L. 2013. The earliest records of internally stratified cyanobacterial and algal lichens from the Lower Devonian of the Welsh Borderland. *New Phytologist* 197: 264–275.

Huelsenbeck JP, Andolfatto P, Huelsenbeck ET. 2011. Structurama: bayesian inference of population structure. *Evolutionary bioinformatics online* 7: 55–59.

Hussa EA, Goodrich-Blair H. 2013. It takes a village: Ecological and fitness impacts of multipartite mutualism. *Annual Review of Microbiology* 67: 161–178.

Hutchinson GE. 1957. Cold spring harbor symposium on quantitative biology. In: 22. Concluding remarks. 415–427.

Iglesias-Prieto R, Beltran VH, LaJeunesse TC, Reyes-Bonilla H, Thome PE. 2004. Different algal symbionts explain the vertical distribution of dominant reef corals in the eastern Pacific. *Proceedings of the Royal Society of London B: Biological Sciences* 271: 1757–1763.

Ivanova NV, Depriest PT, Bobrova VK, Troitsky AV. 1999. Phylogenetic analysis of the lichen family Umbilicariaceae based on nuclear ITS1 and ITS2 rDNA sequences. *The Lichenologist* 31: 477–489.

Jackson ND, Fahrig L. 2014. Landscape context affects genetic diversity at a much larger spatial extent than population abundance. *Ecology* 95: 871–881.

Jackson HB, Fahrig L. 2015. Are ecologists conducting research at the optimal scale? *Global Ecology and Biogeography* 24: 52–63.

Janzen DH. 1985. On Ecological Fitting.

Jones G, Oxelman B. 2014. DISSECT: an assignment-free Bayesian discovery method for species delimitation under the multispecies coalescent. *bioRxiv*: 3178.

Joy JB. 2013. Symbiosis catalyses niche expansion and diversification. *Proceedings of the Royal Society B: Biological Sciences* 280.

Kazenel MR, Debban CL, Ranelli L, Hendricks WQ, Chung YA, Pendergast TH, Charlton ND, Young CA, Rudgers JA. 2015. A mutualistic endophyte alters the niche dimensions of its host plant. *AoB PLANTS* 7.

Kingman JFC. 2000. Origins of the coalescent: 1974–1982. Genetics 156: 1461–1463.

Keller I, Alexander JM, Holderegger R, Edwards PJ. 2013. Widespread phenotypic and genetic divergence along altitudinal gradients in animals. *Journal of Evolutionary Biology* 26 (12): 2527-2543.

Kivlin SN, Emery SM, Rudgers JA. 2013. Fungal symbionts alter plant responses to global change. *American Journal of Botany* 100: 1445–1457.

Klanderud K, Totland Ø. 2005. Simulated Climate Change Altered Dominance Hierarchies and Diversity of an Alpine Biodiversity Hotspot. *Ecology* 86: 2047–2054.

Knowles LL, Carstens BC. 2007. Delimiting species without monophyletic gene trees. *Systematic biology* 56: 887–895.

Körner C. 2007. The use of 'altitude' in ecological research. *Trends in Ecology & Evolution* 22: 569–574.

Krienitz L, Bock C, Kotut K, Pröschold T. 2012. Genotypic diversity of *Dictyosphaerium*–morphospecies (Chlorellaceae, Trebouxiophyceae) in African inland waters, including the description of four new genera.

Kroken S, Taylor JW. 2000. Phylogenetic Species, Reproductive Mode, and Specificity of the Green Alga *Trebouxia* Forming Lichens with the Fungal Genus Letharia. *The Bryologist* 103: 645–660.

Kubatko LS, Carstens BC, Knowles LL. 2009. STEM: species tree estimation using maximum likelihood for gene trees under coalescence. *Bioinformatics* 25: 971–973.

LaJeunesse TC, Smith R, Walther M, Pinzón J, Pettay DT, McGinley M, Aschaffenburg M, Medina-Rosas P, Cupul-Magaña AL, Pérez AL, *et al.* 2010. Host-symbiont recombination versus natural selection in the response of coral-dinoflagellate symbioses to environmental disturbance. *Proceedings. Biological Sciences / The Royal Society* 277: 2925–2934.

Leavitt SD, Esslinger TL, Spribille T, Divakar PK, Thorsten Lumbsch H. 2013a. Multilocus phylogeny of the lichen-forming fungal genus *Melanohalea* (Parmeliaceae, Ascomycota): Insights on diversity, distributions, and a comparison of species tree

and concatenated topologies. *Molecular Phylogenetics and Evolution* 66: 138–152.

Leavitt S, Fankhauser JD, Leavitt DH, Porter LD, Johnson LA, St Clair LL. 2011a. Complex patterns of speciation in cosmopolitan 'rock posy' lichens - Discovering and delimiting cryptic fungal species in the lichen-forming *Rhizoplaca melanophthalma* species-complex (Lecanoraceae, Ascomycota). *Molecular phylogenetics and evolution* 59: 587–602.

Leavitt SD, Johnson LA, Goward T, St. Clair LL. 2011b. Species delimitation in taxonomically difficult lichen-forming fungi: An example from morphologically and chemically diverse *Xanthoparmelia* (Parmeliaceae) in North America. *Molecular Phylogenetics and Evolution* 60: 317–332.

Leavitt SD, Kraichak E, Nelsen MP, Altermann S, Divakar PK, Alors D, Esslinger TL, Crespo A, Lumbsch T. 2015a. Fungal specificity and selectivity for algae play a major role in determining lichen partnerships across diverse ecogeographic regions in the lichen-forming family Parmeliaceae (Ascomycota). *Molecular Ecology* 24: 3779–3797.

Leavitt SD, Kraichak E, Vondrak J, Nelsen MP, Sohrabi M, Perez-Ortega S, St Clair LL, Lumbsch HT. 2016. Cryptic diversity and symbiont interactions in rock-posy lichens. *Molecular Phylogenetics and Evolution* 99: 261–274.

Leavitt SD, Moreau CS, Lumbsch HT. 2015b. The dynamic discipline of species delimitation: Progress toward effectively recognizing species boundaries in natural populations. In: Upreti DK, Divakar PK, Shukla V, Bajpai R, eds. Recent Advances in Lichenology. Springer India, 11–44.

Leavitt SD, Nelsen MP, Lumbsch HT, Johnson LA, St. Clair LL. 2013b. Symbiont flexibility in subalpine rock shield lichen communities in the Southwestern USA. *The Bryologist* 116: 149–161.

Lefébure T, Douady CJ, Gouy M, Trontelj P, Briolay J, Gibert J. 2006. Phylogeography of a subterranean amphipod reveals cryptic diversity and dynamic evolution in extreme environments. *Molecular Ecology* 15: 1797–1806.

Leliaert F, De Clerck O. 2017. Refining species boundaries in algae. *Journal of Phycology* 53: 12–16.

Leliaert F, Verbruggen H, Vanormelingen P, Steen F, López-Bautista JM, Zuccarello GC, Clerck OD. 2014. DNA-based species delimitation in algae. *European Journal of Phycology* 49: 179–196.

Lewis LA, Flechtner VR. 2004. Cryptic species of *Scenedesmus* (chlorophyta) from desert soil communities of Western North America. *Journal of Phycology* 40: 1127–1137.

Lindblom L, Ekman S. 2006. Genetic variation and population differentiation in the lichen-forming ascomycete *Xanthoria parietina* on the island Storfosna, central Norway.

Molecular Ecology 15: 1545–1559.

Litterski B. 1999. *Pflanzengeographische und ökologische Bewertung der Flechtenflora Mecklenburg-Vorpommerns*. J. Cramer.

Liu YJ, Hall BD. 2004. Body plan evolution of ascomycetes, as inferred from an RNA polymerase II phylogeny. *Proceedings of the National Academy of Sciences of the United States of America* 101: 4507–4512.

Liu L, Yu L, Kubatko L, Pearl DK, Edwards SV. 2009. Coalescent methods for estimating phylogenetic trees. *Molecular Phylogenetics and Evolution* 53: 320–328.

Logares R, Rengefors K, Kremp A, Shalchian-Tabrizi K, Boltovskoy A, Tengs T, Shurtleff A, Klaveness D. 2007. Phenotypically different microalgal morphospecies with identical ribosomal DNA: A case of rapid adaptive evolution? *Microbial Ecology* 53: 549–561.

Longton RE. 1988. *Biology of Polar Bryophytes and Lichens*. CUP Archive.

Lücking R. 2008. Folicolous lichenized fungi. In: Flora Neotropica Monograph. 1–867.

Lücking R, Dal-Forno M, Sikaroodi M, Gillevet PM, Bungartz F, Moncada B, Yánez-Ayabaca A, Chaves JL, Coca LF, Lawrey JD. 2014. A single macrolichen constitutes hundreds of unrecognized species. *Proceedings of the National Academy of Sciences* 111: 11091–11096.

Lumbsch HT, Leavitt SD. 2011. Goodbye morphology? A paradigm shift in the delimitation of species in lichenized fungi. 50: 59–72.

Lundholm N, Moestrup Ø, Kotaki Y, Hoef-Emden K, Scholin C, Miller P. 2006. Inter- and intraspecific variation of the *Pseudo-nitzschia delicatissima* complex (Bacillariophyceae) illustrated by rRNA probes, morphological data and phylogenetic analyses. *Journal of Phycology* 42: 464–481.

Magain N, Forrest LL, Sérusiaux E, Goffinet B. 2010. Microsatellite primers in the *Peltigera dolichorhiza* complex (lichenized ascomycete, Peltigerales). *American Journal of Botany* 97: e102–e104.

Magain N, Miądlikowska J, Goffinet B, Sérusiaux E, Lutzoni F. 2016. Macroevolution of specificity in cyanolichens of the genus *Peltigera* section *Polydactylon* (Lecanoromycetes, Ascomycota). *Systematic Biology* 66: 74–99.

Maher AMD, Asaiyah MAM, Brophy C, Griffin CT. 2017. An Entomopathogenic Nematode Extends Its Niche by Associating with Different Symbionts. *Microbial Ecology* 73: 211–223.

Malavasi V, Škaloud P, Rindi F, Tempesta S, Paoletti M, Pasqualetti M. 2016. DNA-based taxonomy in ecologically versatile microalgae: A re-evaluation of the species concept within the coccoid green algal genus *Coccomyxa* (Trebouxiophyceae, Chlorophyta).

PLOS ONE 11: e0151137.

Manhart JR, McCourt RM. 1992. Molecular data and species concepts in the algae. *Journal of Phycology* 28: 730–737.

Mansournia MR, Wu B, Matsushita N, Hogetsu T. 2012. Genotypic analysis of the foliose lichen *Parmotrema tinctorum* using microsatellite markers: Association of mycobiont and photobiont, and their reproductive modes. *The Lichenologist* 44: 419–440.

Marini L, Nascimbene J, Nimis PL. 2011. Large-scale patterns of epiphytic lichen species richness: Photobiont-dependent response to climate and forest structure. *Science of The Total Environment* 409: 4381–4386.

Martín MP, Winka K, Llimona X, Lumbsch and HT. 2000. Evaluation of morphological variation in the lichen *Diploschistes ocellatus* (Ascomycota, Ostropales): Evidence from nuclear rDNA ITS sequence data. *Plant Biology* 2: 571–578.

Matheny PB, Liu YJ, Ammirati JF, Hall BD. 2002. Using RPB1 sequences to improve phylogenetic inference among mushrooms (*Inocybe*, Agaricales). *American Journal of Botany* 89: 688–698.

Mayden RL. 1997. A hierarchy of species concepts: The denouement in the saga of the species problem. In: Claridge MF, Dawah HA, Wilson MR, eds. Species: The units of diversity. Chapman and Hall, 381–423.

Mayor, J.R., Sanders, N.J., Classen, A.T., Bardgett, R.D., Clément, J.C., Fajardo, A., Lavorel, S., Sundqvist, M.K., Bahn, M., Chisholm, C. and Cieraad, E., 2017. Elevation alters ecosystem properties across temperate treelines globally. Nature 542(7639): 91.

Mayr E. 1982. Of what use are subspecies? *The Auk* 99: 593–595.

McCourt RM, Hoshaw RW. 1990. Noncorrespondence of breeding groups, morphology, and monophyletic groups in *Spirogyra* (Zygnemataceae: Chlorophyta) and the application of species concepts. *Systematic Botany* 15: 69–78.

McCune B. 2000. Lichen communities as indicators of forest health. *The Bryologist* 103: 353–356.

McEvoy M, Solhaug KA, Gauslaa Y. 2007. Solar radiation screening in usnic acid-containing cortices of the lichen *Nephroma arcticum*. *Symbiosis (Rehovot)* 43: 143–150.

Miądlikowska J, Kauff F, Hofstetter V, Fraker E, Grube M, Hafellner J, Reeb V, Hodkinson BP, Kukwa M, Lücking R, *et al.* 2006. New insights into classification and evolution of the Lecanoromycetes (Pezizomycotina, Ascomycota) from phylogenetic analyses of three ribosomal RNA- and two protein-coding genes. *Mycologia* 98: 1088–1103.

Mieog JC, Van Oppen MJH, Berkelmans R, Stam WT, Olsen JL. 2009. Quantification of

algal endosymbionts (*Symbiodinium*) in coral tissue using real-time PCR. *Molecular Ecology Resources* 9: 74–82.

Miralles A, Vences M. 2013. New metrics for comparison of taxonomies reveal striking discrepancies among species delimitation methods in *Madascincus* lizards. *PLOS ONE* 8: e68242.

Molins A, Moya P, García-Breijo FJ, Reig-Armiñana J, Barreno E. 2018. A multi-tool approach to assess microalgal diversity in lichens: isolation, Sanger sequencing, HTS and ultrastructural correlations. *The Lichenologist* 50: 123–138.

Montecinos AE, Couceiro L, Peters AF, Desrut A, Valero M, Guillemin M-L. 2017. Species delimitation and phylogeographic analyses in the *Ectocarpus* subgroup *siliculosi* (Ectocarpales, Phaeophyceae). *Journal of Phycology* 53: 17–31.

Moon-van der Staay SY, De Wachter R, Vaulot D. 2001. Oceanic 18S rDNA sequences from picoplankton reveal unsuspected eukaryotic diversity. *Nature* 409: 607–610.

Moran NA. 2007. Symbiosis as an adaptive process and source of phenotypic complexity. *Proceedings of the National Academy of Sciences* 104: 8627–8633.

Morgante M, Olivieri A m. 1993. PCR-amplified microsatellites as markers in plant genetics. *The Plant Journal* 3: 175–182.

Moya P, Chiva S, Molins A, Jadrna I, Skaloud P, Peksa O, Barreno E. 2018. *Myrmecia israeliensis* as the primary symbiotic microalga in squamulose lichens growing in European and Canary Island terricolous communities. *Fottea* 18: 72–85.

Moya P, Molins A, Martínez-Alberola F, Muggia L, Barreno E. 2017. Unexpected associated microalgal diversity in the lichen *Ramalina farinacea* is uncovered by pyrosequencing analyses. *PLOS ONE* 12: e0175091.

Moya P, Škaloud P, Chiva S, Reig-Armiñana, Barreno E, Vančurová L, García-Breijo FJ. 2015. Molecular phylogeny and ultrastructure of the lichen microalga *Asterochloris mediterranea* sp. nov. from Mediterranean and Canary Islands ecosystems. *International Journal of Systematic and Evolutionary Microbiology* 65: 1838–1854.

Muggia L, Baloch E, Stabentheiner E, Grube M, Wedin M. 2011. Photobiont association and genetic diversity of the optionally lichenized fungus *Schizoxylon albescens*. *FEMS Microbiology Ecology* 75: 255–272.

Muggia L, Candotto-Carniel F, Grube M. 2017. The Lichen Photobiont Trebouxia: Towards and Appreciation of Species Diversity and Molecular Studies. In: Algal and Cyanobacteria Symbioses. WORLD SCIENTIFIC (EUROPE), 111–146.

Muggia L, Grube M, Tretiach M. 2008. Genetic diversity and photobiont associations in selected taxa of the *Tephromela atra* group (Lecanorales, lichenised Ascomycota). *Mycological Progress* 7: 147–160.

Muggia L, Leavitt S, Barreno E. 2018. The hidden diversity of lichenised Trebouxiophyceae (Chlorophyta). *Phycologia* 57: 503–524.

Muggia L, Pérez-Ortega S, Fryday A, Spribille T, Grube M. 2014a. Global assessment of genetic variation and phenotypic plasticity in the lichen-forming species *Tephromela atra*. *Fungal Diversity* 64: 233–251.

Muggia L, Pérez-Ortega S, Kopun T, Zellnig G, Grube M. 2014b. Photobiont selectivity leads to ecological tolerance and evolutionary divergence in a polymorphic complex of lichenized fungi. *Annals of Botany* 114: 463–475.

Muggia L, Vancurova L, Škaloud P, Peksa O, Wedin M, Grube M. 2013. The symbiotic playground of lichen thalli – a highly flexible photobiont association in rock-inhabiting lichens. *FEMS Microbiology Ecology* 85: 313–323.

Mukhtar A, Garty J, Galun M. 1994. Does the lichen alga *Trebouxia* occur free-living in nature: further immunological evidence. *Symbiosis* 17: 247–253.

Myllys L, Stenroos S, Thell A. 2002. New Genes for Phylogenetic Studies of Lichenized Fungi: Glyceraldehyde-3-Phosphate Dehydrogenase and Beta-Tubulin Genes. *The Lichenologist* 34: 237–246.

Nadyeina O, Cornejo C, Boluda CG, Myllys L, Rico VJ, Crespo A, Scheidegger C. 2014. Characterization of microsatellite loci in lichen-forming fungi of *Bryoria* section *Implexae* (Parmeliaceae). *Applications in Plant Sciences* 2: 1400037.

Nash TH. 2008. *Lichen Biology*. Cambridge University Press.

Nelsen MP, Gargas A. 2008. Dissociation and horizontal transmission of codispersing lichen symbionts in the genus *Lepraria* (Lecanorales: Stereocaulaceae). *New Phytologist* 177: 264–275.

Nelsen MP, Gargas A. 2009. Symbiont flexibility in *Thamnolia vermicularis* (Pertusariales: Icmadophilaceae). *The Bryologist* 112: 404–417.

Niu Y., Wei J. 1993. Variations in ITS sequences of nuclear nrDNA from two *Lasallia* species and their systematic significance. *Mycosystema* 6: 25–29.

Núñez-Zapata J, Divakar PK, Del-Prado R, Cubas P, Hawksworth DL, Crespo A. 2011. Conundrums in species concepts: the discovery of a new cryptic species segregated from *Parmelina tiliacea* (Ascomycota: Parmeliaceae). *The Lichenologist* 43: 603–616.

Nyati S, Beck A, Honegger R. 2007. Fine structure and phylogeny of green algal photobionts in the microfilamentous genus *Psoroglaena* (Verrucariaceae, lichen-forming ascomycetes). *Plant Biology* 9: 390–399.

O'Brien H. 2013. A preliminary look at host association patterns in *Trebouxia*. *PhotobiontDiversity.wordpress.com*.

O'Brien HE, Miadlikowska J, Lutzoni F. 2005. Assessing host specialization in symbiotic

cyanobacteria associated with four closely related species of the lichen fungus Peltigera. *European Journal of Phycology* 40: 363–378.

O'Brien HE, Parrent JL, Jackson JA, Moncalvo J-M, Vilgalys R. 2005. Fungal community analysis by large-scale sequencing of environmental samples. *Applied and Environmental Microbiology* 71: 5544–5550.

Ohmura Y, Kawachi M, Kasai F, Watanabe MM, Takeshita S. 2006. Genetic combinations of symbionts in a vegetatively reproducing lichen, *Parmotrema tinctorum*, based on ITS rDNA sequences. *The Bryologist* 109: 43–59.

Onuț-Brännström I, Benjamin M, Scofield DG, Heiḥmarsson S, Andersson MG, Lindström ES, Johannesson H. 2018. Sharing of photobionts in sympatric populations of *Thamnolia* and *Cetraria* lichens: evidence from high-throughput sequencing. *Scientific reports* 8: 4406.

O'Meara BC. 2010. New heuristic methods for joint species delimitation and species tree inference. *Systematic biology* 59: 59–73.

Opanowicz M, Grube M. 2004. Photobiont genetic variation in *Flavocetraria nivalis* from Poland (Parmeliaceae, lichenized Ascomycota). *Lichenologist The* 36: 125–131.

Osyczka P, Rola K, Lenart-Boroń A, Boroń P. 2014. High intraspecific genetic and morphological variation in the pioneer lichen *Cladonia rei* colonising slag dumps. *Open Life Sciences* 9: 579–591.

Ott S. 1987. Sexual reproduction and developmental adaptations in *Xanthoria parietina*. *Nordic Journal of Botany* 7: 219–228.

Palmer TM, Stanton ML, Young TP. 2003. Competition and coexistence: Exploring mechanisms that restrict and maintain diversity within mutualist guilds. *The American Naturalist* 162: S63–S79.

Parker PG, Snow AA, Schug MD, Booton GC, Fuerst PA. 1998. What molecules can tell us about populations: choosing andusing a molecular marker. *Ecology* 79: 361–382.

Paul F, Otte J, Schmitt I, Grande FD. 2018. Comparing Sanger sequencing and high-throughput metabarcoding for inferring photobiont diversity in lichens. *Scientific Reports* 8: 8624.

Pauls SU, Nowak C, Bálint M, Pfenninger M. 2013. The impact of global climate change on genetic diversity within populations and species. *Molecular Ecology* 22: 925–946.

Payo DA, Leliaert F, Verbruggen H, D'hondt S, Calumpong HP, Clerck OD. 2013. Extensive cryptic species diversity and fine-scale endemism in the marine red alga *Portieria* in the Philippines. *Proc. R. Soc. B* 280: 20122660.

Peay KG. 2016. The mutualistic niche: Mycorrhizal symbiosis and community dynamics. *Annual Review of Ecology, Evolution, and Systematics* 47: 143–164.

Peksa O, Škaloud P. 2011. Do photobionts influence the ecology of lichens? A case study of environmental preferences in symbiotic green alga *Asterochloris* (Trebouxiophyceae). *Molecular ecology* 20: 3936–3948.

Pérez-Ortega S, Ortiz-Álvarez R, Green TGA, Ríos A de los. 2012. Lichen myco- and photobiont diversity and their relationships at the edge of life (McMurdo Dry Valleys, Antarctica). *FEMS Microbiology Ecology* 82: 429–448.

Peterson AT. 2011. *Ecological Niches and Geographic Distributions (MPB-49)*. Princeton University Press.

Pfenninger M, Schwenk K. 2007. Cryptic animal species are homogeneously distributed among taxa and biogeographical regions. *BMC Evolutionary Biology* 7: 121.

Pianka ER. 2011. *Evolutionary Ecology*. Eric R. Pianka.

Piercey-Normore MD. 2004. Selection of algal genotypes by three species of lichen fungi in the genus *Cladonia*. *Canadian Journal of Botany* 82: 947–961.

Piercey-Normore MD. 2005. Lichens from the Hudson Bay Lowlands: northeastern coastal regions of Wapusk National Park in Manitoba. *Canadian Journal of Botany* 83: 1029–1038.

Piercey-Normore MD. 2006. The lichen-forming ascomycete *Evernia mesomorpha* associates with multiple genotypes of *Trebouxia jamesii*. *New Phytologist* 169: 331–344.

Piercey-Normore M. 2009. Vegetatively reproducing fungi in three genera of the Parmeliaceae share divergent algal partners. *The Bryologist* 112: 773–785.

Piercey-Normore MD, DePriest PT. 2001. Algal switching among lichen symbioses. *American Journal of Botany* 88: 1490–1498.

Piganeau G, Eyre-Walker A, Grimsley N, Moreau H. 2011. How and why DNA barcodes underestimate the diversity of microbial eukaryotes. *PLoS ONE* 6: e16342.

Pino-Bodas R, Burgaz AR, Martín MP, Lumbsch HT. 2012. Species delimitations in the *Cladonia cariosa* group (Cladoniaceae, Ascomycota). *The Lichenologist* 44: 121–135.

Pita L, Fraune S, Hentschel U. 2016. Emerging sponge models of animal-microbe symbioses. *Frontiers in Microbiology* 7.

Poelt, J, 1962. Bestimmungsschlüssel der Höheren Flechten von Europa. Mitt. Bot. Staatssamml. München 4: 301–571.

Poisot T, Bever JD, Nemri A, Thrall PH, Hochberg ME. 2011. A conceptual framework for the evolution of ecological specialisation. *Ecology Letters* 14: 841–851.

Pons J, Barraclough TG, Gomez-Zurita J, Cardoso A, Duran DP, Hazell S, Kamoun S, Sumlin WD, Vogler AP. 2006. Sequence-based species delimitation for the DNA taxonomy of undescribed insects. *Systematic biology* 55: 595–609.

Printzen C. 2002. Fungal specific primers for PCR-amplification of mitochondrial LSU in lichens. *Molecular Ecology Notes* 2: 130–132.

Printzen C, Domaschke S, Fernández-Mendoza F, Pérez-Ortega S. 2013. Biogeography and ecology of *Cetraria aculeata*, a widely distributed lichen with a bipolar distribution. *MycoKeys* 6: 33–53.

Printzen C, Ekman S, Tønsberg T. 2003. Phylogeography of *Cavernularia hultenii*: evidence of slow genetic drift in a widely disjunct lichen. *Molecular Ecology* 12: 1473–1486.

Pritchard JK, Stephens M, Donnelly P. 2000. Inference of population structure using multilocus genotype data. *Genetics* 155: 945–959.

Provan J, Bennett KD. 2008. Phylogeographic insights into cryptic glacial refugia. *Trends in Ecology & Evolution* 23: 564–571.

Pröschold T, Darienko T, Silva PC, Reisser W, Krienitz L. 2011. The systematics of *Zoochlorella* revisited employing an integrative approach. *Environmental Microbiology* 13: 350–364.

Puillandre N, Modica MV, Zhang Y, Sirovich L, Boisselier M-C, Cruaud C, Holford M, Samadi S. 2012. Large-scale species delimitation method for hyperdiverse groups. *Molecular ecology* 21: 2671–2691.

Pulliam H r. 2000. On the relationship between niche and distribution. *Ecology Letters* 3: 349–361.

Purvis OW. 1997. The species concept in lichens. *SYSTEMATICS ASSOCIATION* 54: 109–134.

Rambold G, Friedl T, Beck A. 1998. Photobionts in lichens: Possible indicators of phylogenetic relationships? *The Bryologist* 101: 392–397.

Raxworthy CJ, Ingram CM, Rabibisoa N, Pearson RG, Weins J. 2007. Applications of ecological niche modeling for species delimitation: A review and empirical evaluation using day geckos (*Phelsuma*) from Madagascar. *Systematic Biology* 56: 907–923.

Rehner SA. 2001. Primers for Elongation Factor 1-alpha (EF1-alpha). *http://www.aftol.org/pdfs/EF1primer.pdf.*

Ridley M. 1989. The cladistic solution to the species problem. Biol. Philos. 4: 1–16.

Rikkinen J. 2002. Lichen guilds share related cyanobacterial symbionts. *Science* 297: 357–357.

Rikkinen, J., 2003. Ecological and evolutionary role of photobiont-mediated guilds in lichens. *Symbiosis*, *34*: 99-110.

Rindi F, Guiry MD. 2002. Diversity, life history, and ecology of *Trentepohlia* and *Printzina* (Trentepohliales, Chlorophyta) in urban habitats in western Ireland. *Journal of*

Phycology 38: 39–54.

Rodriguez RJ, Henson J, Van Volkenburgh E, Hoy M, Wright L, Beckwith F, Kim Y-O, Redman RS. 2008. Stress tolerance in plants via habitat-adapted symbiosis. *The ISME journal* 2: 404–416.

Rodriguez-Cabal MA, Barrios-Garcia MN, Nuñez MA. 2012. Positive interactions in ecology: filling the fundamental niche. *Ideas in Ecology and Evolution* 5.

Rolshausen G, Grande FD, Sadowska-Deś AD, Otte J, Schmitt I. 2018. Quantifying the climatic niche of symbiont partners in a lichen symbiosis indicates mutualist-mediated niche expansions. *Ecography* 41: 1380–1392.

Romeike J, Friedl T, Helms G, Ott S. 2002. Genetic diversity of algal and fungal partners in four species of *Umbilicaria* (lichenized Ascomycetes) along a transect of the Antarctic Peninsula. *Molecular Biology and Evolution* 19: 1209–1217.

Rowan R. 2004. Coral bleaching: Thermal adaptation in reef coral symbionts. *Nature* 430: 742–742.

Rudi K, Skulberg OM, Jakobsen KS. 1998. Evolution of Cyanobacteria by Exchange of Genetic Material among Phyletically Related Strains. *Journal of Bacteriology* 180: 3453–3461.

Ruiz-Sanchez E, Sosa V. 2010. Delimiting species boundaries within the Neotropical bamboo *Otatea* (Poaceae: Bambusoideae) using molecular, morphological and ecological data. *Molecular Phylogenetics and Evolution* 54: 344–356.

Ruprecht U, Brunauer G, Printzen C. 2012. Genetic diversity of photobionts in Antarctic lecideoid lichens from an ecological view point. *The Lichenologist* 44: 661–678.

Rybalka N, Andersen RA, Kostikov I, Mohr KI, Massalski A, Olech M, Friedl T. 2009. Testing for endemism, genotypic diversity and species concepts in Antarctic terrestrial microalgae of the Tribonemataceae (Stramenopiles, Xanthophyceae). *Environmental Microbiology* 11: 554–565.

Sadowska-Deś AD, Bálint M, Otte J, Schmitt I. 2013. Assessing intraspecific diversity in a lichen-forming fungus and its green algal symbiont: Evaluation of eight molecular markers. *Fungal Ecology* 6: 141–151.

Sadowska-Deś AD, Dal Grande F, Lumbsch HT, Beck A, Otte J, Hur J-S, Kim JA, Schmitt I. 2014. Integrating coalescent and phylogenetic approaches to delimit species in the lichen photobiont *Trebouxia*. *Molecular Phylogenetics and Evolution* 76: 202–210.

Sanders WB. 2005. Observing microscopic phases of lichen life cycles on transparent substrata placed in situ. *The Lichenologist* 37: 373–382.

Sanders WB. 2010. Together and separate: reconstructing life histories of lichen symbionts. *Bibliotheca Lichenologica* 105: 1–16.

Sanger F, Nicklen S, Coulson AR. 1977. DNA sequencing with chain-terminating inhibitors. *Proceedings of the National Academy of Sciences* 74: 5463–5467.

Saunders GW, Kucera H. 2010. An evaluation of rbcL, tufA, UPA, LSU and ITS as DNA barcode markers for the marine green macroalgae. *Cryptogamie. Algologie* 31: 487–528.

Scheidegger C, Schroeter B, Frey B. 1995. Structural and functional processes during water vapour uptake and desiccation in selected lichens with green algal photobionts. *Planta* 197: 399–409.

Schlensog M, Schroeter B, Green T. 2000. Water dependent photosynthetic activity of lichens from New Zealand: differences in the green algal and the cyanobacterial thallus parts of photosymbiodemes. *Bibliotheca Lichenologica* 75: 149–160.

Schmitt I, Crespo A, Divakar PK, Fankhauser JD, Herman-Sackett E, Kalb K, Nelsen MP, Nelson NA, Rivas-Plata E, Shimp AD, *et al.* 2009a. New primers for promising single-copy genes in fungal phylogenetics and systematics. *Persoonia* 23: 35–40.

Schmitt I, Prado R del, Grube M, Lumbsch HT. 2009b. Repeated evolution of closed fruiting bodies is linked to ascoma development in the largest group of lichenized fungi (Lecanoromycetes, Ascomycota). *Molecular Phylogenetics and Evolution* 52: 34–44.

Schoch CL, Seifert KA, Huhndorf S, Robert V, Spouge JL, Levesque CA, Chen W, Bolchacova E, Voigt K, Crous PW, *et al.* 2012. Nuclear Ribosomal Internal Transcribed Spacer (ITS) Region as a Universal DNA Barcode Marker for Fungi. *Proceedings of the National Academy of Sciences*.

Shokralla S, Spall JL, Gibson JF, Hajibabaei M. 2012. Next-generation sequencing technologies for environmental DNA research. *Molecular Ecology* 21: 1794–1805.

Simon UK, Weiß M. 2008. Intragenomic variation of fungal ribosomal genes is higher than previously thought. *Molecular Biology and Evolution* 25: 2251–2254.

Singh G, Dal Grande F, Divakar PK, Otte J, Crespo A, Schmitt I. 2017. Fungal–algal association patterns in lichen symbiosis linked to macroclimate. *New Phytologist* 214: 317–329.

Singh G, Dal Grande F, Divakar PK, Otte J, Leavitt SD, Szczepanska K, Crespo A, Rico VJ, Aptroot A, Cáceres ME da S, *et al.* 2015. Coalescent-based species delimitation approach uncovers high cryptic diversity in the dosmopolitan lichen-forming fungal genus *Protoparmelia* (Lecanorales, Ascomycota). *PLoS ONE* 10: e0124625.

Škaloud P, Peksa O. 2010. Evolutionary inferences based on ITS rDNA and actin sequences reveal extensive diversity of the common lichen alga *Asterochloris* (Trebouxiophyceae, Chlorophyta). *Molecular phylogenetics and evolution* 54: 36–46.

Škaloud P, Steinová J, Řídká T, Vančurová L, Peksa O. 2015. Assembling the challenging puzzle of algal biodiversity: species delimitation within the genus *Asterochloris* (Trebouxiophyceae, Chlorophyta). *Journal of Phycology*: 51.3:507-527.

Sork VL, Werth S. 2014. Phylogeography of *Ramalina menziesii*, a widely distributed lichen-forming fungus in western North America. *Molecular Ecology* 23: 2326–2339.

Spribille T, Klug B, Mayrhofer H. 2011. A phylogenetic analysis of the boreal lichen *Mycoblastus sanguinarius* (Mycoblastaceae, lichenized Ascomycota) reveals cryptic clades correlated with fatty acid profiles. *Molecular Phylogenetics and Evolution* 59: 603–614.

Spribille T, Tuovinen V, Resl P, Vanderpool D, Wolinski H, Aime MC, Schneider K, Stabentheiner E, Toome-Heller M, Thor G, *et al.* 2016. Basidiomycete yeasts in the cortex of ascomycete macrolichens. *Science* 353: 488–492.

Stiller JW, Hall BD. 1997. The origin of red algae: Implications for plastid evolution. *Proceedings of the National Academy of Sciences* 94: 4520–4525.

Sung G-H, Sung J-M, Hywel-Jones NL, Spatafora JW. 2007. A multi-gene phylogeny of Clavicipitaceae (Ascomycota, Fungi): Identification of localized incongruence using a combinational bootstrap approach. *Molecular Phylogenetics and Evolution* 44: 1204–1223.

Talavera G, Dincă V, Vila R. 2013. Factors affecting species delimitations with the GMYC model: insights from a butterfly survey. *Methods in Ecology and Evolution* 4: 1101–1110.

Taylor JW, Jacobson DJ, Kroken S, Kasuga T, Geiser DM, Hibbett DS, Fisher MC. 2000. Phylogenetic species recognition and species concepts in fungi. *Fungal genetics and biology: FG & B* 31: 21–32.

Thompson JN. 1999. Specific Hypotheses on the Geographic Mosaic of Coevolution. *The American Naturalist* 153: S1–S14.

Thompson JN. 2005. *The Geographic Mosaic of Coevolution*. University of Chicago Press.

Tronholm A, Leliaert F, Sansón M, Afonso-Carrillo J, Tyberghein L, Verbruggen H, De Clerck O. 2012. Contrasting geographical distributions as a result of thermal tolerance and long-distance dispersal in two allegedly widespread tropical brown algae. *PLoS ONE* 7: e30813.

Tschermak-Woess E. 1988. New and known taxa of *Chlorella* (Chlorophyceae): Occurrence as lichen phycobionts and observations on living dictyosomes. *Plant Systematics and Evolution* 159: 123–139.

Turner S, Pryer KM, Miao VPW, Palmer JD. 1999. Investigating Deep Phylogenetic

Relationships among Cyanobacteria and Plastids by Small Subunit rRNA Sequence Analysis1. *Journal of Eukaryotic Microbiology* 46: 327–338.

U'Ren JM, Lutzoni F, Miadlikowska J, Laetsch AD, Arnold AE. 2012. Host and geographic structure of endophytic and endolichenic fungi at a continental scale. *American Journal of Botany* 99: 898–914.

Vančurová L, Muggia L, Peksa O, Řídká T, Škaloud P. 2018. The complexity of symbiotic interactions influences the ecological amplitude of the host: A case study in Stereocaulon (lichenized Ascomycota). *Molecular Ecology* 27: 3016–3033.

Van Oppen MJH, Klerk H, Olsen JL, Stam WT. 1996. Hidden diversity in marine algae: some examples of genetic variation below the species level. *Journal of the Marine Biological Association of the United Kingdom* 76: 239–242.

Vargas Castillo R, Beck A. 2012. Photobiont selectivity and specificity in *Caloplaca* species in a fog-induced community in the Atacama Desert, northern Chile. *Fungal Biology* 116: 665–676.

Vargas C de, Norris R, Zaninetti L, Gibb SW, Pawlowski J. 1999. Molecular evidence of cryptic speciation in planktonic foraminifers and their relation to oceanic provinces. *Proceedings of the National Academy of Sciences* 96: 2864–2868.

de Vera J-P, Schulze-Makuch D, Khan A, Lorek A, Koncz A, Möhlmann D, Spohn T. 2014. Adaptation of an Antarctic lichen to Martian niche conditions can occur within 34 days. *Planetary and Space Science* 98: 182–190.

Verbruggen H. 2014. Morphological complexity, plasticity, and species diagnosability in the application of old species names in DNA-based taxonomies. *Journal of Phycology* 50: 26–31.

Verbruggen H, Leliaert F, Maggs CA, Shimada S, Schils T, Provan J, Booth D, Murphy S, De Clerck O, Littler DS, *et al.* 2007. Species boundaries and phylogenetic relationships within the green algal genus *Codium* (Bryopsidales) based on plastid DNA sequences. *Molecular Phylogenetics and Evolution* 44: 240–254.

Vilgalys R, Hester M. 1990. Rapid genetic identification and mapping of enzymatically amplified ribosomal DNA from several *Cryptococcus* species. *Journal of Bacteriology* 172: 4238–4246.

Vobis G, Hawksworth DL. 1981. Conidial lichen-forming fungi. In: Biology of conidial fungi. Elsevier, 245–273.

Victor BC. 2015. How many coral reef fish species are there? Cryptic diversity and the new molecular taxonomy. In: Ecology of Fishes on Coral Reefs. Cambridge University Press, Cambridge, United Kingdom, 76–87.

Vondrák J, Říha P, Arup U, Søchting U. 2009. The taxonomy of the *Caloplaca citrina*

group (Teloschistaceae) in the Black Sea region; with contributions to the cryptic species concept in lichenology. *The Lichenologist* 41: 571–604.

Voytsekhovich A, Beck A. 2016. Lichen photobionts of the rocky outcrops of Karadag massif (Crimean Peninsula). *Symbiosis* 68: 9–24.

Vrijenhoek RC, Schutz SJ, Gustafson RG, Lutz RA. 1994. Cryptic species of deep-sea clams (Mollusca: Bivalvia: Vesicomyidae) from hydrothermal vent and cold-water seep environments. *Deep Sea Research Part I: Oceanographic Research Papers* 41: 1171–1189.

Warren DL, Wright AN, Seifert SN, Shaffer HB. 2014. Incorporating model complexity and spatial sampling bias into ecological niche models of climate change risks faced by 90 California vertebrate species of concern. *Diversity and Distributions* 20: 334–343.

Wedin M, Maier S, Fernández-Brime S, Cronholm B, Westberg M, Grube M. 2016. Microbiome change by symbiotic invasion in lichens. *Environmental Microbiology* 18: 1428–1439.

Wei JC, Jiang YM. 1993. The Asian Umbilicariaceae (Ascomycota). Mycosystema Monographicum Series, No. 1. Beijing: International Academic Publishers.

Weisburg WG, Barns SM, Pelletier DA, Lane DJ. 1991. 16S ribosomal DNA amplification for phylogenetic study. *Journal of Bacteriology* 173: 697–703.

Werth S. 2010. Population genetics of lichen-forming fungi – a review. *The Lichenologist* 42: 499–519.

Werth S, Sork VL. 2010. Identity and genetic structure of the photobiont of the epiphytic lichen *Ramalina menziesii* on three oak species in southern California. *American journal of botany* 97: 821–830.

Werth S, Sork VL. 2014. Ecological specialization in *Trebouxia* (Trebouxiophyceae) photobionts of *Ramalina menziesii* (Ramalinaceae) across six range-covering ecoregions of western North America. *American journal of botany* 101: 1127–1140.

Widmer I, Dal Grande F, Excoffier L, Holderegger R, Keller C, Mikryukov VS, Scheidegger C. 2012. European phylogeography of the epiphytic lichen fungus *Lobaria pulmonaria* and its green algal symbiont. *Molecular Ecology* 21: 5827–5844.

Widmer I, Grande FD, Cornejo C, Scheidegger C. 2010. Highly variable microsatellite markers for the fungal and algal symbionts of the lichen *Lobaria pulmonaria* and challenges in developing biont-specific molecular markers for fungal associations. *Fungal Biology* 114: 538–544.

Williams GC. 2008. *Adaptation and Natural Selection: A Critique of Some Current Evolutionary Thought*. Princeton University Press.

Will-Wolf S, Jovan S, Neitlich P, Peck JE, Rosentreter R. 2015. Lichen-based indices to

quantify responses to climate and air pollution across northeastern U.S.A. *The Bryologist* 118: 59–82.

Wirtz N, Lumbsch HT, Green TGA, Türk R, Pintado A, Sancho L, Schroeter B. 2003. Lichen fungi have low cyanobiont selectivity in maritime Antarctica. *New Phytologist* 160: 177–183.

Wirtz N, Printzen C, Lumbsch HT. 2012. Using haplotype networks, estimation of gene flow and phenotypic characters to understand species delimitation in fungi of a predominantly Antarctic *Usnea* group (Ascomycota, Parmeliaceae). *Organisms Diversity & Evolution* 12: 17–37.

Wornik S, Grube M. 2010. Joint dispersal does not imply maintenance of partnerships in lichen symbioses. *Microbial Ecology* 59: 150–157.

Wright S. 1940. The statistical consequences of Mendelian heredity in relation to speciation. *The new systematics*: 161-183.

Yahr R, Vilgalys R, Depriest PT. 2004. Strong fungal specificity and selectivity for algal symbionts in Florida scrub *Cladonia* lichens. *Molecular Ecology* 13: 3367–3378.

Yahr R, Vilgalys R, DePriest PT. 2006. Geographic variation in algal partners of *Cladonia subtenuis* (Cladoniaceae) highlights the dynamic nature of a lichen symbiosis. *New Phytologist* 171: 847–860.

Yang Z, Rannala B. 2010. Bayesian species delimitation using multilocus sequence data. *Proceedings of the National Academy of Sciences of the United States of America* 107: 9264–9269.

Yung CCM, Chan Y, Lacap DC, Pérez-Ortega S, de los Rios-Murillo A, Lee CK, Cary SC, Pointing SB. 2014. Characterization of Chasmoendolithic Community in Miers Valley, McMurdo Dry Valleys, Antarctica. *Microbial Ecology* 68: 351–359.

Zahradníková M, Andersen HL, Tønsberg T, Beck A. 2017. Molecular Evidence of *Apatococcus*, including *A. fuscideae* sp. nov., as Photobiont in the Genus *Fuscidea*. *Protist*.

Zhang N, Blackwell M. 2002. Molecular phylogeny of *Melanospora* and similar pyrenomycetous fungi. *Mycological Research* 106: 148–155.

Zhang D-X, Hewitt GM. 2003. Nuclear DNA analyses in genetic studies of populations: practice, problems and prospects. *Molecular Ecology* 12: 563–584.

Zhang J, Kapli P, Pavlidis P, Stamatakis A. 2013. A general species delimitation method with applications to phylogenetic placements. *Bioinformatics* 29: 2869–2876.

Zoller S, Lutzoni F. 2003. Slow algae, fast fungi: exceptionally high nucleotide substitution rate differences between lichenized fungi and their symbiotic green algae *Coccomyxa*. *Molecular Phylogenetics and Evolution* 29: 629–640.

Zoller S, Scheidegger C, Sperisen C. 1999. Pcr Primers for the Amplification of Mitochondrial Small Subunit Ribosomal DNA of Lichen-forming Ascomycetes. *The Lichenologist* 31: 511–516.

Zoller S, Lutzoni F, Scheidegger C. 1999. Genetic variation within and among populations of the threatened lichen *Lobaria pulmonaria* in Switzerland and implications for its conservation. *Molecular Ecology* 8: 2049–2059.

11. APPENDICES

APPENDIX 1 A: Assessing intraspecific diversity in a lichen-forming fungus and its green algal symbiont: Evaluation of eight molecular markers.

STATEMENT OF JOINT AUTHORSHIP

Published in Fungal Ecology (online on 22 February 2013, printed in volume 6 on April 2013, Pages 141-151, DOI: 10.1016/j.funeco.2012.12.001)

Involved authors: Anna D. Sadowska-Deś, Miklós Bálint, Jürgen Otte, Imke Schmitt

What did the Ph.D. student or the Co-Authors contribute to this work?

(1) Development and planning:

Anna D. Sadowska-Deś	40%
Miklós Bálint	30%
Imke Schmitt	30%

(2) Performance of the individual investigations and experiments

(2a) Fieldwork 50%

Anna D. Sadowska-Deś	100%	Collected most of the lichen material.

(2b) Labwork 50%

Anna D. Sadowska-Deś	10%	Samples preparation, loci and primer selection.
Jürgen Otte	85%	DNA extraction, PCR and sequencing, design of new primers.
Imke Schmitt	5%	Helped with loci and primer selection.

(3) Preparation of the data collection and figures

Anna D. Sadowska-Deś	80%	Conducted sequence alignments, determined DNA polymorphisms and haplotype numbers with DnaSP, constructed median-joining haplotype networks by using Network 4.6, produced all figures and tables.
Miklós Bálint	10%	Assisted with data compilation.
Imke Schmitt	10%	Provided feedback in preparation of the data and the figures.

(4) Analyses and interpretation of data

Anna D. Sadowska-Deś	50 %	Compared alignments features, RAxML analysis, compared median-joining haplotype networks, interpreted results, carried out literature search.
Miklós Bálint	30%	Conceived analyses, helped in the data analyses and interpretation of data, literature search.
Imke Schmitt	20%	Helped in the interpretation of the results and literature search.

(5) Writing the manuscript

Anna D. Sadowska-Deś	40%
Miklós Bálint	40%
Imke Schmitt	20%

Date/Place: 25.07.2019 /Frankfurt am Main

Signature of the Ph.D. Student: Anna Sadowska-Deś

Verification of the statement above:

Signature of the Supervisor: J. Sch. Date/Place: 25.07.2019/Frankfurt am Main

FUNGAL ECOLOGY 6 (2013) 141–151

available at www.sciencedirect.com

SciVerse ScienceDirect

journal homepage: www.elsevier.com/locate/funeco

Methodological Advances

Assessing intraspecific diversity in a lichen-forming fungus and its green algal symbiont: Evaluation of eight molecular markers

Anna D. SADOWSKA-DEŚ[a,b], *Miklós BÁLINT*[a,c], *Jürgen OTTE*[a], *Imke SCHMITT*[a,b,*]

[a]*LOEWE Biodiversity and Climate Research Centre (BiK-F), Senckenberg Gesellschaft für Naturforschung, Senckenberganlage 25, D-60325 Frankfurt am Main, Germany*
[b]*Department of Biological Sciences, Goethe Universität Frankfurt, Max-von-Laue-Str. 9, D-60438 Frankfurt am Main, Germany*
[c]*Molecular Biology Center, Babeş-Bolyai University, Treboniu Laurian 42, 400270 Cluj, Romania*

ARTICLE INFO

Article history:
Received 19 July 2012
Revision received 2 November 2012
Accepted 24 November 2012
Available online 22 February 2013
Corresponding editor:
Peter Crittenden

Keywords:
Adaptation
Barcoding
Genetic diversity
Lasallia pustulata
Lichen
Mycobiont
Photobiont
Phylogeny
Population biology
Selectivity
Trebouxia

ABSTRACT

To facilitate marker selection in sequence-based studies on genetic diversity and symbiont selectivity in lichens we conducted a comparison of eight molecular markers in the lichen-forming fungus *Lasallia pustulata* and its trebouxioid photobiont. We compared mtSSU rDNA, mtLSU rDNA, *MCM7*, *TSR1* (mycobiont) and nrITS rDNA, *COX2*, psbJ-L intergenic spacer, *rbcL* (photobiont) of 45 individuals from European populations of *L. pustulata*. Mycobiont and photobiont loci had congruent phylogenetic signals. Based on the results of this study we recommend the use of *MCM7* and *TSR1* (mycobiont), and nrITS rDNA and *COX2* (photobiont). In this specific study system we found no sequence variability in the mycobiont loci *EF1*, nrITS rDNA, *RPB1*, and *RPB2*, which we sequenced for a subset of individuals. We had limited success amplifying *GPD* (mycobiont), actin and chloroplast LSU rDNA (photobiont), however, we do not rule out that these loci could be valuable markers in other species.

* *Corresponding author*. Senckenberg Gesellschaft für Naturforschung, Senckenberganlage 25, D-60325 Frankfurt am Main, Germany. Tel.: +49 69 7542 1855; fax: +49 69 7542 1800.
E-mail address: imke.schmitt@senckenberg.de (I. Schmitt).
1754-5048/$ – see front matter © 2013 Elsevier Ltd and The British Mycological Society.
http://dx.doi.org/10.1016/j.funeco.2012.12.001

Introduction

Understanding the phylogeography and population biology of symbiotic organisms is of special interest because symbiosis may be an important mechanism of adaptation. The choice and identity of symbiotic partners can influence the distribution and ecological tolerance of a species. This has been shown, for example, in corals and their photosymbionts (Howells *et al.* 2012), plants and endophytic fungi (Rodriguez *et al.* 2008; Redman *et al.* 2011), or plants and mycorrhizal fungi (Rosendahl 2008; Johnson *et al.* 2010). Recent studies suggest that lichen-forming fungi select their green algal photobionts according to habitat (Muggia *et al.* 2008; Fernandez-Mendoza *et al.* 2011; Peksa & Škaloud 2011; Vargas Castillo & Beck 2012), and that in some species multiple algal genotypes with different ecological tolerances are present in a single lichen individual (Casano *et al.* 2011). These findings support the idea that photobiont selection may influence the lichen's ability to respond to environmental change, and to occupy diverse ecological niches (Piercey-Normore 2006).

Genetic diversity in lichens has been assessed at the species or subspecies level. Some studies focus only on the mycobiont (e.g. Leavitt *et al.* 2011; Spribille *et al.* 2011; and studies summarized by Werth 2010), only the photobiont (e.g. Werth & Sork 2008), or both symbiotic partners (e.g. Yahr *et al.* 2006; Fernandez-Mendoza *et al.* 2011; Vargas Castillo & Beck 2012). Most of these studies are based on molecular sequence markers that can be generated from metagenomic DNA extracts using symbiont specific primers (Gardes & Bruns 1993; Zoller *et al.* 1999; Kroken & Taylor 2000; Printzen 2002; Schmitt *et al.* 2009). While sequence markers have been successfully employed to analyze symbiont diversity, selectivity and evolution, genomic markers, such as single sequence repeats (microsatellites), are probably most promising for high-resolution population studies in lichen-forming fungi (Werth 2010; Dal Grande *et al.* 2012). However, the development of such markers typically requires axenic cultivation of the mycobiont, which is often not feasible. To date, microsatellite markers have only been published for *Lobaria pulmonaria* and its photobiont *Dictyochloropsis reticulata* (Trebouxiophyceae) (Walser *et al.* 2003; Dal Grande *et al.* 2010; Widmer *et al.* 2010), *Parmotrema tinctorum* and its photobiont (Mansournia *et al.* 2012), for the mycobionts of *Peltigera dolichorhiza* (Magain *et al.* 2010) and *Buellia frigida* (Jones *et al.* 2012), and for *Trebouxia decolorans*, the photobiont found in *Xanthoria parietina* and *Anaptychia ciliaris* (Dal Grande *et al.* 2013). Thus, sequence-based approaches to understanding the phylogeography and population structure of lichens are an important method in lichenology. Furthermore, suitable sequence markers are necessary for the analysis of coevolution and symbiont selectivity in the lichen symbiosis. Some mycobiont species are highly selective, forming lichens only with certain photobiont species or lineages, whereas others may utilize a great variety of photobiont lineages (e.g. Blaha *et al.* 2006; Piercey-Normore 2006; Nelsen & Gargas 2009). On the other hand, a single photobiont species can associate with different species of lichen-forming fungi (e.g. Beck *et al.* 2002). For such studies it is important to evaluate the available locus markers in order to maximize the retrieved number of fungal and algal haplotypes, as well as the number of unique symbiotic pairs.

A number of ribosomal, protein coding, and intron markers have been used to study mycobiont and photobiont diversity at the species level or below (e.g. Škaloud & Peksa 2010; Werth & Sork 2010; Fernandez-Mendoza *et al.* 2011; Leavitt *et al.* 2011; Spribille *et al.* 2011). However, an overall comparison of the performance of molecular loci at the population level using a single lichen species is missing. Here, we compared the variability of eight loci (four mycobiont, four photobiont) using 45 specimens from the European populations of *Lasallia pustulata* and its green algal photobiont (*Trebouxia* sp.). For a subset of individuals we tested additional loci. We chose a fungus with trebouxioid photobiont, because unicellular green algae of the genus *Trebouxia* are the most common photobionts in lichens (Tschermak-Woess 1988; Friedl & Büdel 1996). They can be found in more than 60 % of the described taxa, approximately 9 000 species (Ahmadjian 1993; Friedl & Büdel 1996). Thus, *Trebouxia* is the most common and widely distributed terrestrial algal genus in the world (Ahmadjian 2004). Genetic variability and phylogenetic relationships of Trebouxiophyceae are still poorly understood, although this taxon makes up a significant portion of terrestrial algal diversity (Škaloud & Peksa 2010; Leliaert *et al.* 2012). Our comparative study helps to facilitate marker selection for studies in biogeography, population biology, and co-evolution/selectivity of lichens with trebouxioid photobionts.

Methods

Taxon sampling and molecular methods

We selected 45 thalli from 30 populations sampled across the species' Europe-wide range (Table 1). We extracted total genomic DNA using the CTAB method (Cubero & Crespo 2002). PCR reactions (25 μl) contained 0.65 U Ex Taq polymerase (TaKaRa BIO INC.), 1× buffer, 0.2 mM dNTP mixture, 0.5–1.0 μM of each primer, 2–50 ng DNA template, and H_2O. Primers used for PCR and cycle sequencing are referenced in Table 2. We used the following PCR cycling conditions to amplify the photobiont loci nrITS rDNA, psbJ-L, *COX2*, *rbcL*, and the mycobiont loci mtSSU rDNA, mtLSU rDNA, *MCM7*, *TSR1*: initial denaturation 95 °C for 4 min, followed by 38 cycles of 95 °C for 30 s, 50 °C for 40 s, 72 °C for 1 min, and final elongation 72 °C for 5 min. It was our experience that the type of Taq we used (and even the brand of PCR machine) had a higher influence on amplification success than varying the annealing temperature. Methodological details on the amplification of additional loci that we tested for a subset of individuals (photobiont actin, 23S rDNA; mycobiont *GPD*, *EF1*, nrITS, *RPB1*, *RPB2*) are provided in Table S1. For some loci we designed new primers that are specific for *L. pustulata* or its photobiont (Table 2, Table S1). Amplification products were separated on 1 % agarose gels. If single bands were present we diluted the PCR products and added 5–12 ng of the amplicon to 10 μl sequencing reactions. If multiple bands were present we extracted fragments of the expected size using the peqGOLD Gel Extraction Kit (PEQLAB Biotechnologie GmbH). We

Table 1 – Material used in the current study and GenBank accession numbers. Herbarium acronyms follow Thiers (2012)

# Of individual	Source	Photobiont				Mycobiont			
		nrITS rDNA	COX2	psbJ-L	*rbcL*	*MCM7*	*TSR1*	mtLSU rDNA	mtSSU rDNA
A0102	Austria, Styria, hiking path to Sporiroa-Ofen, 760 m, lat. 46.926469, long. 15.178028, leg. Sadowska-Deś, 27.07.2011 (FR)	JX474323	JX474233	JX844291	JX474278	JX474413	JX474458	JX474503	JX474368
E0101	Estonia, Lääne-Virumaa Lahemaa Rahvuspark, Vihula vald, lat. 59.5156104, long. 25.9356541, leg. Jüriado, 31.07.2008 (TU)	JX474324	JX474234	JX844292	JX474279	JX474414	JX474459	JX474504	JX474369
G0116	Germany, Hesse, Eppstein, 342 m, lat. 50.13949, long. 8.40439, leg. Sadowska-Deś, Nuñez Zapata, Schmitt, 26.05.2011 (FR)	JX474325	JX474235	JX844293	JX474280	JX474415	JX474460	JX474505	JX474370
G0126	Germany, Hesse, Eppstein, 342 m, lat. 50.13949, long. 8.40439, leg. Sadowska-Deś, Nuñez Zapata, Schmitt, 26.05.2011 (FR)	JX474326	JX474236	JX844294	JX474281	JX474416	JX474461	JX474506	JX474371
G0136	Germany, Hesse, Eppstein, 342 m, lat. 50.13949, long. 8.40439, leg. Sadowska-Deś, Nuñez Zapata, Schmitt, 26.05.2011 (FR)	JX474327	JX474237	JX844295	JX474282	JX474417	JX474462	JX474507	JX474372
G0305	Germany, Saarland, Lohfelden, Elsenfeld, 400 m, lat. 49.59647222, long. 7.00676389, leg. Sadowska-Deś, John, Nuñez Zapata, Schmitt, 17.06.2011 (FR)	JX474328	JX474238	JX844296	JX474283	JX474418	JX474463	JX474508	JX474373
G0507	Germany, Saarland, Orscholz, 300 m, lat. 49.500876, long. 6.542163, leg. Sadowska-Deś, John, Nuñez Zapata, Schmitt, 17.06.2011 (FR)	JX474329	JX474239	JX844297	JX474284	JX474419	JX474464	JX474509	JX474374
G0703	Germany, Thuringia, Bad Blankenburg, Ingoklippefelsen, 309 m, lat. 50.664914, long. 11.246982, leg. Sadowska-Deś, 25.06.2011 (FR)	JX474330	JX474240	JX844298	JX474285	JX474420	JX474465	JX474510	JX474375
G0910	Germany, Saxony-Anhalt, Bodetal, Rosstrappe, 403 m, lat. 51.735064, long. 11.246982, leg. Sadowska-Deś, 13.08.2011 (FR)	JX474331	JX474241	JX844299	JX474286	JX474421	JX474466	JX474511	JX474376
H0102	Hungary, Baranya district, Kővágószőlős, Mecsek Mts, Jakab-hegy, Zsongor-kő, 450 m, lat. 46.09083333, long. 18.1330555, leg. Farkas, Lőkös, 30.10.2010 (HB Farkas-268)	JX474332	JX474242	JX844300	JX474287	JX474422	JX474467	JX474512	JX474377
H0301	Hungary, Baranya district, Kővágószőlős, Mecsek Mts, Jakab-hegy, Babas-szerkovek, 410 m, lat. 46.09194444, long. 18.12916667, leg. Farkas, Lőkös, 30.10.2010 (HB Farkas-270)	JX474333	JX474243	JX844301	JX474288	JX474423	JX474468	JX474513	JX474378
H0302	Hungary, Baranya district, Kővágószőlős, Mecsek Mts, Jakab-hegy, Babas-szerkovek, 410 m, lat. 46.09194444, long. 18.12916667, leg. Farkas, Lőkös, 07.04. 2011 (HB Farkas-311)	JX474334	JX474244	JX844302	JX474289	JX474424	JX474469	JX474514	JX474379
H0502	Hungary, Pest District, Kamence, Borzsony Mts, Nagy-Mána, 695 m, lat. 46.09083333, long. 18.13305556, leg. Farkas, Lőkös, Molnár, 07.05.2011 (HB Farkas-346)	JX474335	JX474245	JX844303	JX474290	JX474425	JX474470	JX474515	JX474380
N0101	Norway, Aust-Agder, Lilesand: Hellekilen, 1 m, lat. 58.698777, long. 8.088226, leg. Klepsland, Jon, 07.06.2009, L164675 (O)	JX474336	JX474246	JX844304	JX474291	JX474426	JX474471	JX474516	JX474381
N0201	Norway, Hedmark, Ringsaker: Brøttum sag, 125 m, lat. 60.062922, long. 10.737061, 11.05.2008, L159236 (O)	JX474337	JX474247	JX844305	JX474292	JX474427	JX474472	JX474517	JX474382
N0203	Norway, Hedmark, Ringsaker: Brøttum sag, 125 m, lat. 60.910672, long. 10.737061, leg. Breili, Anders, 11.05.2008, L159236 (O)	JX474338	JX474248	JX844306	JX474293	JX474428	JX474473	JX474518	JX474383
N0301	Norway, Akershus, Ski: Nord Bjørke, 110 m, lat. 60.062922, long. 11.375427, leg. Breili, Anders, 18.06.2006, L150858 (O)	JX474339	JX474249	JX844307	JX474294	JX474429	JX474474	JX474519	JX474384
N0701	Norway, Oppland, Vågå: Russvassbue, 1 185 m, lat. 61.11926, long. 10.466137, leg. Haugan, 24.06.2008, L160450 (O)	JX474340	JX474250	JX844308	JX474295	JX474430	JX474475	JX474520	JX474385

(*continued on next page*)

Table 1 – (*continued*)

# Of individual	Source	Photobiont				Mycobiont			
		nrITS rDNA	*COX2*	psbJ-L	*rbcL*	*MCM7*	*TSR1*	mtLSU rDNA	mtSSU rDNA
N0801	Norway, Oppland, Vågå: Trollhø, 1 300 m, lat. 61.752031, long. 9.050303, leg. Breili, Anders, 25.03.2005, L142521 (O)	JX474341	JX474251	JX844309	JX474296	JX474431	JX474476	JX474521	JX474386
N0901	Norway, Rogland, Vindafjord: Saltvika, 1 m, lat. 59.301234, long. 5.985718, leg. Jordal, 02.09.2008, L155335 (O)	JX474342	JX474252	JX844310	JX474297	JX474432	JX474477	JX474522	JX474387
N1001	Norway, Sogn Og Fjordane, Edi: Hamnest, 2 m, lat. 61.665375, long. 6.315307, leg. Breili, Anders, 08.04.2009, L159494 (O)	JX474343	JX474253	JX844311	JX474298	JX474433	JX474478	JX474523	JX474388
N1101	Norway, Vestfold, Larvik, Stavern, 20 m, lat. 58.983333, long. 10.03333, leg. Rui, Timdal, 02.04.2011, L169175 (O)	JX474344	JX474254	JX844312	JX474299	JX474434	JX474479	JX474524	JX474389
N1104	Norway, Vestfold, Larvik, Stavern, 20 m, lat. 58.983333, long. 10.03333, leg. Rui, Timdal, 02.04.2011, L169175 (O)	JX474345	JX474255	JX844313	JX474300	JX474435	JX474480	JX474525	JX474390
P0101	Poland, Lower Silesia, Sobieszów, Zbójeckie Skały, 600 m, lat. 51.0244444, long. 15.904444, leg. Sadowska-Deś, 23.06.2011 (FR)	JX474346	JX474256	JX844314	JX474301	JX474436	JX474481	JX474526	JX474391
P0103	Poland, Lower Silesia, Sobieszów, Zbójeckie Skały, 600 m, lat. 51.0244444, long. 15.904444, leg. Sadowska-Deś, 23.06.2011 (FR)	JX474347	JX474257	JX844315	JX474302	JX474437	JX474482	JX474527	JX474392
P0109	Poland, Lower Silesia, Sobieszów, Zbójeckie Skały, 600 m, lat. 51.0244444, long. 15.904444, leg. Sadowska-Deś, 23.06.2011 (FR)	JX474348	JX474258	JX844316	JX474303	JX474438	JX474483	JX474528	JX474393
P0206	Poland, Lower Silesia, Sobieszów, Chojnik Hill, 530 m, lat. 50.83333, long. 15.63333, leg. Sadowska-Deś, 23.06.2011 (FR)	JX474349	JX474259	JX844317	JX474304	JX474439	JX474484	JX474529	JX474394
P0309	Poland, Lower Silesia, Sobieszów, Chojnik Castle, 530 m, lat. 50.833725, long. 15.644181, leg. Sadowska-Deś, 29.08.2011 (FR)	JX474350	JX474260	JX844318	JX474305	JX474440	JX474485	JX474530	JX474395
P0401	Poland, Lower Silesia, Izery Mts, Bobrowe Skały, 699 m, lat. 50.866666, long. 15.58333, leg. Sadowska-Deś, 25.08.2011 (FR)	JX474351	JX474261	JX844319	JX474306	JX474441	JX474486	JX474531	JX474396
P0501	Poland, Lower Silesia, Ostrzyca Proboszczowicka, Kaczawskie Mts, 501 m, lat. 51.14888889, long. 15.96944444, leg. Sadowska-Deś, 02.09.2011 (FR)	JX474352	JX474262	JX844320	JX474307	JX474442	JX474487	JX474532	JX474397
P0502	Poland, Lower Silesia, Ostrzyca Proboszczowicka, Kaczawskie Mts, 501 m, lat. 51.14888889, long. 15.96944444, leg. Sadowska-Deś, 02.09.2011 (FR)	JX474353	JX474263	JX844321	JX474308	JX474443	JX474488	JX474533	JX474398
P0503	Poland, Lower Silesia, Ostrzyca Proboszczowicka, Kaczawskie Mts, 501 m, lat. 51.14888889, long. 15.96944444, leg. Sadowska-Deś, 02.09.2011 (FR)	JX474354	JX474264	JX844322	JX474309	JX474444	JX474489	JX474534	JX474399
P0601	Poland, Lower Silesia, Rudawy Janowickie, Bolczów Castle, 561 m, lat. 51.03388889, long. 16.08972222, leg. Sadowska-Deś, 30.09.2011 (FR)	JX474355	JX474265	JX844323	JX474310	JX474445	JX474490	JX474535	JX474400
P0602	Poland, Lower Silesia, Rudawy Janowickie, Bolczów Castle, 561 m, lat. 51.03388889, long. 16.08972222, leg. Sadowska-Deś, 30.09.2011 (FR)	JX474356	JX474266	JX844324	JX474311	JX474446	JX474491	JX474536	JX474401

Table 1 – (*continued*)

# Of individual	Source	Photobiont				Mycobiont			
		nrITS rDNA	COX2	psbJ-L	*rbcL*	MCM7	TSR1	mtLSU rDNA	mtSSU rDNA
P0605	Poland, Lower Silesia, Rudawy Janowickie, Bolczów Castle, 561 m, lat. 51.03388889, long. 16.08972222, leg. Sadowska-Deś, 30.09.2011 (FR)	JX474357	JX474267	JX844325	JX474312	JX474447	JX474492	JX474537	JX474402
P0701	Poland, Lower Silesia, Jelenia Góra, 383 m, lat. 50.873319, long. 15.761103, leg. J. and Z. Sadowscy, 12.09.2011 (FR)	JX474358	JX474268	JX844326	JX474313	JX474448	JX474493	JX474538	JX474403
P0716	Poland, Lower Silesia, Jelenia Góra, 383 m, lat. 50.873319, long. 15.761103, leg. J. and Z. Sadowscy, 12.09.2011 (FR)	JX474359	JX474269	JX844327	JX474314	JX474449	JX474494	JX474539	JX474404
S0101	Spain, Almeria, Garganta de Chilla, 1 700 m, lat. 40.2325, long. 5.30722222, leg. Vivas Rebuelta, 11.07.2010 (FR)	JX474360	JX474270	JX844328	JX474315	JX474450	JX474495	JX474540	JX474405
S0401	Spain, Almeria, Garganta de Chilla, 1 000 m, lat. 40.206666, long. −5.29472222, leg. Vivas Rebuelta, 11.07.2010 (FR)	JX474361	JX474271	JX844329	JX474316	JX474451	JX474496	JX474541	JX474406
S0405	Spain, Almeria, Garganta de Chilla, 1 000 m, lat. 40.206666, long. −5.29472222, leg. Vivas Rebuelta, 11.07.2010 (FR)	JX474362	JX474272	JX844330	JX474317	JX474452	JX474497	JX474542	JX474407
W0105	Slovakia, Tribeč Mts, Zobor Mts: Nitra, 546 m, lat. 48.337255, long. 18.10623, leg. Guttova, 27.07.2011 (FR)	JX474363	JX474273	JX844331	JX474318	JX474453	JX474498	JX474543	JX474408
W0131	Slovakia, Tribeč Mts, Zobor Mts: Nitra, 546 m, lat. 48.337255, long. 18.10623, leg. Guttova, 27.07.2011 (FR)	JX474364	JX474274	JX844332	JX474319	JX474454	JX474499	JX474544	JX474409
W0133	Slovakia, Tribeč Mts, Zobor Mts: Nitra, 546 m, lat. 48.337255, long. 18.10623, leg. Guttova, 27.07.2011 (FR)	JX474365	JX474275	JX844333	JX474320	JX474455	JX474500	JX474545	JX474410
X0121	Portugal, Algarve, Serra de Monchique, 890 m, lat. 37.317139, long. −8.590722, leg. Divakar, Agudo, Ruibal, 19.05.2011 (FR)	JX474366	JX474276	JX844334	JX474321	JX474456	JX474501	JX474546	JX474411
Y0103	Serbia, Pčinja District, Surdulica, Vardenik Mts, 1 640 m, lat. 42.647805, long. 22.261555, leg. Lőkös, 24.06.2011 (HB Farkas-446)	JX474367	JX474277	JX844335	JX474322	JX474457	JX474502	JX474547	JX474412

sequenced the amplicons using Big Dye 3.1 chemistry (Applied Biosystems). Cycle sequencing was executed with the following program: initial denaturation for 1 min at 95 °C, followed by 30 cycles of 96 °C for 10 s, 50 °C for 10 s, 60 °C for 2 min. Sequenced products were precipitated and loaded on an ABI PRISMTM 3730 DNA Analyzer (Applied Biosystems). We assembled partial sequences using Geneious v5.4 (Drummond *et al.* 2011) and edited conflicts manually.

Sequence analyses and networks

We aligned sequences of each locus individually using MUSCLE (Edgar 2004) implemented in Geneious. We analyzed the alignments using RAxML (Stamatakis 2006). The maximum likelihood (ML) analyses were performed assuming the general time reversible model of nucleotide substitution with six rate categories including estimation of invariant sites and assuming a discrete gamma distribution (GTR + I + G) for the psbJ-L dataset and GTR + G for all other datasets. These models were determined as best fitting models using the program MrModeltest v2 (Nylander 2004). ML bootstrapping was performed based on 1 000 replicates. We examined the ML trees for the presence of supported conflicts (individuals group in a clade supported by >75 % ML bootstrap support in one dataset, but in a different supported clade in another dataset). We determined DNA polymorphisms and haplotype numbers with DnaSP v5 (Librado & Rozas 2009). For each locus we measured: the number of polymorphic sites to assess locus variability; the number of parsimony informative positions to assess possible use of the locus as a phylogenetic marker; the number of gaps to indicate the potential for ambiguous alignment of the locus; and nucleotide diversity, average differences between individuals, the number of haplotypes, and haplotype diversity to estimate utility of the locus as an intraspecific marker. Gaps were treated as missing data. We constructed median joining haplotype networks using Network 4.6 (Bandelt *et al.* 1999).

Results

We generated 45 sequences of each of the following loci: photobiont nrITS rDNA, psbJ-L intergenic spacer, *COX2*, *rbcL*, and mycobiont mtSSU rDNA, mtLSU rDNA, *MCM7*, *TSR1*.

Table 2 – Loci and primers used in the current study

Locus	Genome	Primer name, orientation	Primer sequence (5′–3′)	Reference
Photobiont				
nrITS rDNA	Nuclear	nrITS1T (f)	GGAAGGATCATTGAATCTATCGT	Kroken & Taylor (2000)
		nrITS4T (r)	GGTTCGCTCGCCGCTACTA	
		nrITSaJOFOR2 (f)	TGAATCTATCGTGCAMACACC	This study
		nrITSaJOREV2 (r)	GCCGCTACTAAGGGAATCCT	
COX2	Mitochondrial	Cox2-P2fw-5′ (f)	GGCATGAAAGCATGGTTAGC	Fernandez-Mendoza *et al.* (2011)
		Cox2-P2rv-3′ (r)	TCTGGATGTTAGCAAGAACTTTGT	
psbJ-L	Chloroplast	psbF (f)	GTWGTWCCAGTATTRGACAT	Werth & Sork (2008)
		psbR (r)	AACCRAATCCANAYAAACAA	
rbcL	Chloroplast	a-ch-rbcL-203 (f)	GAATCWTCWACWGGWACTTGGACWAC	Nelsen *et al.* (2011)
		a-ch-rbcL-991 (r)	CCTTCTARTTTACCWACAAC	
Mycobiont				
MCM7	Nuclear	MCM7-709 (f)	ACIMGIGTITCVGAYGTHAARCC	Schmitt *et al.* (2009)
		MCM7-1348 (r)	GAYTTDGCIACICCIGGRTCWCCCAT	
		MCM7FOR2 (f)	AGGTGAACGCTTACACATGC	This study
		MCM7REV2 (r)	CGGGAGCTATGGATCTTGAG	
TSR1	Nuclear	TSR1-1453F (f)	GARTTCCCIGAYGARATYGARCT	Schmitt *et al.* (2009)
		TSR1-2308R (r)	CTTRAARTAICCRTGIGTICC	
		TSR1LAPUFOR (f)	ACTACAAAGGCGCAAAGAGC	This study
		TSR1LAPUREV (r)	TGAACCAGTTGACGTCTTCG	
mtLSU rDNA	Mitochondrial	mtLSU3A (f)	GCTGGTTTTCTGCGAAACCTATATAAG	Printzen (2002)
		mtLSU4A (r)	GTTAGTTTGCCGAGTTCCTTAATG	
mtSSU rDNA	Mitochondrial	mrSSU1 (f)	AGCAGTGAGGGATATTGGTC	Zoller *et al.* (1999), Zhou & Stanosz (2001)
		MSU7 (r)	GTCGAGTTACAGACTACAATCC	

Detailed information on specimens and corresponding GenBank accession numbers is given in Table 1. We also generated 12 sequences of chloroplast 23S rDNA (GenBank accession numbers JX474221–JX474232).

A comparison of alignment features and variability among photobiont loci (nrITS rDNA, psbJ-L, *COX2*, *rbcL*) and mycobiont loci (mtSSU rDNA, mtLSU rDNA, *MCM7*, *TSR1*) is presented in Table 3. The ML 75 % bootstrap support method for testing datasets for incongruence indicated no supported conflicts among photobiont or mycobiont alignments. This suggests that the tested loci have similar evolutionary histories. ML trees are presented in Fig S1. The median joining networks of the four photobiont loci are also largely congruent (Fig 1).

Variability of the photobiont loci was higher than that of the mycobiont loci (Table 3). Nuclear ITS rDNA of the photobiont showed the highest number of variable sites (71) and haplotypes (13), followed by the mitochondrial loci psbJ-L intergenic spacer and *COX2*. The psbJ-L intergenic spacer is non-coding and highly variable, thus causing ambiguities/gaps in the alignment. *RbcL* was the least variable photobiont locus (Table 3). Among the mycobiont loci, the nuclear protein-coding gene *MCM7* possessed the highest number of polymorphic sites, average differences between individuals,

Table 3 – Comparison of variability among four photobiont and four mycobiont loci. The alignment included 45 sequences from the European populations of *Lasallia pustulata*

Symbiont	Photobiont				Mycobiont			
Locus	nrITS rDNA	*COX2*	psbJ-L	*rbcL*	*MCM7*	*TSR1*	mtLSU rDNA	mtSSU rDNA
Alignment length	507	419	614	441	370	485	728	706
Polymorphic sites [N] (%)	71 (14.0 %)	44 (10.5 %)	44 (7.2 %)	5 (1.1 %)	6 (1.6 %)	5 (1.0 %)	2 (0.3 %)	1 (0.1 %)
Parsimony informative positions [N]	69	44	43	5	6	5	2	1
Gaps [N]	5	0	331	0	0	0	1	4
Nucleotide diversity[a]	0.051	0.045	0.075	0.005	0.0029	0.002	0.0008	0.0003
Ø differences between individuals[a]	26.24	18.6	26.7	2.04	1.07	0.97	0.58	0.24
Haplotypes [N]	13	5	10	4	3	3	3	2
Haplotype diversity	0.81	0.66	0.7	0.61	0.47	0.24	0.52	0.24

a Based on pairwise comparisons.

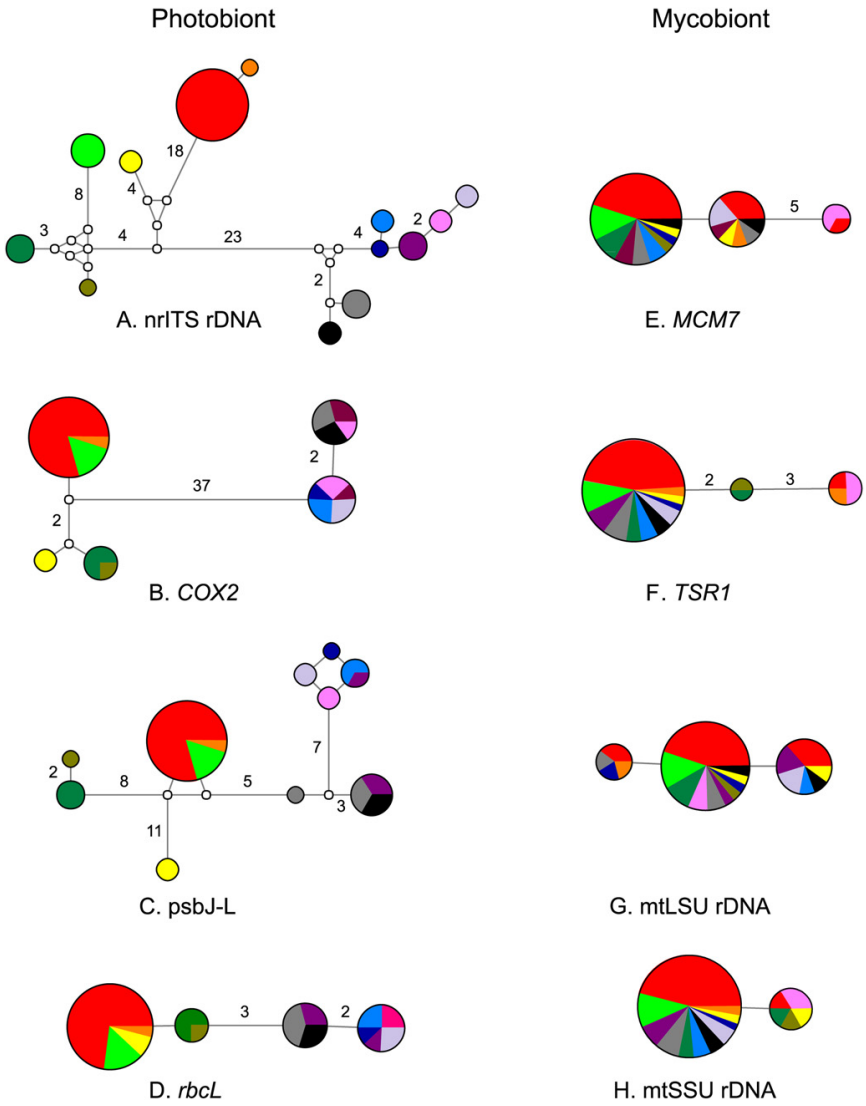

Fig 1 – Median joining haplotype networks. (A–D) photobiont, (E–H) mycobiont. (A) nrITS rDNA, (B) *COX2*, (C) psbJ-L intergenic spacer, (D) *rbcL*, (E) *MCM7*, (F) *TSR1*, (G) mtLSU rDNA, (H) mtSSU rDNA. Colored circles indicate haplotypes; the size of circles is relative to the number of individuals carrying the haplotype. Empty circles indicate missing haplotypes. Individuals are color-coded based on the nrITS rDNA photobiont haplotype they carry. Numbers indicate mutational steps > 1.

and the highest nucleotide diversity. It also had the shortest alignment. The second nuclear, protein-coding locus (*TSR1*) was only marginally less polymorphic than *MCM7* (Table 3). Despite much longer alignments, the mitochondrial ribosomal loci yielded very little variability (1–2 polymorphic sites). However, the little variation observed among mycobiont loci was largely congruent. For example, the largest haplotype group in the nuclear *TSR1* and in the mitochondrial mtSSU rDNA consisted of the same individuals (Fig 1F, H).

For a subset of individuals we tested additional loci (Table S1). The mycobiont loci *EF1*, nrITS rDNA, *RPB1*, and *RPB2* showed no sequence variability in *L. pustulata*. Despite PCR optimization we had very limited success in amplifying/sequencing the mycobiont locus *GPD* and the photobiont locus actin in the present study system (methodological details and experimental outcomes are provided in Table S1). We were able to generate 12 sequences of chloroplast LSU rDNA (23S rDNA). This marker was recently recommended for diversity assessment in the genus *Trebouxia* (del Campo *et al.* 2009, 2010). The new 23S rDNA sequences contained no introns. We compared 23S rDNA and nrITS rDNA variability of these 12 individuals, and found nrITS rDNA to be more variable (alignment length excluding sites with gaps 23S rDNA: 1 072, nrITS rDNA: 503; polymorphic sites 23S rDNA: 20 (1.9 %), nrITS:

64 (12.7 %); nucleotide diversity 23S rDNA: 0.00594, nrITS: 0.03915; number of haplotypes 23S rDNA: 6, nrITS rDNA: 9).

Discussion

It is difficult to find mycobiont loci with sufficient variability at the population level. Intraspecific variability has been reported for nuclear ITS rDNA in some lichen-forming fungi (e.g. Printzen *et al.* 2003; Lindblom & Ekman 2006; Del Prado *et al.* 2011; Núñez-Zapata *et al.* 2011; Wirtz *et al.* 2012), and also in a number of non-lichenized fungi (e.g. Nilsson *et al.* 2008; Bonito *et al.* 2010; Kovács *et al.* 2011). However, a factor complicating the use of nrITS rDNA as a population marker in fungi is the potential presence of intragenomic variation (e.g. Simon & Weiss 2008). Furthermore, species boundaries in fungi are often not well understood and different ITS types may indicate the presence of morphologically cryptic species complexes (Del Prado *et al.* 2011; Núñez-Zapata *et al.* 2011; Wirtz *et al.* 2008, 2012). Overall, nrITS rDNA is conserved enough in the majority of fungal species to serve as a species identifier, rather than a population marker (Schoch *et al.* 2012). Our finding of lack of sequence variability in the nrITS rDNA of *L. pustulata* is consistent with this observation. A second locus from the nuclear ribosomal cistron, IGS rDNA, has also been employed at the subspecies level, sometimes showing slightly lower (Lindblom & Ekman 2006), sometimes slightly higher variability than nrITS rDNA (Printzen *et al.* 2003; Leavitt *et al.* 2011; Wirtz *et al.* 2012).

Protein-coding genes, such as *GPD*, *MCM7*, *RPB1*, *RPB2*, *TSR1* or *TUB* may be alternatives to ribosomal loci for population studies of fungi (Buschbom & Mueller 2006; Fernandez-Mendoza *et al.* 2011; Leavitt *et al.* 2011; Spribille *et al.* 2011; Wirtz *et al.* 2012). Paralogs, sometimes present in these genes, are typically too divergent to cause problems in studies at the species level or below (Buschbom & Mueller 2006). *RPB1* and *RPB2* had very little or no variability (Buschbom & Mueller 2006; Wirtz *et al.* 2012; this study), while *MCM7* showed an acceptable level of polymorphism in the present and other studies (Leavitt *et al.* 2011; Spribille *et al.* 2011). *TSR1*, which was tested at the population level for the first time in the present study, performed very similarly to *MCM7*. For both markers (*MCM7* and *TSR1*) it is best to generate a few sequences using universal ascomycete primers (Schmitt *et al.* 2009) and then design more specific primers for the target group, as PCR and sequencing can be problematic using universal primers for protein-coding genes (Schoch *et al.* 2012). In the present study we had very limited success sequencing *GPD* (see Table S1), a marker that was successfully used to analyze population dynamics in *Cetraria aculeata* (Fernandez-Mendoza *et al.* 2011). This suggests that utility of certain loci may depend on the species studied.

Markers covering the entire genome, such as short sequence repeats (microsatellites), or single nucleotide polymorphisms (SNPs), are likely to be more powerful in resolving population structure in lichen mycobionts. However, the development of such markers typically requires axenic cultivation of fungal partners, which is often time consuming due to the slow growth rates of isolated mycobionts (Widmer *et al.* 2010). As more genome sequences of lichen-forming fungi and their photobionts become available, we expect that bioinformatics approaches will become important tools for separating the genomes of the symbiotic partners. Genomic data generated with next generation sequencing technology will be a valuable resource for marker development in population studies in non-model organisms (Davey *et al.* 2011).

Photobionts can be highly diverse, and it has been shown repeatedly that multiple photobiont lineages can form associations with a single fungus (e.g. Blaha *et al.* 2006; Piercey-Normore 2006; Nelsen & Gargas 2009; Bačkor *et al.* 2010). In this study, too, the trebouxioid photobiont showed considerable variation, indicating that multiple genetic lineages of algae form symbioses with *L. pustulata*. Three out of four tested photobiont loci showed substantial variability. The nrITS rDNA and *COX2* median joining networks indicate that there are at least two major photobiont haplotype groups separated from each other by 23/37 steps (Fig 1A, B). These highly divergent genotype groups probably belong to different *Trebouxia* species. Nuclear ITS rDNA and *COX2* are therefore most useful to assess the phylogenetic range of possible trebouxioid symbiotic partners in a lichen mycobiont, i.e. they are suitable markers for studies of selectivity. Our study shows that phylogenetic signal in all tested photobiont loci is congruent, with nrITS rDNA providing the highest resolution. Thus, nrITS rDNA, *COX2*, *rbcL*, and psbJ-L are probably all useful markers for multi-locus phylogenetic studies at different taxonomic levels within the genetically diverse genus *Trebouxia*. Whether these loci are sufficiently polymorphic to assess population structure at the level of individuals remains to be tested. Since trebouxioid photobionts of lichens are considered mostly clonal organisms, care needs to be taken not to underestimate their potential genetic diversity by relying on a single marker type (Arnaud-Haond *et al.* 2005). However, the loci analyzed here are likely to be very useful to define genetic lineages in *Trebouxia*, for which more powerful, high-resolution markers can then be developed (Dal Grande *et al.* 2013).

Additional loci have been used successfully in other studies of lichen photobiont diversity, for example actin (Fernandez-Mendoza *et al.* 2011), or chloroplast LSU (del Campo *et al.* 2010), demonstrating their value as phylogenetic or population markers. In the present study we confirm that nrITS rDNA appears to be more suitable for analyzing genetic variability at the intraspecific level, whereas chloroplast LSU seems to be adequate at the interspecific level in the genus *Trebouxia* (del Campo *et al.* 2010). The chloroplast LSU sequences generated in the present study belong to the same general group of species analyzed by del Campo *et al.* (2010). In BLAST searches they were most similar to *Trebouxia simplex* FJ804756: N1104, P0206, W0133 (identities 1 070 out of 1 072 bp), P0103, P0309, W0133 (identities 1 069 out of 1 072), W0105, P0701, P0101, X0121, G0910 (identities 1 066 out of 1 072), or to *Trebouxia brindabellae* FJ804757: G0507 (identities 1 071 out of 1 072). The sequence deviations between the new sequences and the BLAST hits may be an indication of unexplored cryptic diversity in *Trebouxia*. The fact that we had only limited success in generating chloroplast LSU and actin sequences (Table S1) indicates that – in analogy to the mycobiont loci – not all photobiont markers appear to be equally suitable for all species/lineages.

Understanding the genetic variability of lichens may provide insights into basic ecological phenomena, such as local adaptation (Peksa & Škaloud 2011; Vargas Castillo & Beck 2012), symbiont specificity (Nelsen & Gargas 2008; Dal Grande *et al.* 2012), and cryptic speciation (Leavitt *et al.* 2011). We have yet much to learn about the local and global distribution of genetic diversity in populations of lichen-forming fungi and their photobionts, selectivity of the symbiotic partners, and the reaction of lichens to anthropogenic change. While a number of appropriate markers are available to assess photobiont selectivity in lichenized fungi with trebouxioid green algae, it will be our challenge to develop powerful markers for assessing variability within and among populations of both symbionts.

Acknowledgments

We thank the following curators and collectors for their generous support in collecting or making available material used in this study: P. Divakar (Madrid), E. Farkas (Vácrátót), M. Grube (Graz), A. Guttova (Bratislava), J. Hafellner (Graz), V. John (Bad Dürkheim), L. Lőkös (Budapest), H. Mayrhofer (Graz), L. Muggia (Graz), T. Randle (Tartu), J. and Z. Sadowscy (Jelenia Góra), T. Spribille (Graz), A. Suija (Tartu), E. Timdal (Oslo), M. Vivas Rebuelta (Madrid). F. Dal Grande (Frankfurt) provided valuable comments on an earlier draft of the manuscript. This study was funded by 'LOEWE, Landes-Offensive zur Entwicklung Wissenschaftlich-ökonomischer Exzellenz' of Hesse's Ministry of Higher Education, Research, and the Arts. A.S-D. was supported by Deutsche Bundesstiftung Umwelt (DBU), and the German Academic Exchange Service (DAAD).

Supplementary data

Supplementary data related to this article can be found at http://dx.doi.org/10.1016/j.funeco.2012.12.001.

REFERENCES

Ahmadjian V, 1993. *The Lichen Symbiosis*. Wiley & Sons, New York.

Ahmadjian V, 2004. *Trebouxia*: reflections on a perplexing and controversial lichen photobiont. In: Seckbach J (ed), *Symbiosis Mechanisms and Model Systems*. Springer, Netherlands, pp. 373–383.

Arnaud-Haond S, Alberto F, Teixeira S, et al., 2005. Assessing genetic diversity in clonal organisms: low diversity or low resolution? Combining power and cost efficiency in selecting markers. *Journal of Heredity* **96**: 434–440.

Bandelt HJ, Forster P, Röhl A, 1999. Median-joining networks for inferring intraspecific phylogenies. *Molecular Biology and Evolution* **16**: 37–48.

Bačkor M, Peksa O, Škaloud P, et al., 2010. Photobiont diversity in lichens from metal-rich substrata based on nrITS rDNA sequences. *Ecotoxicology and Environmental Safety* **73**: 603–612.

Beck A, Kasalicky T, Rambold G, 2002. Myco-photobiontal selection in a Mediterranean cryptogam community with *Fulgensia fulgida*. *New Phytologist* **153**: 317–326.

Blaha J, Baloch E, Grube M, 2006. High photobiont diversity associated with the euryoecious lichen-forming ascomycete *Lecanora rupicola* (Lecanoraceae, Ascomycota). *Biological Journal of the Linnean Society* **88**: 283–293.

Bonito GM, Gryganskyi AP, Trappe JM, et al., 2010. A global meta-analysis of *Tuber* ITS rDNA sequences: species diversity, host associations and long-distance dispersal. *Molecular Ecology* **19**: 4994–5008.

Buschbom J, Mueller GM, 2006. Testing "species pair" hypotheses: evolutionary processes in the lichen-forming species complex *Porpidia flavocoerulescens* and *Porpidia melinodes*. *Molecular Biology and Evolution* **23**: 574–586.

Casano LM, del Campo EM, García-Breijo FJ, et al., 2011. Two *Trebouxia* algae with different physiological performances are ever-present in lichen thalli of *Ramalina farinacea*. Coexistence versus competition? *Environmental Microbiology* **13**: 806–818.

Cubero OF, Crespo A, 2002. Isolation of nucleic acids from lichens. In: Kranner I, Beckett R, Varma A (eds), *Protocols in Lichenology*. Springer, Berlin, pp. 381–391.

Dal Grande F, Widmer I, Beck A, et al., 2010. Microsatellite markers for *Dictyochloropsis reticulata* (Trebouxiophyceae), the symbiotic alga of the lichen *Lobaria pulmonaria* (L.). *Conservation Genetics* **11**: 1147–1149.

Dal Grande F, Widmer I, Wagner HH, et al., 2012. Vertical and horizontal photobiont transmission within populations of a lichen symbiosis. *Molecular Ecology* **13**: 3159–3172.

Dal Grande F, Beck A, Singh G, et al., 2013. Microsatellite primers in the lichen symbiotic alga *Trebouxia decolorans* (Trebouxiophyceae). *Applications in Plant Sciences*, doi:10.3732/apps.1200400.

Davey JW, Hohenlohe PA, Etter PD, et al., 2011. Genome-wide genetic marker discovery and genotyping using next-generation sequencing. *Nature Reviews Genetics* **12**: 499–510.

del Campo EM, Casano LM, Gasulla F, et al., 2009. Presence of multiple group I introns closely related to bacteria and fungi in plastid 23S rRNAs of lichen-forming *Trebouxia*. *International Microbiology* **12**: 59–67.

del Campo EM, Casano LM, Gasulla F, et al., 2010. Suitability of chloroplast LSU rDNA and its diverse group I introns for species recognition and phylogenetic analyses of lichen-forming *Trebouxia* algae. *Molecular Phylogenetics and Evolution* **54**: 437–444.

Del Prado R, Divakar PK, Crespo A, 2011. Using genetic distances in addition to ITS molecular phylogeny to identify potential species in the *Parmotrema reticulatum* complex: a case study. *The Lichenologist* **43**: 569–583.

Drummond A, Ashton B, Buxton S, et al., 2011. *Geneious v5.4*. Available from: http://www.geneious.com/

Edgar RC, 2004. MUSCLE: multiple sequence alignment with high accuracy and high throughput. *Nucleic Acids Research* **32**: 1792–1797.

Fernandez-Mendoza F, Domaschke S, Garcia MA, et al., 2011. Population structure of mycobionts and photobionts of the widespread lichen *Cetraria aculeata*. *Molecular Ecology* **20**: 1208–1232.

Friedl T, Büdel B, 1996. Photobionts. In: Nash TH (ed), *Lichen Biology*. Cambridge University Press, Cambridge, UK, pp. 8–23.

Gardes M, Bruns TD, 1993. nrITS primers with enhanced specificity for basidiomycetes – application to the identification of mycorrhizae and rusts. *Molecular Ecology* **2**: 113–118.

Howells EJ, Beltran VH, Larsen NW, et al., 2012. Coral thermal tolerance shaped by local adaptation of photosymbionts. *Nature Climate Change* **2**: 116–120.

Johnson NC, Wilson GWT, Bowker MA, Wilson JA, Miller RM, 2010. Resource limitation is a driver of local adaptation in

mycorrhizal symbioses. *Proceedings of the National Academy of Sciences of the United States of America* **107**: 2093–2098.
Jones TC, Green TGA, Hogg ID, Wilkins RJ, 2012. Isolation and characterization of microsatellites in the lichen *Buellia frigida* (Physciaceae), an Antarctic endemic. *American Journal of Botany* **99**: e131–e133.
Kovács GM, Jankovics T, Kiss L, 2011. Variation in the nrDNA nrITS sequences of some powdery mildew species: do routine molecular identification procedures hide valuable information? *European Journal of Plant Pathology* **131**: 135–141.
Kroken S, Taylor JW, 2000. Phylogenetic species, reproductive mode, and specificity of the green alga *Trebouxia* forming lichens with the fungal genus *Letharia*. *The Bryologist* **103**: 645–660.
Leavitt SD, Johnson L, St. Clair LL, 2011. Species delimitation and evolution in morphologically and chemically diverse communities of the lichen-forming genus *Xanthoparmelia* (Parmeliaceae, Ascomycota) in western North America. *American Journal of Botany* **98**: 175–188.
Leliaert F, Smith DR, Moreau H, et al., 2012. Phylogeny and molecular evolution of the green algae. *Critical Reviews in Plant Sciences* **31**: 1–46.
Librado P, Rozas J, 2009. DnaSP v5: a software for comprehensive analysis of DNA polymorphism data. *Bioinformatics* **25**: 1451–1452.
Lindblom L, Ekman S, 2006. Genetic variation and population differentiation in the lichen-forming ascomycete *Xanthoria parietina* on the island Storfosna, central Norway. *Molecular Ecology* **15**: 1545–1559.
Magain N, Forrest LL, Sérusiaux E, Goffinet B, 2010. Microsatellite primers in the *Peltigera dolichorhiza* complex (lichenized ascomycete, Peltigerales). *American Journal of Botany*: e102–e104.
Mansournia MR, Wu B, Matsushita N, et al., 2012. Genotypic analysis of the foliose lichen *Parmotrema tinctorum* using microsatellite markers: association of mycobiont and photobiont, and their reproductive modes. *The Lichenologist* **44**: 419–440.
Muggia L, Grube M, Tretiach M, 2008. Genetic diversity and photobiont associations in selected taxa of the *Tephromela atra* group (Lecanorales, lichenised Ascomycota). *Mycological Progress* **7**: 147–160.
Nelsen MP, Gargas A, 2008. Dissociation and horizontal transmission of codispersing lichen symbionts in the genus *Lepraria* (Lecanorales: Stereocaulaceae). *New Phytologist* **177**: 264–275.
Nelsen MP, Gargas A, 2009. Symbiont flexibility in *Thamnolia vermicularis* (Pertusariales: Icmadophilaceae). *The Bryologist* **112**: 404–417.
Nelsen MP, Plata ER, Andrew CJ, et al., 2011. Phylogenetic diversity of trentepohlialean algae associated with lichen-forming fungi. *Journal of Phycology* **47**: 282–290.
Nilsson RH, Kristiansson E, Ryberg M, et al., 2008. Intraspecific nrITS variability in the kingdom Fungi as expressed in the international sequence databases and its implications for molecular species identification. *Evolutionary Bioinformatics Online* **4**: 193–201.
Núñez-Zapata J, Divakar PK, Del Prado R, et al., 2011. Conundrums in species concepts: the discovery of a new cryptic species segregated from *Parmelina tiliacea* (Ascomycota: Parmeliaceae). *The Lichenologist* **43**: 603–616.
Nylander JAA, 2004. MrModeltest 2.2. Program distributed by the author.
Peksa O, Škaloud P, 2011. Do photobionts influence the ecology of lichens? A case study of environmental preferences in symbiotic green alga *Asterochloris* (Trebouxiophyceae). *Molecular Ecology* **20**: 3936–3948.
Piercey-Normore MD, 2006. The lichen-forming ascomycete *Evernia mesomorpha* associates with multiple genotypes of *Trebouxia jamesii*. *New Phytologist* **169**: 331–344.
Printzen C, 2002. Fungal specific primers for PCR-amplification of mitochondrial LSU in lichens. *Molecular Ecology Notes* **2**: 130–132.
Printzen C, Ekman S, Tønsberg T, 2003. Phylogeography of *Cavernularia hultenii*: evidence of slow genetic drift in a widely disjunct lichen. *Molecular Ecology* **12**: 1473–1486.
Redman RS, Kim YO, Woodward CJDA, et al., 2011. Increased fitness of rice plants to abiotic stress via habitat adapted symbiosis: a strategy for mitigating impacts of climate change. *PLoS One* **6**: e14823.
Rodriguez RJ, Henson J, Van Volkenburgh E, et al., 2008. Stress tolerance in plants via habitat-adapted symbiosis. *The ISME Journal* **2**: 404–416.
Rosendahl S, 2008. Communities, populations and individuals of arbuscular mycorrhizal fungi. *New Phytologist* **178**: 253–266.
Schmitt I, Crespo A, Divakar PK, et al., 2009. New primers for promising single-copy genes in fungal phylogenetics and systematics. *Persoonia* **23**: 35–40.
Schoch CL, Seifert KA, Huhndorf S, et al., 2012. Nuclear ribosomal internal transcribed spacer (ITS) region as a universal DNA barcode marker for Fungi. *Proceedings of the National Academy of Sciences of the United States of America* **109**: 6241–6246.
Simon UK, Weiss M, 2008. Intragenomic variation of fungal ribosomal genes is higher than previously thought. *Molecular Biology and Evolution* **25**: 2251–2254.
Škaloud P, Peksa O, 2010. Evolutionary inferences based on nrITS rDNA and actin sequences reveal extensive diversity of the common lichen alga *Asterochloris* (Trebouxiophyceae, Chlorophyta). *Molecular Phylogenetics and Evolution* **54**: 36–46.
Spribille T, Klug B, Mayrhofer H, 2011. A phylogenetic analysis of the boreal lichen *Mycoblastus sanguinarius* (Mycoblastaceae, lichenized Ascomycota) reveals cryptic clades correlated with fatty acid profiles. *Molecular Phylogenetics and Evolution* **59**: 603–614.
Stamatakis A, 2006. RAxML-VI-HPC: maximum likelihood-based phylogenetic analyses with thousands of taxa and mixed models. *Bioinformatics* **22**: 2688–2690.
Thiers B, 2012. *Index Herbariorum: a global directory of public herbaria and associated staff*. New York Botanical Garden's Virtual Herbarium, New York Botanical Garden, New York.
Tschermak-Woess E, 1988. The algal partner. In: Galun M (ed), *CRC Handbook of Lichenology*. Boca Raton, FL, USA, pp. 39–92.
Vargas Castillo R, Beck A, 2012. Photobiont selectivity and specificity in *Caloplaca* species in a fog-induced community in the Atacama Desert, northern Chile. *Fungal Biology* **116**: 665–676.
Walser J-C, Sperisen C, Soliva M, et al., 2003. Fungus-specific microsatellite primers of lichens: application for the assessment of genetic variation on different spatial scales in *Lobaria pulmonaria*. *Fungal Genetics and Biology* **40**: 72–82.
Werth S, 2010. Population genetics of lichen-forming fungi – a review. *The Lichenologist* **42**: 499–519.
Werth S, Sork VL, 2008. Local genetic structure in a North American epiphytic lichen, *Ramalina menziesii* (Ramalinaceae). *American Journal of Botany* **95**: 568–576.
Werth S, Sork VL, 2010. Identity and genetic structure of the photobiont of the epiphytic lichen *Ramalina menziesii* on three oak species in southern California. *American Journal of Botany* **97**: 821–830.
Widmer I, Dal Grande F, Cornejo C, et al., 2010. Highly variable microsatellite markers for the fungal and algal symbionts of the lichen *Lobaria pulmonaria* and challenges in developing biont-specific molecular markers for fungal associations. *Fungal Biology* **114**: 538–544.
Wirtz N, Printzen C, Lumbsch HT, 2008. The delimitation of Antarctic and bipolar species of neuropogonoid *Usnea*

(Ascomycota, Lecanorales): a cohesion approach of species recognition for the *Usnea perpusilla* complex. *Mycological Research* **112**: 472–484.

Wirtz N, Printzen C, Lumbsch HT, 2012. Using haplotype networks, estimation of gene flow and phenotypic characters to understand species delimitation in fungi of a predominantly Antarctic *Usnea* group (Ascomycota, Parmeliaceae). *Organisms Diversity & Evolution* **12**: 17–37.

Yahr R, Vilgalys R, DePriest PT, 2006. Geographic variation in algal partners of *Cladonia subtenuis* (Cladoniaceae) highlights the dynamic nature of a lichen symbiosis. *New Phytologist* **171**: 847–860.

Zhou S, Stanosz GR, 2001. Primers for amplification of mt SSU rDNA, and a phylogenetic study of *Botryosphaeria* and associated anamorphic fungi. *Mycological Research* **105**: 1033–1044.

Zoller S, Scheidegger C, Sperisen C, 1999. PCR primers for the amplification of mitochondrial small subunit ribosomal DNA of lichen-forming ascomycetes. *The Lichenologist* **31**: 511–516.

SUPPLEMENTARY MATERIALS

Table S1. Additional loci tested for a subset of individuals. Experimental conditions and outcomes are provided.

PHOTOBIONT							
Locus	**Genome**	**Primer name, orientation**	**Primer sequence (5'-3')**	**Reference***	**Annealing temperatures tested**	**Type of Taq tested**	**Comments**
23S rDNA	chloroplast	ST1 (f) ST4 (r)	CCGAAAGGCGTAGTCGATGG CCGTCGATGTGAACTCTTGG	del Campo *et al.* 2009	52°C, 55°C, 58°C	ExTaq	PCR successful, but in most reactions two similar sized bands (also at higher temperatures). Out of 45 samples we generated 12 correct sequences, 11 bacterial sequences. Using primer combinations that amplify shorter fragments (ST1/ST2, ST3/ST4 from del Campo et al. 2009) might help avoiding bacterial DNA. Alignment (12 sequences) was less polymorphic than nrITS.
actin	nuclear	Act1T (f) Act4T (r)	CACACRGTRCCCATCTAYGAGG GTTGAACAGCACCTCAGGGCA	Kroken & Taylor 2000	48°C, 50°C, 53°C, 54°C, 56°C, and touchdown protocol from Fernandez-Mendoza *et al.* 2011	ExTaq, ExTaq HS, Molegene, Molegene HS, Phusion, GoTaq	Only some samples amplified, multiple bands, sequencing problems, few sequences generated
		ActinAlgFOR1 (f) ActinAlgREV1 (r)	CACGCAATCACAAGGCTAG TGGTAATGACCTGCAGCAA	this study	50°C-54°*C*	ExTaq, ExTaq HS	*Lasallia pustulata* specific, only some samples amplified, multiple bands, sequencing problems

(Table S1 continued) MYCOBIONT							
Locus	**Genome**	**Primer name, orientation**	**Primer sequence (5'-3')**	**Reference**	**Annealing temperatures tested**	**Type of Taq tested**	**Comments**
RPB1	nuclear	gRPB1Af (f) fRPB1cR (r)	GADTGTCCDGGDCATTTTGG CNGGCDATNTCRTTRTCCATRTA	Stiller & Hall 1997 Matheny *et al.* 2002	48°C-52°C	ExTaq, ExTaq HS, Molgene, Molegene HS,	PCR/sequencing successful, two bands, gel purification necessary, alignment (12 sequences) without polymorphic sites
RPB2	nuclear	fRPB2-5F (f) fRPB2-7cR (r)	GAYGAYMGWGATCAYTTYGG CCCATRGCTTGYTTRCCCAT	Liu et al. 1999	48°C-52°C	ExTaq, ExTaq HS, Molegene, Molegene HS,	PCR/sequencing successful, alignment (10 sequences) without polymorphic sites
EF1	nuclear	EF1-983F (f) EF1-2218R (r)	GCYCCYGGHCAYCGTGAYTTYAT ATGACACCRACRGCRACRGTYTG	Rehner 2001	48°C-50°C	ExTaq, ExTaq HS, Molgene, Molegene HS	PCR/sequencing successful, multiple bands, gel purification necessary
		E1FLAPUFOR1 (f) E1FLAPUREV1 (r)	GACTCGTGAGCACGCTCTG GTGCGCAGTGTGGCAGTC	this study	50°C-52°C	ExTaq, ExTaq HS, Molegene, Molegene HS	*Lasallia pustulata* specific, PCR/sequencing successful, multiple bands, gel purification necessary, alignment (13 sequences) without polymorphic sites
nrITS rDNA	nuclear	ITS1f ITS4	CTTGGTCATTTAGAGGAAGTAA TCCTCCGCTTATTGATATGC	White *et al.* 1990; Gardes & Bruns 1993	48°C-56°C (gradient)	ExTaq, ExTaq HS, Molgene, Molegene HS, Phusion, GoTaq	Only 30% of the samples amplified, multiple bands, gel purifications necessary, alignment (12 sequences) without polymorphic sites
GPD	nuclear	Gpdl-LM Gpd2-LM	ATTGGCCGCATCGTCTTCCGCAA CCCACTCGTTGTCGTACCA	Myllys *et al.* 2002	48°C, 50°C, 52°C, 54°C, 56°C, and touchdown protocol from Fernandez-Mendoza *et al.* 2011	ExTaq, Molegene Taq (all temperatures), ExTaq HS, Molegene HS, Phusion, GoTaq (selected temperatures)	Only some samples amplified, multiple bands often close together, sequencing problems, gel purifications necessary, no sequences generated

References:

del Campo EM, Casano LM, Gasulla F, *et al.*, 2009. Presence of multiple group I introns closely related to bacteria and fungi in plastid 23S rRNAs of lichen-forming *Trebouxia*. *International Microbiology* 12: 59-67.

Gardes M, Bruns TD, 1993. ITS primers with enhanced specificity for basidiomycetes - application to the identification of mycorrhizae and rusts. Molecular Ecology 2: 113-118

Kroken S, Taylor JW, 2000. Phylogenetic species, reproductive mode, and specificity of the green alga *Trebouxia* forming lichens with the fungal genus *Letharia*. *The Bryologist* 103: 645-660.

Liu YJ, Whelen S, Hall BD, 1999. Phylogenetic relationships among ascomycetes: evidence from an RNA polymerse II subunit. *Molecular Biology and Evolution* 16: 1799-1808.

Matheny PB, Liu YJ, Ammirati JF, Hall BD, 2002. Using *RPB1* sequences to improve phylogenetic inference among mushrooms (Inocybe, Agaricales). *American Journal of Botany* 89: 688-698.

Myllys L, Stenroos S, Thell A, 2002. New genes for phylogenetic studies of lichenized fungi: glyceraldehyde-3-phosphate dehydrogenase and beta-tubulin genes. *The Lichenologist* 34: 237-246.

Stiller JW, Hall BD, 1997. The origin of red algae: Implications for plastid evolution. *Proceedings of the National Academy of Sciences* 94: 4520-4525.

Rehner S, 2001. Primers for Elongation Factor 1-a (EF1-a)

White TJ, Bruns T, Lee S, Taylor JW (1990) Amplification and direct sequencing of fungal ribosomal RNA genes for phylogenetics. In *PCR Protocols: A Guide to Methods and Applications*, Innis MA, Gelfand DH, Sninsky JJ, White TJ (eds), pp 315-322. New York: Academic Press, Inc.

Figure S1: Maximum likelihood trees of eight tested loci. Trees were generated in RAxML. ML bootstrap support is based on 1000 replicates.

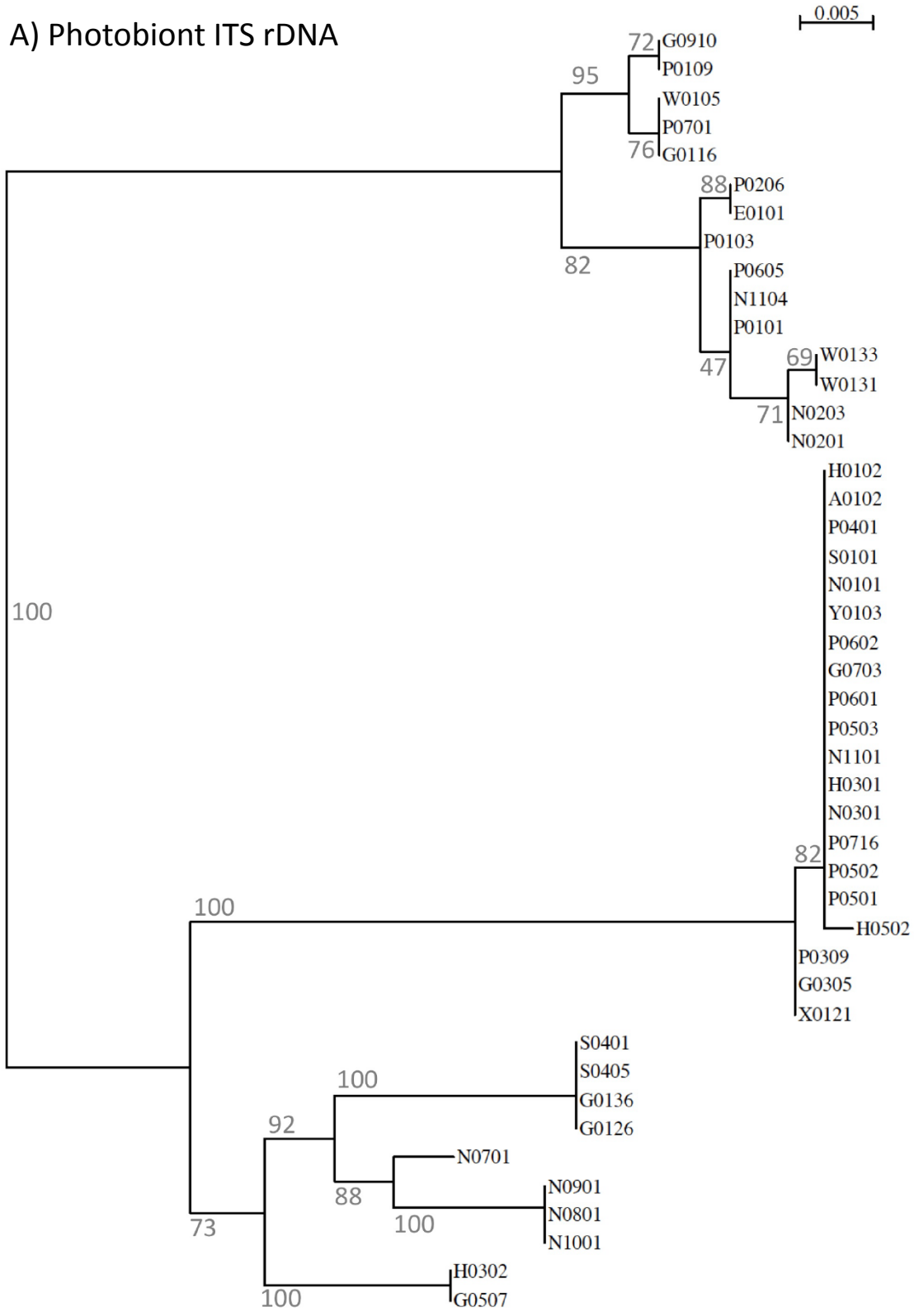

B) Photobiont COX2

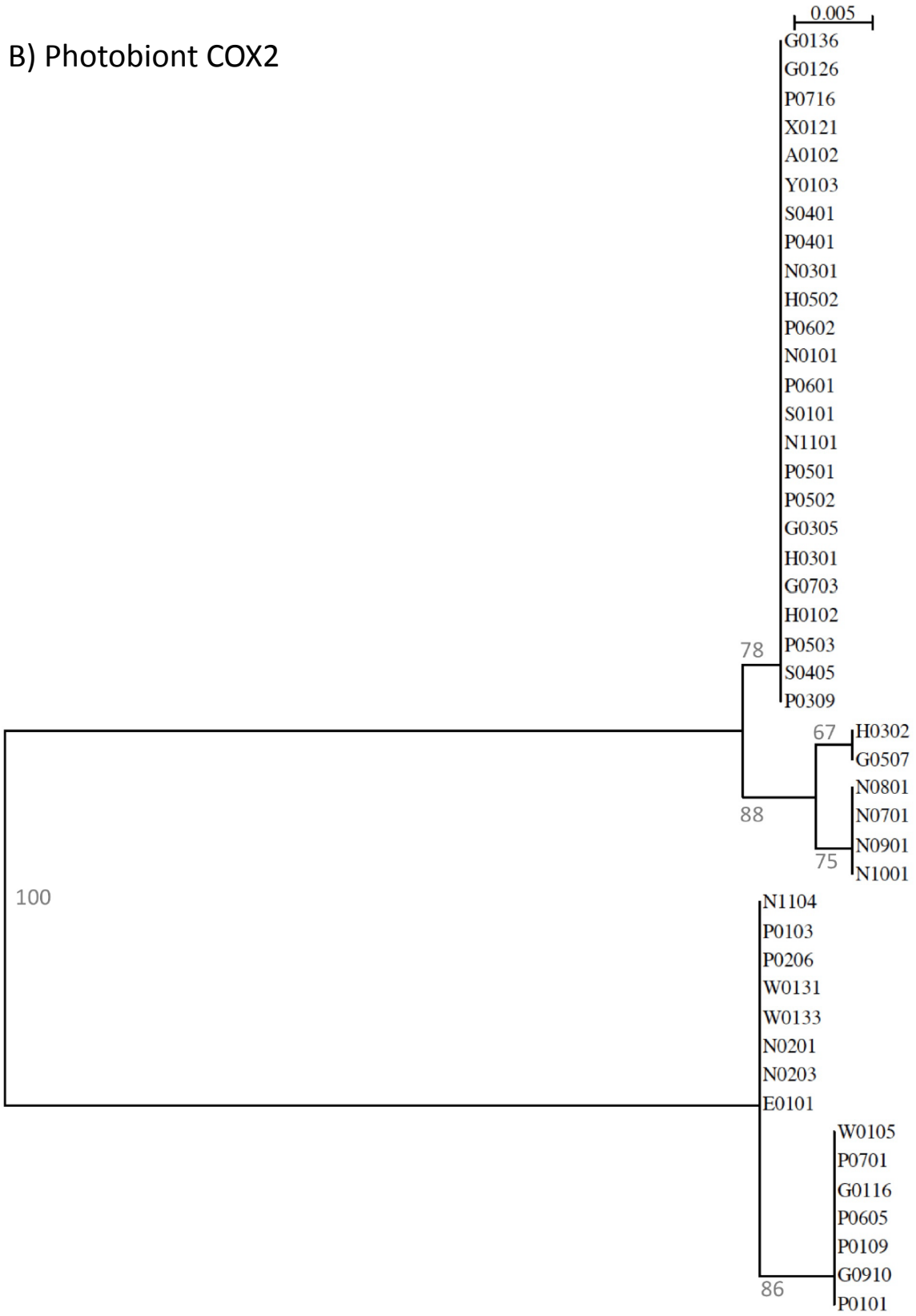

C) Photobiont *psbJ-L*

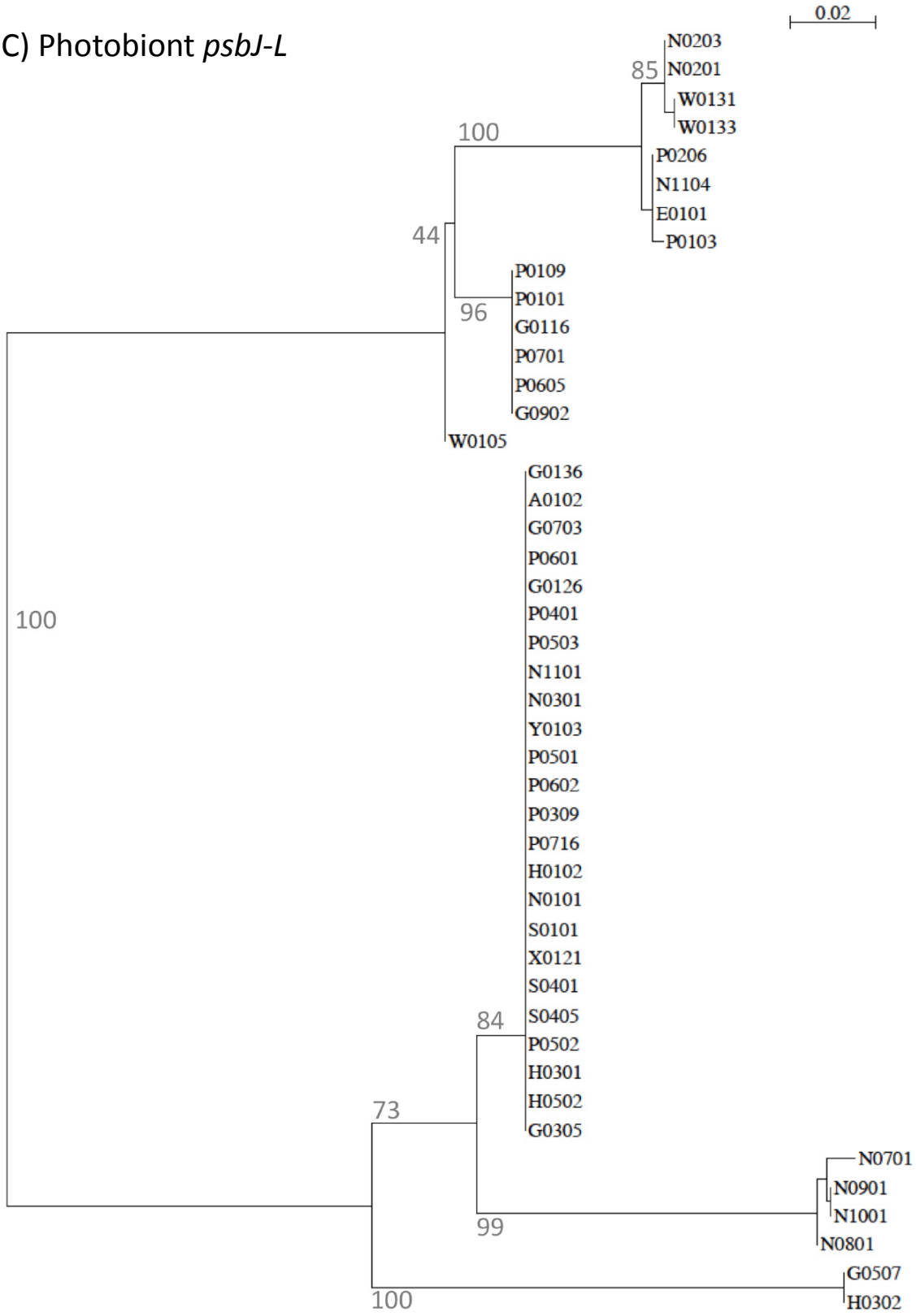

D) Photobiont *rbcL*

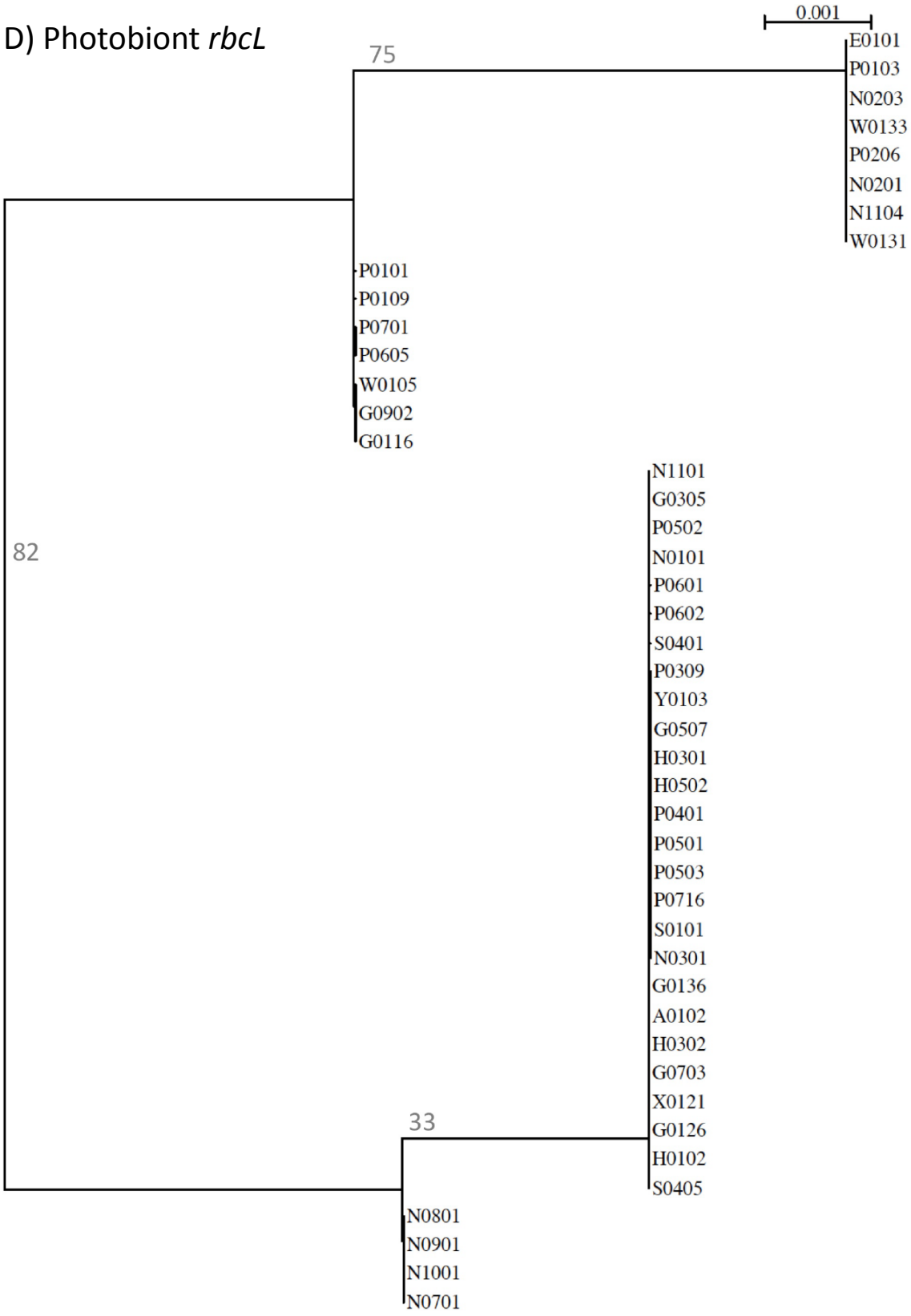

E) Mycobiont *MCM7*

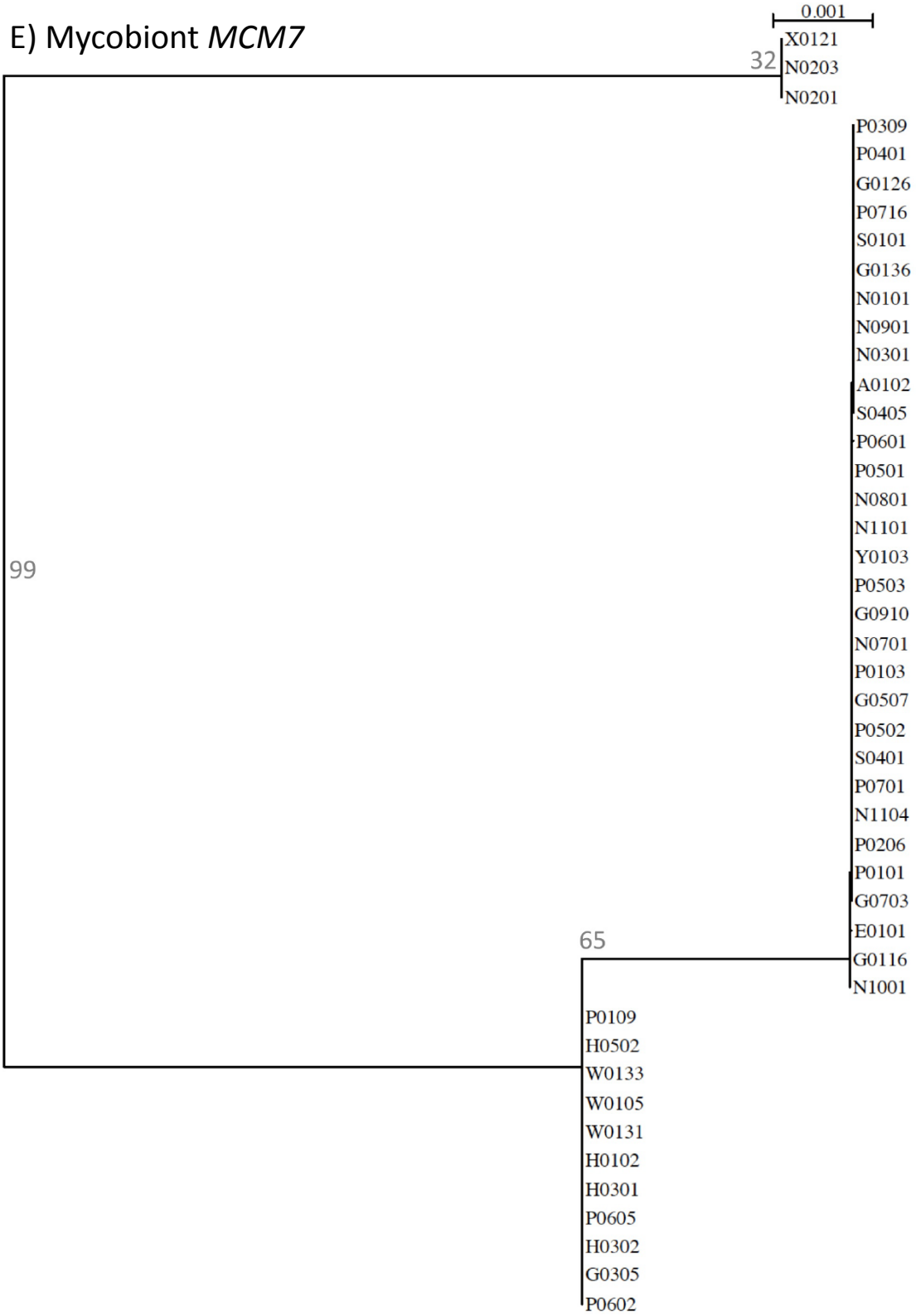

E) Mycobiont *TSR1*

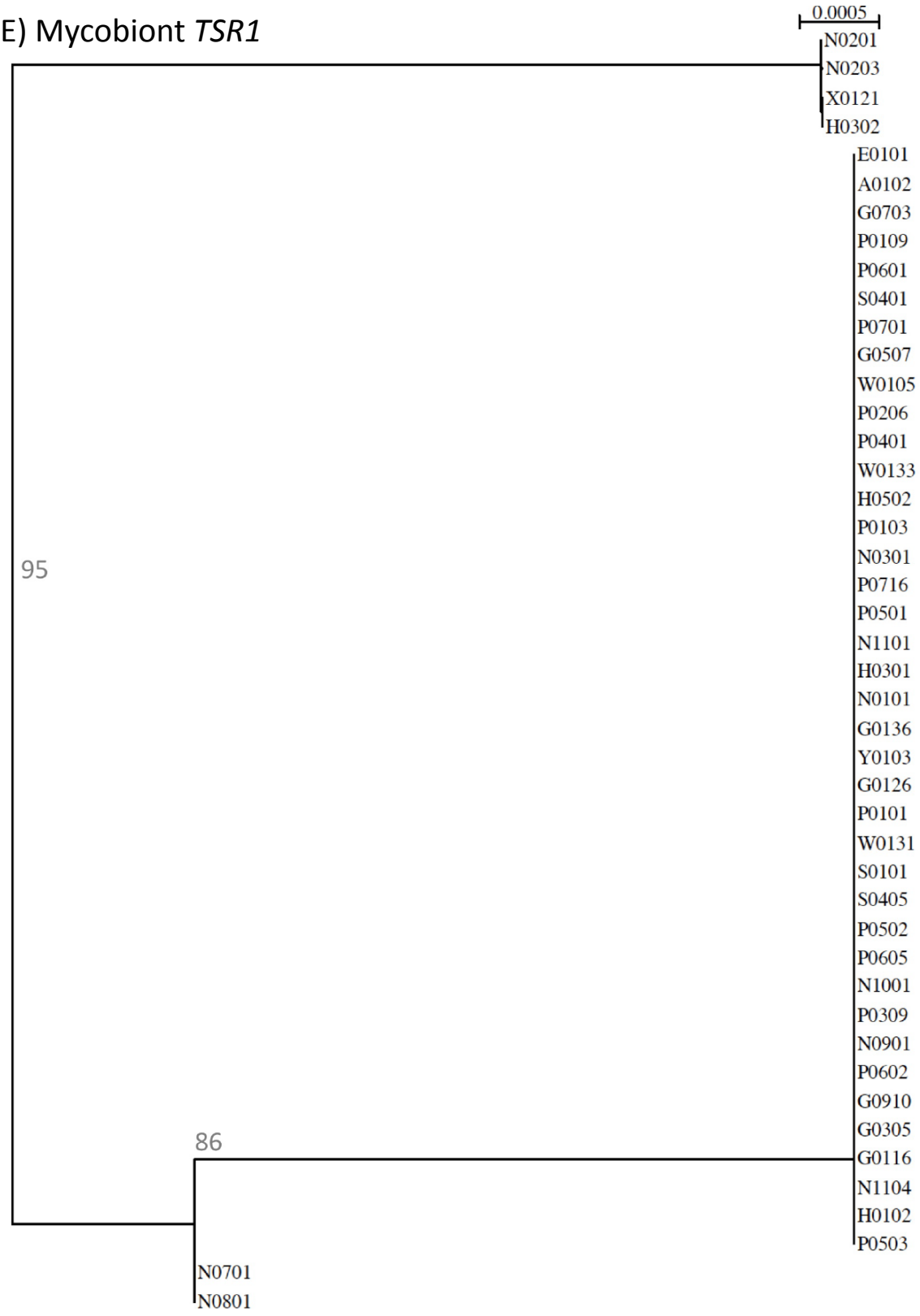

F) Mycobiont mtLSU

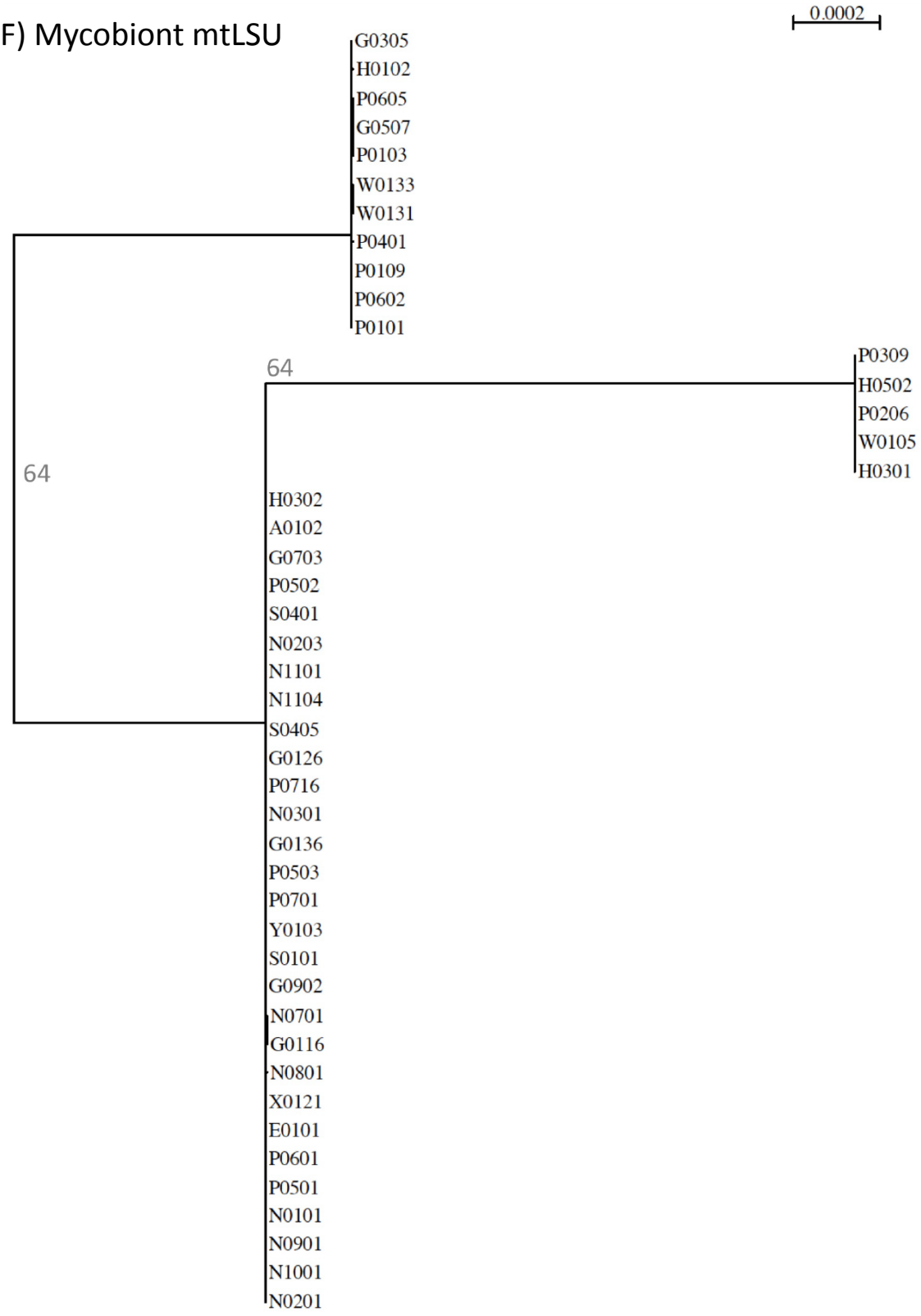

G) Mycobiont mtSSU

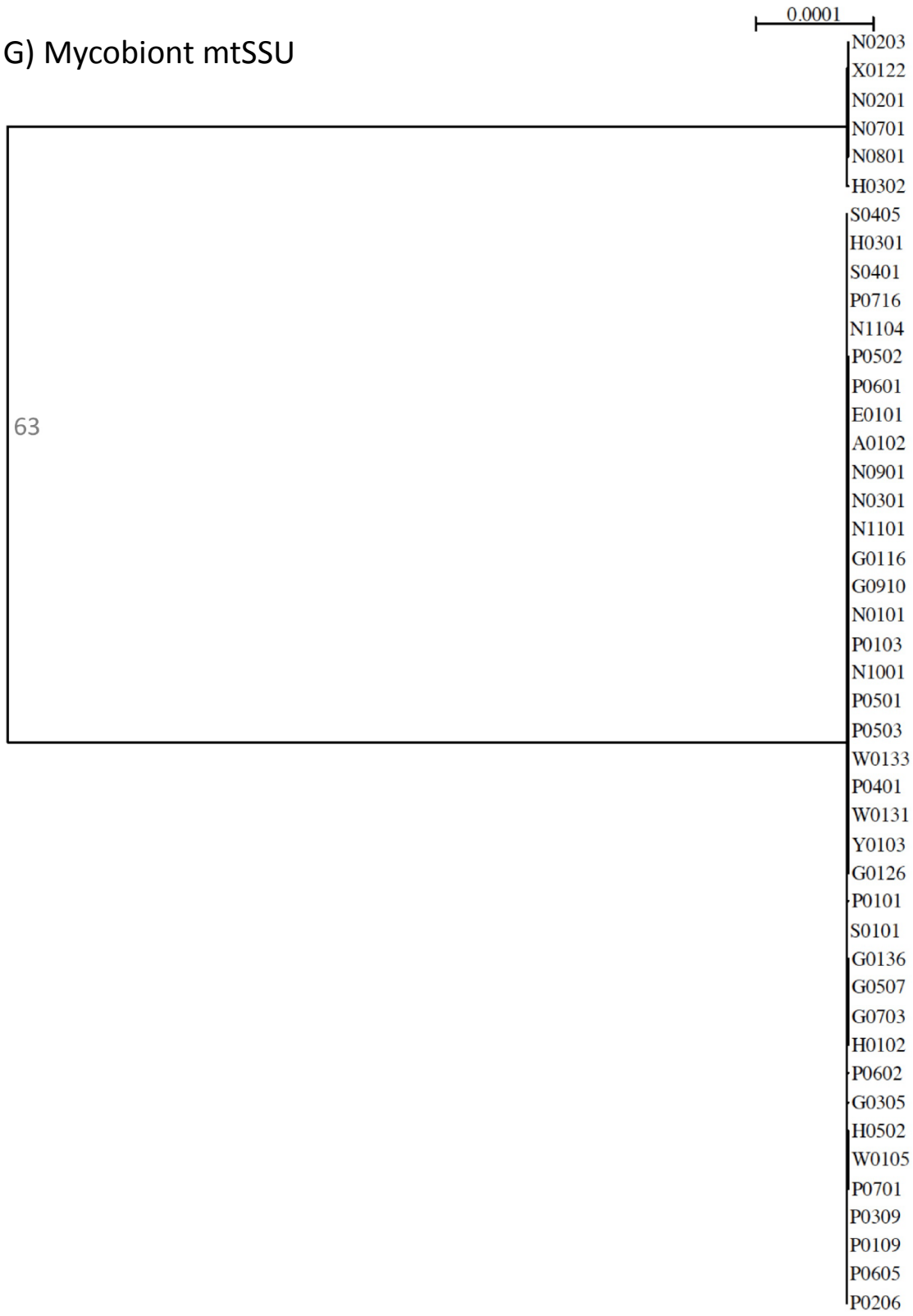

APPENDIX 1 B: Corrigendum to "Assessing intraspecific diversity in a lichen-forming fungus and its green algal symbiont: Evaluation of eight molecular markers.

FUNGAL ECOLOGY 6 (2013) 466–470

available at www.sciencedirect.com

SciVerse ScienceDirect

journal homepage: www.elsevier.com/locate/funeco

Corrigendum

Corrigendum to "Assessing intraspecific diversity in a lichen-forming fungus and its green algal symbiont: Evaluation of eight molecular markers" [Fungal Ecology (2012) 141–151]

Anna D. SADOWSKA-DEŚ[a,b], *Miklós BÁLINT*[a,c], *Jürgen OTTE*[a], *Imke SCHMITT*[a,b,*]

[a]*LOEWE Biodiversity and Climate Research Centre (BiK-F), Senckenberg Gesellschaft für Naturforschung, Senckenberganlage 25, D-60325 Frankfurt am Main, Germany*
[b]*Department of Biological Sciences, Goethe Universität Frankfurt, Max-von-Laue-Str. 9, D-60438 Frankfurt am Main, Germany*
[c]*Molecular Biology Center, Babeş-Bolyai University, Treboniu Laurian 42, 400270 Cluj, Romania*

The authors regret that the GenBank Accession Numbers in Table 1 were not listed in the correct fields. Please see corrected Table 1, below:

The authors would like to apologise for any inconvenience caused.

Table 1 – Material used in the current study and GenBank accession numbers. Herbarium acronyms follow Thiers (2012).

# of individual	Source	Photobiont				Mycobiony			
		nrITS rDNA	COX2	psbJ-L	*rbcL*	MCM7	TSR1	mtLSU rDNA	mtSSU rDNA
A0102	Austria, Styria, hiking path to Sporiroa-Ofen, 760 m, lat. 46.926469, long. 15.178028, leg. Sadowska-Deś, 27.07.2011 (FR)	JX474350	JX474260	JX844318	JX474305	JX474440	JX474485	JX474530	JX474395
E0101	Estonia, Lääne-Virumaa Lahemaa Rahvuspark, Vihula vald, lat. 59.5156104, long. 25.9356541, leg. Jüriado, 31.07.2008 (TU)	JX474351	JX474261	JX844319	JX474306	JX474441	JX474486	JX474531	JX474396
G0116	Germany, Hesse, Eppstein, 342 m, lat. 50.13949, long. 8.40439, leg. Sadowska-Deś, Nuñez Zapata, Schmitt, 26.05.2011 (FR)	JX474337	JX474247	JX844305	JX474292	JX474427	JX474472	JX474517	JX474382

DOI of original article: http://dx.doi.org/10.1016/j.funeco.2012.12.001.
* *Corresponding author*. Senckenberg Gesellschaft für Naturforschung, Senckenberganlage 25, D-60325 Frankfurt am Main, Germany. Tel.: +49 69 7542 1855; fax: +49 69 7542 1800.
E-mail address: imke.schmitt@senckenberg.de (I. Schmitt).

http://dx.doi.org/10.1016/j.funeco.2013.06.001

Table 1 – (continued)

# of individual	Source	Photobiont				Mycobiony			
		nrITS rDNA	COX2	psbJ-L	*rbcL*	*MCM7*	TSR1	mtLSU rDNA	mtSSU rDNA
G0126	Germany, Hesse, Eppstein, 342 m, lat. 50.13949, long. 8.40439, leg. Sadowska-Deś, Nuñez Zapata, Schmitt, 26.05.2011 (FR)	JX474338	JX474248	JX844306	JX474293	JX474428	JX474473	JX474518	JX474383
G0136	Germany, Hesse, Eppstein, 342 m, lat. 50.13949, long. 8.40439, leg. Sadowska-Deś, Nuñez Zapata, Schmitt, 26.05.2011 (FR)	JX474339	JX474249	JX844307	JX474294	JX474429	JX474474	JX474519	JX474384
G0305	Germany, Saarland, Lohfelden, Elsenfels, 400 m, lat. 49.59647222, long. 7.00676389, leg. Sadowska-Deś, John, Nuñez Zapata, Schmitt 17.06.2011 (FR)	JX474347	JX474257	JX844315	JX474302	JX474437	JX474482	JX474527	JX474392
G0507	Germany, Saarland, Orscholz, 300 m, lat. 49.500876, long. 6.542163, leg. Sadowska-Deś, John, Nuñez Zapata, Schmitt 17.06.2011 (FR)	JX474348	JX474258	JX844316	JX474303	JX474438	JX474483	JX474528	JX474393
G0703	Germany, Thuringia, Bad Blankenburg, Ingoklippefelsen, 309 m, lat. 50.664914, long. 11.246982, leg. Sadowska-Deś, 25.06.2011 (FR)	JX474349	JX474259	JX844317	JX474304	JX474439	JX474484	JX474529	JX474394
G0910	Germany, Saxony-Anhalt, Bodetal, Rosstrappe, 403 m, lat. 51.735064, long. 11.246982, leg. Sadowska-Deś, 13.08.2011 (FR)	JX474358	JX474268	JX844326	JX474313	JX474448	JX474493	JX474538	JX474403
H0102	Hungary, Baranya district, Kővágószőlős, Mecsek Mts, Jakab-hegy, Zsongor-kő, 450 m, lat. 46.09083333, long. 18.1330555, leg. Farkas, Lőkös, 30.10.2010 (HB Farkas-268)	JX474354	JX474264	JX844322	JX474309	JX474444	JX474489	JX474534	JX474399
H0301	Hungary, Baranya district, Kővágószőlős, Mecsek Mts, Jakab-hegy, Babas-szerkovek, 410 m, lat. 46.09194444, long. 18.12916667 leg. Farkas, Lőkös, 30.10.2010 (HB Farkas-270)	JX474355	JX474265	JX844323	JX474310	JX474445	JX474490	JX474535	JX474400
H0302	Hungary, Baranya district, Kővágószőlős, Mecsek Mts, Jakab-hegy, Babas-szerkovek, 410 m, lat. 46.09194444, long. 18.12916667, leg. Farkas, *Lőkös*, 07.04. 2011 (HB Farkas-311)	JX474356	JX474266	JX844324	JX474311	JX474446	JX474491	JX474536	JX474401
H0502	Hungary, Pest District, Kamence, Borzsony Mts, Nagy-Mána, 695 m, lat. 46.09083333, long. 18.13305556, leg. Farkas, *Lőkös*, *Molnár*, 07.05.2011 (HB Farkas-346)	JX474357	JX474267	JX844325	JX474312	JX474447	JX474492	JX474537	JX474402
N0101	Norway, Aust – Agder, Lillesand: Hellekilen, 1 m, lat. 58.698777, long. 8.088226, leg. Klepsland, Jon, 07.06.2009, L164675 (O)	JX474333	JX474243	JX844301	JX474288	JX474423	JX474468	JX474513	JX474378

(*continued on next page*)

Table 1 – (*continued*)

# of individual	Source	Photobiont				Mycobiony			
		nrITS rDNA	COX2	psbJ-L	*rbcL*	*MCM7*	*TSR1*	mtLSU rDNA	mtSSU rDNA
N0201	Norway, Hedmark, Ringdaker: Brøttum sag, 125 m, lat. 60.062922, long. 10.737061, 11.05.2008, L159236 (O)	JX474328	JX474238	JX844296	JX474283	JX474418	JX474463	JX474508	JX474373
N0203	Norway, Hedmark, Ringsaker: Brøttum sag, 125 m, lat. 60.910672, long. 10.737061, leg. Breili, Anders, 11.05.2008, L159236 (O)	JX474345	JX474255	JX844313	JX474300	JX474435	JX474480	JX474525	JX474390
N0301	Norway, Akershus, Ski: Norde Bjørke, 110 m, lat. 60.062922, long. 11.375427, leg. Breili, Anders, 18.06.2006, L150858 (O)	JX474365	JX474275	JX844333	JX474320	JX474455	JX474500	JX474545	JX474410
N0701	Norway, Oppland, Vågå: Russvassbue, 1185 m, lat. 61.11926, long. 10.466137, leg. Haugan, 24.06.2008, L160450 (O)	JX474331	JX474241	JX844330	JX474286	JX474421	JX474497	JX474511	JX474376
N0801	Norway, Oppland, Vågå: Trollhø, 1300 m, lat. 61.752031, long. 9.050303, leg. Breili, Anders, 25.03.2005, L142521 (O)	JX474332	JX474242	JX844300	JX474287	JX474422	JX474467	JX474512	JX474377
N0901	Norway, Rogland, Vindafjord: Saltvika, 1 m, lat. 59.301234, long. 5.985718, leg. Jordal, 02.09.2008, L155335 (O)	JX474329	JX474239	JX844297	JX474284	JX474419	JX474464	JX474509	JX474374
N1001	Norway, Sogn Og Fjordane, Edi: Hamnest, 2 m, lat. 61.665375, long. 6.315307, leg. Breili, Anders, 08.04.2009, L159494 (O)	JX474330	JX474240	JX844298	JX474285	JX474420	JX474465	JX474510	JX474375
N1101	Norway, Vestfold, Larvik, Stavern, 20 m, lat. 58.983333, long. 10.03333, leg. Rui, Timdal, 02.04.2011, L169175 (O)	JX474364	JX474274	JX844332	JX474319	JX474454	JX474499	JX474544	JX474409
N1104	Norway, Vestfold, Larvik, Stavern, 20 m, lat. 58.983333, long. 10.03333, leg. Rui, Timdal, 02.04.2011, L169175 (O)	JX474344	JX474254	JX844312	JX474299	JX474434	JX474479	JX474524	JX474389
P0101	Poland, Lower Silesia, Sobieszów, Zbójeckie Skały, 600 m, lat. 51.0244444, long. 15.904444, leg. Sadowska-Deś, 23.06.2011 (FR)	JX474327	JX474237	JX844295	JX474282	JX474417	JX474462	JX474507	JX474372
P0103	Poland, Lower Silesia, Sobieszów, Zbójeckie Skały, 600 m, lat. 51.0244444, long. 15.904444, leg. Sadowska-Deś, 23.06.2011 (FR)	JX474340	JX474250	JX844308	JX474295	JX474430	JX474475	JX474520	JX474385
P0109	Poland, Lower Silesia, Sobieszów, Zbójeckie Skały, 600 m, lat. 51.0244444, long. 15.904444, leg. Sadowska-Deś, 23.06.2011 (FR)	JX474367	JX474277	JX844335	JX474322	JX474457	JX474502	JX474547	JX474412
P0206	Poland, Lower Silesia, Sobieszów, Chojnik Hill, 530 m, lat. 50.83333, long. 15.63333, leg. Sadowska-Deś, 23.06.2011 (FR)	JX474346	JX474256	JX844314	JX474301	JX474436	JX474481	JX474526	JX474391
P0309	Poland, Lower Silesia, Sobieszów, Chojnik Castle, 530 m, lat. 50.833725, long. 15.644181, leg. Sadowska-Deś, 29.08.2011 (FR)	JX474341	JX474251	JX844309	JX474296	JX474431	JX474476	JX474521	JX474386

Table 1 – (*continued*)

# of individual	Source	Photobiont				Mycobiony			
		nrITS rDNA	COX2	psbJ-L	*rbcL*	*MCM7*	TSR1	mtLSU rDNA	mtSSU rDNA
P0401	Poland, Lower Silesia, Izery Mts, Bobrowe Skały, 699 m, lat. 50.866666, long. 15.58333, leg. Sadowska-Deś, 25.08.2011 (FR)	JX474366	JX474276	JX844334	JX474321	JX474456	JX474501	JX474546	JX474411
P0501	Poland, Lower Silesia, Ostrzyca Proboszczowicka, Kaczawskie Mts, 501 m, lat. 51.14888889, long. 15.96944444, leg. Sadowska-Deś, 02.09.2011 (FR)	JX474326	JX474236	JX844294	JX474281	JX474416	JX474461	JX474506	JX474371
P0502	Poland, Lower Silesia, Ostrzyca Proboszczowicka, Kaczawskie Mts, 501 m, lat. 51.14888889, long. 15.96944444, leg. Sadowska-Deś, 02.09.2011 (FR)	JX474342	JX474252	JX844310	JX474297	JX474432	JX474477	JX474522	JX474387
P0503	Poland, Lower Silesia, Ostrzyca Proboszczowicka, Kaczawskie Mts, 501 m, lat. 51.14888889, long. 15.96944444, leg. Sadowska-Deś, 02.09.2011 (FR)	JX474343	JX474253	JX844311	JX474298	JX474433	JX474478	JX474523	JX474388
P0601	Poland, Lower Silesia, Rudawy Janowickie, Bolczów Castle, 561 m, lat. 51.03388889, long. 16.08972222, leg. Sadowska-Deś, 30.09.2011 (FR)	JX474325	JX474235	JX844293	JX474280	JX474415	JX474460	JX474505	JX474370
P0602	Poland, Lower Silesia, Rudawy Janowickie, Bolczów Castle, 561 m, lat. 51.03388889, long. 16.08972222, leg. Sadowska-Deś, 30.09.2011 (FR)	JX474323	JX474233	JX844291	JX474278	JX474413	JX474458	JX474503	JX474368
P0605	Poland, Lower Silesia, Rudawy Janowickie, Bolczów Castle, 561 m, lat. 51.03388889, long. 16.08972222, leg. Sadowska-Deś, 30.09.2011 (FR)	JX474324	JX474234	JX844292	JX474279	JX474414	JX474459	JX474504	JX474369
P0701	Poland, Lower Silesia, Jelenia Góra, 383 m, lat. 50.873319, long. 15.761103, leg. J., Z. Sadowscy, 12.09.2011 (FR)	JX474362	JX474272	JX844299	JX474317	JX474452	JX474466	JX474542	JX474407
P0716	Poland, Lower Silesia, Jelenia Góra, 383 m, lat. 50.873319, long. 15.761103, leg. J.,Z. Sadowscy, 12.09.2011 (FR)	JX474363	JX474273	JX844331	JX474318	JX474453	JX474498	JX474543	JX474408
S0101	Spain, Ávila, Garganta de Chilla, 1700 m, lat. 40.2325, long. -5.30722222, leg. Vivas Rebuelta, 11.07.2010 (FR)	JX474334	JX474244	JX844302	JX474289	JX474424	JX474469	JX474514	JX474379
S0401	Spain, Ávila, Garganta de Chilla, 1000 m, lat. 40.206666, long. -5.29472222, leg. Vivas Rebuelta, 11.07.2010 (FR)	JX474335	JX474245	JX844303	JX474290	JX474425	JX474470	JX474515	JX474380
S0405	Spain, Ávila, Garganta de Chilla, 1000 m, lat. 40.206666, long. -5.29472222, leg. Vivas Rebuelta, 11.07.2010 (FR)	JX474336	JX474246	JX844304	JX474291	JX474426	JX474471	JX474516	JX474381
W0105	Slovakia, Tribeč Mts, Zobor Mts: Nitra, 546 m, lat. 48.337255, long. 18.10623, leg. Guttova, 27.07.2011 (FR)	JX474359	JX474269	JX844327	JX474314	JX474449	JX474494	JX474539	JX474404

(*continued on next page*)

Table 1 – (*continued*)

# of individual	Source	Photobiont				Mycobiony			
		nrITS rDNA	*COX2*	psbJ-L	*rbcL*	*MCM7*	*TSR1*	mtLSU rDNA	mtSSU rDNA
W0131	Slovakia, Tribeč Mts, Zobor Mts: Nitra, 546 m, lat. 48.337255, long. 18.10623, leg. Guttova, 27.07.2011 (FR)	JX474360	JX474270	JX844328	JX474315	JX474450	JX474495	JX474540	JX474405
W0133	Slovakia, Tribeč Mts, Zobor Mts: Nitra, 546 m, lat. 48.337255, long. 18.10623, leg. Guttova, 27.07.2011 (FR)	JX474361	JX474271	JX844329	JX474316	JX474451	JX474496	JX474541	JX474406
X0121	Portugal, Algarve, Serra de Monchique, 890 m, lat. 37.317139, long. -8.590722, leg. Divakar, Agudo, Ruibal, 19.05.2011 (FR)	JX474352	JX474262	JX844320	JX474307	JX474442	JX474487	JX474532	JX474397
Y0103	Serbia, Pčinja District, Surdulica, Vardenik Mts, 1640 m, lat. 42.647805, long. 22.261555, leg. *Lőkös*, 24.06.2011 (HB Farkas-446)	JX474353	JX474263	JX844321	JX474308	JX474443	JX474488	JX474533	JX474398

APPENDIX 2: Integrating coalescent and phylogenetic approaches to delimit species in the lichen photobiont *Trebouxia.*

STATEMENT OF JOINT AUTHORSHIP

Published in Molecular Phylogenetics and Evolution (online on 28 March 2014, printed in volume 76 on July 2014, Pages 202-210, DOI: 10.1016/j.ympev.2014.03.020)

Involved authors: Anna D. Sadowska-Deś, Francesco Dal Grande, H. Thorsten Lumbsch, Andreas Beck, Jürgen Otte, Jae-Seoun Hur, Jung A. Kim, Imke Schmitt

What did the Ph.D. student or the Co-Authors contribute to this work?

(1) Development and planning:

Anna D. Sadowska-Deś	30%
Francesco Dal Grande	20%
H. Thorsten Lumbsch	20%
Imke Schmitt	10%

(2) Performance of the individual investigations and experiments

(2a) Fieldwork 30%

Anna D. Sadowska-Deś	95%	Collected most of the lichen material.
Imke Schmitt	5%	Assisted with obtaining permits.

(2b) Labwork 70%

Anna D. Sadowska-Deś	30%	Samples preparation, DNA extraction, PCR and sequencing.
Jürgen Otte	50%	Conducted most of the DNA extraction, PCR and sequencing.

Andreas Beck Jae-Seoun Hur Jung A. Kim Anna D. Sadowska-Deś	20%	Cultivation of the photobionts.

(3) Preparation of the data collection and figures

Anna D. Sadowska-Deś	70%	Conducted sequence alignments, produced all figures and tables.
Francesco Dal Grande	20%	Helped in data generation.
Imke Schmitt	10%	Provided feedback on preparation of the data and the figures.

(4) Analyses and interpretation of data

Anna D. Sadowska-Deś	30%	Conducted phylogenetic analyses, species delimitation analyses, photobiont sharing analysis, interpreted data, carried out literature search.
Francesco Dal Grande	30%	Helped in the data analyses and interpretation of data, literature search.
H. Thorsten Lumbsch	10%	Provided feedback on data analyses.
Imke Schmitt	20%	Helped in the interpretation of the results and literature search.
Andreas Beck Jae-Seoun Hur Jung A. Kim Anna D. Sadowska-Deś	10%	Performed morphological analyses of the cultivated photobionts

(5) Writing the manuscript

Anna D. Sadowska-Deś	60%
Francesco Dal Grande	30%

H. Thorsten Lumbsch Andreas Beck Imke Schmitt	10%

Date/Place: 25.07.2019 /Frankfurt am Main

Signature of the Ph.D. Student: Anna Sadowska-Deś

Verification of the statement above:

Signature of the Supervisor: J. Sch. Date/Place: 25.07.2019/Frankfurt am Main

Molecular Phylogenetics and Evolution 76 (2014) 202–210

Contents lists available at ScienceDirect

Molecular Phylogenetics and Evolution

journal homepage: www.elsevier.com/locate/ympev

Integrating coalescent and phylogenetic approaches to delimit species in the lichen photobiont *Trebouxia*

Anna D. Sadowska-Deś [a,b,*,1], Francesco Dal Grande [b,1], H. Thorsten Lumbsch [c], Andreas Beck [d,e], Jürgen Otte [b], Jae-Seoun Hur [f], Jung A. Kim [f], Imke Schmitt [a,b,*]

[a] Department of Biological Sciences, Institute of Ecology, Evolution and Diversity, Goethe Universität, Max-von-Laue-Str. 13, D-60438 Frankfurt, Germany
[b] Biodiversity and Climate Research Centre (BiK-F), Senckenberg Gesellschaft für Naturforschung, Senckenberganlage 25, D-60325 Frankfurt, Germany
[c] Science & Education, The Field Museum, 1400 S. Lake Shore Drive, Chicago, IL 60605, USA
[d] Department of Lichenology and Bryology, Botanische Staatssammlung München, Menzinger Straße 67, D-80638 München, Germany
[e] GeoBio-Center, Ludwig-Maximilians Universität München, Richard-Wagner-Str. 10, D-80333 München, Germany
[f] Korean Lichen Research Institute, Sunchon National University, Suncheon 540-742, South Korea

ARTICLE INFO

Article history:
Received 7 October 2013
Revised 4 March 2014
Accepted 17 March 2014
Available online 28 March 2014

Keywords:
Terrestrial green algae
Cryptic species
Environmental specialization
Photobiont sharing
Lasallia pustulata

ABSTRACT

The accurate assessment of species boundaries in symbiotic systems is a prerequisite for the study of speciation, co-evolution and selectivity. Many studies have shown the high genetic diversity of green algae from the genus *Trebouxia*, the most common photobiont of lichen-forming fungi. However, the phylogenetic relationships, and the amount of cryptic diversity of these algae are still poorly understood, and an adequate species concept for trebouxiophycean algae is still missing. In this study we used a multifaceted approach based on coalescence (GMYC, STEM) and phylogenetic relationships to assess species boundaries in the trebouxioid photobionts of the lichen-forming fungus *Lasallia pustulata*. We further investigated whether putative species of *Trebouxia* found in *L. pustulata* are shared with other lichen-forming fungi. We found that *L. pustulata* is associated with at least five species of *Trebouxia* and most of them are shared with other lichen-forming fungi, showing different patterns of species-to-species and species-to-community interactions. We also show that one of the putative *Trebouxia* species is found exclusively in association with *L. pustulata* and is restricted to thalli from localities with Mediterranean microclimate. We suggest that the species delimitation method presented in this study is a promising tool to address species boundaries within the heterogeneous genus *Trebouxia*.

1. Introduction

Cryptic diversity is a common phenomenon in many groups of organisms (e.g. Bálint et al., 2011; Bickford et al., 2007; Hebert et al., 2004; Lumbsch and Leavitt, 2011). Different lineages of species can display different adaptive responses to environmental changes, thus overlooking cryptic diversity may lead to inefficient conservation practices (Pauls et al., 2013). Furthermore, in symbiotic associations, it is important to assess diversity of symbiotic partners at the species level to understand patterns of co-evolution and co-distribution. A correct assessment of species boundaries may provide information about species-to-species and species-to-community interactions, as well as co-distribution and co-speciation. For example, it has been proposed that lichen-forming fungi form ecological guilds by sharing the same algae. These horizontally linked fungal networks may become evident once the system is studied at the level of species and communities (Rikkinen, 2002).

Lichens are symbiotic systems composed of at least one fungal partner (mycobiont) and green algae and/or cyanobacteria (photobiont). Generally, more than one lichen-forming fungus forms associations with a single algal lineage (Friedl and Büdel, 2008). Recent studies using a combination of molecular, chemical and morphological data have shown that several groups of lichen-forming fungi may include cryptic species (Crespo and Lumbsch, 2010; Crespo and Perez-Ortega, 2009). Some studies have also highlighted the presence of cryptic diversity in algae associated with lichen-forming fungi, e.g. in the genera *Asterochloris* and *Trebouxia* (Casano et al., 2011; Škaloud and Peksa, 2010). The coccoid green algae of the genus *Trebouxia* are the most common

* Corresponding authors at: Biodiversity and Climate Research Centre (BiK-F), Senckenberg Gesellschaft für Naturforschung, Senckenberganlage 25, D-60325 Frankfurt, Germany.
E-mail addresses: Anna.Sadowska-Des@senckenberg.de (A.D. Sadowska-Deś), Imke.Schmitt@senckenberg.de (I. Schmitt).
[1] These authors contributed equally to this work.

http://dx.doi.org/10.1016/j.ympev.2014.03.020
1055-7903/

and widespread photobionts involved in symbiotic associations with fungi (Friedl and Büdel, 2008; Tschermak-Woess, 1988). Studies exploring the genetic diversity of *Trebouxia* did usually not go beyond designating phylogenetic clades with letters and numerals (Helms, 2003; Ruprecht et al., 2012; Yahr et al., 2006). Despite the fact that molecular phylogenies are often not entirely congruent with current taxonomy of *Trebouxia* (Blaha et al., 2006; Romeike et al., 2002), attempts to assign species in a systematic way based on molecular and morphological data are rare. A self-organizing classification tool based on algal sequence information and single strand conformation polymorphism (SSCP) analysis has been proposed (Grube and Muggia, 2010), however, it is not widely employed. At present we lack a clear understanding of species boundaries and species richness within this genus (Škaloud and Peksa, 2010).

The traditional way to describe species is based on phenotypical characters (e.g. Gärtner, 1985). When working with groups that show limited morphological characters, this approach may lead to underestimation of the real number of species. To improve the assessment of species boundaries there is need to test morphological characters together with molecular data (e.g. Knowles and Carstens, 2007; Welton et al., 2013). Some species delimitation methods assign samples to groups without a priori information, e.g. the general mixed Yule coalescent model (GMYC, Pons et al., 2006), Gaussian Clustering (Hausdorf and Hennig, 2010), Structurama (Huelsenbeck et al., 2011), or O'Meara's heuristic method (O'Meara, 2010), while others require prior assignment of samples to putative lineages such as species tree estimation using maximum likelihood for gene trees under coalescence (e.g. STEM, Kubatko et al., 2009). One of the first widely used methods based on molecular data was the genealogical concordance phylogenetic species approach comparing the presence of putative species in single-locus analyses (e.g. Avise and Ball, 1990; Kroken and Taylor, 2001; Taylor et al., 2000). This method accommodates for incomplete lineage sorting of several genes and evaluates concordance among single-gene trees. Although this method is widely used, it has been shown to be flawed when attempting to delimitate closely related species (Carstens et al., 2013). Clades that are present in the majority of single-locus genealogies are likely to represent isolated lineages (Dettman et al., 2003). In the GMYC method the species delimitation is based on branch length differences (Monaghan et al., 2009; Pons et al., 2006). This approach has been widely applied to delimit species in many different groups such as bats (Esselstyn et al., 2012), insects (Hamilton et al., 2011), snails (Puillandre et al., 2012), lizards (Wiens and Penkrot, 2002) and lichen-forming fungi (Leavitt et al., 2013, 2012; Parnmen et al., 2012). The assumption of GMYC models is that the independent evolution leads to appearance of genetically distinct clusters, which are separated by long internal branches (Barraclough et al., 2003; Fujisawa and Barraclough, 2013; Queiroz, 2007). Another widely used coalescence model is STEM (Kubatko et al., 2009), which was developed to assess species boundaries in systems with existing subspecies taxonomy (Carstens and Dewey, 2010). This test computes the gene tree probability for all hierarchical permutations of lineage groupings. In this method the species delimitation is not affected by the phylogenetic uncertainty in the species tree, however the correctness of the method depends on the accuracy of the gene tree (Carstens and Dewey, 2010).

In the present study we used a multifaceted approach combining phylogenetic and coalescent methods to delimit species boundaries in the trebouxioid photobiont of the lichen *Lasallia pustulata* (L.) Mérat. *Lasallia pustulata* is an umbilicate macrolichen reproducing mainly by asexual propagules (isidia). From this mode of reproduction we would expect little variability of the photobiont as a result of predominantly clonal dispersal. However, genetic variability of the photobiont in *L. pustulata* populations is in fact high (Sadowska-Deś et al., 2013), an observation that has also been made in other asexually reproducing lichen species (Dal Grande et al., 2012; Nelsen and Gargas, 2009; Ohmura et al., 2006; Opanowicz and Grube, 2004; Piercey-Normore, 2006, 2009; Werth and Sork, 2010; Wornik and Grube, 2010). These studies suggest that multiple photobiont species associate with a single fungal species, and that various photobionts may be commonly available in a given environment. In this study we aimed to answer the following questions: (i) is *Lasallia pustulata* associated with a single or multiple *Trebouxia* species?, and (ii) does the range of compatible photobiont partners found in *L. pustulata* overlap with that of other lichen-forming fungi?

2. Materials and methods

2.1. Taxon sampling

We collected specimens of *L. pustulata* across the species distribution range. Out of a total of 469 thalli we selected 22 samples that had a unique haplotype at either of four photobiont loci. Fresh samples were dried and stored at −20 °C until preparation. Information about sampling locality, haplotypes and GenBank accession numbers are given in Table S1. Specimens are deposited in the herbaria Berlin (B), Frankfurt (FR), and Oslo (O).

2.2. DNA isolation, polymerase chain reaction (PCR) amplification and sequencing

Total genomic DNA was extracted from a small part of the thallus using the CTAB method (Cubero and Crespo, 2002). We sequenced the algal symbiont at the following loci: internal transcribed spacer region (nrITS rDNA), chloroplast intergenic spacer (psbJ-L), cytochrome C oxidase II (*COX2*) and ribulose-bisphosphate carboxylase (*rbcL*). Primers for PCR amplification were: nrITS: nrITS1T, nrITS4T (Kroken and Taylor, 1990) and nrITSaJOFOR2, nrITSaJOREV2 (Sadowska-Deś et al., 2013); psbJ-L: psbF and psbR (Werth and Sork, 2008); *COX2*: Cox2-P2fw-50, Cox2-P2rv-30 (Fernandez-Mendoza et al., 2011); rbcL: a-ch-rbcL-203, a-ch-rbcL-991 (Nelsen et al., 2011).

Standard PCR amplification (25 μl) contained 0.65 U Ex Taq polymerase (TaKaRa BIO INC.), 1× buffer, 0.2 mM dNTP mixture, 0.5–1.0 μM of each primer, 2–50 ng DNA template, and H_2O. Thermal cycling parameters for all loci were: initial denaturation 95 °C for 4 min, followed by 35 cycles of 95 °C for 30 s, 50 °C for 40 s, 72 °C for 1 min, and final elongation 72 °C for 5 min. PCR products were separated on 1% agarose gels stained with ethidium bromide. When multiple bands were present, fragments of the expected length were extracted using the peq-GOLD Gel Extraction Kit (PEQLAB Biotechnologie GmbH). The amplicons were sequenced using Big Dye 3.1 chemistry (Applied Biosystems, Foster City, CA, USA). The following cycle sequencing program was used: initial denaturation for 1 min at 95 °C, followed by 30 cycles of 96 °C for 10 s, 50 °C for 10 s, 60 °C for 2 min. Products were run on an ABI PRISMTM 3730 DNA Analyzer (Applied Biosystems).

2.3. Sequence alignment

Sequences of each locus were aligned using the MUSCLE alignment algorithm (Edgar, 2004) as implemented in Geneious v5.4.2 (Drummond et al., 2011). Before the analysis, ambiguous regions from all loci were manually removed. We confirmed sequence identity by using BLAST searches in GenBank.

2.4. Phylogenetic analyses

To test the level of compatibility among loci, we applied the Congruence Among Distance Matrices test (CADM, Campbell et al., 2011; Legendre and Lapointe, 2004). The null hypothesis assumes that all tested phylogenetic trees are completely incongruent. We performed maximum likelihood (ML) and Bayesian analyses on the single-locus and the combined four-locus datasets.

ML analysis with 1000 bootstrap pseudoreplicates (Felsenstein, 1985) was performed on the concatenated dataset using RAxML v7.4.2 (Stamatakis, 2006) with the GTRGAMMA model implemented. We treated each locus as separate partition, as well as first, second and third codon positions of the protein-coding genes.

We conducted Bayesian analyses in MrBayes 3.2.1 (Huelsenbeck and Ronquist, 2001). The best-fitting model was selected with the corrected Akaike Information Criterion as implemented in jModelTest 2.1.1 (model SYM, −lnL = 1275.4812 for nrITS; model GTR, −lnL = 4089.2736 for psbJ-L; model GTR, −lnL = 992.0584 for *COX2* and model GTR, −lnL = 632.2397 for *rbcL*; Darriba et al., 2012; Guindon and Gascuel, 2003; Posada, 2008). We ran MrBayes for 10 million generations, and sampled one out of every 1000 trees. The first 40,000 trees were discarded as burn-in (likelihoods below stationary level). No molecular clock was assumed. Sequences of *Trebouxia decolorans* from the lichen *Anaptychia ciliaris* were used as outgroup in all analyses.

The phylogenetic trees were visualized using FigTree v 1.4.0 (Morariu et al., 2009). All clades with ML equal or above 75% and posterior probabilities (PP) equal or greater than 0.95 were considered as strongly supported (Fig. 1).

2.5. Identification of putative species

We applied a GMYC approach (Monaghan et al., 2009; Pons et al., 2006) to identify putative species. This method uses chronograms for comparison of the following models: (i) null model which assumes that all samples derived from one population and (ii) alternative GMYC model which identifies intraspecific and interspecific relationships based on different branch lengths and position of nodes that define putative species. Based on the likelihood ratio test (LRT) the null hypothesis can be rejected, and if the GMYC model is significantly better than null model, the number of putative species within dataset can be estimated.

To calculate the number of species we used the chronogram calculated from the Bayesian tree of the combined dataset. Subsequently we applied single and multiple threshold methods by using the GMYC package implemented in SPLITS in R v2.15.3 (Meyer et al., 2011). A chronogram was calculated based on the penalized likelihood method (Sanderson, 2002) and obtained by using the "chronopol" command in the package *ape* (Meyer et al., 2011). Outgroup sequences were excluded from the dataset using the drop.tip command. To convert the chronogram into a fully dichotomous chronogram we used multidivtime (Thorne and Kishino, 2002). The lineages-through-time plot (Fig. 2) shows the overall pattern of diversification over time. The number of reconstructed lineages is depicted by a line. Time is presented as a proportion of the total time since the first cladogenesis event inferred for the taxon. The two vertical lines show sharp increases in branching rate, which indicate the change from interspecies to intraspecies branching events. We summarized the analysis to obtain indication of the number of recognized lineages.

We used *BEAST (Heled and Drummond, 2010) implemented in the program BEAST v.1.7.5 (Drummond et al., 2012) to estimate species trees from putative species-level lineages and supported clades. We employed STEM (Kubatko et al., 2009) to generate species trees based on different species delimitation scenarios. To obtain likelihood scores for alternative species delimitation scenarios we followed the protocol by Carstens and Dewey (2010). We tested the following scenarios: 1-species scenario, 2-species scenario, 4-species scenario based on multiple threshold of GMYC, 5-species scenario, and the 6-species scenario based on a combination of multiple threshold of GMYC and phylogeny.

In addition we also used a genealogical concordance approach (Avise and Ball, 1990). This approach recognizes species based on presence of clades in the majority of single-locus genealogies (Dettman et al., 2003, 2008).

2.6. Photobiont sharing analysis

We performed BLAST searches with each nrITS haplotype of the photobiont of *L. pustulata* to find other lichen-forming fungi that are associated with the same algal strains. We set the identity threshold to 98%. A heatmap of the lichen-forming fungi and algal nrITS haplotypes was made using the package *pheatmap* in R.

3. Results

3.1. Congruence of the data

To assess the congruence of the four loci we performed CADM test (Campbell et al., 2011; Legendre and Lapointe, 2004). The null hypothesis, which assumes complete incongruence of the phylogenetic trees, was rejected for all examined loci. Kendall's coefficient of concordance (W) showed that nrITS and psbJ-L were completely congruent with other loci (W = 0.982, $p = 0.001$), whereas *rbcL* and *COX2* were partially congruent (W = 0.581, $p = 0.03$; Table S2). Additionally, we checked the phylogenetic congruence by comparing ML trees of all single loci (Fig. S1). No supported conflicts between single-loci ML phylogenetic trees were found that could influence the compatibility of the combined dataset. According to these tests all datasets of nrITS rDNA, psbJ-L, *COX2* and *rbcL* are congruent and can be analyzed simultaneously in one combined dataset.

3.2. Phylogenetic analysis

The alignment length of the concatenated dataset was 2566 base pairs (nrITS rDNA ~430 bp; psbJ-L ~558 bp; *COX2* ~419 bp, and *rbcL* ~441 bp), including 328 variable positions. Statistical information about sequences used in this study is included in Table 1. The presence of outgroups, especially for psbJ-L, changed the length of the alignment and number of variable characters.

The phylogenetic tree (Fig. 1) was divided into two main clades and five subclades. The first subclade comprising of four haplotypes (001, 002, 003, 004) was highly supported (ML = 99%, PP = 1). The second subclade was divided into a single haplotype 009 (ML = 100%, PP = 0.98), sister to a clade including haplotypes 005, 006, 007 and 008 (ML = 81%, PP = 0.98). Haplotypes 010, 011, 012 formed a highly supported third subclade (ML = 100%, PP = 1). The fourth subclade was divided into two groups of haplotypes 013, 014 (ML = 83%, PP = 0.84) and 015, 016 (ML = 84%, PP = 0.47). The fifth subclade (ML = 100%, PP = 1) was split into two groups: haplotypes 017 and 018 (not supported), and haplotypes 019, 020, 021, 022 (ML = 99%, PP = 1).

3.2.1. Identification of putative species based on the GMYC method

Species delimitation was estimated using the GMYC method. We used the tree obtained from *BEAST (Heled and Drummond, 2010) to visualize the delimitation of putative species recognized by the single and multiple threshold GMYC methods (Fig. 1). Outgroups were removed from the analysis. The putative delimitations

Table 1
Sequence characteristics of sampled markers used in this study. In psbJ-L all ambiguities in outgroup were considered as gaps (not informative positions).

	Alignment length (bp)		Variable characters		Model selected
	+ Outgroup	− Outgroup	+ Outgroup	− Outgroup	
nrITS	430	430	81	59	SYM
psbJ-L	1276	558	165	60	GTR
COX2	419	419	77	48	GTR
rbcL	441	441	5	5	GTR
Combined	2566	1848	328	172	SYM

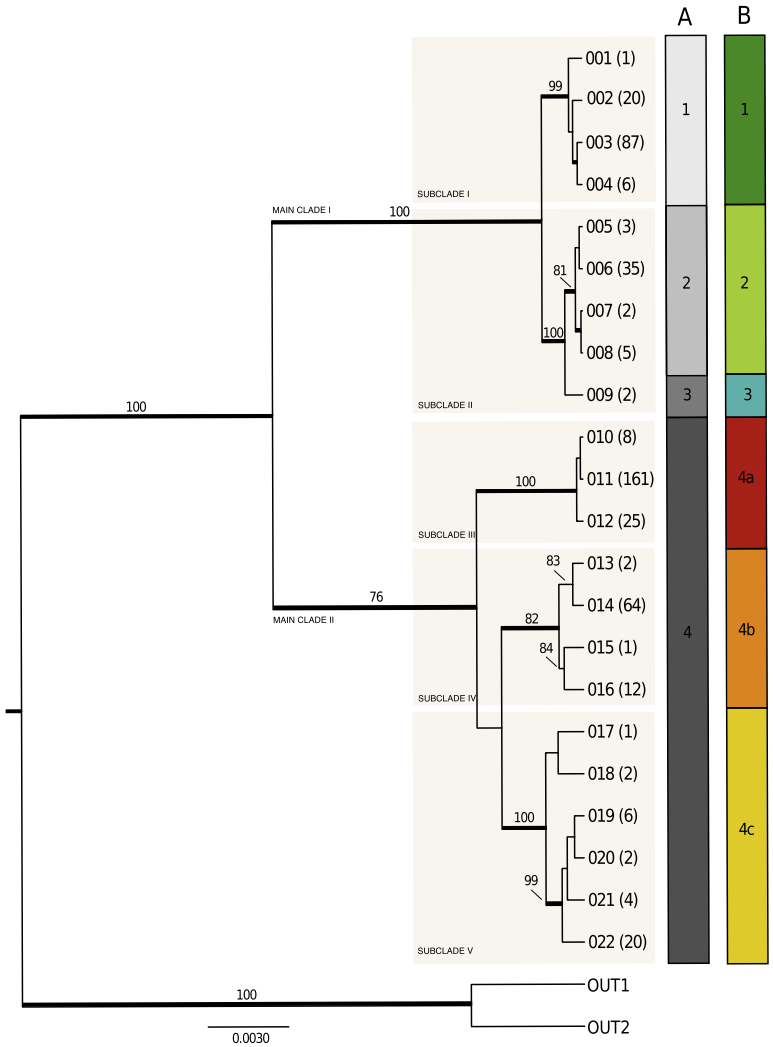

Fig. 1. Maximum likelihood tree based on the concatenated dataset including nrITS, psbJ-L, *COX* and *rbcL* sequences. Branches in bold represent Bayesian posterior probabilities support greater than 0.95. ML bootstrap support greater than 75% is shown above branches. Column A depicts species recognized by the multiple threshold GMYC model, and column B depicts the most probable 6-species scenario suggested by STEM analyses.

of a single and multiple threshold modes were visualized as ultrametric trees obtained from SPLITS (Meyer et al., 2011).

The single threshold method was not preferred over the null model of uniform (coalescence) branching rate ($logL_{GMYC}$ = 44.40021 vs. $\log L_0 = 44.03784$, $2\Delta L = 0.7247428$, $p > 0.05$). The confidence intervals ranged from 1 to 6. The model fitted the switch in the branching pattern at −0.714659, resulting in four putative species. Because this model was not significant we did

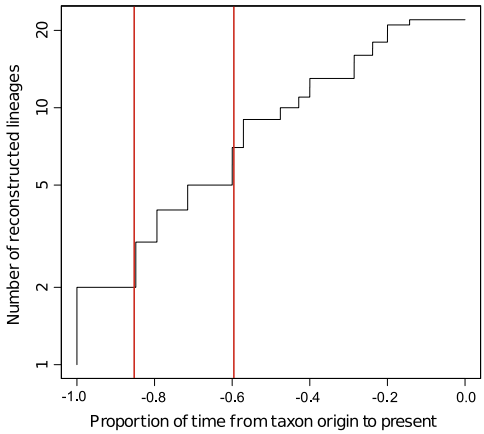

Fig. 2. Lineage-through-time (LTT) plot of the multiple threshold analysis of GMYC model. Lines depict numbers of reconstructed lineages for the clades.

not consider it as informative and we excluded it from further analyses.

Two switches were present in the multiple threshold method (Fig. 2). This model was preferred over the null model of uniform branching rates ($\log L_{GMYC} = 49.74622$ vs. $\log L_0 = 44.03784$, $2\Delta L = 11.41676$, $p < 0.05$). The confidence interval was equal to 3. The model fitted the switch in the branching pattern at −0.8482913 and −0.5998106 and resulted in four putative species. No unclassified individuals were present and all 22 haplotypes were categorized into putative species (Fig. 3).

The multiple threshold model was preferred over the single threshold model ($\log L_{GMYC\text{-}MUL} = 49.74622$ vs. $\log L_{GMYC\text{-}SIN} = 44.40021$, $2\Delta L = 10.69202$, $p < 0.05$). All putative species derived by multiple threshold mode of GMYC were supported by ML and Bayesian analyses (species 1: ML = 99%, PP = 1; species 2: ML = 81%, PP = 0.98; species 3: ML = 100%, PP = 0.98; species 4: ML = 76%, PP = 1).

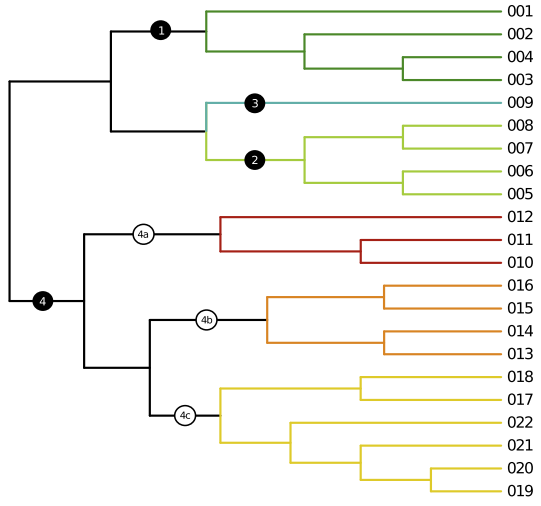

Fig. 3. Ultrametric gene genealogy and clusters of haplotypes recognized as a putative species by multiple-threshold of GMYC (numbers in black circles). Nodes of genetic clusters recognized as putative species (best supported STEM scenario) are highlighted in colors. (For interpretation of the references to color in this figure legend, the reader is referred to the web version of this article.)

3.2.2. Putative species tree analyses

To select the best species delimitation scenario we used a hierarchical Bayesian model *BEAST implemented in the program BEAST (Heled and Drummond, 2010). Species trees were estimated directly from the sequence data, incorporating the coalescent process and nucleotide substitution model parameters. The *BEAST topology tree was congruent with the 4-locus ML phylogeny. For the analysis we followed the protocol by Carsten and Dewey (2010) and compared five different delimitation scenarios based on different assumptions of species boundaries (Table 2): 1-species scenario (all haplotypes were treated as one species – GMYC null model), 4-species scenario based on multiple-threshold results from GMYC (Fig. 1, column A), and another two scenarios (2-, 5-species) based on different phylogenetic assumptions. The 2-species scenario consisted of two main clades of haplotypes: 001–009 (ML = 100%, PP = 1) and 010–022 (ML = 76%, PP = 1). The 5-species scenario consisted of 5 subclades: haplotypes 001–004 (ML = 99%, PP = 1), haplotypes 005–009 (ML = 51%, PP = 0.98), haplotypes 010–012 (ML = 100%, PP = 1), haplotypes 013–016 (ML = 82%, PP = 1) and haplotypes 017–022 (ML = 100%, PP = 1). The 6-species scenario was selected based on results obtained from the multiple-threshold of GMYC method and combined ML and Bayesian support values (Fig. 1, column B), i.e. within the putative species 4 proposed by the multiple-threshold method we distinguished three well-supported subclades: 4a (ML = 100%, PP = 1), 4b (ML = 82%, PP = 1) and 4c (ML = 100%, PP = 1).

To evaluate different scenarios we used species tree estimation using Maximum likelihood STEM as implemented in v 2.0 (Kubatko et al., 2009). This program infers ML species tree from estimated gene trees under coalescent model. Results are presented in Table 2. The best fitting scenario was the 6-species scenario (−lnL 25.29879, $p < 0.001$), although the difference in ΔlnL between 5- and 6-species scenarios was not significant ($p = 0.9$). The number of specimens composing the 6 putative species scenario was as following: species 1–114 samples; species 2–45 samples; species 3–2 samples; species 4a–194; species 4b–79 samples and species 4c–35 samples (Fig. 1, column B).

3.2.3. Evolution of putative species in a genealogical framework

We also used a genealogical concordance approach (Avise and Ball, 1990; Baum and Shaw, 1995) that delimits well-separated lineages using molecular data. Relationships of putative species inferred in the concatenated dataset were evaluated among individual loci (Hudson and Coyne, 2002). Genealogical concordance results based on ML bootstrap values for 4-species and 6-species scenarios are shown in Table 3. Four clades of the 6-species delimitation scenario were present and highly supported in psbJ-L (species 1: ML = 100%, PP = 1; species 4a: ML = 100%, PP = 1; species 4b: ML = 95%, PP = 1; species 4c: ML = 100%, PP = 1). Putative species 1, 2, 3 and 4a were present in nrITS, but only the latter two were

Table 2
Likelihood scores for STEM analysis of species delimitation scenarios based on the concatenated nrITS rDNA, psbJ-L, *COX2*, *rbcL* dataset. High log-likelihood means high support for a given scenario (k = number of parameters, MTM = multiple threshold method of GMYC).

Scenario	−lnL	k	ΔlnL	Bonferroni corrected P
6-Species	25.29879	7	0	
5-Species	27.46663	6	2.1678	0.9
4-Species/MTM	94.3019	5	69.003	<0.001
2-Species	108.0971	3	82.798	<0.001
1-Species	220.32715	3	195.0283	<0.001

Table 3
Genealogical concordance. Presence of clades suggested by multiple threshold of GMYC and STEM (+ = present, but not supported, – = not present), with ML bootstrap support values (%)/Bayesian posterior probabilities values.

	GMYC	Combined	nrITS	psbJ-L	*COX2*	*rbcL*
Multiple threshold	1	99/1	+/0.98	100/1	–/–	–/–
	2	81/0.98	+/+	–/–	93/0.98	–/–
	3	100/0.98	90/1	–/–	–/–	–/–
	4	76/1	+/0.98	96/0.99	99/1	–/–
6-Species scenario	1	99/1	+/0.98	100/1	–/–	–/–
	2	81/0.98	+/+	–/–	93/98	–/–
	3	100/0.98	90/1	–/–	–/–	–/–
	4a	100/1	98/1	100/1	89/–	–/–
	4b	82/1	–/–	95/0.99	+/–	–/–
	4c	100/1	–/–	100/1	–/–	–/–

supported (species 3 ML = 90%, PP = 1, species 4a ML = 98%, PP = 1). Putative species 2 (ML = 93%, PP = 0.98) and 4a (ML = 89%, PP – not present) as well as 4b (not supported) were found in *COX2*. None of the six putative species were found in *rbcL*.

3.3. Photobiont sharing analysis

We compared 22 nrITS *Trebouxia* haplotypes with all similar sequences (98% threshold of pairwise identity) available in GenBank. We found 47 lichen-forming fungi belonging to 19 genera that shared at least one photobiont haplotype found in *L. pustulata*. Seventeen out of 22 *Trebouxia* haplotypes, belonging to five putative species, were included into the heatmap-sharing matrix (Fig. 4).

According to heatmap distribution we divided the fungal species into two blocks: block one contained putative photobiont species 1, 2, 3 and block two included species 4b and 4c. Many of the 47 included lichen-forming fungi belonged to Lecideaceae (10 species) or Umbilicariaceae (8 species). Ten species of lichenized fungi are associated only with algal haplotypes from block one, while 34 species are exclusively associated with algal haplotypes from block two. Only two fungal species, *Boreoplaca ultrafrigida* and *Evernia mesomorpha*, are associated with haplotypes from all putative algal species presented in the heatmap. *Pseudevernia cladoniae* shares haplotypes from both blocks of haplotypes (putative species 2, 3 and 4c). Although *Cetraria aculeata* and *C. islandica* are among the most extensively sampled lichens in GenBank, they share haplotypes only with the putative species 4b and 4c. The algal haplotype shared by most species of lichenized fungi (022, putative species 4c) was found in 29 fungal taxa, in 11 of them exclusively. Five different species of *Umbilicaria* were associated with haplotype 022. The photobiont of *Lasallia hispanica* was related only to putative species 4c (haplotype 019 and 022). Haplotype 017 and 021 from the putative species 4c were not found among the sequences available in GenBank. The haplotypes of the putative species 4a (010, 011, 012) were so far only found in *L. pustulata*.

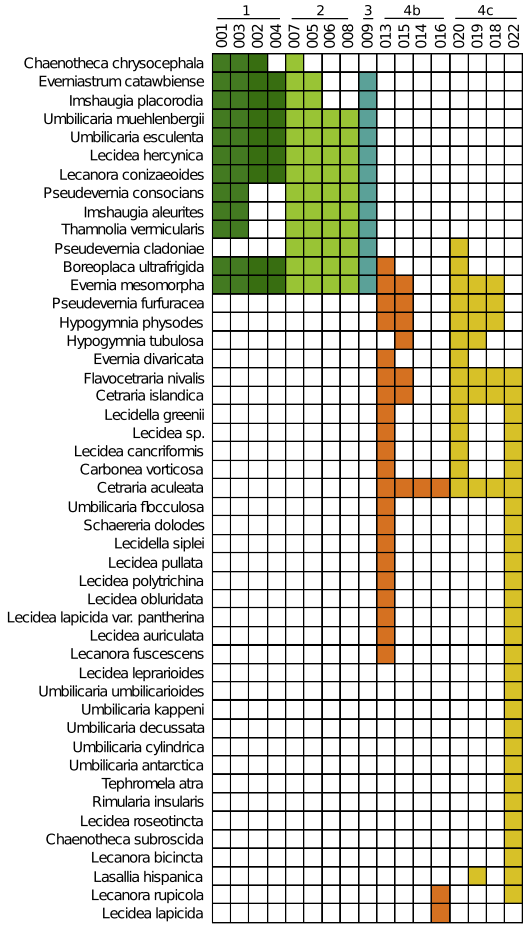

Fig. 4. Heatmap of nrITS algal haplotypes shared among different lichen-forming fungi (98% identity threshold).

4. Discussion

In this study we showed that *L. pustulata* is associated with multiple species of *Trebouxia*. This is supported by phylogenetic and coalescence-based analyses (GMYC, STEM). High diversity of algae associated with a single species of lichen-forming fungus has been shown in other studies (Blaha et al., 2006; Doering and Piercey-Normore, 2009; Leavitt et al., 2011; Muggia et al., 2013; Nelsen and Gargas, 2009; Ohmura et al., 2006; Opanowicz and Grube, 2004; Piercey-Normore, 2006; Ruprecht et al., 2012; Vargas and Beck, 2012). In these studies algal groups/clades were inferred solely from phylogenetic tree topologies, most of which were based on a single locus. In our study we show that the high diversity of photobionts found in *L. pustulata* is consistent with the presence of several algal species.

Low selectivity of the mycobiont towards the photobiont seems to be an important strategy in constantly changing environments, and symbiont-switching has been proposed as an adaptive strategy of lichen-forming fungi (Beck et al., 1998; Muggia et al., 2013;

Wirtz et al., 2003). The high diversity of photobionts associated with lichen-forming fungi could be the effect of photobiont replacement with more compatible algae derived from other lichen symbioses, i.e. from vegetative diaspores (Friedl, 1987; Rambold and Triebel, 1992), or photobiont uptake from free-living strains (Ahmadjian, 1987; Macedo et al., 2009; Sanders, 2005; Sanders and Lücking, 2002). By selecting locally adapted photosynthetic partners, lichens may be able to occupy wider ecological niches (Dal Grande et al., 2014a; Peksa and Škaloud, 2011). As already suggested in other studies (*Xanthoria sp.*, Beck and Mayr, 2012; *Parmotrema tinctorum*, Ohmura et al., 2006; *Umbilicaria sp.*, Romeike et al., 2002) during differentiation of the thallus, the photobiont may be replaced with algal strains that are better adapted to the local environmental conditions or symbiotic chimeras may be formed as the result of fusion between genetically different individuals. *Lasallia pustulata* is a facultative sexual fungus. Even a low rate of sexual recombination seems sufficient to reshuffle the symbiotic association via horizontal photobiont transmission. Additionally, this sexual mode of reproduction plays an important role in shaping the symbiotic association at larger distances, and leads to occupy new, distinct niches (Dal Grande et al., 2012; Grube and Spribille, 2012; Wornik and Grube, 2010).

Being able to assign algal haplotypes to species helps us understand association patterns among unrelated fungal species. This is particularly important if we consider that co-evolution may be evident at a higher phylogenetic level, i.e. knowing the entire spectrum of photobiont species gives us the opportunity to evaluate the possibility of co-evolution leading to co-speciation (Beck, 1999; Beck et al., 2002; Rikkinen, 2002). Photobiont haplotypes of *L. pustulata* were found to be associated with many other lichen-forming fungi with different ecological requirements, and showed various association patterns. In our study lichen-forming fungi were either associated with putative algal species 1, 2 and 3, or with species 4b, 4c. Only very few lichen-forming fungi were associated with all putative *Trebouxia* species. This can be a result of biased sampling represented in GenBank. However, even species with large sample sizes (e.g. *Cetraria aculeata*) showed association with only some of the *Trebouxia* species (4b and 4c), suggesting preference of the fungi for only one or a few algal species. Although co-evolution between symbionts is considered to be rather low in lichen-forming fungi, and algal symbiont switching is common, signals of co-evolution can be inferred from the presence of one-to-one fungal–algal interactions. In our study we found one putative *Trebouxia* species (4a) associated exclusively with *L. pustulata*. Interestingly, all specimens carrying this exclusive photobiont were found in the Mediterranean, or at localities with sub-Mediterranean climatic conditions (Haffner, 1982; John, 1986). However these algal haplotypes were not genetically similar to putative "Mediterranean" *Trebouxia* haplotypes reported in earlier studies (Del Campo et al., 2013; Fernandez-Mendoza et al., 2011; Muggia et al., 2010).

4.1. Caveats to the analyses

All available delimitation methods have some disadvantages, and applying a wide range of analyses can result in more than one outcome (Carstens et al., 2013). In our analyses we used a multifaceted approach based on coalescent (GMYC, STEM) and phylogenetic analyses. The GMYC method delimits well-supported clades of haplotypes and treats them as independent lineages. Although this approach is widely used in many different systems, the main disadvantage of this method is the susceptibility to over-delimitation. A similar problem is present in STEM analyses, as they tend to support delimitation of too many species. As shown in Harrington and Near (2012), STEM strategy leads to over-splitting by increasing the number of branches in the species tree and decreasing the average number of lineages in each branch. In addition, STEM, BEAST and *BEAST rely on the prior assignment of individuals into species categories so they are not designed to explicitly test hypotheses of species delimitation (Harrington and Near, 2012). The genealogical concordance method (Avise and Ball, 1990) provides a rather conservative approach to delimit well-separated lineages using molecular data. The probability of observing reciprocal monophyly at a sample of multiple loci requires a substantial amount of time after the initial divergence of species. Therefore recently derived species may remain undiscovered with this method due to incomplete lineage sorting and other factors (Hickerson et al., 2006; Hudson and Coyne, 2002; Knowles and Carstens, 2007). Because of different rates of evolutionary process of speciation in different loci, this approach can give conflicting information (Dettman et al., 2003).

Another problem in species delimitation methods is the issue of sample size. The recommended number of specimens for species delimitation is of at least 10 samples from all putative lineages. However, optimal sampling number depends on the model organism and the method used to assess species boundaries (Carstens et al., 2013; Esselstyn et al., 2012). It is possible that the low number of specimens for the putative species 3 influenced the final putative number of species.

Despite of the above mentioned caveats, these methods are gaining popularity for delimitating species in groups with cryptic diversity and few phenotypic characters. Morphology in fact can lead to underestimating diversity. It has been shown for instance that chances of encountering multiple species with identical morphologies increase quickly in taxa of lower morphological complexity such as unicellular coccoid green algae investigated in our study (Leliaert et al., 2014; van Oppen et al., 1996; Verbruggen, 2014; Verbruggen et al., 2009). Many studies using molecular phylogenetic data have shown that morphologically indistinguishable species included indeed numerous (closely related) species (e.g. Dal Grande et al., 2014b; Payo et al., 2013; Souffreau et al., 2013). However, preliminary morphological analyses on two of the putative species show that some morphological variability is present (Fig. S2).

Based on the present results, we conclude that photobionts of *L. pustulata* most likely belong to six *Trebouxia* species. Different methods (such as coalescent approaches and phylogenetic analyses) yielded congruent results. All six clades were phylogenetically supported in the concatenated dataset, and the most likely scenario in STEM suggested six species, four of which were also present in the multiple-threshold of the GMYC model. Despite certain caveats implied in the methods, we think the species delimitation method presented in this study is an improvement over existing descriptions of diversity within *Trebouxia* and a promising tool to address species boundaries within the genus.

Acknowledgments

We thank the following collectors and curators for providing us with lichen material: Eva Farkas (Vácrátót), Anna Guttova (Bratislava), László Lőkös (Budapest), Jano Nuñez-Zapata (Madrid), Zdenek Palice (Praha), Raquel Pino-Bodas (Madrid), Garima Singh (Frankfurt), Einar Timdal (Oslo), Mercedes Vivas-Rebuelta (Madrid), Robert Vogt (Berlin), Jan Vondrak (Ceske Budejovice). We are also grateful to Steffen Pauls (Frankfurt) and Volker John (Bad Dürkheim) for valuable discussions, and Jan Schnitzler (Frankfurt) for contributing to data analysis. This study was funded by 'LOEWE, Landes-Offensive zur Entwicklung Wissenschaftlich-ökonomischer Exzellenz' of Hesse's Ministry of Higher Education, Research and the Arts. A. S-D. was supported by a fellowship from the German Academic Exchange Service (DAAD).

Appendix A. Supplementary material

Supplementary data associated with this article can be found, in the online version, at http://dx.doi.org/10.1016/j.ympev.2014.03.020.

References

Ahmadjian, V., 1987. Coevolution in Lichens. Ann. N. Y. Acad. Sci. 503, 307–315.

Avise, J.C., Ball, R.M., 1990. Principles of genealogical concordance in species concepts and biological taxonomy. Oxf. Surv. Evol. Biol. 7, 45–67.

Bálint, M., Domisch, S., Engelhardt, C.H.M., Haase, P., Lehrian, S., Sauer, J., Theissinger, K., Pauls, S.U., Nowak, C., 2011. Cryptic biodiversity loss linked to global climate change. Nat. Clim. Change 1, 313–318.

Barraclough, T.G., Birky, C.W., Burt, A., 2003. Diversification in sexual and asexual organisms. Evolution 57, 2166–2172.

Baum, D.A., Shaw, K.L., 1995. Genealogical perspectives on the species problem. In: Hoch, P.C., Stephenson A.G. (Eds.), Experimental and Molecular Approaches to Plant Biosystematics. Missouri Botanical Garden, St. Louis, pp. 289–303.

Beck, A., 1999. Photobiont inventory of a lichen community growing on heavy-metal-rich rock. Lichenologist 31, 501–510.

Beck, A., Mayr, C., 2012. Nitrogen and carbon isotope variability in the green-algal lichen *Xanthoria parietina* and their implications on mycobiont–photobiont interactions. Ecol. Evol. 2, 3132–3144.

Beck, A., Friedl, T., Rambold, G., 1998. Selectivity of photobiont choice in a defined lichen community: inferences from cultural and molecular studies. New Phytol. 139, 709–720.

Beck, A., Kasalicky, T., Rambold, G., 2002. Myco-photobiontal selection in a Mediterranean cryptogam community with *Fulgensia fulgida*. New Phytol. 153, 317–326.

Bickford, D., Lohman, D.J., Sodhi, N.S., Ng, P.K.L., Meier, R., Winker, K., Ingram, K.K., Das, I., 2007. Cryptic species as a window on diversity and conservation. Trends Ecol. Evol. 22, 148–155.

Blaha, J., Baloch, E., Grube, M., 2006. High photobiont diversity associated with the euryoecious lichen-forming ascomycete *Lecanora rupicola* (Lecanoraceae, Ascomycota). Biol. J. Linn. Soc. 88, 283–293.

Campbell, V., Legendre, P., Lapointe, F.J., 2011. The performance of the Congruence Among Distance Matrices (CADM) test in phylogenetic analysis. BMC Evol. Biol. 11, 64.

Carstens, B.C., Dewey, T.A., 2010. Species delimitation using a Combined Coalescent and Information-Theoretic approach: an example from North American *Myotis* bats. Syst. Biol. 59, 400–414.

Carstens, B.C., Pelletier, T.A., Reid, N.M., Satler, J.D., 2013. How to fail at species delimitation. Mol. Ecol. 22, 4369–4383.

Casano, L.M., del Campo, E.M., García-Breijo, F.J., Reig-Armiñana, J., Gasulla, F., del Hoyo, A., Guéra, A., Barreno, E., 2011. Two *Trebouxia* algae with different physiological performances are ever-present in lichen thalli of *Ramalina farinacea*. Coexistence versus competition? Environ. Microbiol. 13, 806–818.

Crespo, A., Lumbsch, H.T., 2010. Cryptic species in lichen-forming fungi. IMA Fungus: Glob. Mycol. J. 1, 167–170.

Crespo, A., Perez-Ortega, S., 2009. Cryptic species and species pairs in lichens: a discussion on the relationship between molecular phylogenies and morphological characters. An. Jard. Bot. Madr. 66, 71–81.

Cubero, O.F., Crespo, A., 2002. Isolation of nucleic acids from lichens. In: Kranner, I.C., Beckett, R.P., Varma, A.K. (Eds.), Protocols in Lichenology. Springer, Berlin, pp. 381–391.

Dal Grande, F., Widmer, I., Wagner, H.H., Scheidegger, C., 2012. Vertical and horizontal photobiont transmission within populations of a lichen symbiosis. Mol. Ecol. 21, 3159–3172.

Dal Grande, F., Alors, D., Divakar, P.K., Bálint, M., Crespo, A., Schmitt, I., 2014a. Insights into intrathalline genetic diversity of the cosmopolitan lichen symbiotic green alga Trebouxia decolorans Ahmadjian using microsatellite markers. Mol. Phylogenet. Evol. 72, 54–60.

Dal Grande, F., Beck, A., Cornejo, C., Singh, G., Cheenacharoen, S., Nelsen, M.P., Scheidegger, C., 2014b. Molecular phylogeny and symbiotic selectivity of the green algal genus *Dictyochloropsis* s.l. (Trebouxiophyceae): a polyphyletic and widespread group forming photobiont-mediated guilds in the lichen family Lobariaceae. New Phytol. 202, 455–470. http://dx.doi.org/10.1111/nph.12678.

Darriba, D., Taboada, G.L., Doallo, R., Posada, D., 2012. jModelTest 2: more models, new heuristics and parallel computing. Nat. Methods 9, 772.

Del Campo, E.M., Catalá, S., Gimeno, J., del Hoyo, A., Martínez-Alberola, F., Casano, L.M., Grube, M., Barreno, E., 2013. The genetic structure of the cosmopolitan three-partner lichen *Ramalina farinacea* evidences the concerted diversification of symbionts. FEMS Microbiol. Ecol. 83, 310–323.

Dettman, J., Jacobson, D.J., Taylor, J.W., 2003. A multilocus genealogical approach to phylogenetic species recognition in the model eukaryote *Neurospora*. Evol. Int. J. Org. Evol. 57, 2703–2720.

Dettman, J., Anderson, J.B., Kohn, L.M., 2008. Divergent adaptation promotes reproductive isolation among experimental populations of the filamentous fungus *Neurospora*. BMC Evol. Biol. 8, 35.

Doering, M., Piercey-Normore, M.D., 2009. Genetically divergent algae shape an epiphyticlichen community on Jack Pine in Manitoba. Lichenologist 41, 69–80.

Drummond, A.J., Ashton, B., Buxton, S., Cheung, M., 2011. Geneious v5.4. <http://www.geneious.com/>.

Drummond, A.J., Suchard, M.A., Xie, D., Rambaut, A., 2012. Bayesian phylogenetics with BEAUti and the BEAST 1.7. Mol. Biol. Evol. 29, 1969–1973.

Edgar, R.C., 2004. MUSCLE: multiple sequence alignment with high accuracy and high throughput. Nucleic Acids Res. 32, 1792–1797.

Esselstyn, J.A., Evans, B.J., Sedlock, J.L., Anwarali Khan, F.A., Heaney, L.R., 2012. Single-locus species delimitation: a test of the mixed Yule-coalescent model, with an empirical application to Philippine round-leaf bats. Proc. Biol. Sci. 279, 3678–3686.

Felsenstein, J., 1985. Confidence limits on phylogenies: an approach using the bootstrap. Evolution 39, 783.

Fernandez-Mendoza, Domaschke, S., Gracía, M.A., Jordan, P., Martín, M.P., Printzen, C., 2011. Population structure of mycobionts and photobionts of the widespread lichen *Cetraria aculeata*. Mol. Ecol. 20, 1208–1232.

Friedl, T., 1987. Thallus development and phycobionts of the parasitic lichen *Diploschistes muscorum*. Lichenologist 19, 183–191.

Friedl, T., Büdel, B., 2008. Photobionts. In: Nash, T.H. (Ed.), Lichen Biology, third ed. Cambridge University Press, Cambridge, UK, pp. 9–26.

Fujisawa, T., Barraclough, T.G., 2013. Delimiting species using single-locus data and the generalized mixed Yule coalescent approach: a revised method and evaluation on simulated datasets. Syst. Biol. 62, 707–724.

Gärtner, G., 1985. Die Gattung *Trebouxia* Puymaly (Chlorellales, Chlorophyceae). Arch. Hydrobiol. Suppl. Algol. Stud. 41, 495–548.

Grube, M., Muggia, L., 2010. Identifying Algal Symbionts in Lichen Symbioses. EUT Edizioni Università di Trieste.

Grube, M., Spribille, T., 2012. Exploring symbiont management in lichens. Mol. Ecol. 21, 3098–3099.

Guindon, S., Gascuel, O., 2003. A simple, fast, and accurate algorithm to estimate large phylogenies by maximum likelihood. Syst. Biol. 52, 696–704.

Haffner, P., 1982. Landschaftsschutzgebiet Saarschleife: Vegetationskarte mit Erläuterungen. Institut für Landeskunde im Saarland.

Hamilton, C.A., Formanowicz, D.R., Bond, J.E., 2011. Species delimitation and phylogeography of *Aphonopelma hentzi* (Araneae, Mygalomorphae, Theraphosidae): cryptic diversity in North American tarantulas. PLoS One 6, e26207.

Harrington, R.C., Near, T.J., 2012. Phylogenetic and coalescent strategies of species delimitation in snubnose darters (Percidae: *Etheostoma*). Syst. Biol. 61, 63–79.

Hausdorf, B., Hennig, C., 2010. Species delimitation using dominant and codominant multilocus markers. Syst. Biol. 59, 491–503.

Hebert, P.D.N., Penton, E.H., Burns, J.M., Janzen, D.H., Hallwachs, W., 2004. Ten species in one: DNA barcoding reveals cryptic species in the neotropical skipper butterfly *Astraptes fulgerator*. Proc. Natl. Acad. Sci. USA 101, 14812–14817.

Heled, J., Drummond, A.J., 2010. Bayesian inference of species trees from multilocus data. Mol. Biol. Evol. 27, 570–580.

Helms, G., 2003. Taxonomy and Symbiosis in Associations of Physciaceae and *Trebouxia*. Unpublished PhD Thesis, Georg-August Universität, Göttingen.

Hickerson, M.J., Meyer, C.P., Moritz, C., 2006. DNA barcoding will often fail to discover new animal species over broad parameter space. Syst. Biol. 55, 729–739.

Hudson, R.R., Coyne, J.A., 2002. Mathematical consequences of the genealogical species concept. Evol. Int. J. Org. Evol. 56, 1557–1565.

Huelsenbeck, J.P., Ronquist, F., 2001. MRBAYES: Bayesian inference of phylogenetic trees. Bioinformatics Oxf. Engl. 17, 754–755.

Huelsenbeck, J.P., Andolfatto, P., Huelsenbeck, E.T., 2011. Structurama: bayesian inference of population structure. Evol. Bioinformatics Online 7, 55–59.

John, V., 1986. Verbreitungstypen von Flechten im Saarland – eine Orientierungshilfe für die Raumbewertung. Abh. Delattinia 15, 1–170.

Knowles, L.L., Carstens, B.C., 2007. Delimiting species without monophyletic gene trees. Syst. Biol. 56, 887–895.

Kroken, S., Taylor, J.W., 1990. Principles of genealogical concordance in species concepts and biological taxonomy. Oxf. Surv. Evol. Biol., 45–67.

Kroken, S., Taylor, J.W., 2001. Outcrossing and recombination in the lichenized fungus *Letharia*. Fungal Genet. Biol. 34, 83–92.

Kubatko, L.S., Carstens, B.C., Knowles, L.L., 2009. STEM: species tree estimation using maximum likelihood for gene trees under coalescence. Bioinformatics 25, 971–973.

Leavitt, S.D., Johnson, L., St. Clair, L.L., 2011. Species delimitation and evolution in morphologically and chemically diverse communities of the lichen-forming genus *Xanthoparmelia* (Parmeliaceae, Ascomycota) in western North America. Am. J. Bot. 98, 175–188.

Leavitt, S.D., Esslinger, T.L., Lumbsch, H.T., 2012. Neogene-dominated diversification in neotropical montane lichens: dating divergence events in the lichen-forming fungal genus *Oropogon* (Parmeliaceae). Am. J. Bot. 99, 1764–1777.

Leavitt, S., Fernández-Mendoza, F., Pérez-Ortega, S., Sohrabi, M., Divakar, P., Lumbsch, T., Clair, L.S., 2013. DNA barcode identification of lichen-forming fungal species in the *Rhizoplaca melanophthalma* species-complex (Lecanorales, Lecanoraceae), including five new species. MycoKeys 7, 1–22.

Legendre, P., Lapointe, F.J., 2004. Assessing congruence among distance matrices: single-Malt Scotch Whiskies Revisited. Aust. N. Z. J. Stat. 46, 615–629.

Leliaert, F., Verbruggen, H., Vanormelingen, P., Steen, F., Lopez-Bautista, J.M., Zuccarello, G.C., De Clerck, O., 2014. DNA-based species delimitation in algae. J. Phycol. (in press).

Lumbsch, H.T., Leavitt, S.D., 2011. Goodbye morphology? A paradigm shift in the delimitation of species in lichenized fungi. Fungal Divers. 50, 59–72.

Macedo, M.F., Miller, A.Z., Dionísio, A., Saiz-Jimenez, C., 2009. Biodiversity of cyanobacteria and green algae on monuments in the Mediterranean Basin: an overview. Microbiol. Read. Engl. 155, 3476–3490.

Meyer, D., Zeileis, A., Hornik, K., Friendly, M., 2011. vcd: Visualizing Categorical Data. <http://www.cran.r–project.org/web/packages/vcd/index.html>.
Monaghan, M.T., Wild, R., Elliot, M., Fujisawa, T., Balke, M., Inward, D.J.G., Lees, D.C., Ranaivosolo, R., Eggleton, P., Barraclough, T.G., Vogler, A.P., 2009. Accelerated species inventory on Madagascar using coalescent-based models of species delineation. Syst. Biol. 58, 298–311.
Morariu, V., Srinivasan, B.V., Raykar, V.C., Duraiswami, R., Davis, L., 2009. Automatic online tuning for fast Gaussian summation. In: Koller, D., Schuurmans, D., Bengio, Y., Bottou, L. (Eds.), Adv. Neural Inf. Process. Syst., vol. 21, pp. 1113–1120.
Muggia, L., Zellnig, G., Rabensteiner, J., Grube, M., 2010. Morphological and phylogenetic study of algal partners associated with the lichen-forming fungus *Tephromela atra* from the Mediterranean region. Symbiosis 51, 149–160.
Muggia, L., Vancurova, L., Škaloud, P., Peksa, O., Wedin, M., Grube, M., 2013. The symbiotic playground of lichen thalli – a highly flexible photobiont association in rock-inhabiting lichens. FEMS Microbiol. Ecol. 85, 313–323.
Nelsen, M.P., Gargas, A., 2009. Symbiont flexibility in *Thamnolia vermicularis* (Pertusariales: Icmadophilaceae). Bryologist 112, 404–417.
Nelsen, M.P., Plata, E.R., Andrew, C.J., Lücking, R., Lumbsch, H.T., 2011. Phylogenetic diversity of Trentepohlialean algae associated with lichen-forming fungi. J. Phycol. 47, 282–290.
Ohmura, Y., Kawachi, M., Kasai, F., Watanabe, M.M., Takeshita, S., 2006. Genetic combinations of symbionts in a vegetatively reproducing lichen, *Parmotrema tinctorum*, based on ITS rDNA sequences. Bryologist 109, 43–59.
O'Meara, B.C., 2010. New heuristic methods for joint species delimitation and species tree inference. Syst. Biol. 59, 59–73.
Opanowicz, M., Grube, M., 2004. Photobiont genetic variation in *Flavocetraria nivalis* from Poland (Parmeliaceae, lichenized Ascomycota). Lichenologist 36, 125–131.
Parnmen, S., Rangsiruji, A., Mongkolsuk, P., Boonpragob, K., Nutakki, A., Lumbsch, H.T., 2012. Using phylogenetic and coalescent methods to understand the species diversity in the *Cladia aggregata* complex (Ascomycota, Lecanorales). PLoS One 7, e52245.
Pauls, S.U., Nowak, C., Bálint, M., Pfenninger, M., 2013. The impact of global climate change on genetic diversity within populations and species. Mol. Ecol. 22, 925–946.
Payo, D.A., Leliaert, F., Verbruggen, H., D'Hondt, S., Calumpong, H.P., De Clerck, O., 2013. Extensive cryptic species diversity and fine-scale endemism in the marine red alga *Portieria* in the Philippines. Proc. R. Soc. B 280, 20122660.
Peksa, O., Škaloud, P., 2011. Do photobionts influence the ecology of lichens? A case study of environmental preferences in symbiotic green alga *Asterochloris* (Trebouxiophyceae). Mol. Ecol. 20, 3936–3948.
Piercey-Normore, M.D., 2006. The lichen-forming ascomycete *Evernia mesomorpha* associates with multiple genotypes of *Trebouxia jamesii*. New Phytol. 169, 331–344.
Piercey-Normore, M.D., 2009. Vegetatively reproducing fungi in three genera of the Parmeliaceae share divergent algal partners. Bryologist 112, 773–785.
Pons, J., Barraclough, T.G., Gomez-Zurita, J., Cardoso, A., Duran, D.P., Hazell, S., Kamoun, S., Sumlin, W.D., Vogler, A.P., 2006. Sequence-based species delimitation for the DNA taxonomy of undescribed insects. Syst. Biol. 55, 595–609.
Posada, D., 2008. JModelTest: phylogenetic model averaging. Mol. Biol. Evol. 25, 1253–1256.
Puillandre, N., Modica, M.V., Zhang, Y., Sirovich, L., Boisselier, M.C., Cruaud, C., Holford, M., Samadi, S., 2012. Large-scale species delimitation method for hyperdiverse groups. Mol. Ecol. 21, 2671–2691.
Queiroz, K.D., 2007. Species concepts and species delimitation. Syst. Biol. 56, 879–886.
Rambold, G., Triebel, D., 1992. The inter-Lecanoralean associations. Bibl. Lichenol. 4, 1–201.
Rikkinen, J., 2002. Lichen guilds share related cyanobacterial symbionts. Science 297, 357.
Romeike, J., Friedl, T., Helms, G., Ott, S., 2002. Genetic diversity of algal and fungal partners in four species of *Umbilicaria* (lichenized Ascomycetes) along a transect of the Antarctic Peninsula. Mol. Biol. Evol. 19, 1209–1217.
Ruprecht, U., Brunauer, G., Printzen, C., 2012. Genetic diversity of photobionts in Antarctic lecideoid lichens from an ecological view point. Lichenologist 44, 661–678.
Sadowska-Deś, A.D., Bálint, M., Otte, J., Schmitt, I., 2013. Assessing intraspecific diversity in a lichen-forming fungus and its green algal symbiont: evaluation of eight molecular markers. Fungal Ecol. 6, 141–151.
Sanders, W.B., 2005. Observing microscopic phases of lichen life cycles on transparent substrata placed in situ. Lichenologist 37, 373–382.
Sanders, W.B., Lücking, R., 2002. Reproductive strategies, relichenization and thallus development observed *in situ* in leaf-dwelling lichen communities. New Phytol. 155, 425–435.
Sanderson, M.J., 2002. Estimating absolute rates of molecular evolution and divergence times: a penalized likelihood approach. Mol. Biol. Evol. 19, 101–109.
Škaloud, P., Peksa, O., 2010. Evolutionary inferences based on nrITS rDNA and actin sequences reveal extensive diversity of the common lichen alga *Asterochloris* (Trebouxiophyceae, Chlorophyta). Mol. Phylogenet. Evol. 54, 36–46.
Souffreau, C., Vanormelingen, P., Van de Vijver, B., Isheva, T., Verleyen, E., Sabbe, K., Vyverman, W., 2013. Molecular evidence for distinct Antarctic lineages in the cosmopolitan terrestrial diatoms *Pinnularia borealis* and *Hantzschia amphioxys*. Protist 164, 101–115.
Stamatakis, A., 2006. RAxML-VI-HPC: maximum likelihood-based phylogenetic analyses with thousands of taxa and mixed models. Bioinformatics Oxf. Engl. 22, 2688–2690.
Taylor, J.W., Jacobson, D.J., Kroken, S., Kasuga, T., Geiser, D.M., Hibbett, D.S., Fisher, M.C., 2000. Phylogenetic species recognition and species concepts in fungi. Fungal Genet. Biol. 31, 21–32.
Thorne, J.L., Kishino, H., 2002. Divergence time and evolutionary rate estimation with multilocus data. Syst. Biol. 51, 689–702.
Tschermak-Woess, E., 1988. New and known taxa of *Chlorella* (Chlorophyceae): occurrence as lichen phycobionts and observations on living dictyosomes. Plant Syst. Evol. 159, 123–139.
van Oppen, M.J.H., Klerk, H., Olsen, J.L., Stam, W.T., 1996. Hidden diversity in marine algae: some examples of genetic variation below the species level. J. Mar. Biol. Assoc. UK 76, 239–242.
Vargas, R., Beck, A., 2012. Photobiont selectivity and specificity in *Caloplaca* species in a fog-induced community in the Atacama Desert, northern Chile. Fungal Biol. 116, 665–676.
Verbruggen, H., 2014. Morphological complexity, plasticity, and species diagnosability in the application of old species names in DNA-based taxonomies. J. Phycol. 50, 26–31.
Verbruggen, H., Vlaeminck, C., Sauvage, T., Sherwood, A.R., Leliaert, F., De Clerck, O., 2009. Phylogenetic analysis of *Pseudochlorodesmis* strains reveals cryptic diversity above the family level in the siphonous green algae (Bryopsidales, Chlorophyta). J. Phycol. 45, 726–731.
Welton, L.J., Siler, C.D., Oaks, J.R., Diesmos, A.C., Brown, R.M., 2013. Multilocus phylogeny and Bayesian estimates of species boundaries reveal hidden evolutionary relationships and cryptic diversity in Southeast Asian monitor lizards. Mol. Ecol. 22, 3495–3510.
Werth, S., Sork, V.L., 2008. Local genetic structure in a North American epiphytic lichen, *Ramalina menziesii* (Ramalinaceae). Am. J. Bot. 95, 568–576.
Werth, S., Sork, V.L., 2010. Identity and genetic structure of the photobiont of the epiphytic lichen *Ramalina menziesii* on three oak species in southern California. Am. J. Bot. 97, 821–830.
Wiens, J.J., Penkrot, T.A., 2002. Delimiting species using DNA and morphological variation and discordant species limits in spiny lizards (*Sceloporus*). Syst. Biol. 51, 69–91.
Wirtz, N., Lumbsch, H.T., Green, T.G.A., Türk, R., Pintado, A., Sancho, L., Schroeter, B., 2003. Lichen fungi have low cyanobiont selectivity in maritime Antarctica. New Phytol. 160, 177–183.
Wornik, S., Grube, M., 2010. Joint dispersal does not imply maintenance of partnerships in lichen symbioses. Microb. Ecol. 59, 150–157.
Yahr, R., Vilgalys, R., DePriest, P.T., 2006. Geographic variation in algal partners of *Cladonia subtenuis* (Cladoniaceae) highlights the dynamic nature of a lichen symbiosis. New Phytol. 171, 847–860.

SUPPLEMENTARY MATERIALS

Table S1. Material used in the current study and GenBank accession numbers. Herbarium acronyms follow Thiers (2012).

Haplotype	Putative species	Locality	Accession number			
			nrITS rDNA	**psbJ-L**	***COX2***	***rbcL***
001	1	Czech Republic, S. Bohemia, Cesky Krumlov, Kaplice, 785 m, lat. 48.753333, long. 14.606667, leg. Palice, 15.08. 2012 (FR)	KJ623927	KJ623999	KJ623951	KJ623975
002	1	Slovakia, Tribeč Mts, Zobor Mts: Nitra, 546 m, lat. 48.337255, long. 18.10623, leg. Guttova, 27.07.2011 (FR)	KJ623928	KJ624000	KJ623952	KJ623976
003	1	Norway, Vestfold, Larvik, Stavern, 20m, lat. 58.983333, long. 10.03333, leg. Rui, Timdal, 2.04.2011 (O)	KJ623929	KJ624001	KJ623953	KJ623977
004	1	Poland, Lower Silesia, Sobieszów, Chojnik Hill, 530 m, lat. 50.83333, long. 15.63333, leg. Sadowska-Deś, 23.06.2011 (FR)	KJ623930	KJ624002	KJ623954	KJ623978
005	2	Poland, Lower Silesia, Sobieszów, Chojnik Castle, 530 m, lat. 50.833725, long. 15.644181, leg. Sadowska-Deś, 29.08.2011 (FR)	KJ623931	KJ624003	KJ623955	KJ623979
006	2	Germany, Hesse, Eppstein, 342 m, lat. 50.13949, long. 8.40439, leg. Sadowska-Deś, Nuñez Zapata, Schmitt, 26.05.2011 (FR)	KJ623932	KJ624004	KJ623956	KJ623980
007	2	Poland, Lower Silesia, Sobieszów, Zbójeckie Skały, 600 m, lat. 51.0244444, long. 15.904444, leg. Sadowska-Deś, 23.06.2011 (FR)	KJ623933	KJ624005	KJ623957	KJ623981
008	2	Germany, Saxony, Anhalt, Bodetal, Rosstrappe, 403 m, lat. 51.735064, long. 11.246982, leg. Sadowska-Deś, 13.08.2011 (FR)	KJ623934	KJ624006	KJ623958	KJ623982
009	3	Poland, Lower Silesia, Sobieszów, Chojnik Hill, 530 m, lat. 50.83333, long. 15.63333, leg. Sadowska-Deś, 23.06.2011 (FR)	KJ623935	KJ624007	KJ623959	KJ623983
010	4a	Italy, Sardinia, Olbia, San Pantaleo, 100m, lat. 41.046111, long. 9.446111, leg. Vondrak, 30.04.2012 (FR)	KJ623936	KJ624008	KJ623960	KJ623984
011	4a	Germany, Saarland, Orscholz, 300 m, lat. 49.500876, long. 6.542163, leg. Sadowska-Deś, John, Nuñez Zapata, Schmitt, 17.06.2011 (FR)	KJ623937	KJ624009	KJ623961	KJ623985
012	4a	Spain, Toledo, Aldeanueva de Barbarrolla, 550m, lat. 39.755000, long. -5.069756, leg. Pino Bodas, 22.01.2012 (FR)	KJ623938	KJ624010	KJ623962	KJ623986
013	4b	Slovakia, Mala Fatra Mts., Varin Nezdubska Lucka, 459m, lat. 49.178186, long. 18.892347, leg. Guttova, 13.08.2011(FR)	KJ623939	KJ624011	KJ623963	KJ623987

014	4b	Germany, Hesse, Eppstein, 342 m, lat. 50.13949, long. 8.40439, leg. Sadowska-Deś, Nuñez Zapata, Schmitt, 26.05.2011 (FR)	KJ623940	KJ624012	KJ623964	KJ623988
015	4b	Norway, Hedmark, Ringsaker: Mjøsstranda, 123m, lat. 60.910672, long. 10.737576, leg. Breili, Anders, 0605.2007, L 158696 (O)	KJ623941	KJ624013	KJ623965	KJ623989
016	4b	Hungary, Pest District, Kamence, Borzsony Mts, Nagy- Mána, 695m, lat. 46.09083333, long. 18.13305556, leg. Farkas, *Lőkös*, *Molnár*, 07.05.2011 (Farkas-346)	KJ623942	KJ624014	KJ623966	KJ623990
017	4c	Portugal, Serra da Estrela. Subida a Torre, 1300m, alt. 40.296389, long. -7.536111, leg. Vivas Rebuelta, 26.03.2009 (FR)	KJ623943	KJ624015	KJ623967	KJ623991
018	4c	Greece,W Aegean,Nomos Evvias, 1370m, long. 38.051389, lat. 24.452500, leg. Sipman, Raus, 26.09.2010 (B)	KJ623944	KJ624016	KJ623968	KJ623992
019	4c	Norway, Akershus Ski: Nord Bjørke, 110m, lat. 60.062922, long. 11.375427, leg. Haugan 18.06.2006, L150858 (O)	KJ623945	KJ624017	KJ623969	KJ623993
020	4c	Norway, Oppland, Vågå: ussvassbue, 1185m, lat. 61.11926, long. 10.466137, leg. Haugan, 24.06.2008, L160450 (O)	KJ623946	KJ624018	KJ623970	KJ623994
021	4c	Norway, Asmaløy, Hvaler, 2m, long. 59.13271, lat. 10.92875, leg Singh, Dal Grande, 15.08.2012 (FR)	KJ623947	KJ624019	KJ623971	KJ623995
022	4c	Norway, Rogland, Vindafjord: Saltvika, 1m, lat. 59.301234, long. 5.985718, leg. Breili, Anders, 02.09.2008, L155335 (O)	KJ623948	KJ624020	KJ623972	KJ623996
OUT1	-	*Anaptychia cilicaris*, Norway, 1890 Rakkestad, 110m, lat. 59.41096, long. 11.36843, leg. Singh, Dal Grande, 15.08.2012 (FR)	KJ623949	KJ624021	KJ623973	KJ623997
OUT2	-	*Anaptychia cilicaris*, Norway, 1890 Rakkestad, 110m, lat. 59.41096, long. 11.36843, leg. Singh, Dal Grande, 15.08.2012 (FR)	KJ623950	KJ624022	KJ623974	KJ623998

Table S2. Congruence Among Distance Matrices (CADM) test results. Kendall's coefficient of concordance (W) gives an estimate of the level of congruence (0 = complete incongruence, 1= complete congruence).

Loci pair	**W**	**P**
nrITS - psbJ–L	0.982	0.001
nrITS - *COX2*	0.964	0.001
psbJ–L - *COX2*	0.952	0.001
psbJ–L - *rbcL*	0.723	0.001
nrITS - *rbcL*	0.696	0.001
COX2 - *rbcL*	0.581	0.03

Figure S1. Maximum likelihood trees of the nrITS (A), psbJ-L (B), *COX* (C) and *rbcL* (D) sequences. Branches in bold represent Bayesian posterior probabilities support greater than 0.95%. ML bootstrap support greater than 75% is shown above branches.

A) nrITS

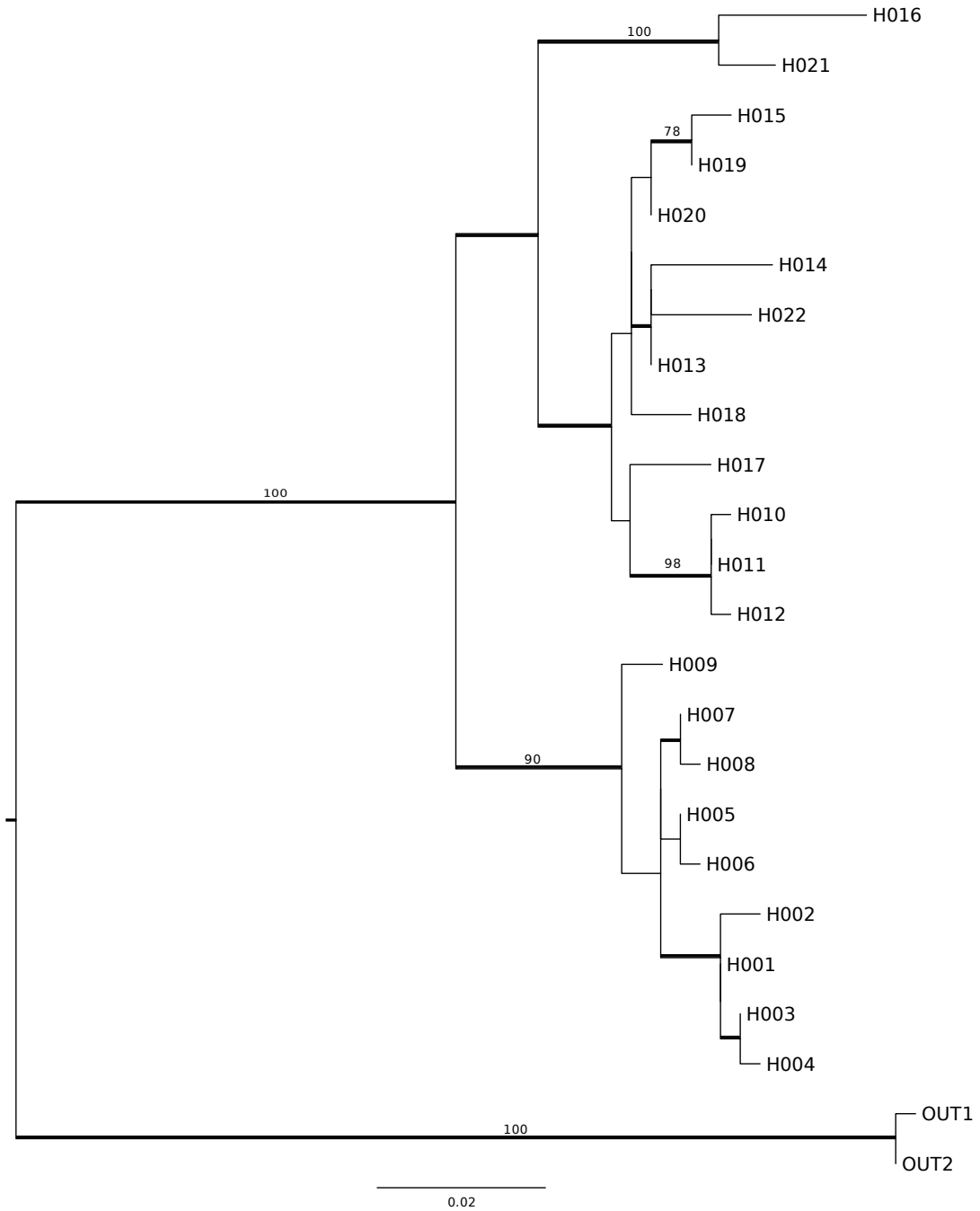

B) psbJ–L

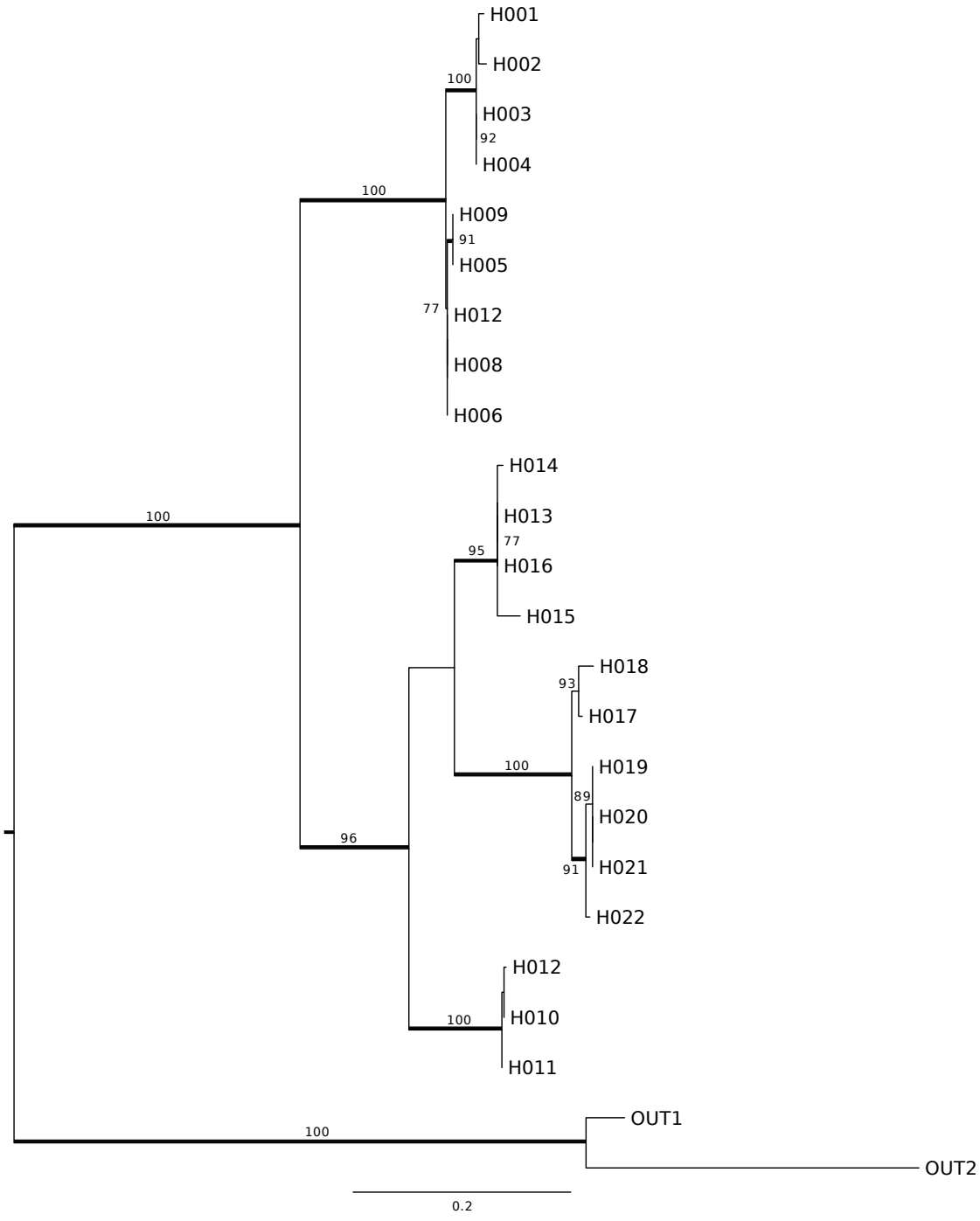
H001
H002
100
H003
92
H004
100
H009
91
H005
77
H012
H008
H006
H014
100
H013
77
95
H016
H015
H018
93
H017
100
H019
89
H020
96
91
H021
H022
H012
100
H010
H011
OUT1
100
OUT2
0.2

C) *COX2*

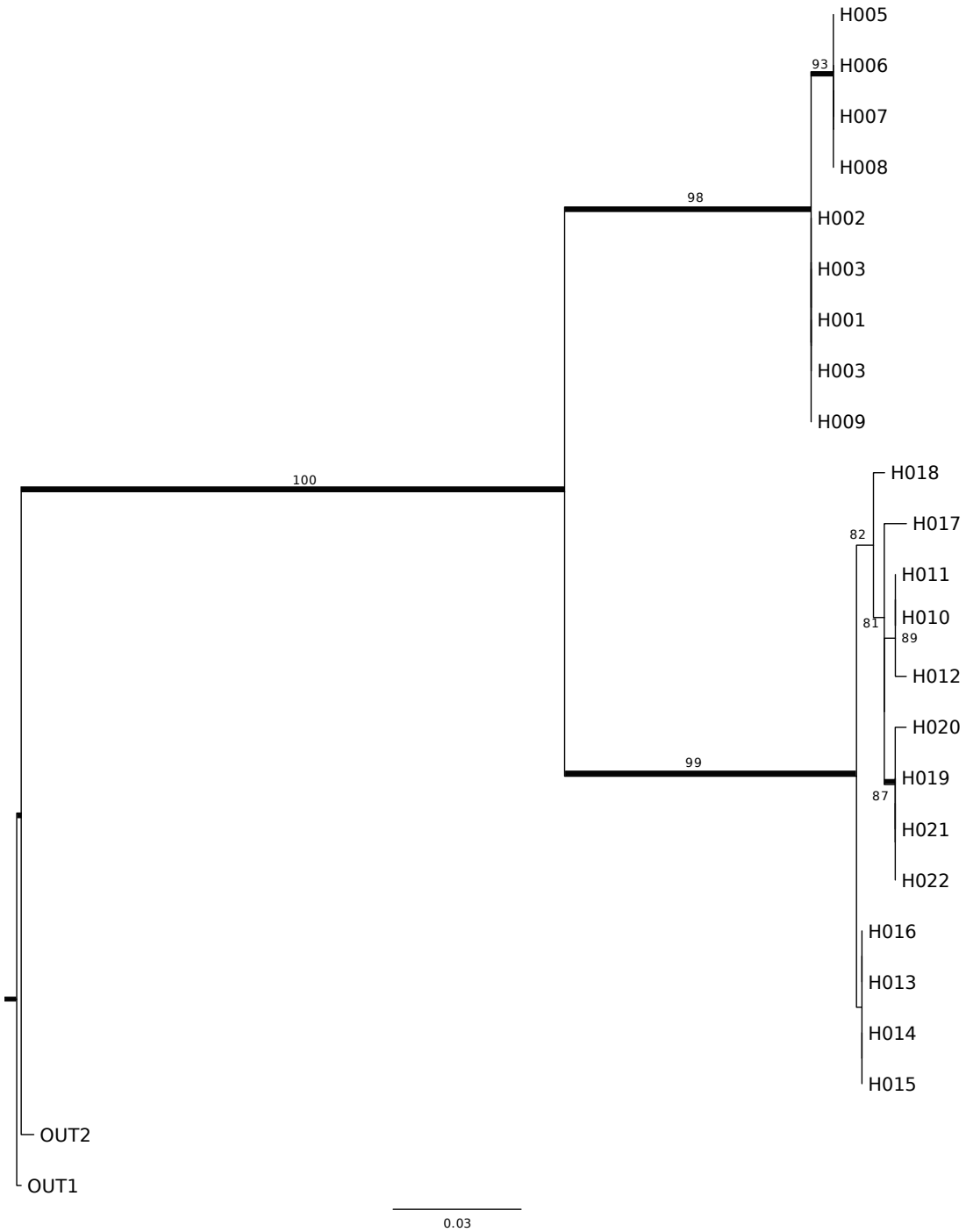
H005
93
H006
H007
H008
98
H002
H003
H001
H003
H009
100
H018
82
H017
H011
81
H010
89
H012
H020
99
H019
87
H021
H022
H016
H013
H014
H015
OUT2
OUT1
0.03

D) *rbcL*

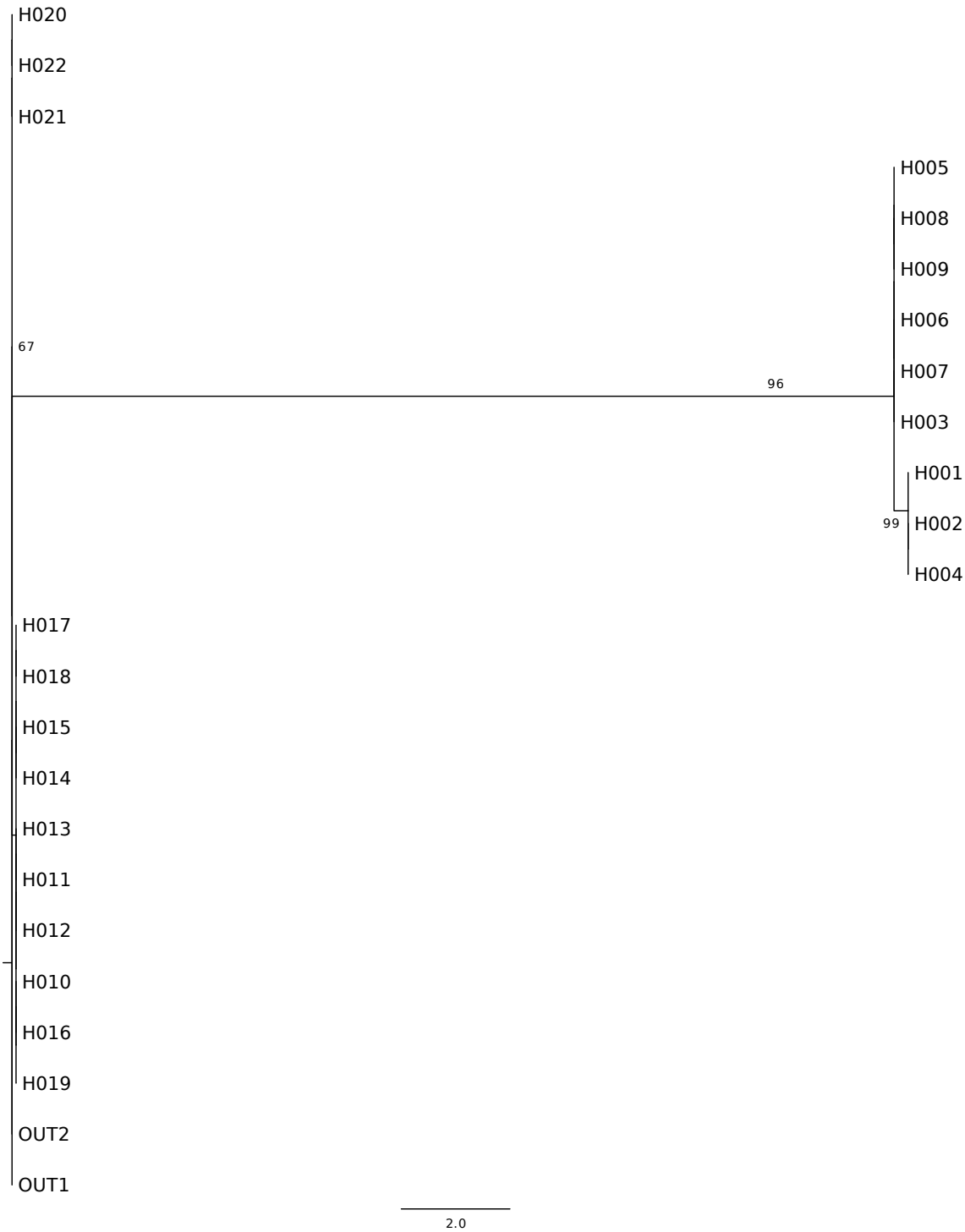
H020
H022
H021
H005
H008
H009
H006
67
H007
96
H003
H001
99
H002
H004
H017
H018
H015
H014
H013
H011
H012
H010
H016
H019
OUT2
OUT1
2.0

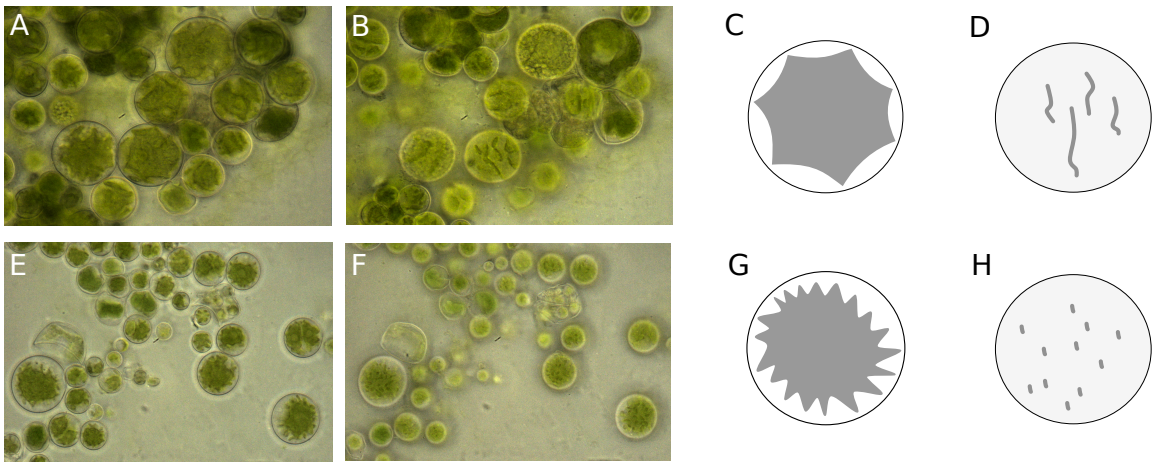

Figure S2. Morphological characters of representatives of the putative species 1 (A-D) and 4a (E-H). A, C, E, G: optical section; B, D, F, H: surface view. Morphological comparisons were carried out on algal cultures established from a single cell progenitor using a micromanipulator (Beck and Koop, *Symbiosis*, 2001): 110811E0103_H02_A2 (Estonia, haplotype 003), 12079I0103_H24_D5 (Italy, haplotype 011), or from multiple cell isolates 120101S1408_H33 (Spain, haplotype 012). Before preparation the samples were washed with distilled water to avoid contamination with aerophytic algae. Identity of the cultured strains was confirmed via PCR and sequencing of the nrITS. In order to obtain enough material for DNA isolation, all algal strains were inoculated on agar medium containing Bold's mineral solution (Ahmadjian, *Phycologia*, 1967) under sterile conditions. Cultivation took place under a diurnal light (12h) and darkness (12h) cycle with a constant temperature of 16°C. We checked 3-7 replicate isolations obtained from the same lichen thallus. After four weeks we repeated the analyses on the same material to confirm our observations. Culture strains of the isolated photobionts are deposited in the algal collection at the Biodiversity and Climate Research Centre, Frankfurt. Three algal cultures obtained from two different putative species were checked using a light microscope at 400 x magnification. Based on chloroplast characters, two different morphotypes of algae were distinguished. The chloroplasts in algae from haplotype 003 (putative species 1) were deeply incised, forming long narrow ridges at the margin of the cell (Fig. S2 a-d). The chloroplast in haplotype 011/012 (putative species 4a; Fig. S2 e-h) formed shorter narrow ridges at the margin of the cells and appeared somewhat spotted. The space between chloroplast and cell wall in putative species 4a was also wider compared to putative species 1, i.e. the chloroplast occupied a smaller fraction of the total cell volume.

APPENDIX 3: Quantifying the climatic niche of symbiont partners in a lichen symbiosis indicates mutualist-mediated niche expansions.

STATEMENT OF JOINT AUTHORSHIP

Published in Ecography (online on 31 July 2018, printed in volume 41 on August 2018, Pages 1380-1392, DOI: 10.1111/ecog.03457)

Involved authors: Gregor Rolshausen, Francesco Dal Grande, Anna D. Sadowska-Deś, Jürgen Otte, Imke Schmitt

What did the Ph.D. student or the Co-Authors contribute to this work?

(3) Development and planning:

Gregor Rolshausen	70%
Francesco Dal Grande	10%
Anna D. Sadowska-Deś	10%
Imke Schmitt	10%

(4) Performance of the individual investigations and experiments

(2a) Fieldwork 30%

Anna D. Sadowska-Deś	100%	Conducted fieldwork and sampling.

(2b) Labwork 70%

Anna D. Sadowska-Deś	20%	Curation and preparation of samples.
Jürgen Otte	80%	DNA extraction, PCR and sequencing.

(3) Preparation of the data collection and figures

Gregor Rolshausen	80%	Produced all figures and tables.

Francesco Dal Grande	10%	Helped with data generation.
Anna D. Sadowska-Deś	10%	Assisted with collecting and organizing data.

(4) Analyses and interpretation of data

Gregor Rolshausen	80%	OTUs delimitation analyses, climatic niche construction, species distribution modeling.
Francesco Dal Grande	10%	Assisted with data analyses and interpretation, literature search.
Imke Schmitt	10%	Provided feedback on data analyses.

(5) Writing the manuscript

Gregor Rolshausen	60%
Francesco Dal Grande	20%
Anna D. Sadowska-Deś	10%
Imke Schmitt	10%

Date/Place: 25.07.2019 /Frankfurt am Main

Signature of the Ph.D. Student: Anna Sadowska-Deś

Verification of the statement above:

Signature of the Supervisor: J. Schmitt Date/Place: 25.07.2019/Frankfurt am Main

ECOGRAPHY

Research

Quantifying the climatic niche of symbiont partners in a lichen symbiosis indicates mutualist-mediated niche expansions

Gregor Rolshausen, Francesco Dal Grande, Anna D. Sadowska-Deś, Jürgen Otte and Imke Schmitt

G. Rolshausen (http://orcid.org/0000-0003-1398-7396) (grolshausen@senckenberg.de), F. Dal Grande, A. D. Sadowska-Deś, J. Otte and I. Schmitt, Senckenberg Biodiversity and Climate Research Centre (SBiK-F), Frankfurt am Main, Germany. ADS-D and IS also at: Dept of Biological Sciences, Inst. of Ecology, Evolution and Diversity, Goethe Univ., Frankfurt, Germany.

Ecography
41: 1380–1392, 2018
doi: 10.1111/ecog.03457

Subject Editor: Fernando T. Maestre
Editor-in-Chief: Miguel Araújo
Accepted 6 November 2017

The large distributional areas and ecological niches of many lichenized fungi may in part be due to the plasticity in interactions between the fungus (mycobiont) and its algal or cyanobacterial partners (photobionts). On the one hand, broad-scale phylogenetic analyses show that partner compatibility in lichens is rather constrained and shaped by reciprocal selection pressures and codiversification independent of ecological drivers. On the other hand, sub-species-level associations among lichen symbionts appear to be environmentally structured rather than phylogenetically constrained. In particular, switching between photobiont ecotypes with distinct environmental preferences has been hypothesized as an adaptive strategy for lichen-forming fungi to broaden their ecological niche. The extent and direction of photobiont-mediated range expansions in lichens, however, have not been examined comprehensively at a broad geographic scale. Here we investigate the population genetic structure of *Lasallia pustulata* symbionts at sub-species-level resolution across the mycobiont's Europe-wide range, using fungal *MCM7* and algal ITS rDNA sequence markers. We show that variance in occurrence probabilities in the geographic distribution of genetic diversity in mycobiont-photobiont interactions is closely related to changes in climatic niches. Quantification of niche extent and overlap based on species distribution modeling and construction of Hutchinsonian climatic hypervolumes revealed that combinations of fungal–algal interactions change at the sub-species level along latitudinal temperature gradients and in Mediterranean climate zones. Our study provides evidence for symbiont-mediated niche expansion in lichens. We discuss our results in the light of symbiont polymorphism and partner switching as potential mechanisms of environmental adaptation and niche evolution in mutualisms.

Introduction

Associations between species in obligate mutualisms, such as lichens or corals, evolve under two main sets of constraints: a broad-scale phylogenetic component, determined by the general compatibility of host genera with their symbiotic partners; and a local-scale ecological component determined by adaptive dynamics, environmental

NORDIC SOCIETY OIKOS

www.ecography.org

tolerances, and dispersal abilities of partners in the symbiosis. For instance, the majority of lichen-forming fungi (mycobionts) in nature are known to be exclusively associated with particular genera of autotrophic photobionts (i.e. *Trebouxia* algae or *Nostoc* cyanobacteria), suggesting an inherent deep phylogenetic constraint in partner compatibility (Beck et al. 1998, Rambold et al. 1998, Piercey-Normore and DePriest 2001, DePriest 2004). Likewise, comprehensive analyses of symbiont associations in the species-rich lichen family Parmeliaceae revealed that, at the scale of ecoregions, the fungal host genus determines the composition of photobionts more than ecological predictors (Leavitt et al. 2015).

At the level of species, however, and especially at the level of populations, the phylogenetic specificity of associating lichen partners appears to be less stringent. On the one hand, several mycobiont species may associate with the same photobiont species, often forming so called lichen guilds (e.g. cyanobacteria: Rikkinen et al. 2002, Wirtz et al. 2003, green algae: Doering and Piercey-Normore 2009, Dal Grande et al. 2014, Singh et al. 2017). On the other hand, a particular mycobiont can associate with multiple strains of photobionts, as well as switch between those strains within its distributional range (Piercey-Normore and DePriest 2001, Blaha et al. 2006, Piercey-Normore 2006, Yahr et al. 2006, Muggia et al. 2010). Moreover, photobionts are not exclusively transmitted vertically during propagation and reproduction of their mycobiont partners, but can also be transmitted horizontally between mycobionts (Friedl 1987, Piercey-Normore and DePriest 2001, Werth and Sork 2008, 2010) and potentially even occur free-living (Mukhtar et al. 1994, Beck et al. 1998). Thus, while environmental preferences in lichen photobionts can evolve independently of a particular mycobiont, the spatial distribution and (realized) niche breadth of lichen-forming fungi will inherently depend on the adaptation of their photobionts to local environmental conditions (Piercey-Normore and DePriest 2001, Yahr et al. 2006, Fernández-Mendoza et al. 2011).

Evidence that association with differentially adapted photobionts alters the niche breadth of lichen-forming fungi comes from explicit phylogeographic approaches that relate the congruency in genetic structures of symbiotic partners to their geographic distributions. A common pattern found in studies addressing this question is that the fungal partner often exhibits substantially less genetic structure at the subspecies level across habitats compared to its photobiont partners; thereby suggesting a generalist strategy in the former, and a central role for local adaptation in the latter (Piercey-Normore 2006, Yahr et al. 2006, Werth and Sork 2008, 2010, Widmer et al. 2012, Muggia et al. 2014). Moreover, horizontal transfer of photobionts of the genus *Trebouxia* or the genus *Asterochloris* between different populations of mycobionts seems to have occurred with high ecological specificity both at a local-scale (Piercey-Normore 2006, Werth and Sork 2010, Peksa and Škaloud 2011) and at larger scales of ecogeographic regions (Yahr et al. 2006, Fernández-Mendoza et al. 2011, Werth and Sork 2014). By and large, inferences in these studies are drawn from methods that aim at 1) explaining the molecular variance observed for a particular taxonomic group (i.e. photobionts or mycobionts) via categorical predictors for habitat and/or symbiotic partners (e.g. F_{ST} and AMOVA methods, Werth and Sork 2008, 2010); 2) evaluating phylogenetic correspondence between associated symbiotic partners and habitat (e.g. Mantel tests and phylogenetic signal; Yahr et al. 2006, Peksa and Škaloud 2011, Singh et al. 2017); or 3) partitioning presence/absence variation for particular symbiont haplotypes onto environmental variables (e.g. redundancy analysis; Fernández-Mendoza et al. 2011, Werth and Sork 2014). Yet, while these approaches do consider environmental variables as predictors for the distribution of molecular variance, none of them places special emphasis on explicitly quantifying the niche breadth of, or the niche overlap between, symbiotic partners.

If mycobionts broaden their distributional range by associating with differently adapted photobionts, we would expect to find a patchwork of genetically differentiated populations of interacting partners throughout that range. Moreover, we expect such a geographic mosaic of interactions to be structured by the mode of dispersal (and reproduction) of partners, as well as by their capabilities to adapt to spatially varying selection regimes (Thompson 1999, 2005). More specifically, in the case of predominantly vertical transmission of photobionts (i.e. no algal switches) during mycobiont reproduction and dispersal, the spatial genetic structure of partners should be congruent throughout the geographic mosaic. In contrast, if algal switches are frequent, the spatial genetic structure of partners should be incongruent, resembling a broad generalistic distribution for mycobionts associating with distinct, locally restricted, photobionts (Werth and Sork 2010, Fernández-Mendoza et al. 2011, Dal Grande et al. 2012, O'Brien et al. 2013). Notably, these scenarios should also translate into distinct patterns of overlap in (climatic) niche space among genetically differentiated symbiont partners, given that their observed ecological preferences are the result of adaptation. Thus, modeling niche dimensions (and spatial distributions) for photobionts and mycobionts respectively will provide a more detailed picture of potential coevolutionary 'hotspots', where reciprocal selection between partners is strong, and 'coldspots', where reciprocal selection is weak or absent throughout the lichen's range (Thompson 1999, 2005, Brodie et al. 2002). Furthermore, while there are studies addressing climate change impacts on lichens (Klanderud and Totland 2005, Crabtree and Ellis 2010, Bjerke 2011, Ellis et al. 2014, Lendemer and Allen 2014, Allen and Lendemer 2016), none of them considers environmental preferences of symbiont partners separately. However, assuming that photobiont switches are an adaptive strategy, at least in some lichens (Piercey-Normore and DePriest 2001, Werth and Sork 2008, 2010), and that some photobionts may even occur free-living (Mukhtar et al. 1994, Beck et al. 1998), an important question then arises as to what extent particular photobionts are climatically

suitable in order to facilitate future range shifts in lichens (Ellis 2012).

In the present study, we address the above questions with a model-based framework in the widespread macrolichen *Lasallia pustulata*, using a comprehensive dataset of presence/absence occurrences throughout the species distributional range, together with a marker-based delineation of sub-species level molecular variance in photobionts and mycobionts (for similar approaches see Gotelli and Stanton-Geddes 2015, Marcer et al. 2016). Despite its predominantly clonal dispersal, *L. pustulata* exhibits a high variability of *Trebouxia* sp. photobionts throughout its range; and most of the *Trebouxia* lineages are shared with other lichen-forming fungi (Sadowska-Deś et al. 2013, 2014), a pattern that suggests frequent switches of photobionts across the species' range. We explore species distribution models (SDMs; Guisan and Zimmermann 2000) together with Hutchinsonian niche hypervolumes (Hutchinson 1957) to ask 1) which climatic factors govern the distribution of photobionts and mycobionts in *L. pustulata* and 2) whether associating with different photobionts influences range expansion of this lichen. Notably, niche quantifications and SDMs calculated from large-scale occurrence data can only give an incomplete description of a species' ecological requirements (or its predicted geographic distribution), because they ignore biotic factors, such as dispersal, competition, and the physiological properties of the organism (Chase and Leibold 2003, Keaney 2006). Our models therefore aim at a dimensional comparison (e.g., uniqueness, extent, overlap) of potential habitat space within a given climatic envelope, rather than at predicting the realized niches of species (Guisan and Zimmermann 2000). Interestingly, however, the quantification of one species' extent in abiotic space (in our study the *Trebouxia* photobionts) can directly correspond to a major biotic niche dimension of another species (in our study the *L. pustulata* mycobionts). Thus, in order to understand potential partner switching strategies, particularly in obligate mutualisms, it is important to quantify the (potential) outcomes of partner switches based on each partner's potential habitat space. To our knowledge, this is the first study approaching the question of preferential photobiont association in lichens from a niche modeling perspective.

Material and methods

Field sampling and molecular methods

We sampled specimens of *L. pustulata* across the species' entire core range, i.e. central Scandinavia to the Canary Islands, and the British Isles to Ukraine and Turkey. In total, we obtained molecular data for 1940 samples (individual thalli) from 119 unique sampling locations (Fig. 1A). Fresh samples were dried and stored at –20°C until DNA extraction. Detailed information about sampling locations and haplotypes are given in Supplementary material Table S1, together with GenBank accession numbers.

From all samples, total genomic DNA was extracted using a small part of the thallus following the CTAB protocol (Cubero and Crespo 2002). Algal symbionts were sequenced at the internal transcribed spacer region nrITS rDNA (primers nrITS1T (f) and nrITS4T (r) based on Kroken and Taylor 2000), and mycobionts were sequenced at the *MCM7*

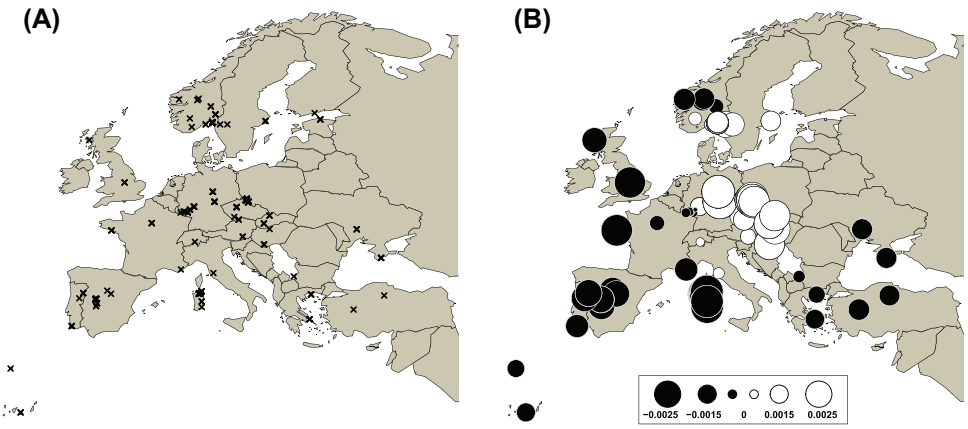

Figure 1. (A) Map depicting 119 unique sampling locations across the core distributional range of *L. pustulata.* (B) Visualization of spatial genetic patterns of *Trebouxia* photobionts using MEMGENE projection (Galpern et al. 2014). Circles represent individual haplotypes. Size and color of the circles depict genetic similarity, with large black and large white circles at opposite extremes of the MEMGENE axis. The legend indicates MEMGENE score values. Visualization of scores for the first MEMGENE axis (explaining 72% of genetic variation among 42 algal haplotypes) suggests the presence of a central genetic cluster (in central Europe) and a peripheral cluster (see Supplementary material Appendix 1 Fig. S1, for the MEMGENE projection of fungal haplotypes).

locus (primers MCM7-709 (f) and MCM7-1348 (r) based on Schmitt et al. 2009). We chose these markers because we have previously shown that they provide the highest intra-population resolution among commonly used sequence-based molecular markers in *L. pustulata* and its associated photobionts (Sadowska-Deś et al. 2013). PCR amplification, amplicon sequencing, and sequence alignment followed established protocols for *L. pustulata* described in Sadowska-Deś et al. (2013, 2014). *Trebouxia* and *Lasallia* sequence identities were confirmed using BLAST searches in GenBank.

Genetic variance and spatial genetic structure

From the aligned sequences, we extracted a total of 42 nrITS rDNA haplotypes for the *Trebouxia* photobionts, and 11 *MCM7* haplotypes for the mycobiont. To characterize the geographic distribution of molecular variance among these haplotypes, we used a regression-based framework to describe the genetic distances – using Kimura's 2-parameter distance – with spatial predictor variables that were generated using Moran's eigenvector maps (MEM; Borcard and Legendre 2002, Griffith and Peres-Neto 2006), as implemented in the 'MEMGENE' R package (Galpern et al. 2014). This approach detects spatial neighborhoods in distance-based data and has been widely used in spatial ecological and genetic contexts (Dray et al. 2012, Manel et al. 2012, Wagner and Fortin 2013, Roffler et al. 2016). The resulting scores for each individual haplotype on the MEM-variables were then used to visualize the spatial genetic structure in our data. Moreover, to examine the genetic variance structure of *Trebouxia* photobionts within and among their fungal partners, we calculated a hierarchical analysis of molecular variance (AMOVA, Excoffier et al. 1992) that considered all algal haplotypes that were associated with one or more of the 11 fungal haplotypes.

Haplotype clustering and OTU delimitation

To circumscribe the molecular variance in our samples for downstream ecological analyses, we used two different approaches to delineate algal and fungal genetic clusters, or operational taxonomic units (hereafter OTUs). Starting from the 42 nrITS rDNA algal haplotypes and the 11 *MCM7* fungal haplotypes respectively, we used the Automatic Barcode Gap Discovery method (ABGD; Puillandre et al. 2012) to delineate photobiont and mycobiont OTUs. Barcode gap discovery infers a model-based confidence limit for intra- and inter-specific genetic distances based on the distribution of all pairwise distances. Depending on this threshold, the method then detects 'barcode gaps' that separate candidate OTUs (Hebert et al. 2003, Puillandre et al. 2012). Notably, the ABGD method has previously been applied to a comprehensive ITS database of *Trebouxia* photobionts from the lichen family Parmeliaceae across a worldwide distribution (Leavitt et al. 2015). In their study, Leavitt et al. (2015) propose a practical ABGD-based classification system for *Trebouxia* photobionts in order to facilitate communication and consistency across future studies. Thus, we carried out the classification of *Trebouxia* OTUs in our study in accordance with the methods used in Leavitt et al. (2015). For this, genetic distances for the ABGD approach were calculated using the JC69 model, and other parameters were set as follows: Pmin = 0.001, Pmax = 0.01, steps = 10, bins = 20, gap width ranging from 0.1 to 1.5 for consistency assessment of inferred groups. The same settings were used for the *MCM7* data obtained from the mycobionts – although here, no general classification reference for the mycobiont exists. Moreover, in order to investigate the robustness of our algal OTUs, we compared the result of the ABGD delimitation against results from a comprehensive set of alternative delimitation and clustering methods (see Supplementary material Appendix 2, for a detailed description of methods and results of all algal OTU robustness analyses). For downstream analyses, algal and fungal OTUs with too few sampling locations ($n < 5$) were omitted (see Results).

Niche hypervolumes and species distribution modeling

Delineated clusters/OTUs of photobionts and mycobionts were subjected to two distinct approaches to characterize their respective ecological niches: 1) direct estimation of n-dimensional hypervolumes from observation points (Blonder et al. 2014), and 2) species distribution modeling (SDM) using maximum entropy (MaxEnt, Phillips et al. 2006). We focus on the Hutchinsonian niche concept that describes a species' niche as an n-dimensional hypervolume, where the dimensions are environmental variables, such as climatic variables or resource distributions (Hutchinson 1957). In our study, we describe these environmental dimensions based on a comprehensive set of 12 bioclim variables from the WorldClim dataset (Supplementary material Table S2), drawn at the highest spatial resolution (~1 km) for our sampling area (WorldClim; Hijmans et al. 2005). We chose this restricted but straightforward set of environmental predictor variables to facilitate the interpretation of our models along the main climatic dimensions of temperature and precipitation in wet and dry periods. In addition to the bioclim variable set reported in the main text, we ran all analyses 1) based on the full set of 19 bioclim variables, and 2) based on a reduced set of seven bioclim variables that showed the weakest correlation structure in our dataset. The former set of analyses addresses the issue of variable set completeness, whereas the latter set of analyses addresses issues of collinearity and non-independence among variables (Dormann et al. 2013). We report all results based on the additional variable sets in the supplementary material (i.e. robustness analyses, Supplementary material Appendix 3). Because all results from these robustness analyses of variable sets were highly congruent with the results based on our original variable choice (Supplementary material), we here present results based on the above mentioned set of 12 bioclim variables that facilitate the interpretation of climatic dimensions in our study area.

Based on the aforesaid environmental predictors, we constructed climatic hypervolumes using multivariate kernel

density estimation, described in Blonder et al. (2014). We first condensed the 12 environmental variables into principal component variables (PCs), where PC1–PC2 already described 90% of the total variance. Hypervolumes for each of the photobiont and mycobiont OTUs were then calculated based on n = 5000 random background points across PC1–PC2, applying a range of bandwidth values (0.2–0.8) to test for stability of results. Varying bandwidths did not change the interpretation of our data and we here show results based on a bandwidth of 0.3. To characterize individual differences in climatic preferences among OTUs, reflected by different niche dimensions, we visually examined hypervolume overlaps in niche space. For this, the individual hypervolume of a particular target OTU (fungal or algal) was projected onto the merged hypervolume of the remaining set of OTUs (fungal or algal). The resulting projection in niche space then allows the identification of particular niche dimensions that are uniquely covered by the respective target OTU. Analyses were carried out using the 'hypervolume' R package (Blonder et al. 2014). Notably, the described hypervolume kernel density estimation has been shown to be sensitive to sample sizes and/or environmental dimensionality (Qaio et al. 2016). Thus, in order to test for robustness of our hypervolume analyses, we additionally calculated all niche quantifications based on the approach developed by Broennimann et al. (2012), implemented in the 'ecospat' R package (Di Cola et al. 2017). We show all additional results from these robustness tests, including the above mentioned robust variable sets, in the supplementary material (Supplementary material Appendix 3). Because the alternative niche quantification approach did not reveal significant differences compared to our original hypervolume analyses, we here report the latter and refer the reader to the Supplementary material Appendix 3 for a detailed comparison of methods.

In addition to hypervolume construction, we used MaxEnt species distribution modeling (Elith et al. 2011, Renner and Warton 2013) as a predictive framework to infer niche breadth and geographic overlap of fungal and algal OTUs. MaxEnt is the most commonly used SDM algorithm that has been shown to perform well for datasets with few occurrence sample points (Elith et al. 2006, Phillips et al. 2006, Elith and Graham 2009, Allen and Lendemer 2016). All MaxEnt models were run for the basic set of 12 bioclim variables, the full set of 19 bioclim variables, and the set of seven bioclim variables that were the least correlated (see Supplementary material Appendix 2 for detailed results). To address issues of model complexity, overfitting, and evaluation, we first applied a jackknife data-partitioning approach to distribute occurrence and background localities (n = 5000) into training and testing bins for k – 1 crossvalidations of k occurrence localities (Shcheglovitova and Anderson 2013, Mateo et al. 2015). Different levels of model complexity were then explored across varying classes of response curves (L: linear, LQ: linear and quadratic, LQH: linear quadratic hinge, H: hinge, and LQHP: linear quadratic hinge product) and regularization multipliers (ranging from 0.5–4), as implemented in the R packages 'dismo' and 'ENMeval' (Muscarella et al. 2014, Hijmans et al. 2015). From a total of 48 different parameter sets, we chose the best model complexity based on AICc values and the AUC criterion (Phillips et al. 2006, Warren and Seifert 2011). In addition to visualizing the predicted spatial distribution of OTUs, we used MaxEnt model outcomes to infer potential interaction hotspots, defined as geographic areas where the encounter probability of particular symbiont partners (i.e. their combined occurrence probabilities) is predicted to be high. Moreover, we calculated pairwise overlap scores for all mycobionts and photobionts in total niche space, based on Schoener's D (ranging from 0: no overlap, to 1: complete overlap; Schoener 1968). For both sets of analyses (hypervolumes and SDMs) we omitted OTUs with too few sampling locations (n < 5), or combined their distributions (see Results). All analyses were carried out in R 3.3.2 (R Core Development Team).

Data deposition

Data available from the Dryad Digital Repository: <http://dx.doi.org/10.5061/dryad.64149> (Rolshausen et al. 2017).

Results

Genetic structure and OTU delimitation

Most of the genetic variance among *Trebouxia* photobionts was detected within mycobionts (93.61%), whereas only 6.39% variation was explained between mycobionts (AMOVA), indicating that only a small fraction of the total variance among photobionts is structured by mycobiont partners. The spatial structure of ITS variation in photobionts across our sampling area, as described by the first MEMGENE axis (explaining 72% of the genetic variation) reveals the greatest differentiation between haplotypes occurring in central Europe and haplotypes from the Mediterranean regions, the British Isles, and south-eastern Europe (Fig. 1B). Comparing the amount of spatial genetic pattern explained by the full analysis ($R^2 = 16.31$) with recently published simulation results further indicates that more of the genetic structure in our data is explicable by spatial structure than might be expected under a pure isolation-by-distance (IBD) scenario where R^2 values typically fall below 0.10 (Galpern et al. 2014). For fungal haplotypes, spatial structuring of *MCM7* variation was non-significant (i.e. no significant MEMGENE axes found) and a low R^2 value of 0.06 did not exclude the IBD null model (distribution plot based on non-significant MEMGENE axis 1 is shown in Supplementary material Appendix 1 Fig. S1).

The two approaches to delineate clusters of genetic variance in mycobionts and photobionts yielded very similar results. For *Trebouxia* photobionts, the 42 ITS

haplotypes were grouped into seven distinct clusters based on hierarchical clustering of pairwise genetic distances. Using the alternative ABGD method (Puillandre et al. 2012), we recovered six OTUs (hereafter OTU_{alga}, based on JC69 distance model with prior maximal distance, $p = 0.0046$), one of which merged two of the aforesaid clusters (Supplementary material Appendix 1 Fig. S2A, Supplementary material Table S1). For the *L. pustulata* mycobiont, hierarchical clustering of 11 haplotypes yielded nine clusters, of which two were merged by the ABGD method into a total of seven OTUs (hereafter OTU_{fungus}, based on JC69 distance model with prior maximal distance, $p = 0.0028$; Supplementary material Appendix 1 Fig. S2B). Haplotype networks for photobionts and mycobionts respectively are shown in Supplementary material Appendix 1 Fig. S3. Furthermore, comparing the *Trebouxia* haplotypes from our study to the 69 ITS OTUs underlying the recently proposed classification system for *Trebouxia* photobionts (Leavitt et al. 2015) revealed that all of our haplotypes fall into the 'S' clade (*simplex/letharii/jamesii* group; Supplementary material Appendix 1 Fig. S2A). For downstream ecological analyses, we omitted algal and fungal OTUs with too few sampling locations ($n < 5$), leading to the exclusion of three mycobionts (OTU_{fungus} 5–7), and one photobiont (OTU_{alga} 6) for niche construction and SDM analyses (Supplementary material Table S1). In order to complete results for the omitted mycobionts, we also combined the distribution data of OTU_{fungus} 5–7 and examined their merged niche dimensions.

Climatic niche construction and SDM

We constructed 2-dimensional (BioClim PC1–PC2; explaining 90% variation) hypervolumes for each OTU (i.e. the target OTU) versus all of the remaining OTUs combined. Inspection of overlaps between these two projections in PCA space allows the following interpretation regarding environmental preferences of target OTUs: in photobionts, we found the environmental preferences of OTU_{alga} 1 to span most of the total *Trebouxia* niche space (here defined as the *Trebouxia* niche space in association with *L. pustulata* in our study), extending into all main climatic dimensions of the depicted PCA space (Fig. 2A). Two other OTU_{alga}, 2 and 3, showed restricted niche dimensions, and neither of them covered a unique area of the total *Trebouxia* niche. Interestingly, the two remaining OTU_{alga} showed non-overlapping dimensions compared to the remaining overall niche projection (OTU_{alga} 1–3), both at opposite ends of niche space: OTU_{alga} 4 spreading uniquely into colder and wetter regions, and OTU_{alga} 5 spreading uniquely into warmer and potentially drier regions (Fig. 2A). Applying the same logic to projections of OTU_{fungus} niches revealed a different picture for the environmental preferences among the mycobionts. Here, OTU_{fungus} 1 broadly covered the full *L. pustulata* niche space depicted in our study, including several unique portions (Fig. 2B). In contrast, the remaining four OTU_{fungus} (2–4, and 5–7 merged) indeed showed differences in their niche dimensions, but none comprised unique (i.e. non-overlapping) portions of the full niche projection, except a small fraction for OTU_{fungus} 2 (Fig. 2B).

A similar picture emerged from MaxEnt SDM predictions. After evaluation of the best parameter sets for each OTU (Supplementary material Table S3), MaxEnt was run for OTUs (alga and fungus) with > 15 sampling locations. From this, we highlight SDM results for three OTU_{alga} (1, 4, and 5) that already showed distinguished patterns of habitat suitability in hypervolume projections. In particular, the geographic SDM predictions for habitat suitability in OTU_{alga} 1 confirmed its relatively generalistic climatic preferences (in association with *L. pustulata*), with the highest suitability values for central European regions, northern Spain, and northern Turkey (Fig. 3, upper panel). In contrast, OTU_{alga} 4 had the highest suitability scores in arctic-alpine regions, such as the Alps, the Pyrenees, the Cantabrian mountain ridge, Scotland, and Norway. OTU_{alga} 5, the putatively more warm-tolerant photobiont, was predicted to occur with the highest probability in the Mediterranean region (southern Spain, southern Italy, Corsica, Sardinia, and the Aegean Sea), as well as the Canary Islands (Fig. 3, upper panel). To further explore how these niche preferences in photobionts might translate into geographic hotspots of symbiotic interactions, we overlaid the SDM predictions for each of the three OTU_{alga} (1, 4, and 5) with the overall SDM prediction for the mycobionts (combining predictions for all OTU_{fungus}). Using multiplication as the connecting operation between SDM prediction layers of symbiont partners then yielded a map of potential interaction hotspots where it is most likely that the (generalist) mycobiont overlaps with particular photobionts (depicted as encounter probability in Fig. 3, lower panel). In accordance with hypervolume projections and SDM model predictions, the OTU_{fungus}–OTU_{alga}–overlap quantification depicts interaction hotspots for OTU_{alga} 1 (generalist) to be broadly distributed, hotspots for OTU_{alga} 4 (cold preferring) located in colder regions and higher elevations, and hotspots for OTU_{alga} 5 (warm preferring) in warmer Mediterranean regions and the Canary Islands (Fig. 3, lower panel). A complete overview of separate MaxEnt model projections for all OTUs with sufficient data is given in Supplementary material Appendix 1 Fig. S4, while Fig. S5 gives pairwise niche overlap scores between all OTU_{alga} and OTU_{fungus} based on Schoener's D metric.

Discussion

Theory predicts that mutualists may augment the environmental tolerance of host species and increase the potential for a host to expand its ecological niche and geographic range (Moran 2007, Poisot et al. 2011, Friesen and Jones 2012, Hussa and Goodrich-Blair 2013). Empirical examples come from fungal or bacterial symbionts that catalyse niche expansion in plants and invertebrates (Joy 2013, Afkhami et al. 2014, Chong and Moran 2016, Maher et al. 2017), or from photosynthetic algal symbionts that govern distinct environmental zonation in corals and sea anemones (Bates 2000,

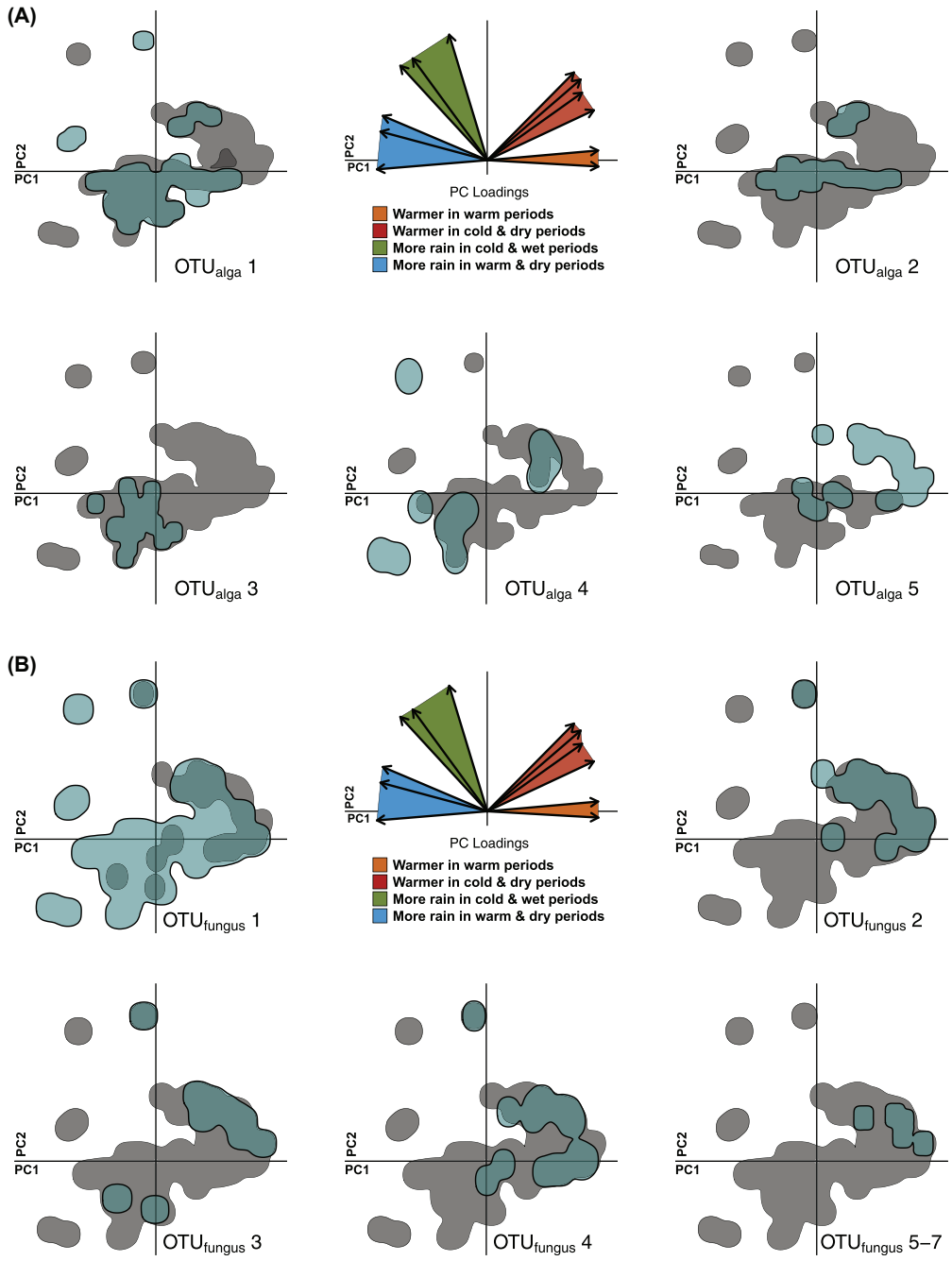

Figure 2. Niche hypervolumes for (A) *Trebouxia* photobionts and (B) *L. pustulata* mycobionts based on environmental PC1–PC2 axes (explaining 94% of variation; PC loadings are depicted in mid-upper panel together with their general interpretations; Supplementary material Table S2). Each of the five projections in (A) and (B) shows the niche hypervolume of a particular $OTU_{alga\ (A)/fungus\ (B)}$ (in cyan) superimposed on the complete niche hypervolume of all remaining $OTU_{alga/fungus}$ (in grey). Non-overlapping portions of cyan and grey projections indicate unique contributions of a particular OTU to the overall fungal or algal niche space.

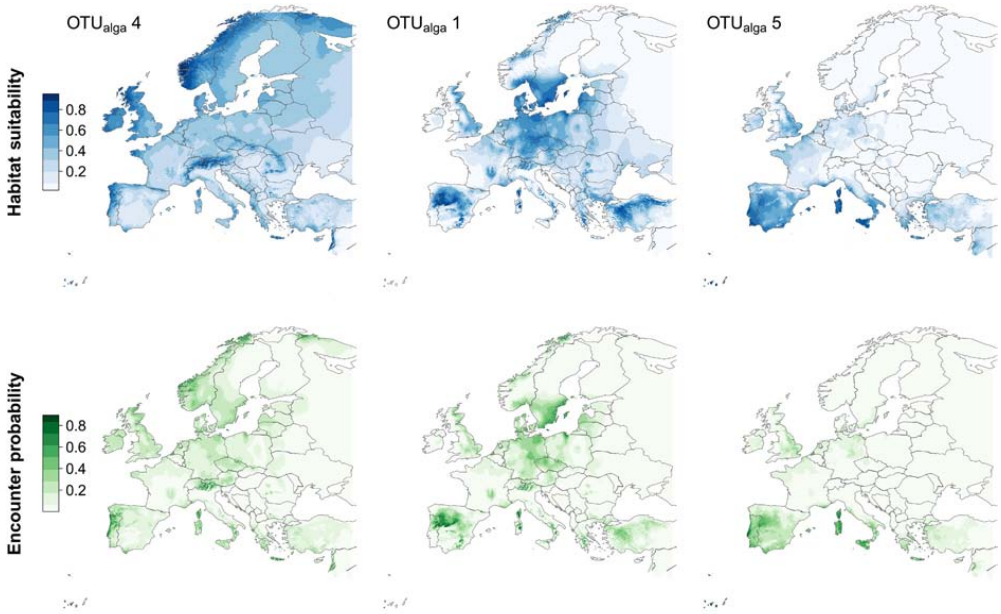

Figure 3. Upper panel: habitat suitability predictions from MaxEnt species distribution models for three prominent algal OTUs (generalistic ecotype OTU$_{alga}$ 1, arctic-alpine ecotype OTU$_{alga}$ 4, and Mediterranean ecotype OTU$_{alga}$ 5). Lower panel: encounter probability of the above ecotypes with the fungal mycobiont (all OTU$_{fungus}$) throughout the distributional range of *L. pustulata*. Probability scores were calculated as the product of model-based habitat suitabilities for the respective photobionts (OTU$_{alga}$ 1, 4, and 5) and the mycobiont (combining all OTU$_{fungus}$). Separate model predictions for all symbiont partners are depicted in Supplementary material Appendix 1 Fig. S4.

Iglesias-Prieto et al. 2004, Mieog et al. 2009, Bongaerts et al. 2015). Similar patterns are also observed in lichen symbioses where a particular mycobiont can associate with genetically differentiated photobionts across a broad eco-geographic range (Opanowicz and Grube 2004, Yahr et al. 2006, Muggia et al. 2010, Fernández-Mendoza et al. 2011, Werth and Sork 2014). Yet, to what extent ecological differentiation (e.g. climatic tolerance) among distinct mutualists alters the overall niche breadth of a symbiosis, is less well understood. To investigate this question, we quantified individual niche contributions of genetically differentiated photobionts and mycobionts in the lichen *L. pustulata* across its core range. The particular distribution pattern we found resembles a climatically structured interaction mosaic between symbionts, and highlights the association with different photobionts as an adaptive strategy in this lichen.

Genetic variance and spatial structure

All 42 *Trebouxia* algae haplotypes we found for our broad-scale European dataset (Fig. 1A) fall within the 'S' clade of the recently published *Trebouxia* phylogeny (Leavitt et al. 2015), where they mainly comprise two distinct clades together with the already existing stock of 'S'-clade photobionts. One of these clades includes OTU$_{alga}$ 1, 3, and 6 – showing more generalistic environmental preferences; whereas the other clade includes, along with OTU$_{alga}$ 2, the two environmentally specialized OTU$_{alga}$ 4, and 5 (Supplementary material Appendix 1 Fig. S2A). A closer look at the spatial distribution of ITS variance among photobionts reveals a central cluster, surrounded by a differentiated peripheral cluster (Fig. 1B). Regression modeling that involved spatially explicit predictors to explain genetic distances among photobiont haplotypes, further indicated that the basic negative relationship between distance and gene flow (isolation-by-distance, IBD) might not be sufficient to explain the genetic structure in our data. We thus interpret the pattern of spatial differentiation to be not only governed by IBD dynamics, but also by adaptive dynamics of particular photobionts evolving distinct environmental preferences. As for the mycobiont, we did not discover significant spatial structure in *MCM7* variation compared to ITS variation in photobionts (Supplementary material Appendix 1 Fig. S1). The analyses of spatial genetic variation among haplotypes of these markers therefore suggests environmental structuring in photobionts, but not in mycobionts; a pattern that was then further corroborated through niche modeling of algal and fungal OTUs.

Among the five photobiont OTUs that were further scrutinized for their environmental preferences (in association with *L. pustulata*), we found one generalist (OTU$_{alga}$ 1) with a broad climatic niche, and two putative specialists (OTU$_{alga}$ 4 and 5) with unique preferences at opposite ends of the

climatic niche space governing our sampling area (Fig. 2A). Notably, although our delineation approach is based on only a single genetic marker, the barcode gap detection approach (ABGD, Puillandre et al. 2012) we applied to define OTUs has recently been tested extensively for *Trebouxia* algal ITS sequences where it reliably depicted OTU boundaries (Leavitt et al. 2015). Accordingly, we consider the photobiont OTUs recovered from our data as evolutionary independent, non-recombining units for which the described pattern of non-overlapping niches (in OTU_{alga} 4 and 5) suggests distinct climatic preferences in response to environmental selection (Graham et al. 2004, Kozak et al. 2008). However, for an in-depth examination of adaptive divergence among *Trebouxia* photobionts – which was not the focus of our study – the description of genetic variance has to include genome-wide patterns that surmount the scope of a single (or a few) barcode markers.

In comparison to the niche spaces we found for the photobionts of *L. pustulata*, the mycobionts showed a different pattern, involving a broadly distributed generalistic type (OTU_{fungus} 1) that occurred throughout the sampling area, together with a few genetically differentiated sub-types that did, however, not show unique climatic preferences in their spatial distributions (Fig. 2B). Interestingly, the selective regimes potentially associated with the genetic variation among photobionts lie on opposite ends of the full climatic spectrum of *L. pustulata* (Fig. 2A). Hence, variation in environmental preferences among algal OTUs significantly broadens the overall niche space of *L. pustulata* towards colder and wetter climates (OTU_{alga} 4 associating with OTU_{fungus} 1), as well as towards warmer and drier climates (OTU_{alga} 5 associating with OTU_{fungus} 1–4). Taken together, the analyses of spatial genetic variance and niche hypervolumes in *L. pustulata* lichens thus support the hypothesis of photobiont switches as an adaptive strategy for a (generalist) mycobiont to broaden its distributional range (Piercey-Normore and DePriest 2001, Werth and Sork 2008, 2010, Fernández-Mendoza et al. 2011, O'Brien et al. 2013).

Distribution modeling and interaction hotspots

Given that photobiont switches occur throughout the distributional range of *L. pustulata*, such that the generalist mycobiont will associate with locally frequent photobionts, the question then arises as to where these switches are most likely to take place. Based on species distribution models (SDM), we approached this question by translating environmental preferences of symbiont partners into their respective geographic distributions. With regard to algal switches and niche expansion, we focused on interactions between the generalist mycobiont and the three photobiont OTUs that showed either generalistic (OTU_{alga} 1), cold-tolerant (OTU_{alga} 4), or warm-tolerant (OTU_{alga} 5) distributions in their association with *L. pustulata*. In accordance with niche hypervolume analyses, SDMs predicted OTU_{alga} 1 to span most of central Europe, whereas habitat suitability for OTU_{alga} 4 peaked in arctic-alpine regions, and OTU_{alga} 5 appeared to be restricted to the Mediterranean (Fig. 3; Supplementary material Appendix 1 Fig. S4A). Moreover, as would be expected, SDMs for the mycobionts predicted a broad central European distribution with no particular specialization for OTU_{fungus} 1, and a clustered distribution in the Mediterranean region for OTU_{fungus} 2–4 (Supplementary material Appendix 1 Fig. S4B). We also point out that the suggested pattern of photobiont switches from the generalistic OTU_{alga} 1 to the warm preferring OTU_{alga} 5 in our broad-scale analyses has recently been detected along a local-scale altitudinal gradient in the Mediterranean (Dal Grande et al. 2017a; see Supplementary material Appendix 2 for congruency between OTU delimitations).

Interestingly, the overall distribution of suitable habitat for *Trebouxia* photobionts was predicted to be significantly larger than the overall distribution of *L. pustulata* mycobionts (Supplementary material Appendix 1 Fig. S4C). Here, it is important to note that the data only include *Trebouxia* strains that were found to be associated with *L. pustulata*, whereas other lichen-forming fungi occurring in the same range were not examined. Hence, given the low specificity of *Trebouxia* algae towards their fungal partners (Friedl and Büdel 1996, Piercey-Normore and DePriest 2001, Peksa and Ŝkaloud 2011), we can currently not resolve whether the differentiated model distributions (and niches) of algal OTUs correspond to locally adapted strains, or whether their distributions are in fact broader considering additional fungal partners. In order to fully understand local adaptation in strains of lichen-associated algae, the spatial extent and dispersal capacities of the entire lichen community harboring those strains has to be taken into account.

Notwithstanding, the modeled distributions of algal OTUs from our data do strengthen the assumption that the range of *L. pustulata* lichens is probably not restricted, but broadened, by environmental preferences of *Trebouxia* algae. In particular, range expansions via photobiont switches will be most effective either towards colder and wetter climates, such as in arctic-alpine regions (switching to OTU_{alga} 4), or towards warmer and drier climates, such as in the Mediterranean (switching to OTU_{alga} 5, see also Dal Grande et al. 2017a). Accordingly, regarding the interaction hotspots of symbiont partners (depicted as the product of their respective occurrence probabilities), the generalist mycobiont (OTU_{fungus} 1) will also likely encounter these *Trebouxia* strains at the outer margins of its distribution (Fig. 3, lower panel). Notably, the remaining genetically differentiated mycobionts (OTU_{fungus} 2–4) primarily clustered in the Mediterranean (Supplementary material Appendix 1 Fig. S4B), suggesting diversification of mycobionts to be more likely in that region. However, to further explore the adaptive significance of this pattern, particularly in regard to photobiont switching and niche overlap (Supplementary material Appendix 1 Fig. S5), additional genome-wide analyses – as opposed to our rather conservative set of genetic markers (ITS rDNA for algae and *MCM7* for fungi) – would be valuable. For instance,

a recent study found genome-wide differentiation among *L. pustulata* mycobionts from the Mediterranean (Sardinia, Italy) that is likely driven by adaptive divergence along an elevational cline (Dal Grande et al. 2017b). Taken together, our results provide evidence for mutualist-mediated niche (and range) expansion in lichens – a strategy also observed in other mutualisms (Afkhami et al. 2014, Bongaerts et al. 2015, Maher et al. 2017) – thereby corroborating theoretical predictions for symbiosis as an adaptive process (Moran 2007, Poisot et al. 2011, Friesen and Jones 2012). We also highlight the importance of niche and distribution models to quantify or locate unique ranges and overlaps of distinct partners involved in a symbiosis (see also Peksa and Ŝkaloud 2011, Afkhami et al. 2014, Allen and Lendemer 2016).

Coevolution and ecological fitting

Regarding the underlying mechanisms structuring *L. pustulata* lichen symbioses across ecological gradients, the spatial genetic pattern of symbiont partners together with their model-based niche predictions can also help to distinguish between two fundamental mechanistic concepts of species associations: coevolution and ecological fitting. Coevolution requires reciprocal selection pressures between interacting species, such that the fitnesses of particular genotypes in one species depend on the distribution of genotypes in the other species (Ehrlich and Raven 1964, Thompson 1999, 2005). Moreover, this reciprocity in fitness functions will often be geographically structured based on local genotype-by-genotype-by-environment interactions, thereby creating a geographic mosaic of strong and weak (or absent) coevolution (Thompson 1999, 2005). On the one hand, strong interdependence of genotype distributions will lead to codiversification and phylogenetic conservatism among interacting partners. On the other hand, weak genetic interdependence can lead to breaks in codiversification, specifically if one genotype obtains realized fitness after colonizing a new habitat where fitnesses are not strongly dependent on the distribution of genotypes in the other species (Thompson 1999, Gomulkiewisz et al. 2000, Nuismer et al. 2000, 2003). The latter scenario is often related to the concept of ecological fitting which is based on the evolutionary history of interacting species being co-opted in a new selective environment with little to no adaptive divergence to the current partner (Janzen 1985, Agosta and Klemens 2008, Agosta et al. 2010).

The spatial genetic pattern we observed in *L. pustulata* lichens – i.e. a generalistic mycobiont switches between genetically differentiated photobionts with divergent ecological amplitudes – appears to be in agreement with the concept of ecological fitting, rather than with strong coevolution between specific genotypes. Indeed, our study thereby confirms a commonly observed pattern found in other lichen symbioses at the level of sub-species or populations (Piercey-Normore 2006, Yahr et al. 2006, Werth and Sork 2008, 2010, Muggia et al. 2014). On a larger phylogenetic scale, however, lichen symbioses are certainly structured by coevolution, as is evident from strong phylogenetic constraint in partner compatibility (DePriest 2004, Yahr et al. 2004, Miadlikowska et al. 2006, Leavitt et al. 2015, Singh et al. 2017). Interestingly, despite only weak codiversification among partners on the sub-species level, their spatial interaction pattern – especially in regard to niche expansion – will often still resemble a mosaic of interaction hotspots (where putatively specialized partners are more frequently available) and coldspots (where there are mainly generalist partners). Hence, it is important for our understanding of lichen symbioses to identify such hotspots where photobiont switches will most likely occur with adaptive benefits.

Conclusions

This study highlights the importance of spatial genetic approaches in order to determine the ecological drivers that structure mutualisms (Yahr et al. 2006, Werth and Sork 2008, 2010, Muggia et al. 2014). Our results confirm a commonly observed pattern in lichen symbioses, where a generalist mycobiont associates with genetically differentiated and ecologically divergent photobionts, thereby potentially expanding its distributional range. Particularly with regard to ongoing climate change, the identification of interaction hotspots among symbiont partners will not only help to understand how lichens can cope with shifting climatic selection regimes, but also to inform conservation strategies on potentially vulnerable populations (Klanderud and Totland 2005, Ellis 2012, Allen and Lendemer 2016). Importantly, given that our assessment of genetic differentiation is currently based on a rather conservative set of genetic markers (ITS rDNA for algae and *MCM7* for fungi), additional analyses with broad-scale genomic tools are needed. To conclude, quantifying the ecological contribution of different genotypes to the overall (climatic) niche of a symbiosis will help to inform future molecular and genomic approaches aiming to understand eco-evolutionary dynamics in mutualisms.

Acknowledgements – We thank the following colleagues for valuable support in field work and sampling: A. Agudo, J. E. Anonby, O. Blum, A. Breili, M. Candan, B. Coppins, P. K. Divakar, C. Ellis, E. Farkas, T. Feuerer, M. Grube, A. Guttova, R. Haugan, H. Holien, V. John, J. Johnsen, J. B. Jordal, B. Kanz, K. Kinalioglu, J. T. Klepsland, J. Liska, L. Lőkös, O. Nadyeina, Z. Palice, L. Paoli, I. Pedley, R. Pino-Bodas, T. Pisani, C. Printzen, T. Randlane, T. Raus, C. Ruibal, J. Sadowscy, C. Scheidegger, G. Singh, H. Sipman, M. Sohrabi, A. Suija, K. Szczepanska, E. Timdal, M. Vivas-Rebuelta, J. Vondrak and M. Wedin.
Author contributions – IS and AS-D designed the study; FDG and AS-D conducted field work and sampling; JO performed laboratory work; GR analyzed the data and wrote the manuscript, with input from IS, FDG and AS-D.

References

Afkhami, M. E. et al. 2014. Mutualist-mediated effects on species' range limits across large geographic scales. – Ecol. Lett. 17: 1265–1273.

Agosta, S. J. and Klemens, J. A. 2008. Ecological fitting by phenotypically flexible genotypes: implications for species associations, community assembly and evolution. – Ecol. Lett. 11: 1123–1134.
Agosta, S. J. et al. 2010. How specialists can be generalists: resolving the "parasite paradox" and implications for emerging infectious disease. – Zoologia 27: 151–162.
Allen, J. L. and Lendemer, J. C. 2016. Climate change impacts on endemic, high-elevation lichens in a biodiversity hotspot. – Biodivers. Conserv. 25: 555–568.
Bates, A. 2000. The intertidal distribution of two algal symbionts hosted by *Anthopleura xanthogrammica* (Brandt 1835). – J. Exp. Mar. Biol. Ecol. 249: 249–262.
Beck, A. et al. 1998. Selectivity of photobiont choice in a defined lichen community: inferences from cultural and molecular studies. – New Phytol. 139: 709–720.
Bjerke, J. W. 2011. Winter climate change: ice encapsulation at mild subfreezing temperatures kills freeze-tolerant lichens. – Environ. Exp. Bot. 72: 404–408.
Blaha, J. et al. 2006. High photobiont diversity associated with the euryoecious lichen-forming ascomycete *Lecanora rupicola* (Lecanoraceae, Ascomycota). – Biol. J. Linn. Soc. 88: 283–293.
Blonder, B. et al. 2014. The n-dimensional hypervolume. – Global Ecol. Biogeogr. 23: 595–609.
Bongaerts, P. et al. 2015. Prevalent endosymbiont zonation shapes the depth distributions of scleractinian coral species. – R. Soc. Open Sci. 2: 140297.
Borcard, D. and Legendre, P. 2002. All-scale spatial analysis of ecological data by means of principal coordinates of neighbour matrices. – Ecol. Model. 153: 51–68.
Brodie, E. D. et al. 2002. The evolutionary response of predators to dangerous prey: hotspots and coldspots in the geographic mosaic of coevolution between garter snakes and newts. – Evolution 56: 2067–2082.
Broennimann, O. et al. 2012. Measuring ecological niche overlap from occurrence and spatial environmental data. – Global Ecol. Biogeogr. 21: 481–497.
Chase, J. M. and Leibold, M. A. 2003. Ecological niches – linking classical and contemporary approaches. – Univ. of Chicago Press.
Chong, R. A. and Moran, N. A. 2016. Intraspecific genetic variation in hosts affects regulation of obligate heritable symbionts. – Proc. Natl Acad. Sci. USA 113: 13114–13119.
Crabtree, D. and Ellis, C. J. 2010. Species interaction and response to wind speed alter the impact of projected temperature change in a montane ecosystem. – J. Veg. Sci. 21: 744–760.
Cubero, O. F. and Crespo, A. 2002. Isolation of nucleic acids from lichens. – In: Kranner, I. C. et al. (eds), Protocols in lichenology. Springer, pp. 381–391.
Dal Grande, F. et al. 2012. Vertical and horizontal photobiont transmission within populations of a lichen symbiosis. – Mol. Ecol. 21: 3159–3172.
Dal Grande, F. et al. 2014. Molecular phylogeny and symbiotic selectivity of the green algal genus *Dictyochloropsis* s.l. (Trebouxiophyceae): a polyphyletic and widespread group forming photobiont-mediated guilds in the lichen family Lobariaceae. – New Phytol. 202: 455–470.
Dal Grande, F. et al. 2017a. Environment and host identity structure communities of green algal symbionts in lichens. – New Phytol. doi:10.1111/nph.14770
Dal Grande, F. et al. 2017b. Adaptive differentiation coincides with local bioclimatic conditions along an elevational cline in populations of a lichen-forming fungus. – BMC Evol. Biol. 17: 93.
DePriest, P. T. 2004. Early molecular investigations of lichen-forming symbionts: 1986–2001. – Annu. Rev. Microbiol. 58: 273–301.
Di Cola, V. et al. 2017. Ecospat: an R package to support spatial analyses and modeling of species niches and distributions. – Ecography 40: 774–787.
Doering, M. and Piercey-Normore, M. D. 2009. Genetically divergent algae shape an epiphytic lichen community on Jack Pine in Manitoba. – Lichenology 41: 69–80.
Dormann, C. F. et al. 2013. Collinearity: a review of methods to deal with it and a simulation study evaluating their performance. – Ecography 36: 27–46.
Dray, S. et al. 2012. Community ecology in the age of multivariate multiscale spatial analysis. – Ecol. Monogr. 82: 257–275.
Ehrlich, P. R. and Raven, P. H. 1964. Butterflies and plants: a study in coevolution. – Evolution 18: 586–608.
Elith, J. and Graham, C. H. 2009. Do they? How do they? WHY do they differ? On finding reasons for differing performances of species distribution models. – Ecography 32: 66–77.
Elith, J. et al. 2006. Novel methods improve prediction of species' distributions from occurrence data. – Ecography 29: 129–151.
Elith, J. et al. 2011. A statistical explanation of MaxEnt for ecologists. – Divers. Distrib. 17: 43–57.
Ellis, C. J. 2012. Lichen epiphyte diversity: a species, community and trait-based review. – Perspect. Plant Ecol. Evol. Syst. 14: 131–152.
Ellis, C. J. et al. 2014. Response of epiphytic lichens to 21st century climate change and tree disease scenarios. – Biol. Conserv. 180: 153–164.
Excoffier, L. et al. 1992. Analysis of molecular variance inferred from metric distances among DNA haplotypes: application to human mitochondrial DNA restriction data. – Genetics 131: 479–491.
Fernández-Mendoza, F. et al. 2011. Population structure of mycobionts and photobionts of the widespread lichen *Cetraria aculeata*. – Mol. Ecol. 20: 1208–1232.
Friedl, T. 1987. Thallus development and phycobionts of the parasitic lichen *Diploschistes muscorum*. – Lichenology 19: 183–191.
Friedl, T. and Büdel, B. 1996. Photobionts. – In: Nash, T. H. (ed.), Lichen biology. Cambridge Univ. Press, pp. 8–23.
Friesen, M. L. and Jones, E. I. 2012. Modelling the evolution of mutualistic symbioses. – In: van Helden, J. et al. (eds), Bacterial molecular networks. Springer, pp. 481–499.
Galpern, P. et al. 2014. MEMGENE: Spatial pattern detection in genetic distance data. – Methods Ecol. Evol. 5: 1116–1120.
Gomulkiewicz, R. et al. 2000. Hot spots, cold spots, and the geographic mosaic theory of coevolution. – Am. Nat. 156: 156–174.
Gotelli, N. J. and Stanton-Geddes, J. 2015. Climate change, genetic markers and species distribution modelling. – J. Biogeogr. 42: 1577–1585.
Graham, C. H. et al. 2004. Integrating phylogenetics and environmental niche models to explore speciation mechanisms in dendrobatid frogs. – Evolution 58: 1781–1793.
Griffith, D. A. and Peres-Neto, P. R. 2006. Spatial modeling in ecology: the flexibility of eigenfunction spatial analyses. – Ecology 87: 2603–2613.

Guisan, A. and Zimmermann, N. E. 2000. Predictive habitat distribution models in ecology. – Ecol. Model. 135: 147–186.
Hebert, P. D. N. et al. 2003. Biological identifications through DNA barcodes. – Proc. R. Soc. B 270: 313–321.
Hijmans, R. J. et al. 2005. Very high resolution interpolated climate surfaces for global land areas. – Int. J. Climatol. 25: 1965–1978.
Hijmans, R. J. et al. 2015. dismo: species distribution modeling. – R package ver. 1.0-12. <http://cran.r-project.org>.
Hussa, E. A. and Goodrich-Blair, H. 2013. It takes a village: ecological and fitness impacts of multipartite mutualism. – Annu. Rev. Microbiol. 67: 161–178.
Hutchinson, G. 1957. Concluding remarks. – Cold Spring Harb. Symp. Quant. Biol. 22: 415–427.
Iglesias-Prieto, R. et al. 2004. Different algal symbionts explain the vertical distribution of dominant reef corals in the Eastern Pacific. – Proc. R. Soc. B 271: 1757–1763.
Janzen, D. H. 1985. On ecological fitting. – Oikos 45: 308–310.
Joy, J. B. 2013. Symbiosis catalyses niche expansion and diversification. – Proc. R. Soc. B 280: 20122820.
Keaney, M. 2006. Habitat, environment and niche: what are we modelling? – Oikos 115: 186–191.
Klanderud, K. and Totland, O. 2005. Simulated climate change altered dominance hierarchies and diversity of an alpine biodiversity hotspot. – Ecology 86: 2047–2054.
Kozak, K. H. et al. 2008. Integrating GIS-based environmental data into evolutionary biology. – Trends Ecol. Evol. 23: 141–148.
Kroken, S. and Taylor, J. W. 2000. Phylogenetic species, reproductive mode, and specificity of the green alga *Trebouxia* forming lichens with the fungal genus *Letharia*. – Bryologist 103: 645–660.
Leavitt, S. D. et al. 2015. Fungal specificity and selectivity for algae play a major role in determining lichen partnerships across diverse ecogeographic regions in the lichen-forming family Parmeliaceae (Ascomycota). – Mol. Ecol. 24: 3779–3797.
Lendemer, J. C. and Allen, J. L. 2014. Lichen biodiversity under threat from sea-level rise in the Atlantic Coastal Plain. – Bioscience 64: 923–931.
Maher, A. M. D. et al. 2017. An entomopathogenic nematode extends its niche by associating with different symbionts. – Microb. Ecol. 73: 211–223.
Manel, S. et al. 2012. Broad-scale adaptive genetic variation in alpine plants is driven by temperature and precipitation. – Mol. Ecol. 21: 3729–3738.
Marcer, A. et al. 2016. Geographical restructuring of *Arabidopsis thaliana*'s genetic makeup in the Iberian Peninsula due to climate change based on genetic cluster membership. – BioRxiv <http://dx.doi.org/10.1101/091686>.
Mateo, R. G. et al. 2015. What is the potential of spread in invasive bryophytes? – Ecography 38: 480–487
Miadlikowska, J. et al. 2006. New insights into classification and evolution of the Lecanoromycetes (Pezizomycotina, Ascomycota) from phylogenetic analyses of three Ribosomal RNA- and two protein-coding genes. – Mycologia 98: 1088–1103.
Mieog, J. C. et al. 2009. The roles and interactions of symbiont, host and environment in defining coral fitness. – PLoS One 4: e6364.
Moran, N. A. 2007. Symbiosis as an adaptive process and source of phenotypic complexity. – Proc. Natl Acad. Sci. USA 104: 8627–8633.
Muggia, L. et al. 2010. Morphological and phylogenetic study of algal partners associated with the lichen-forming fungus *Tephromela atra* from the Mediterranean region. – Symbiosis 51: 149–160.
Muggia, L. et al. 2014. Photobiont selectivity leads to ecological tolerance and evolutionary divergence in a polymorphic complex of lichenized fungi. – Ann. Bot. 114: 463–475.
Mukhtar, A. et al. 1994. Does the lichen alga *Trebouxia* occur free-living in nature: further immunological evidence. – Symbiosis 17: 247–253.
Muscarella, R. et al. 2014. ENMeval: an R package for conducting spatially independent evaluations and estimating optimal model complexity for Maxent ecological niche models. – Methods Ecol. Evol. 5: 1198–1205.
Nuismer, S. L. et al. 2000. Coevolutionary clines across selection mosaics. – Evolution 54: 1102–1115.
Nuismer, S. L. et al. 2003. Coevolution in temporally variable environments. – Am. Nat. 162: 195–204.
O'Brien, H. E. et al. 2013. Assessing population structure and host specialization in lichenized cyanobacteria. – New Phytol. 198: 557–566.
Opanowicz, M. and Grube, M. 2004. Photobiont genetic variation in *Flavocetraria nivalis* from Poland (Parmeliaceae, lichenized Ascomycota). – Lichenology 36: 125–131.
Peksa, O. and Ŝkaloud, P. 2011. Do photobionts influence the ecology of lichens? A case study of environmental preferences in symbiotic green alga *Asterochloris* (Trebouxiophyceae). – Mol. Ecol. 20: 3936–3948.
Phillips, S. J. et al. 2006. Maximum entropy modeling of species geographic distributions. – Ecol. Model. 190: 231–259.
Piercey-Normore, M. D. 2006. The lichen-forming ascomycete *Evernia mesomorpha* associates with multiple genotypes of *Trebouxia jamesii*. – New Phytol. 169: 331–344.
Piercey-Normore, M. D. and DePriest, P. T. 2001. Algal switching among lichen symbioses. – Am. J. Bot. 88: 1490–1498.
Poisot, T. et al. 2011. A conceptual framework for the evolution of ecological specialisation. – Ecol. Lett. 14: 841–851.
Puillandre, N. et al. 2012. ABGD, automatic barcode gap discovery for primary species delimitation. – Mol. Ecol. 21: 1864–1877.
Qaio, H. et al. 2016. A cautionary note on the use of hypervolume kernel density estimators in ecological niche modelling. – Global Ecol. Biogeogr. 26: 1066–1070.
Rambold, G. et al. 1998. Photobionts in lichens: possible indicators of phylogenetic relationships – Bryologist 101: 392–397.
Renner, I. W. and Warton, D. I. 2013. Equivalence of MAXENT and Poisson point process models for species distribution modeling in ecology. – Biometrics 69: 274–281.
Rikkinen, J. et al. 2002. Lichen guilds share related cyanobacterial symbionts. – Science 297: 357.
Roffler, G. H. et al. 2016. Identification of landscape features influencing gene flow: how useful are habitat selection models? – Evol. Appl. 9: 805–817.
Rolshausen, G. et al. 2017. Data from: Quantifying the climatic niche of symbiont partners in a lichen symbiosis indicates mutualist-mediated niche expansions. – Dryad Digital Repository, <http://dx.doi.org/10.5061/dryad.64149>.
Sadowska-Deś, A. D. et al. 2013. Assessing intraspecific diversity in a lichen-forming fungus and its green algal symbiont: evaluation of eight molecular markers. – Fungal Ecol. 6: 141–151.

Sadowska-Deś, A. D. et al. 2014. Integrating coalescent and phylogenetic approaches to delimit species in the lichen photobiont *Trebouxia*. – Mol. Phylogenet. Evol. 76: 202–210.
Schmitt, I. et al. 2009. New primers for promising single-copy genes in fungal phylogenetics and systematics. – Persoonia 23: 35–40.
Schoener, T. W. 1968. The *Anolis* lizards of Bimini: resource partitioning in a complex fauna. – Ecology 49: 704–726.
Shcheglovitova, M. and Anderson, R. P. 2013. Estimating optimal complexity for ecological niche models: a jackknife approach for species with small sample sizes. – Ecol. Model. 269: 9–17.
Singh, G. et al. 2017. Fungal–algal association patterns in lichen symbiosis linked to macroclimate. – New Phytol. 214: 317–329.
Thompson, J. N. 1999. Specific hypotheses on the geographic mosaic of coevolution. – Am. Nat. 153: S1–S14.
Thompson, J. N. 2005. The geographic mosaic of coevolution. – Univ. of Chicago Press.
Wagner, H. H. and Fortin, M. J. 2013. A conceptual framework for the spatial analysis of landscape genetic data. – Conserv. Genet. 14: 253–261.
Warren, D. L. and Seifert, S. N. 2011. Ecological niche modeling in Maxent: the importance of model complexity and the performance of model selection criteria. – Ecol. Appl. 21: 335–342.
Werth, S. and Sork, V. L. 2008. Local genetic structure in a North American epiphytic lichen, *Ramalina menziesii* (Ramalinaceae). – Am. J. Bot. 95: 568–576.
Werth, S. and Sork, V. L. 2010. Identity and genetic structure of the photobiont of the epiphytic lichen *Ramalina menziesii* on three oak species in southern California. – Am. J. Bot. 97: 821–830.
Werth, S. and Sork, V. L. 2014. Ecological specialization in *Trebouxia* (Trebouxiophyceae) across six range-covering ecoregions of western North America. – Am. J. Bot. 101: 1127–1140.
Widmer, I. et al. 2012. European phylogeography of the epiphytic lichen fungus *Lobaria pulmonaria* and its green algal symbiont. – Mol. Ecol. 21: 5827–5844.
Wirtz, N. et al. 2003. Lichen fungi have low cyanobiont selectivity in maritime Antarctica. – New Phytol. 160: 177–183.
Yahr, R. et al. 2004. Strong fungal specificity and selectivity for algal symbionts in Florida scrub *Cladonia* lichens. – Mol. Ecol. 13: 3367–3378.
Yahr, R. et al. 2006. Geographic variation in algal partners of *Cladonia subtenuis* (Cladoniaceae) highlights the dynamic nature of a lichen symbiosis. – New Phytol. 171: 847–860.

Supplementary material and GenBank accession numbers (Appendix ECOG-03457 at <www.ecography.org/appendix/ecog-03457>). Appendix 1–4.

SUPPLEMENTARY MATERIAL OVERVIEW

APPENDIX 1 (supplementary figures for main text)

Figure S1

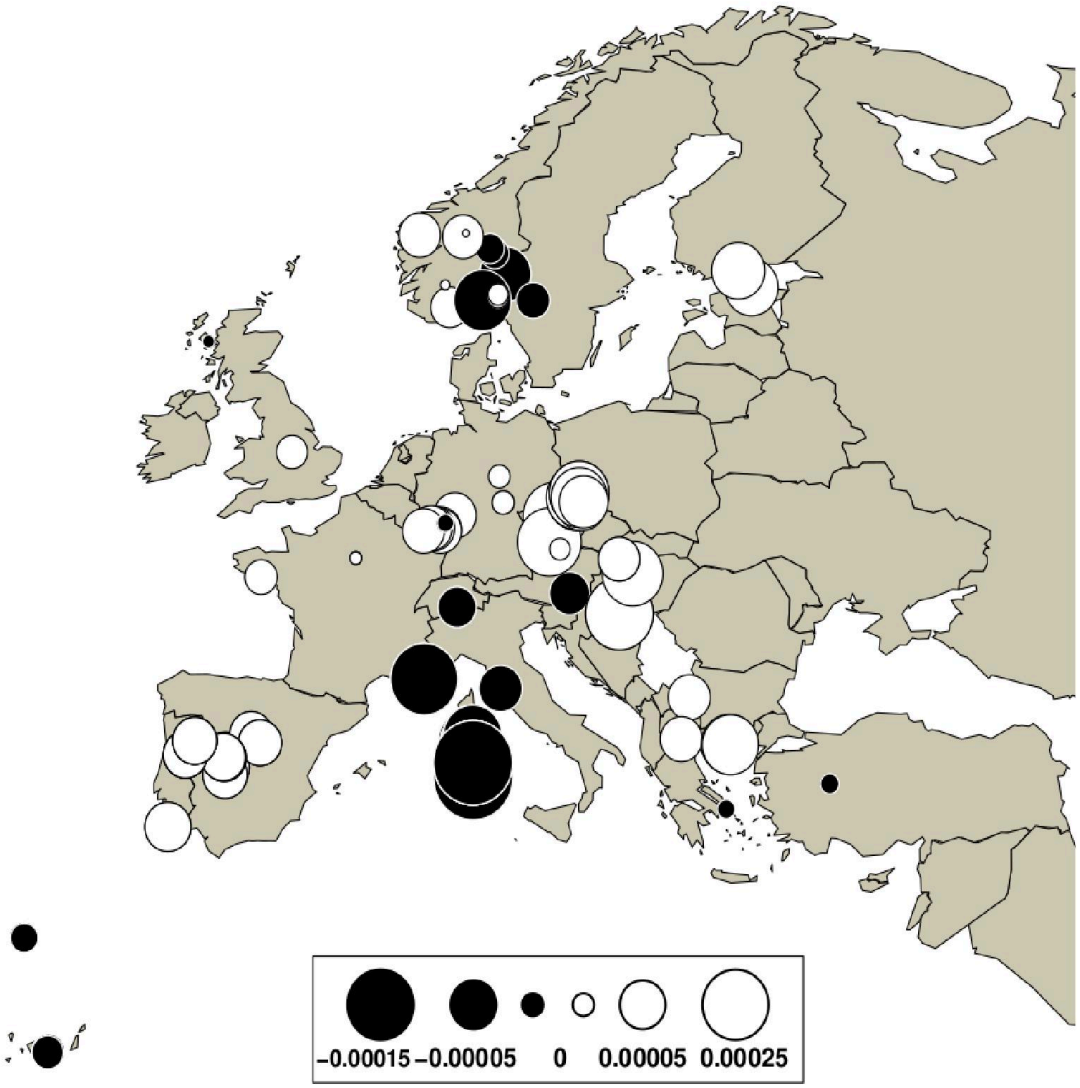

Figure S1. Visualization of individual scores for the first MEMGENE axis explaining >95% of genetic variation among 11 fungal haplotypes. Size and color of the circles depict genetic similarity with large black and large white circles at opposite extremes of the axis, and score values indicated in the legend (Galpern et al. 2014).

Figure S2 (A)

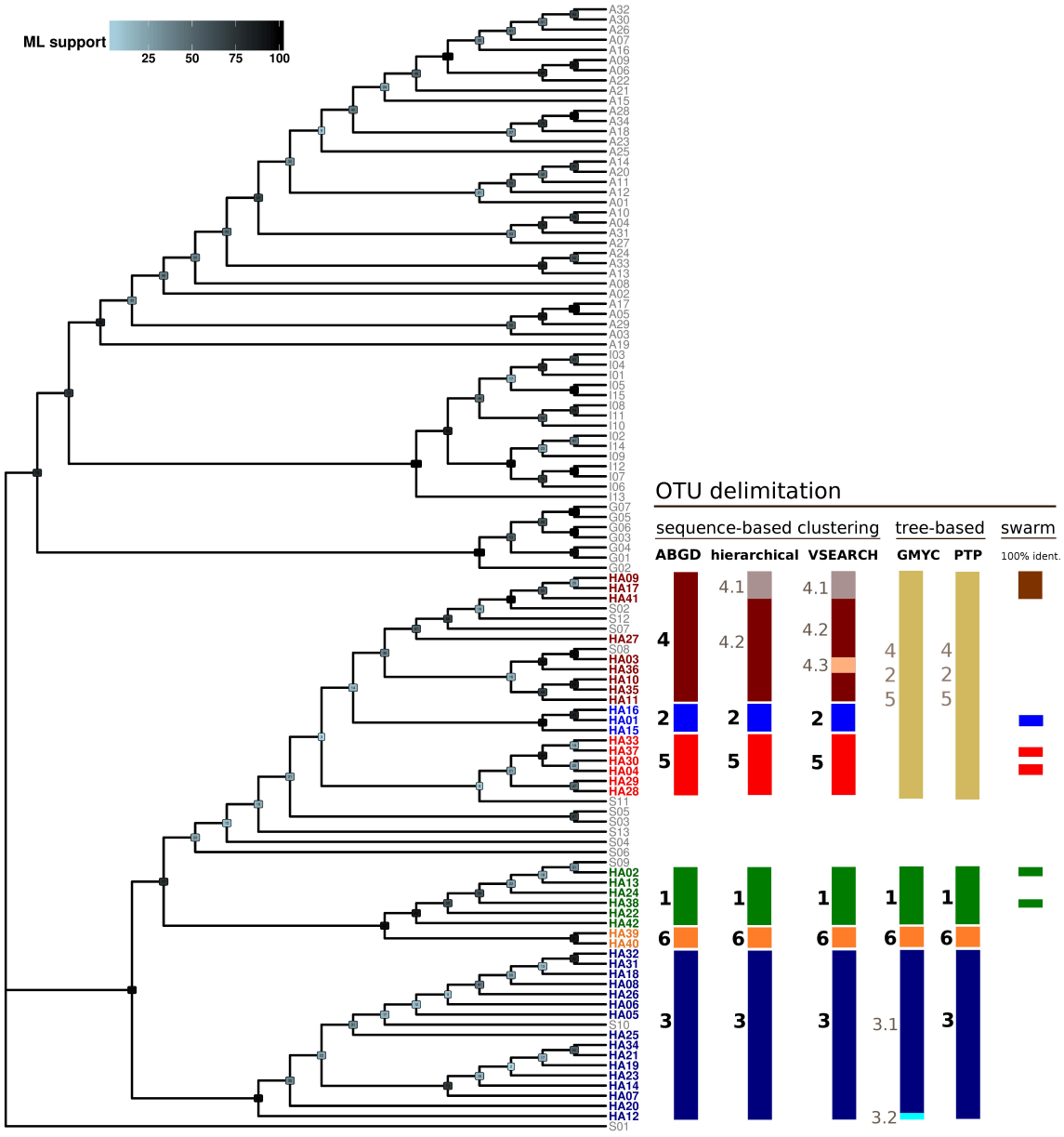
ML support
25
50
75
100
OTU delimitation
sequence-based clustering
tree-based
swarm
ABGD
hierarchical
VSEARCH
GMYC
PTP
100% ident.

Figure S2 (B)

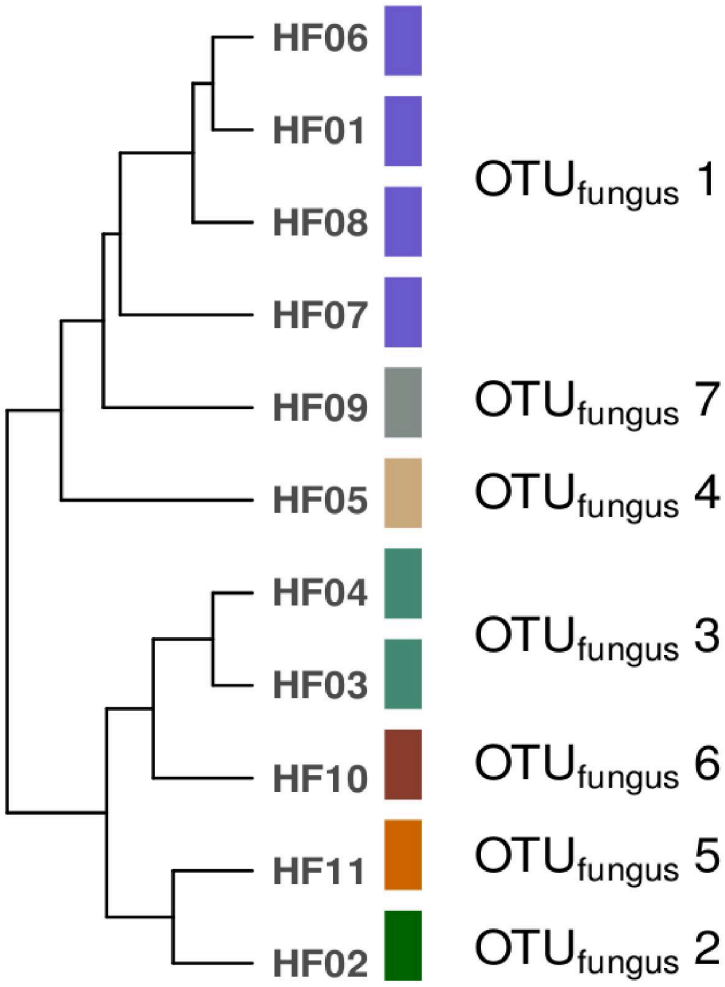

Figure S2. (A) ITS gene tree with bootstrap ML support calculated with RAxML v8 (Stamatakis 2006; Stamatakis et al. 2008) representing all 42 *Trebouxia* haplotypes from our study (colored bold font, grouped into OTUs 1 – 6) together with the 69 Trebouxia OTUs described in Leavitt et al. 2015 (grouped into four clades: 'A', 'I', 'G', 'S'). The color coding of our 42 haplotypes follows the ABGD OTU delimitation (Puillandre et al. 2012) and vertical bars to the right of the tree depict the respective delimitations based on alternative clustering approaches. See supplementary material (Appendix 2) for a detailed description of methods. (B) MCM7 gene tree calculated with RAxML v8 (Stamatakis 2006; Stamatakis et al. 2008) showing all 11 mycobiont haplotypes grouped into 7 OTUs using ABGD (Puillandre et al. 2012).

Figure S3

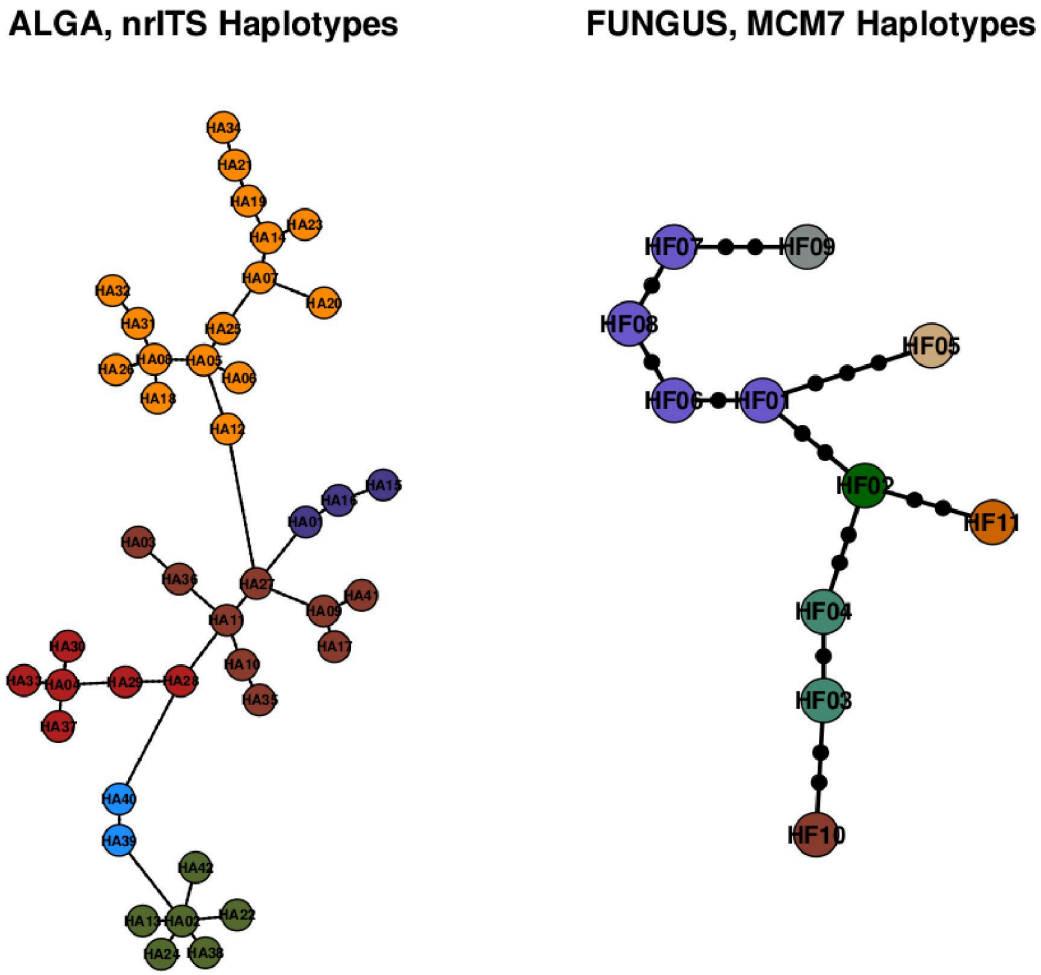

Figure S3. Haplotype networks of 42 ITS *Trebouxia* haplotypes, and 11 MCM7 *Lasallia pustulata* mycobiont haplotypes. Networks were calculated using the 'pegas' package in R (R Core Development Team 2016). Color coding corresponds to the ABGD OTU delimitation.

Figure S4

(A)

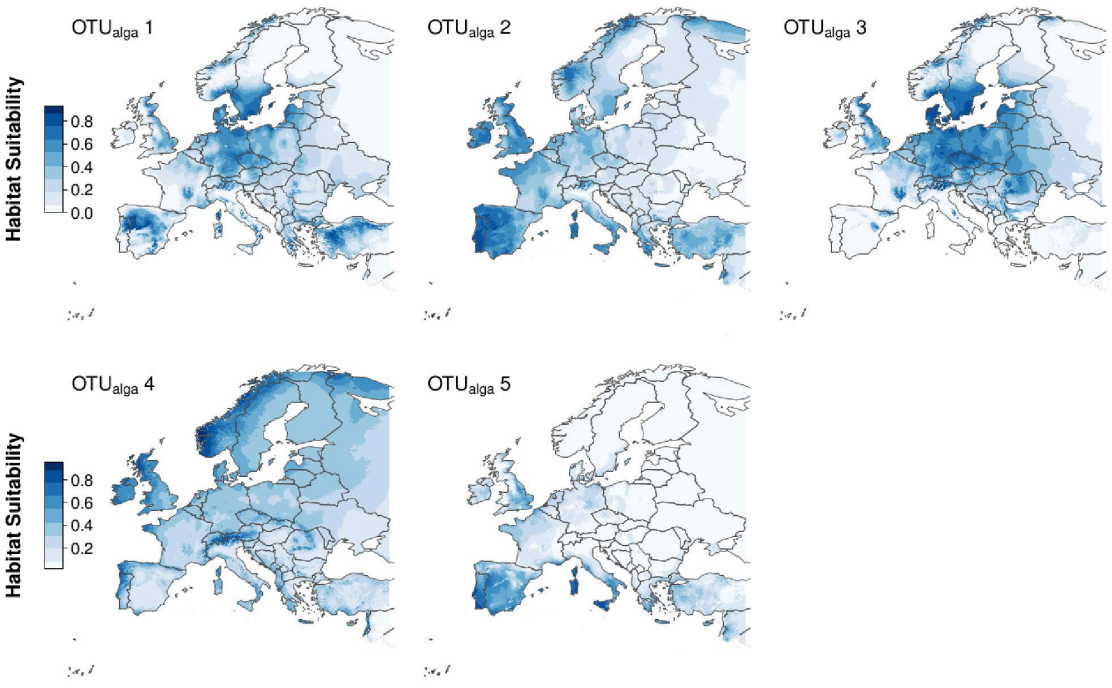
OTU$_{alga}$ 1
OTU$_{alga}$ 2
OTU$_{alga}$ 3
OTU$_{alga}$ 4
OTU$_{alga}$ 5
Habitat Suitability
0.8
0.6
0.4
0.2
0.0

(B)

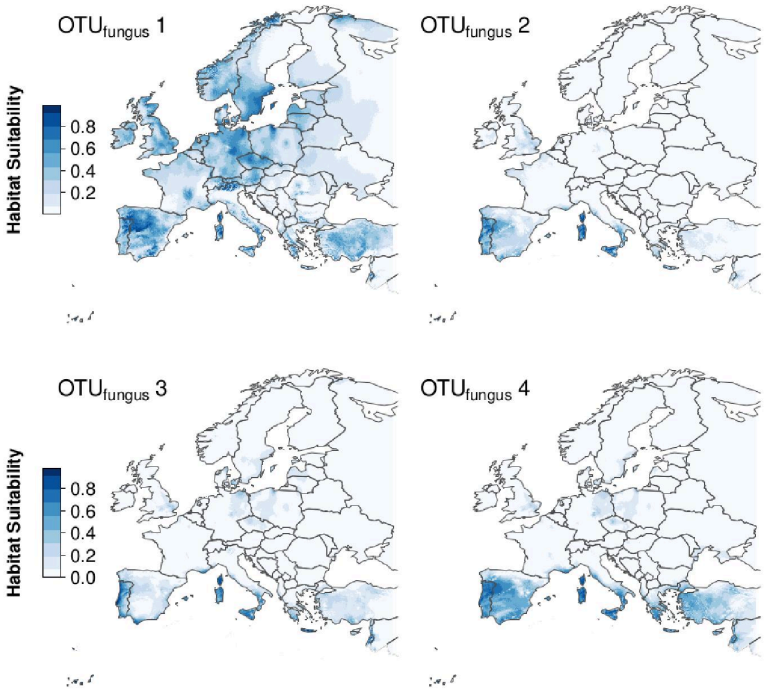
OTU$_{fungus}$ 1
OTU$_{fungus}$ 2
OTU$_{fungus}$ 3
OTU$_{fungus}$ 4
Habitat Suitability
0.8
0.6
0.4
0.2
0.0

(C)

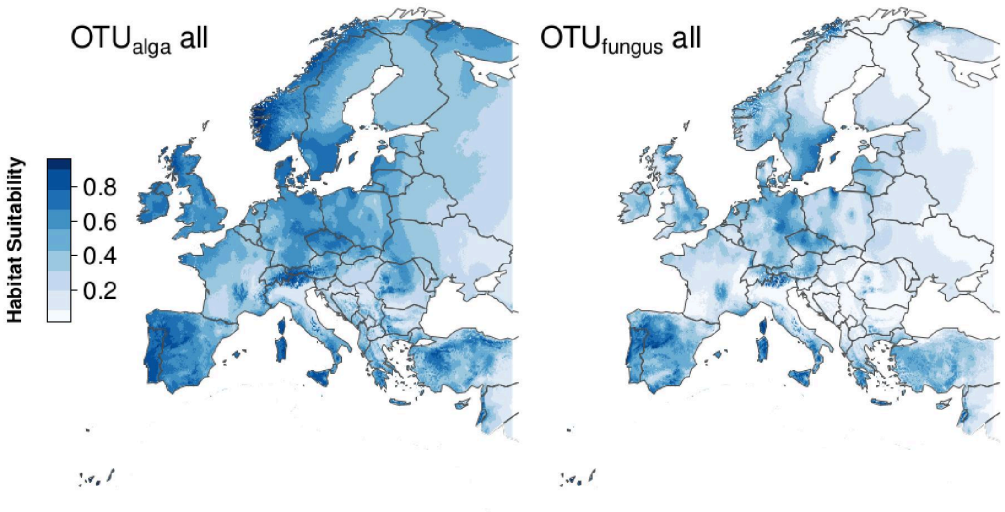

Figure S4 Habitat suitability predictions from MaxEnt species distribution models for all **(A)** algal and **(B)** fungal OTUs with sufficient sampling data (see also Table S1). **(C)** MaxEnt predictions for all algal and all fungal OTUs combined.

Figure S5

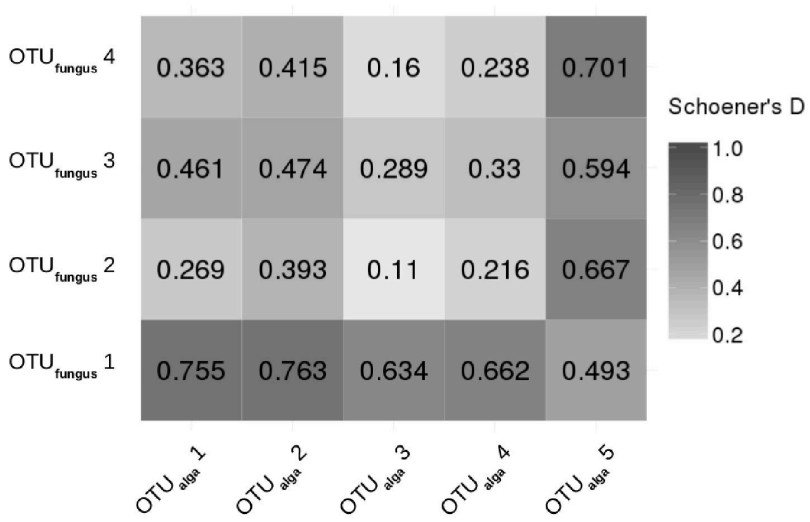

Figure S5 Heatmap depicting pairwise niche overlap scores between algal and fungal OTUs based on Schoener's D metric (ranging from 1: complete overlap, to 0: no overlap; Schoener 1968) calculated via stacking the respective prediction rasters from MaxEnt species distribution models.

APPENDIX 2 (Robustness analyses of OTU delimitations)

In order to scrutinize the robustness of the delimitation of our 42 haplotypes into six OTUs, based on ABGD clustering (Puillandre et al. 2012, Leavitt et al. 2015), we applied alternative clustering approaches in addition to the ABGD approach described in the main text. Here, we give a methodological description of these approaches together with a brief summary of results. These results are also depicted on Figure S2A (supplementary material, Appendix 1).

1. Hierarchical clustering of sequences. Using MAFFT (Katoh and Standley 2013), we aligned ITS raw sequence reads for the 42 haplotypes and calculated the pairwise identity matrix (containing the square root distances) of that alignment. Single linkage hierarchical clustering of this matrix revealed the best solution of seven OTU clusters that were congruent with the ABGD delimitation with the exception of OTU_{alga} 4, which was split further into two OTUs (Figure S2A). The hierarchical clustering thus strongly supports the ABGD delimitation with a minor difference of assigning HA09, HA17, and HA41 to a separate cluster.

2. VSEARCH clustering. Starting from raw sequence reads for 42 haplotypes, we used the software tool *cluster_fast* implemented in the VSEARCH meta-genomics toolkit (Rognes et al. 2016). Each input sequence is used as a query in a search against an initially empty database of centroid sequences. The query sequence is clustered with the first centroid sequence found with similarity equal to or above the threshold of 97% similarity. The search generally finds the most similar sequences first. If no matches are found, the query sequence becomes the centroid of a new cluster and is added to the database.
The results from VSEARCH clustering strongly support the splits between original algal OTUs 1 – 6, but also subdivide $OTU_{alga}4$ further into three sub-OTUs binning HA03, HA36, and HA09 into a separate cluster, as well as HA17, and HA41 in another cluster. Although $OTU_{alga}4$ is subdivided by VSEARCH and hierarchical clustering, the important result regarding our original ABGD delimitation is the congruency of delimitations for OTUalga 1, 2, 3, 5, and 6 – leaving the remaining $OTU_{alga}4$ either as one big cluster (as analyzed in the study) or subdivided further into smaller clusters that would share similar ecological preferences as the inclusive $OTU_{alga}4$.

3. Tree-based delimitation. We used two different tree-based delimitation methods on the ITS gene tree calculated with RAxML. First, we used the GMYC (Generalized Mixed Yule Coalescent) model (Pons et al. 2006; Fujisawa and Barraclough 2013), implementing single and multiple thresholds via the 'splits' package in R. (Ezar et al. 2014, R Core Development Team 2016). The GMYC model detects stochastic birth-death processes between species from neutral coalescent processes within species based on time-calibrated single gene trees. Second, we used the PTP (Poisson Tree Processes) model via the PTP webmask (Zhang et al. 2013) using both ML and Bayesian implementations of the algorithm. PTP aims to discern diversification events among species (i.e. speciation) from diversification processes within species by analyzing the number of substitutions between

branching events (compared to time intervals as in GMYC). Species hypotheses delineated via GMYC and/or PTP correspond to the logic of the phylogenetic species concept.
With regard to our OTU delimitation based on ABGD, the two tree based approaches revealed similar results for OTU_{alga} 1, 3, and 6. However, both tree-based methods did not subdivide the large OTU_{alga} cluster comprising OTU_{alga} 2, 4, and 5, but instead found only one cluster including all three ABGD OTUs (Figure S2A). Thus, GMYC and PTP support OTU_{alga} 1, 3, and 6 but do not distinguish between OTU_{alga} 2, 4, and 5. The latter OTUs, however, showed significant ecological divergence (see main text) and we therefore consider the tree-based methods as less informative against the background of the above mentioned cluster analyses.

4. Sequence identity with SWARM OTUs. In order to scrutinize the validity of sequence identity thresholds between our haplotypes, we used BLAST to compare ITS sequences from our study with core ITS sequences from robust *Trebouxia* OTUs that were recently delimited in Dal Grande et al. (2017) using the meta-genomics software tool SWARM. Dal Grande et al. (2017) use deep-coverage Illumina DNA metabarcoding to examine photobiont communities in *Lasallia pustulata* along an elevational gradient. Testing an extensive set of lichen thalli revealed > 23m quality filtered reads assigned to the genus *Trebouxia*, from which SWARM retained seven unique algal OTUs (see Dal Grande et al. 2017 for detailed a description). Here, the core ITS sequences from these seven OTUs were blasted (100% identity) against the ITS haplotypes in our study in order to validate their distinctiveness. The SWARM OTUs represent a particularly solid delimitation because of the immense amount of background data available from deep-coverage metabarcoding. SWARM is therefore not confronted with the problem of choosing an arbitrary global clustering threshold (e.g. 97% similarity) but rather employs a local clustering threshold by taking into account sequence abundance values to define OTUs.
The resulting assignments of SWARM OTUs to our original ABGD OTUs (based on 100% sequence identity of haplotypes in OTUs) supports our basic delimitation into six algal OTUs. In particular the division of OTU_{alga} 2, 4, and 5 was supported because SWARM retains distinct and strongly supported OTUs whose core ITS sequences were also significantly different in our dataset (Figure S2A).

5. Secondary RNA structure comparison. As a final approach to test the robustness of our original algal OTU delimitation, we reconstructed the ITS RNA secondary structure for each of the six algal OTU cluster centroids using RNAFOLD (Hofacker et al. 1994; Gruber et al. 2008; Lorenz et al. 2011). Differences in minimum free energy (MFE) predictions for RNA secondary structures can be depicted in 'mountain plots', graphs that plot sequence position versus the number of base pairs that enclose that position. MFE based comparisons of ITS sequences have been used elsewhere as complementary evidence resolving interspecific relationships in *Fuscidea* lichens (Zahradníková et al. 2017) and in *Trebouxia* photobionts (Dal Grande et al. 2017).
Figure S6A (see below) reveals clear cut differences in the MFE folding across all six algal OTUs in our study, including differences for OTU_{alga} 4 vs. OTU_{alga} 2 and 5. We consider this independent approach as an additional line of of evidence supporting our original OTU delimitation based on ABGD. Secondary RNA structures are shown in Figure S6B.

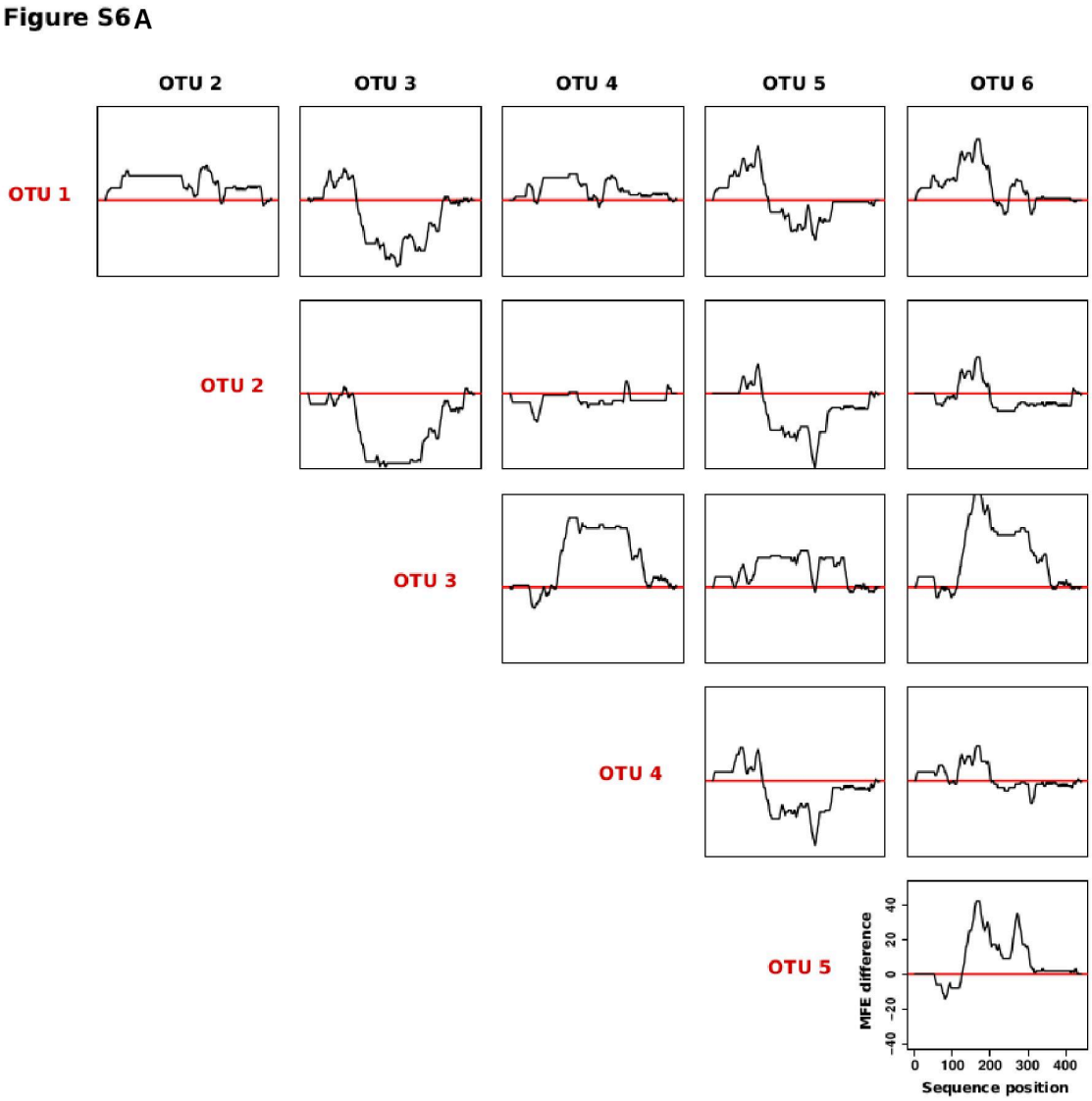

Figure S6. Comparison of RNA secondary structures obtained for the six algal OTU centroid sequences using RNAFOLD . (A) The plots depict the differences in minimum free energy folding along the full sequence. Black lines depict the difference in values between the two respective OTU centroids relative to one OTU's base line value (red line). (B) Depiction of MFE plain structure drawings as obtained from RNAFOLD . Note that we use the RNAFOLD information simply as an additional source of variance in our sequence dataset, which we then use to infer differences between the OTU centroids.

Figure S6 B

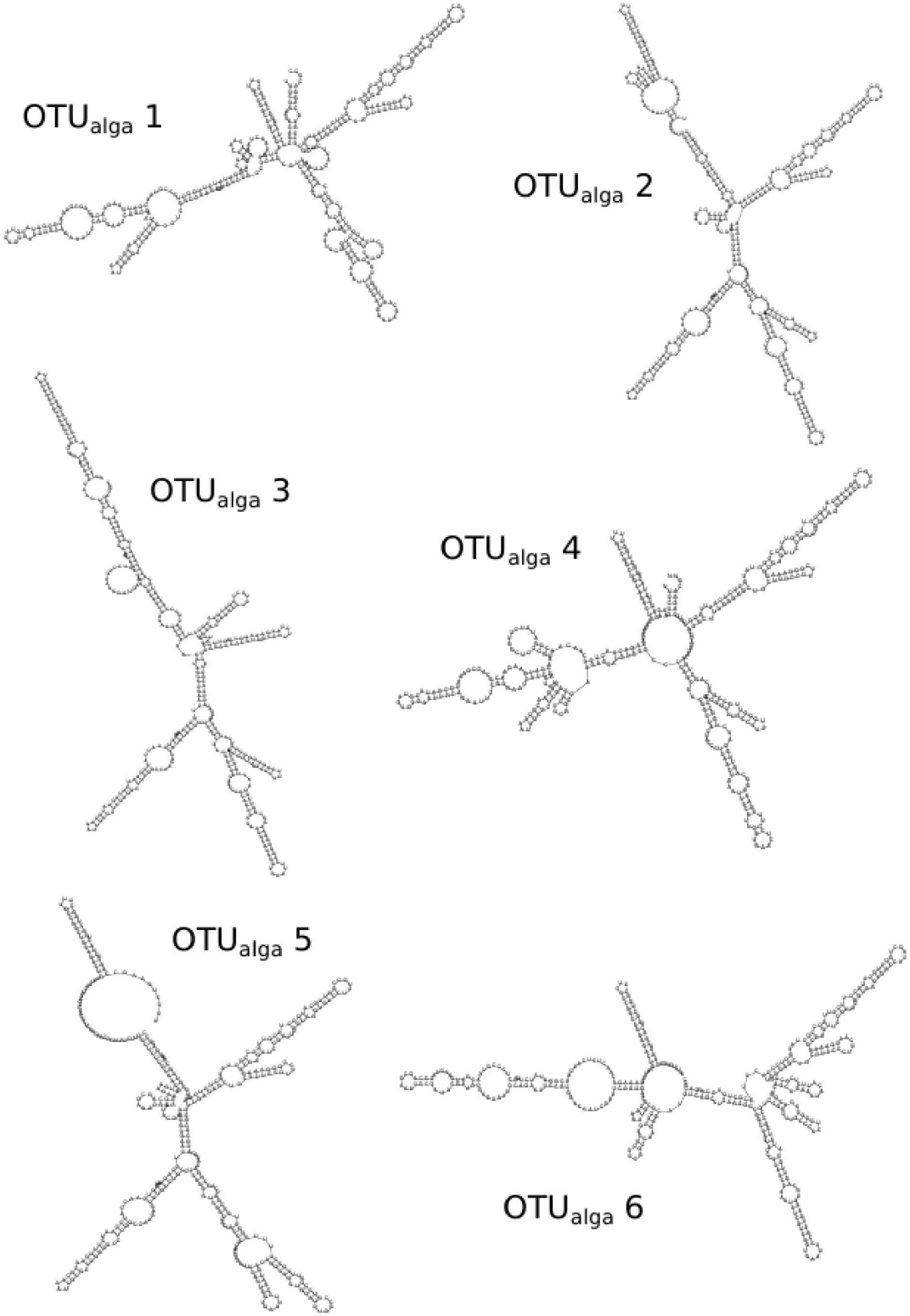

APPENDIX 3 (Robustness analyses of niche quantification, distribution models, and bioclim variable sets)

To scrutinize the robustness of our main findings in niche quantification (hypervolume) and species distribution models (SDMs) across the bioclim envelope of our study area, we here include the full set of analyses discussed in the main text based on (i) the full variable set of 19 bioclims, and (ii) a set of seven uncorrelated bioclims, depicted via cluster analysis (Figure S7). The set of variables discussed in the main text includes correlated bioclim variables and was simply chosen because of its straightforward ecological interpretation. To tackle potential problems with this choice of variables, such as variance inflation and compromised predictions (Dormann et al. 2013), we here compare our original results against results from models based on the two variable sets mentioned above. Parameters underlying the hypervolume quantifications (Figure S8), MaxEnt evaluation runs, and MaxEnt SDM models (Figure S9 & S10) were kept at the same values as for the original analyses (see main text for details).

Furthermore, we scrutinize our basic methodological approach to quantify niche dimensions and overlap. In the main text, niches are quantified based on multivariate kernel density estimations, as implemented in the 'hypervolume' R package (Blonder et al. 2014). This method, however, can be of limited power when dealing with small sample sizes or many environmental dimensions (Qiao et al. 2016). While we are confident that the latter issue does not apply to our study (we run hypervolume estimations for only two PCA axes), the former issue (sample size) could reduce the accuracy of hypervolume geometries. To address this potential problem, we here run the same set of analyses based on the alternative niche quantification algorithm developed by Broennimann et al. (2012) and implemented in the 'ecospat' R package (Di Cola et al. 2017). For this, we follow the same logic as outlined in the main text (i.e., quantifying the niche of a particular target OTU against the combined niche dimensions of all remaining OTUs, for fungi and algae respectively). Because the issue of collinearity among explanatory variables also applies indirectly to PCA based niche quantification, we ran all ecospat analyses based on two variable sets: the full 19 bioclim set (Figure S11 & S12), and the uncorrelated bioclim set (Figure S13 & S14). Congruency between 'hypervolume' and 'ecospat' methods provides additional confidence in our original interpretations of niche dimensions and niche overlaps. More details are given in the figure captions below.

Figure S7

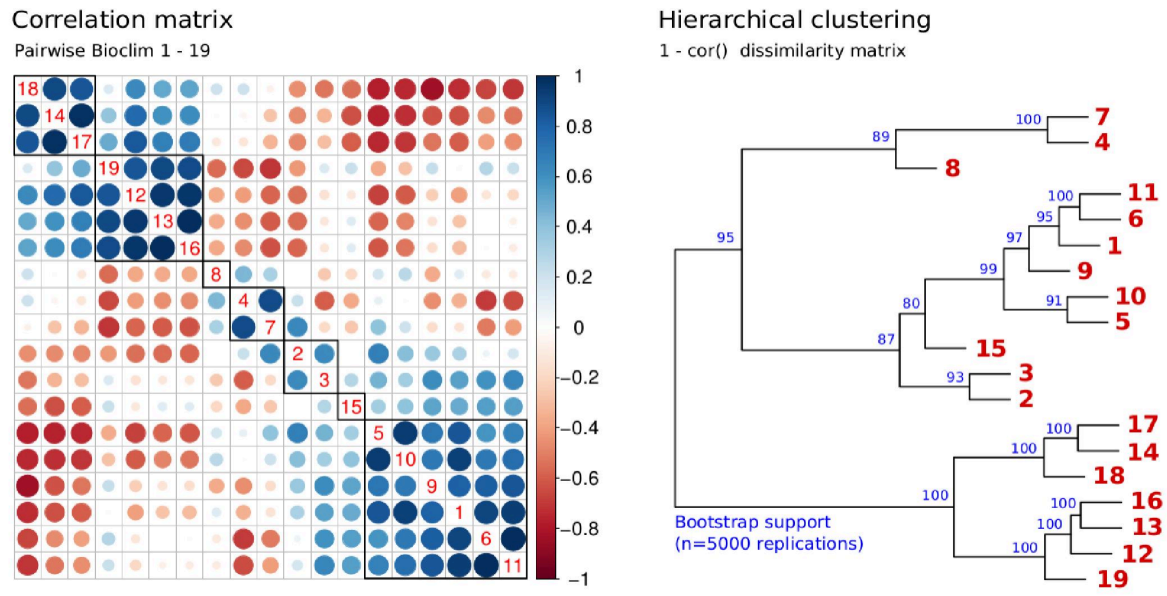

Figure S7. Correlation analysis of bioclim variables in our study area. Left panel: Visual depiction of the 19x19 correlation matrix for all bioclims. Numbers in red on the diagonal indicate the bioclim variable, colored dots indicate the sign and strength of the correlation (red: negative, blue: positive; legend gives the respective Pearson coefficients, and diameter of dots indicate their statistical significance at threshold p=0.05). The matrix is ordered based on hierarchical clustering of the dissimilarity matrix calculated from the correlation matrix as: 1 – cor() matrix. Accordingly, black frames cluster together highly correlated variables and depict the seven variable clusters that were chosen for further analysis. Right panel: Bootstrap supported cluster dendrogram for the dissimilarity matrix based on correlation analysis of 19 bioclim variables. For clusters containing more than one variable we calculated the average correlation coefficient for each cluster member with all non-cluster members and chose the lowest average coefficient to depict the cluster representative. This lead to the following set of uncorrelated bioclim variables: 2, 4, 6, 8, 14, 15, 19.

Figure S8A Algal OTUs, 19 bioclims

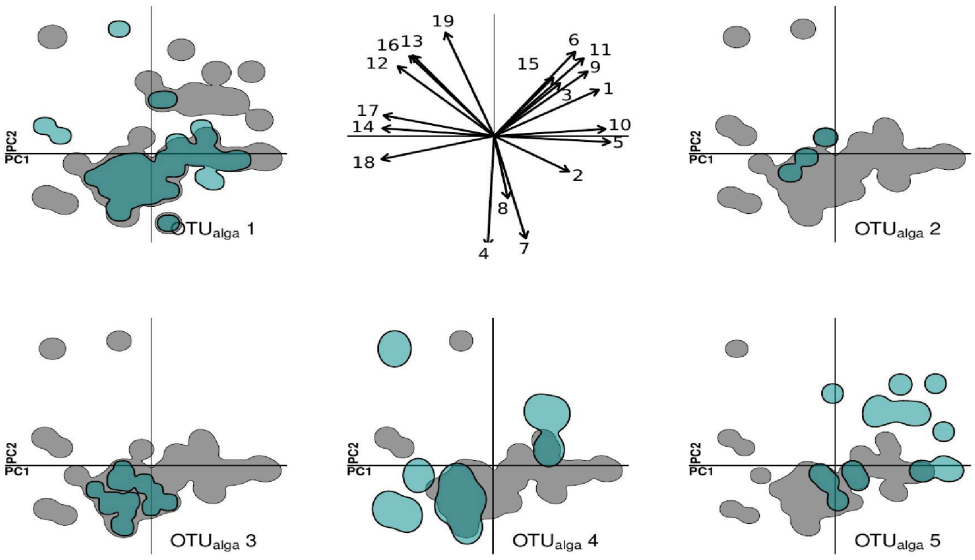

Figure S8B Algal OTUs, 7 uncor bioclims

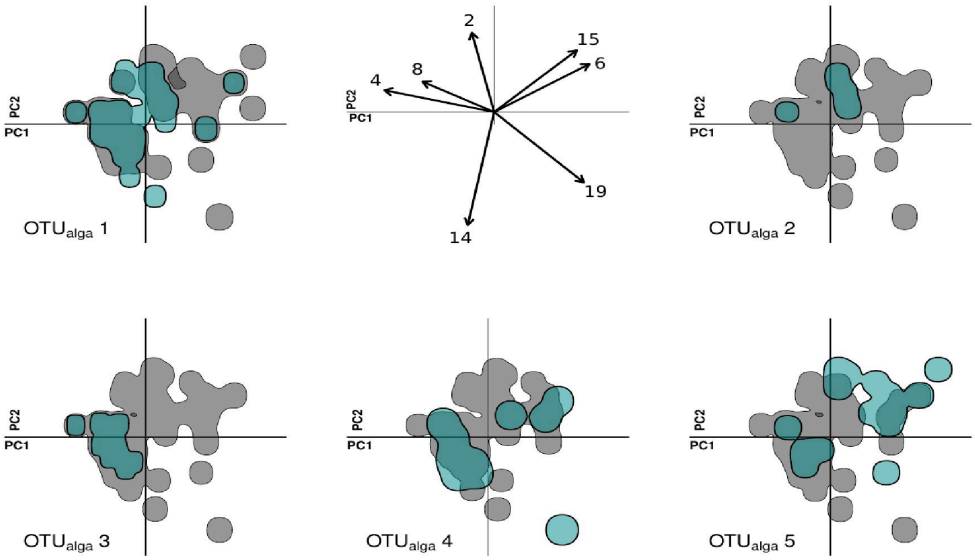

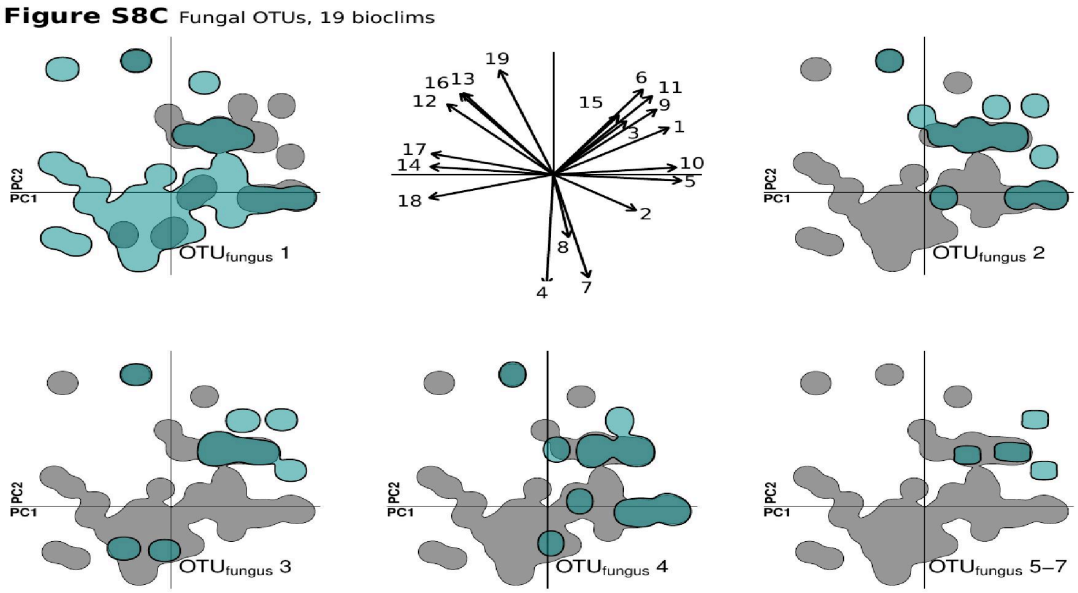

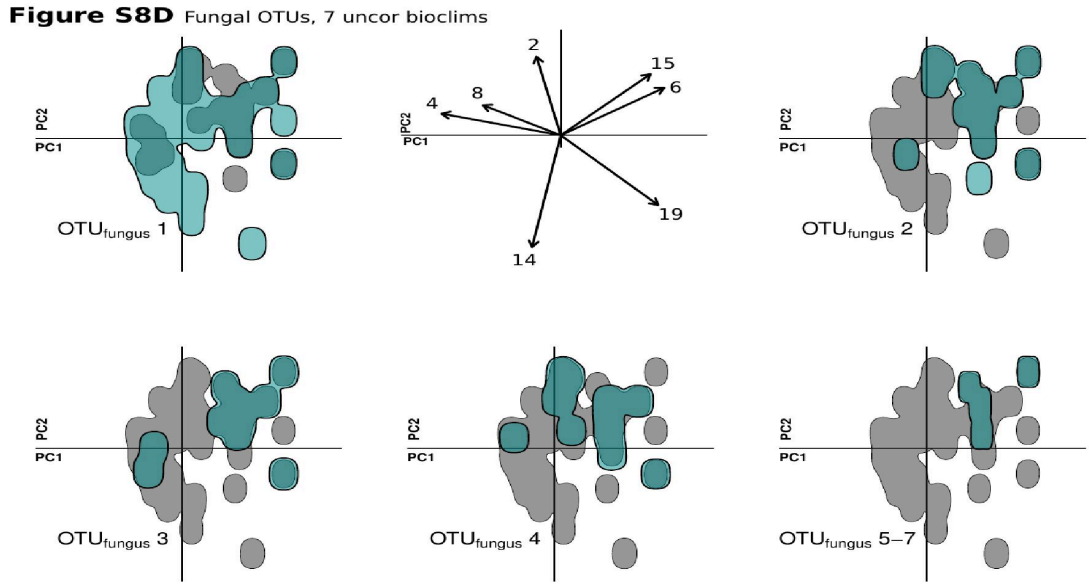

Figure S8. Niche hypervolumes (Blonder et al. 2014) calculated for *Trebouxia* photobionts and *Lasallia pustulata* mycobionts based on the full set of 19 bioclim variables **(A & C)**, and the set of seven uncorrelated bioclim variables **(B & D)**. Each projection shows the niche hypervolume of a particular OTUalga / fungus (in cyan) superimposed on the complete niche hypervolume of all remaining OTUalga / fungus (in grey). Non-overlapping portions of cyan and grey projections indicate unique contributions of a particular OTU to the overall fungal or algal niche space.

Figure S9A SDM predictions, Alga-Fungi overlap, 19 bioclims

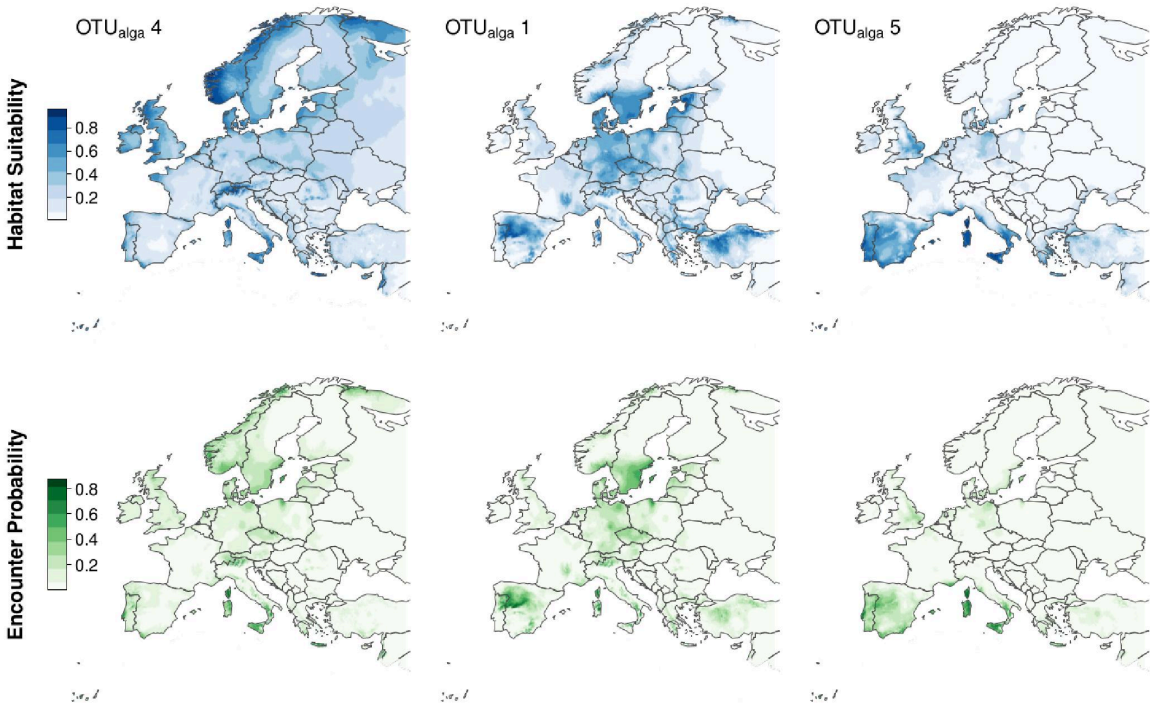

Figure S9B SDM predictions, all algal OTUs, 19 bioclims

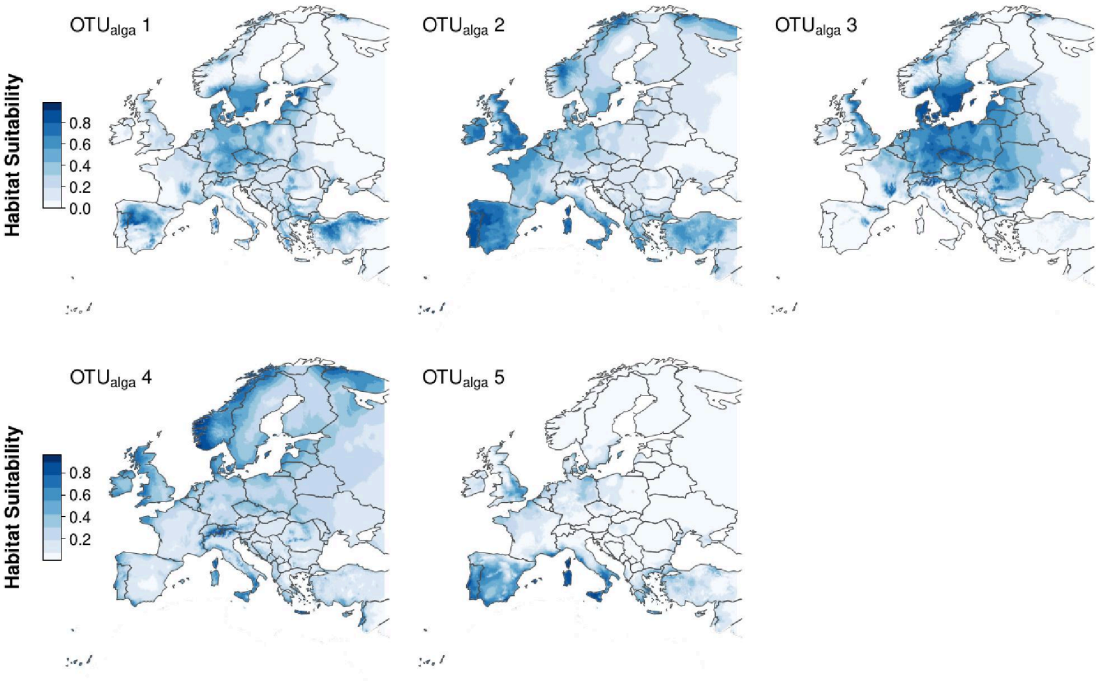

Figure S9C SDM predictions, all fungal OTUs, 19 bioclims

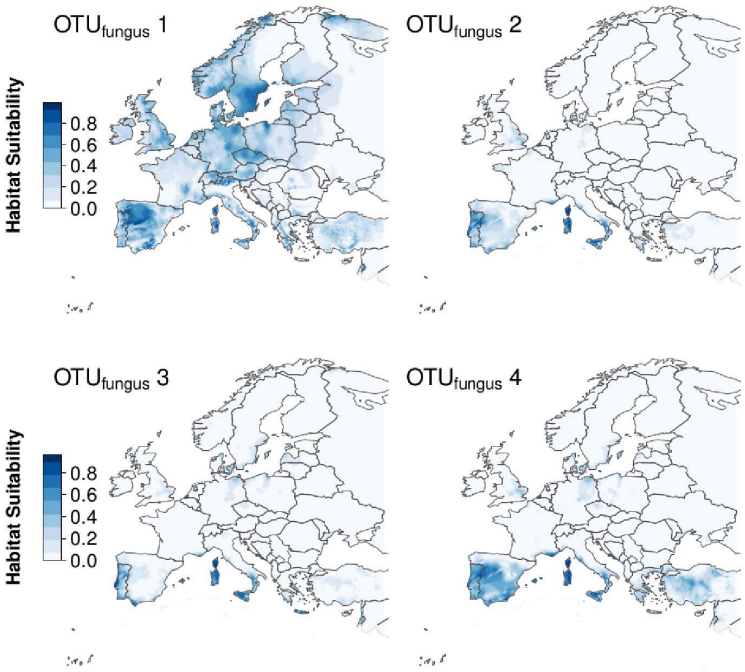

Figure S9D SDM predictions, combined algal & fungal OTUs, 19bioclims

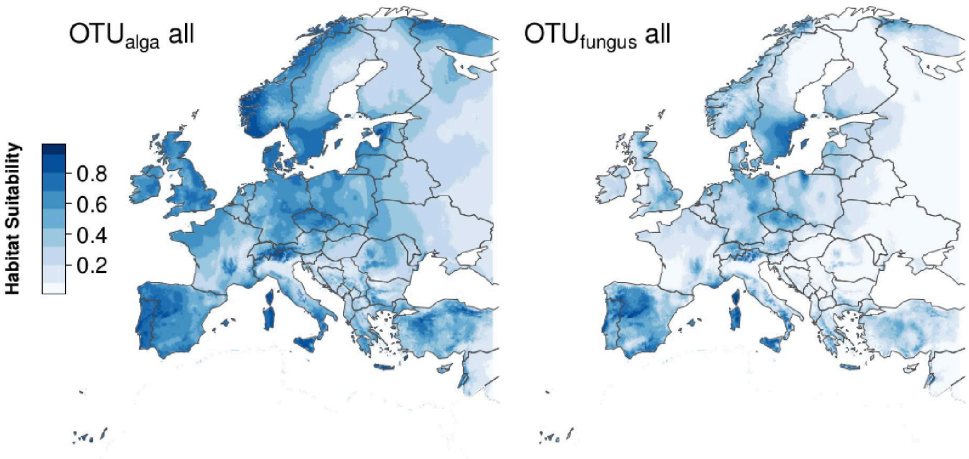

Figure S9. Habitat suitability predictions from MaxEnt species distribution models based on 19 bioclim variables. **(A)** Upper panel: Habitat suitability predictions from MaxEnt models for three prominent algal OTUs (generalistic ecotype OTUalga 1, arctic-alpine ecotype OTUalga 4, and Mediterranean ecotype OTUalga 5). Lower panel: Encounter probability of the above ecotypes with the fungal mycobiont (all OTUfungus) throughout the distributional range of *L. pustulata*. Probability scores were calculated as the product of model-based habitat suitabilities for the respective photobionts (OTUalga 1, 4, and 5) and the mycobiont (combining all OTUfungus). **(B)** Separate MaxEnt predictions for algal and fungal **(C)** OTUs with sufficient sampling data (see Table S1). **(D)** MaxEnt predictions for all algal and all fungal OTUs combined.

Figure S10A SDM predictions, Alga-Fungi overlap, 7 uncor. bioclims

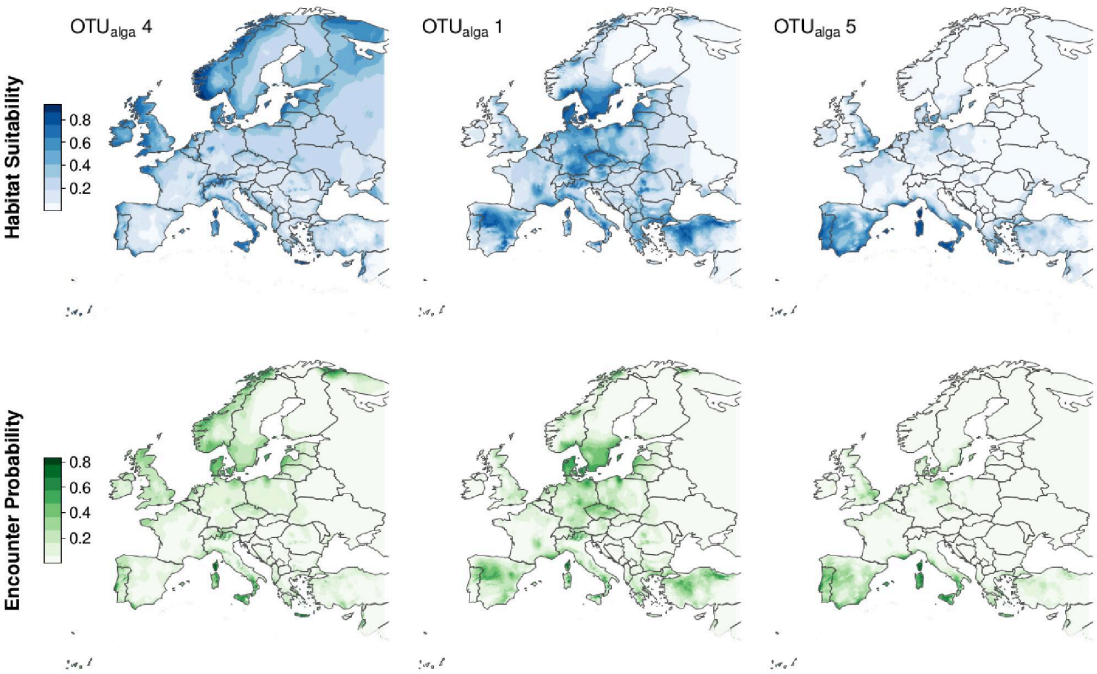

Figure S10B SDM predictions, all algal OTUs, 7 uncor. bioclims

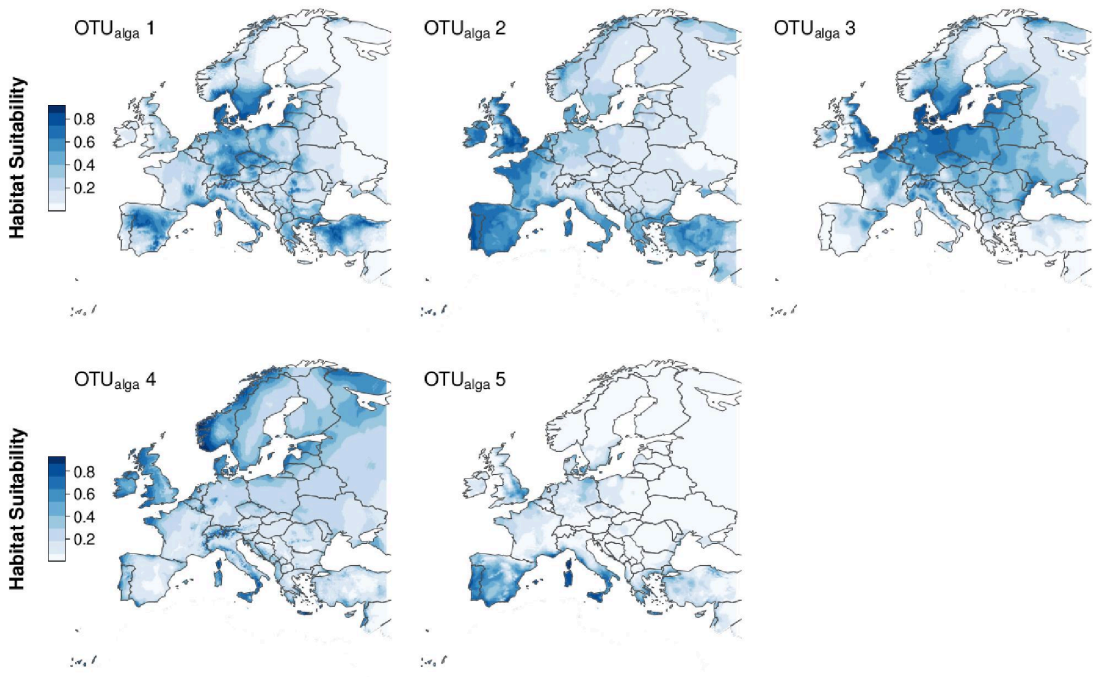

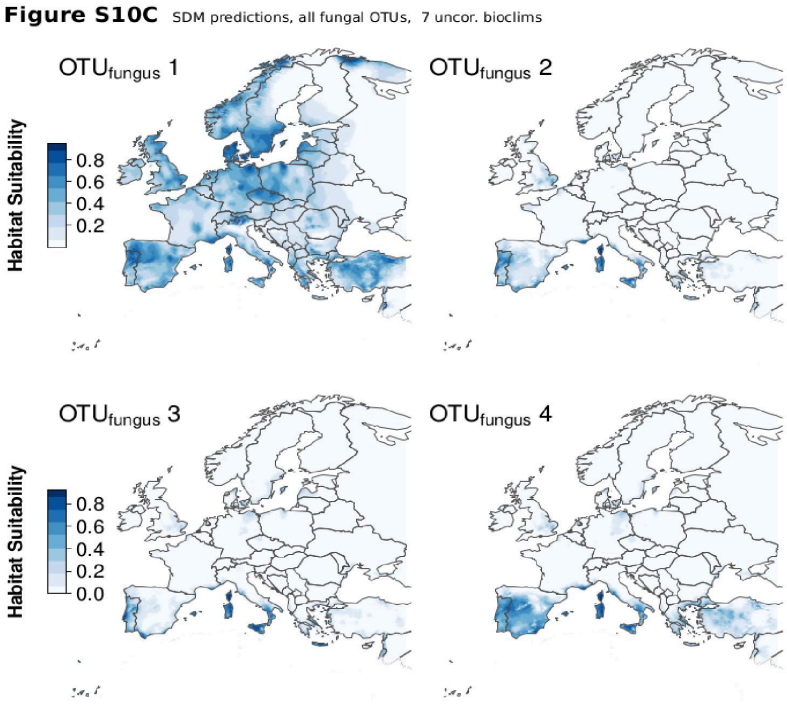

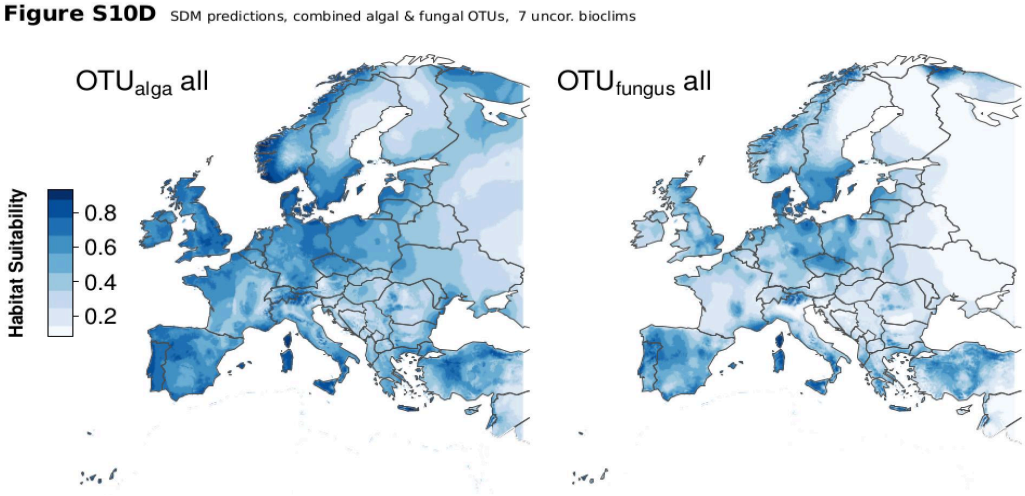

Figure S10. Habitat suitability predictions from MaxEnt species distribution models based on 7 uncorrelated bioclim variables. **(A)** Upper panel: Habitat suitability predictions from MaxEnt models for three prominent algal OTUs (generalistic ecotype OTUalga 1, arctic-alpine ecotype OTUalga 4, and Mediterranean ecotype OTUalga 5). Lower panel: Encounter probability of the above ecotypes with the fungal mycobiont (all OTUfungus) throughout the distributional range of *L. pustulata*. Probability scores were calculated as the product of model-based habitat suitabilities for the respective photobionts (OTUalga 1, 4, and 5) and the mycobiont (combining all OTUfungus). **(B)** Separate MaxEnt predictions for algal and fungal **(C)** OTUs with sufficient sampling data (see Table S1). **(D)** MaxEnt predictions for all algal and all fungal OTUs combined.

Figure S11

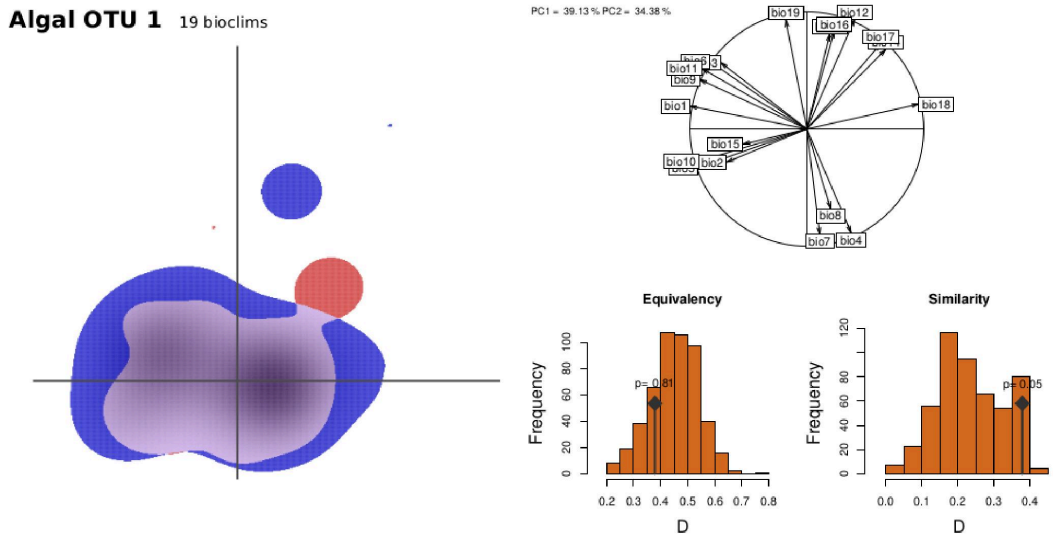
Algal OTU 1 19 bioclims
PC1 = 39.13 % PC2 = 34.38 %
bio19
bio12
bio16
bio17
bio11
bio9
bio1
bio18
bio15
bio10
bio2
bio8
bio7
bio4
Equivalency
Similarity
Frequency
p= 0.81
p= 0.05
D

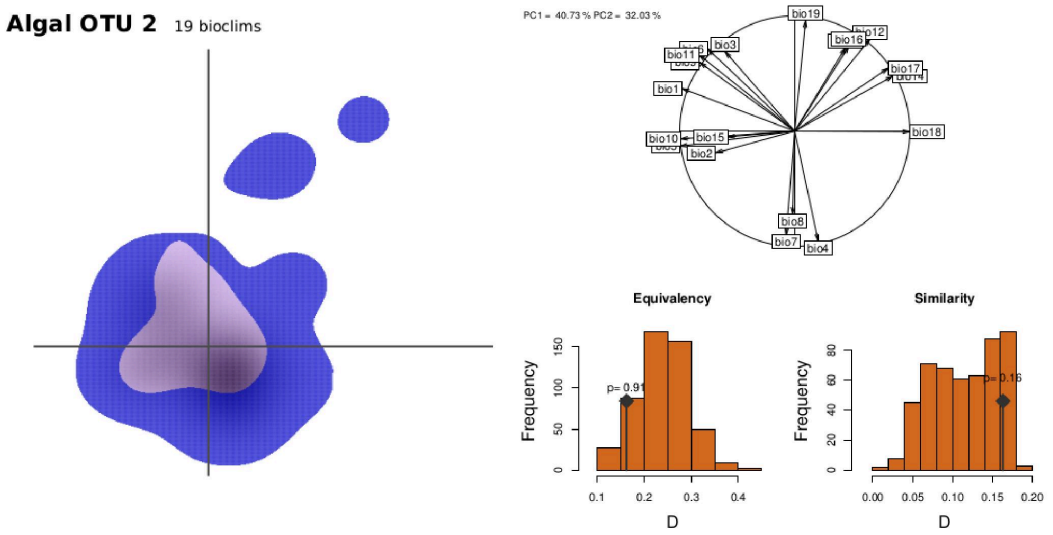
Algal OTU 2 19 bioclims
PC1 = 40.73 % PC2 = 32.03 %
bio19
bio12
bio16
bio3
bio11
bio17
bio1
bio10
bio15
bio18
bio2
bio8
bio7
bio4
Equivalency
Similarity
Frequency
p= 0.91
p= 0.16
D

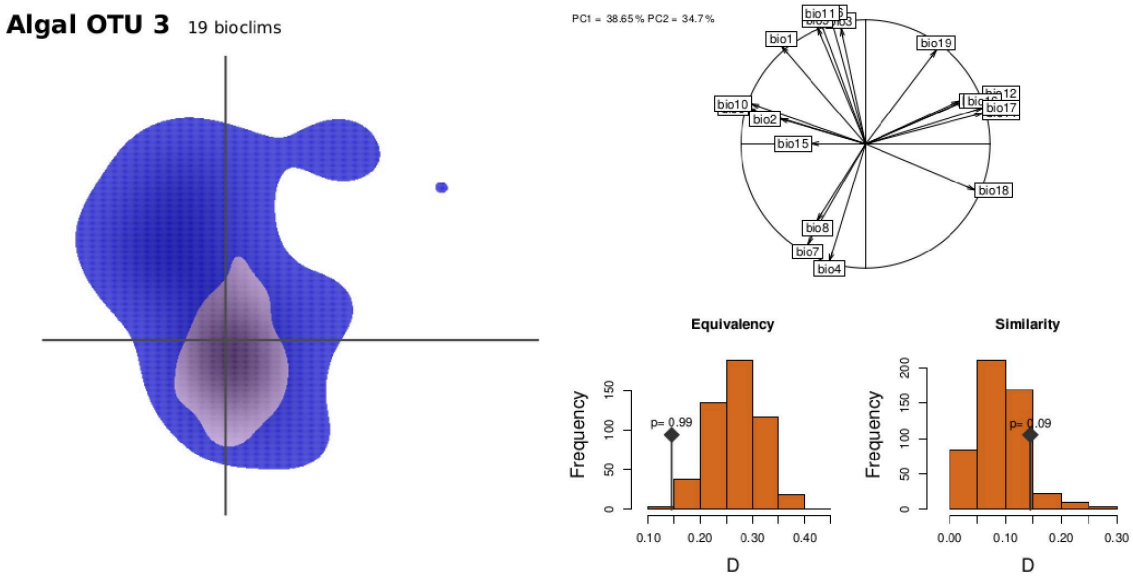
Algal OTU 3
19 bioclims
PC1 = 38.65 % PC2 = 34.7 %
bio1
bio19
bio10
bio2
bio15
bio18
bio8
bio7
bio4
Equivalency
Similarity
Frequency
p= 0.99
p= 0.09
D

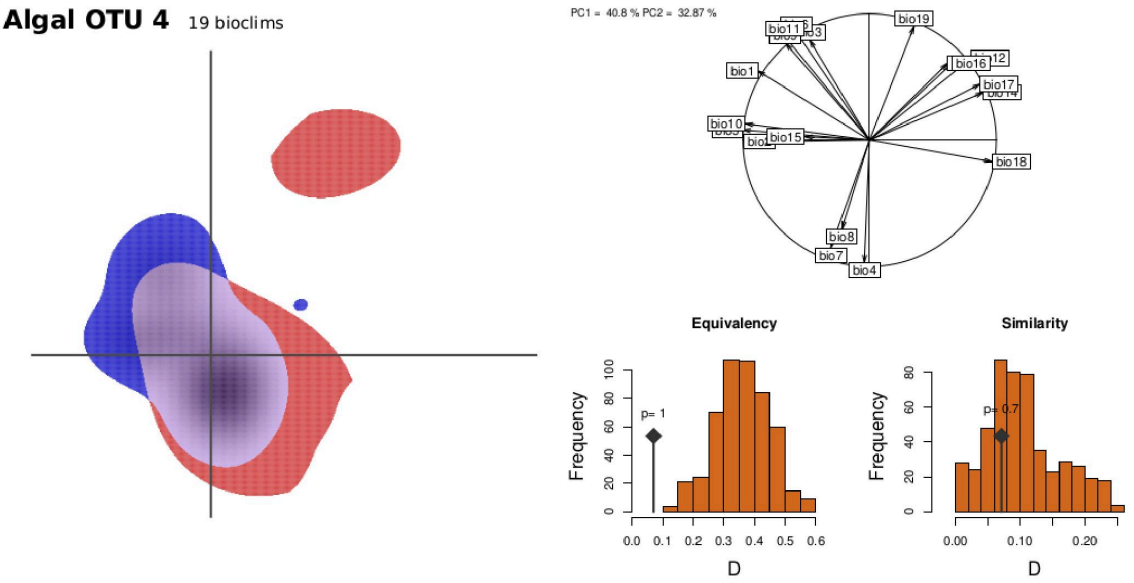
Algal OTU 4
19 bioclims
PC1 = 40.8 % PC2 = 32.87 %
bio19
bio1
bio16
bio17
bio10
bio15
bio18
bio8
bio7
bio4
Equivalency
Similarity
Frequency
p= 1
p= 0.7
D

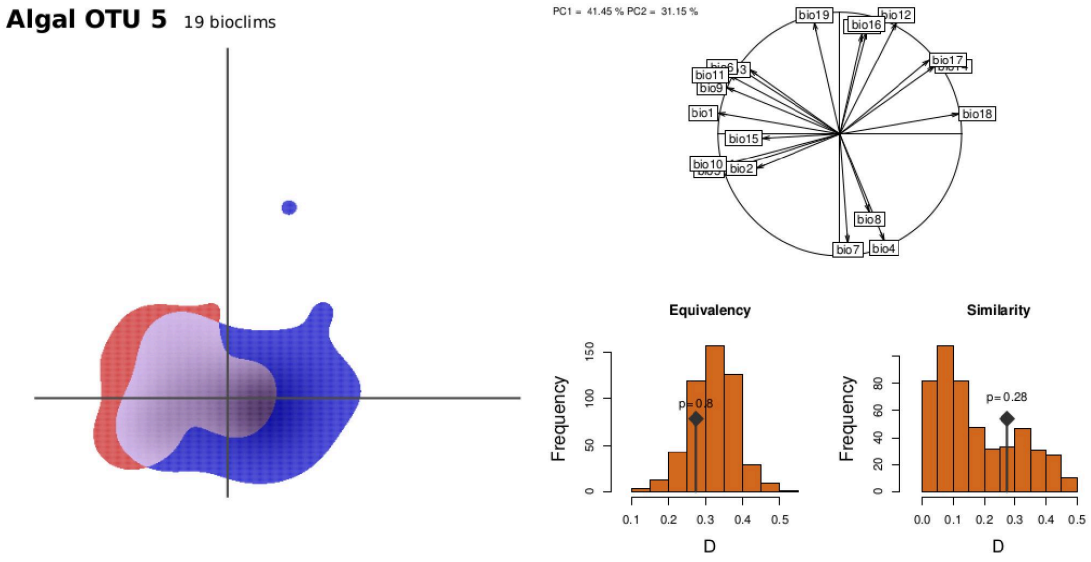

Figure S11. Left panel: Niche quantification and overlap along the two first PCA axes (based on the full set of 19 bioclims). For each algal OTU (indicated in figure header), the particular niche of the OTU is depicted in red, the niche for the remaining OTUalga is depicted in blue, and their overlap is depicted in violet. Note that if there is no red extent plotted, the complete niche of the respective OTU falls within the overall niche of the remaining OTUs (e.g., OTUalga 2 and 3). Right panel: On the top, PCA loadings are shown for the first two PCA axes. On the bottom, histograms show the observed niche overlap score between the OTU's niche and the combined niche of the remaining OTUs calculated as Schoener's D (bars with a diamond). The orange bars show simulated overlaps (n=500 replications) on which tests for niche equivalency (left) and similarity (right) were calculated. Numbers above the bar show the significance based on these simulation runs. All niches were calculated using the algorithm implemented in the 'ecospat' R package with the following parameter set: n background-points = 10 000, grid resolution = 500, low density values were not excluded.

Figure S12

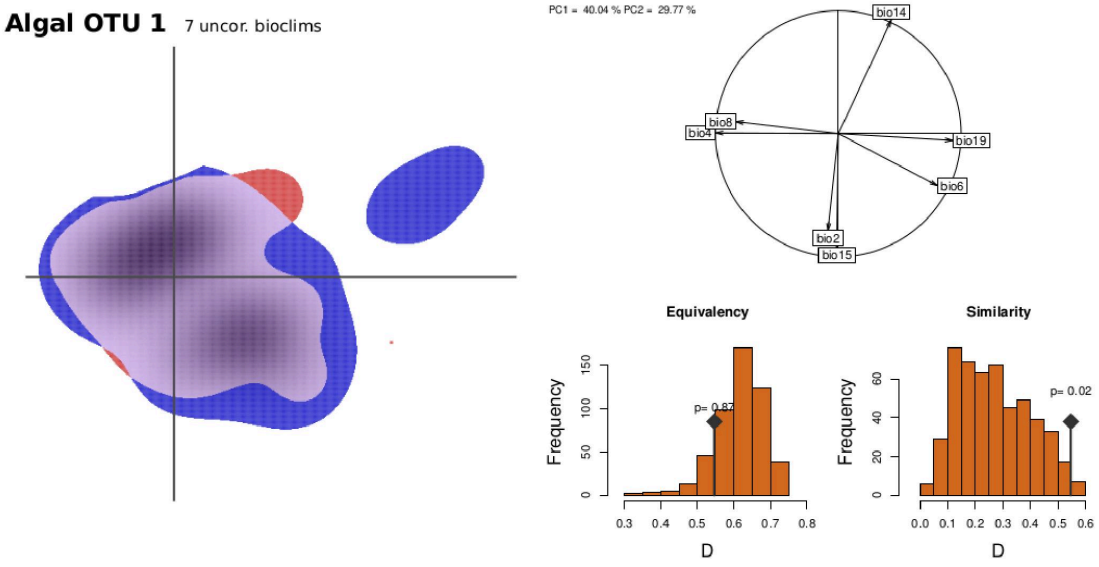
Algal OTU 1
7 uncor. bioclims
PC1 = 40.04 % PC2 = 29.77 %
bio14
bio8
bio4
bio19
bio6
bio2
bio15
Equivalency
Similarity
Frequency
p= 0.87
p= 0.02
D

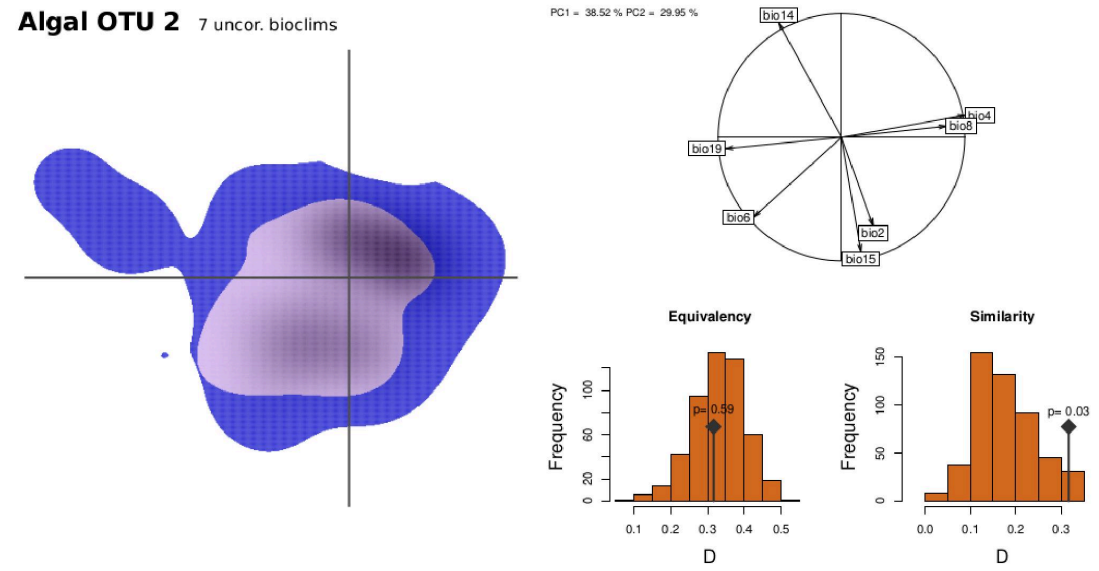
Algal OTU 2
7 uncor. bioclims
PC1 = 38.52 % PC2 = 29.95 %
bio14
bio4
bio8
bio19
bio6
bio2
bio15
Equivalency
Similarity
Frequency
p= 0.59
p= 0.03
D

Algal OTU 3 7 uncor. bioclims

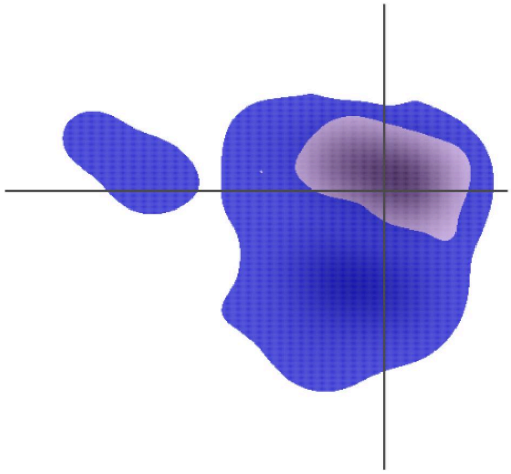

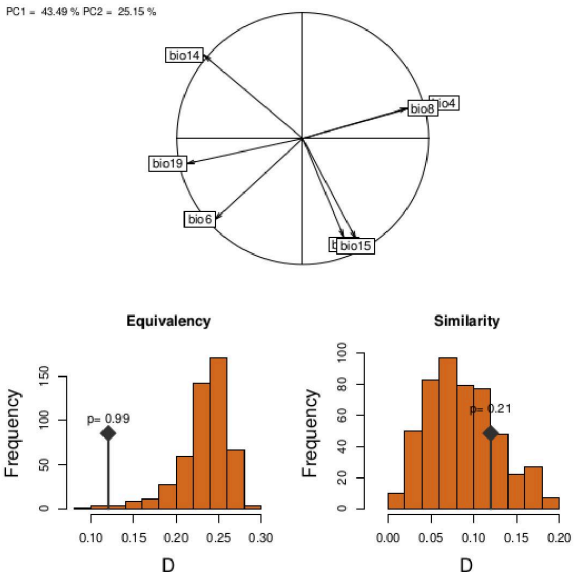

Algal OTU 4 7 uncor. bioclims

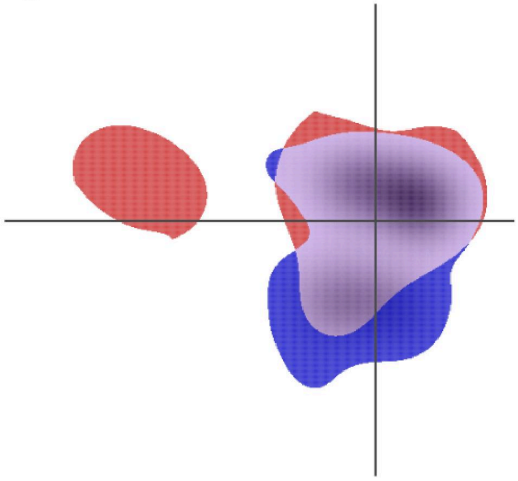

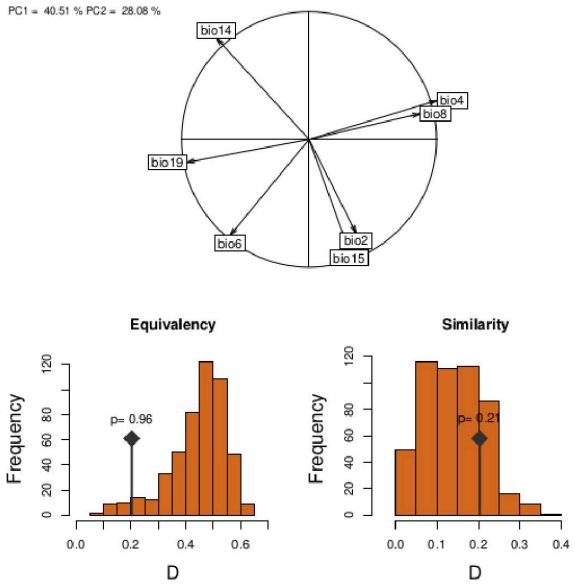

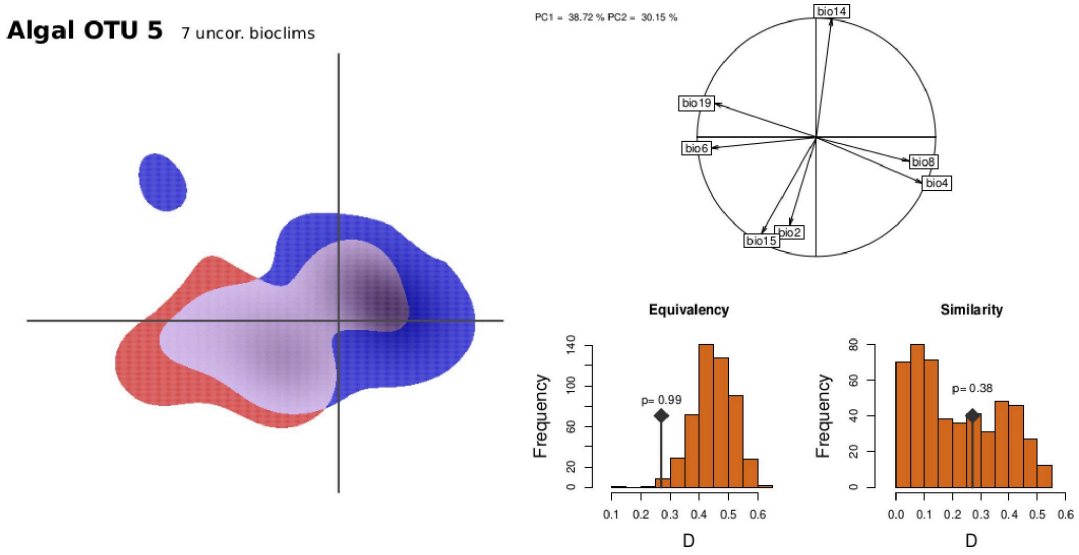

Figure S12. Left panel: Niche quantification and overlap along the two first PCA axes (based on the uncorrelated set of 7 bioclims). For each algal OTU (indicated in figure header), the particular niche of the OTU is depicted in red, the niche for the remaining OTUalga is depicted in blue, and their overlap is depicted in violet. Note that if there is no red extent plotted, the complete niche of the respective OTU falls within the overall niche of the remaining OTUs (e.g., OTUalga 2 and 3). Right panel: On the top, PCA loadings are shown for the first two PCA axes. On the bottom, histograms show the observed niche overlap score between the OTU's niche and the combined niche of the remaining OTUs calculated as Schoener's D (bars with a diamond). The orange bars show simulated overlaps (n=500 replications) on which tests for niche equivalency (left) and similarity (right) were calculated. Numbers above the bar show the significance based on these simulation runs. All niches were calculated using the algorithm implemented in the 'ecospat' R package with the following parameter set: n background-points = 10 000, grid resolution = 500, low density values were not excluded.

Figure S13

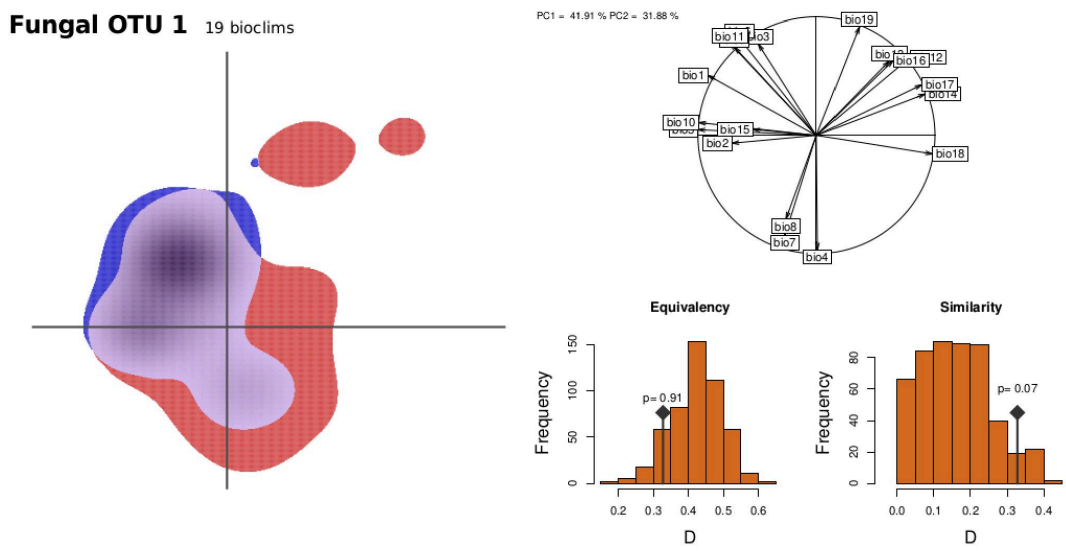
Fungal OTU 1 19 bioclims
PC1 = 41.91 % PC2 = 31.88 %
bio19
bio11
bio3
bio16
bio12
bio1
bio17
bio14
bio10
bio15
bio2
bio18
bio8
bio7
bio4
Equivalency
Similarity
Frequency
p= 0.91
p= 0.07
D

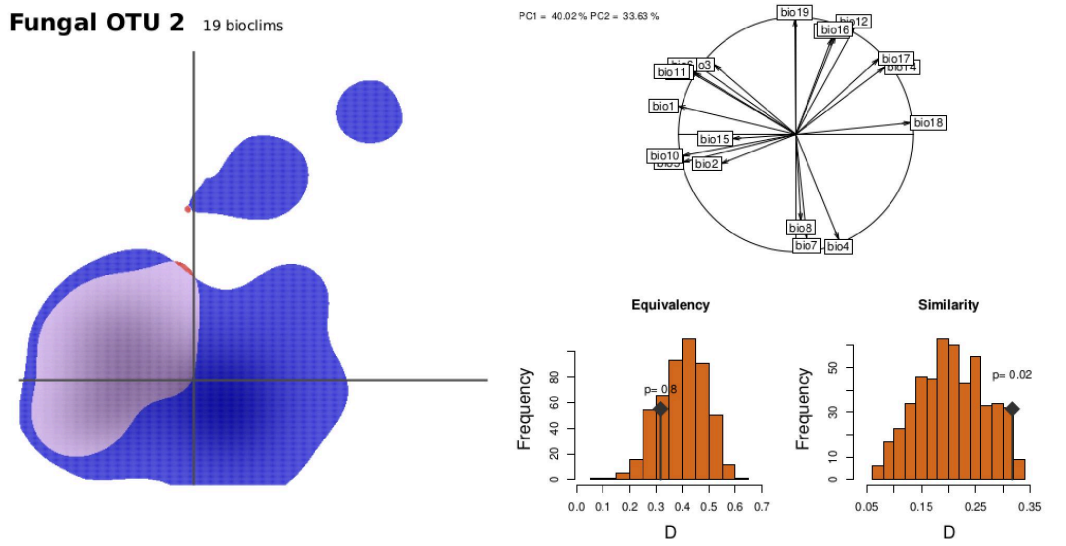
Fungal OTU 2 19 bioclims
PC1 = 40.02 % PC2 = 33.63 %
bio19
bio12
bio16
bio3
bio11
bio17
bio14
bio1
bio18
bio15
bio10
bio2
bio8
bio7
bio4
Equivalency
Similarity
Frequency
p= 0.8
p= 0.02
D

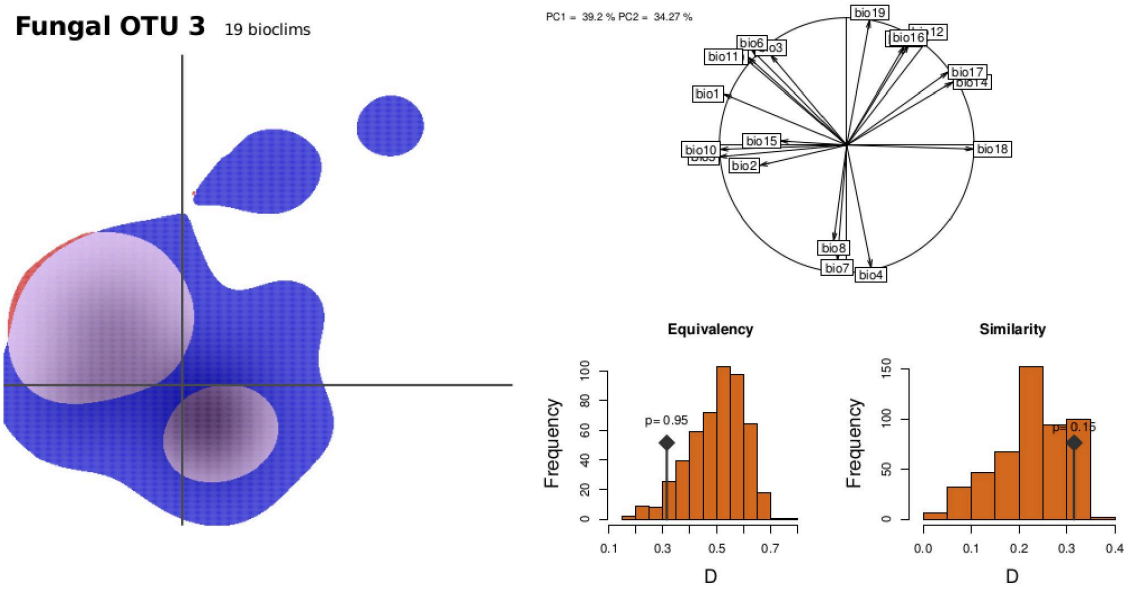
Fungal OTU 3
19 bioclims
PC1 = 39.2 % PC2 = 34.27 %
bio19
bio16
bio17
bio14
bio1
bio15
bio10
bio18
bio2
bio8
bio7
bio4
Equivalency
Similarity
Frequency
p= 0.95
p= 0.15
D

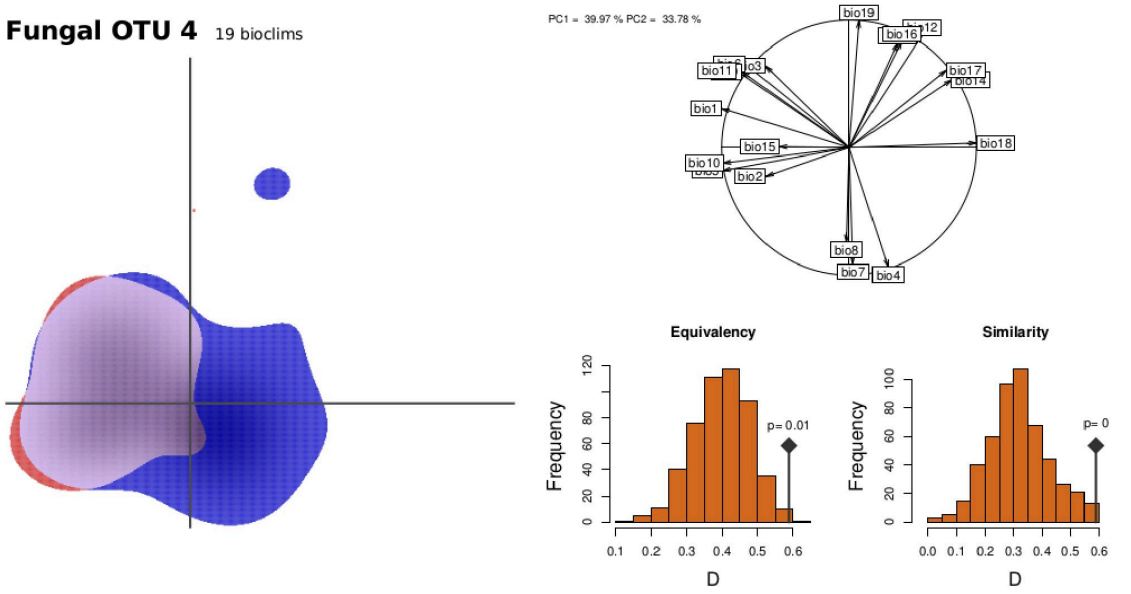
Fungal OTU 4
19 bioclims
PC1 = 39.97 % PC2 = 33.78 %
bio19
bio16
bio17
bio1
bio15
bio18
bio10
bio2
bio8
bio7
bio4
Equivalency
Similarity
Frequency
p= 0.01
p= 0
D

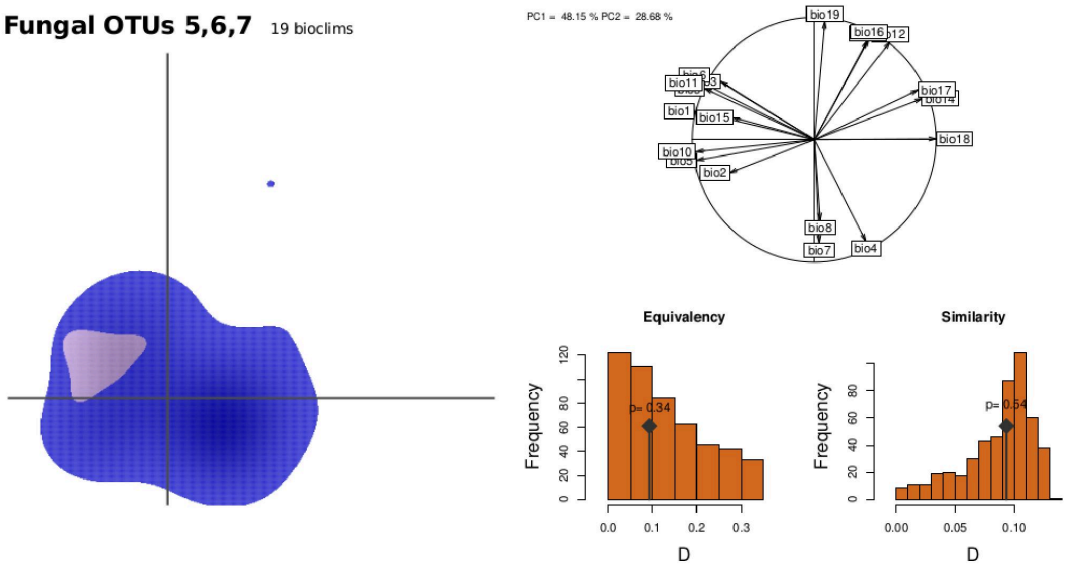

Figure S13. Left panel: Niche quantification and overlap along the two first PCA axes (based on the uncorrelated set of 7 bioclims). For each fungal OTU (indicated in figure header), the particular niche of the OTU is depicted in red, the niche for the remaining OTUfungus is depicted in blue, and their overlap is depicted in violet. Note that if there is no red extent plotted, the complete niche of the respective OTU falls within the overall niche of the remaining OTUs. Right panel: On the top, PCA loadings are shown for the first two PCA axes. On the bottom, histograms show the observed niche overlap score between the OTU's niche and the combined niche of the remaining OTUs calculated as Schoener's D (bars with a diamond). The orange bars show simulated overlaps (n=500 replications) on which tests for niche equivalency (left) and similarity (right) were calculated. Numbers above the bar show the significance based on these simulation runs. All niches were calculated using the algorithm implemented in the 'ecospat' R package with the following parameter set: n background-points = 10 000, grid resolution = 500, low density values were not excluded.

Figure S14

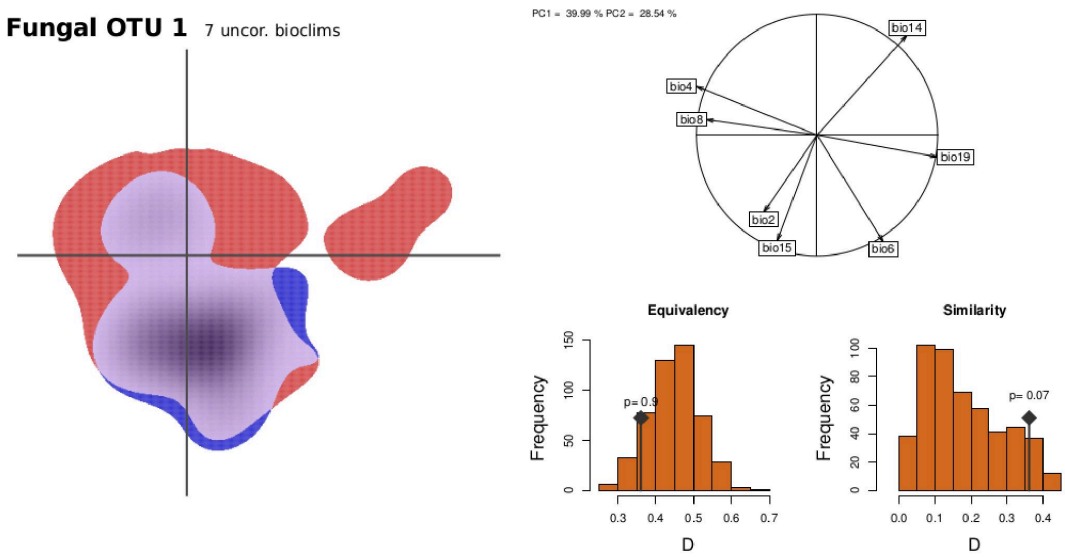
Fungal OTU 1
7 uncor. bioclims
PC1 = 39.99 % PC2 = 28.54 %
bio14
bio4
bio8
bio19
bio2
bio15
bio6
Equivalency
Similarity
Frequency
p= 0.9
p= 0.07
D

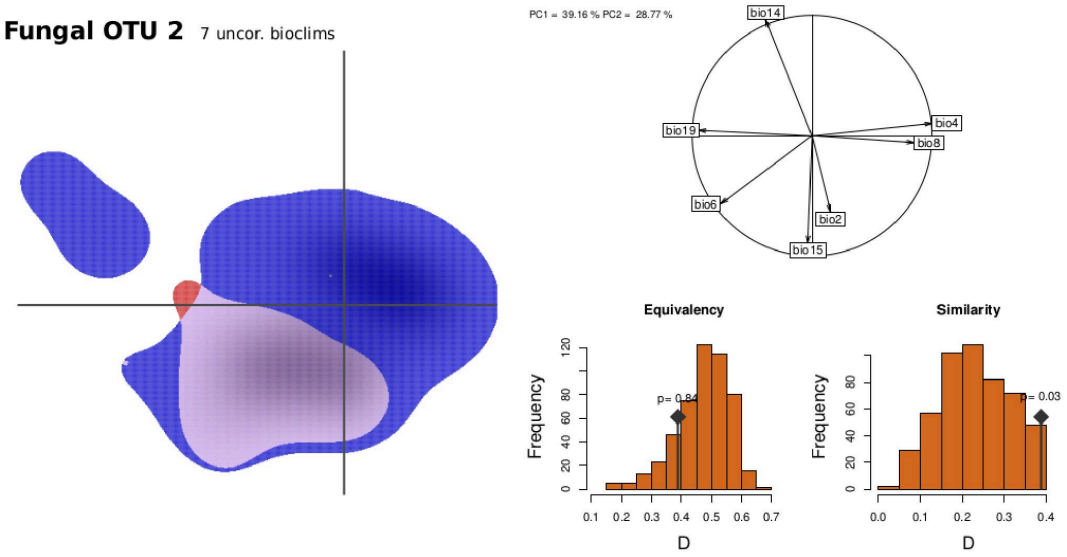
Fungal OTU 2
7 uncor. bioclims
PC1 = 39.16 % PC2 = 28.77 %
bio14
bio19
bio4
bio8
bio6
bio2
bio15
Equivalency
Similarity
Frequency
p= 0.84
p= 0.03
D

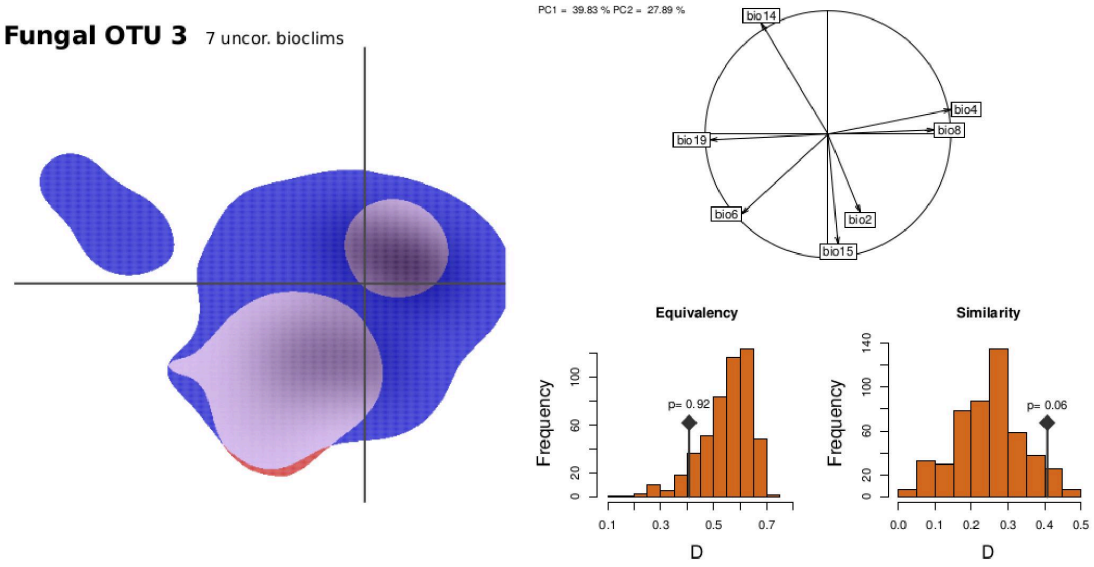
Fungal OTU 3
7 uncor. bioclims
PC1 = 39.83 % PC2 = 27.89 %
bio14
bio4
bio8
bio19
bio6
bio2
bio15
Equivalency
Similarity
Frequency
p= 0.92
p= 0.06
D

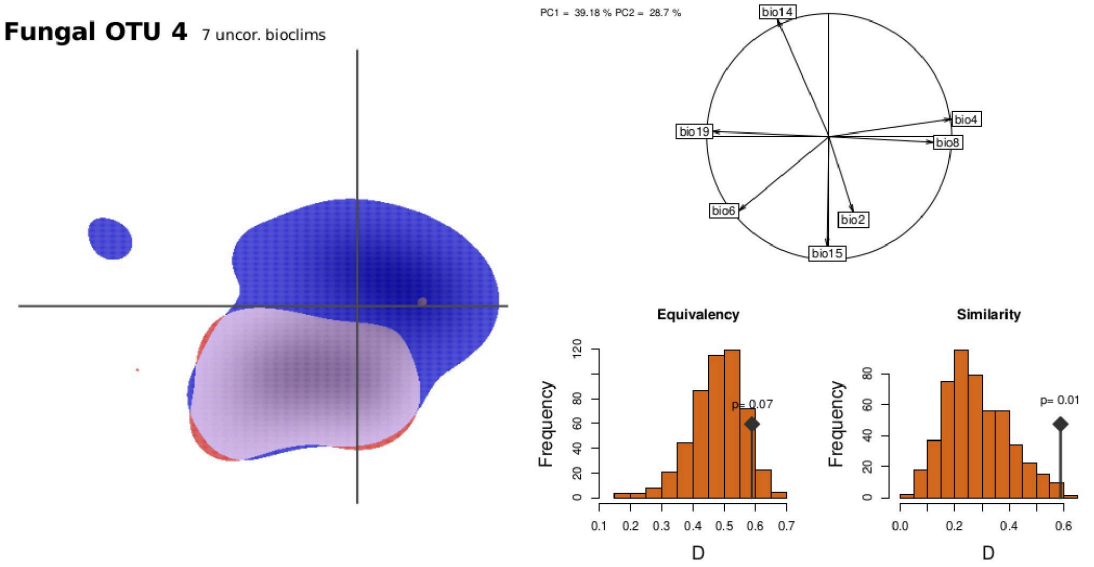
Fungal OTU 4
7 uncor. bioclims
PC1 = 39.18 % PC2 = 28.7 %
bio14
bio4
bio8
bio19
bio6
bio2
bio15
Equivalency
Similarity
Frequency
p= 0.07
p= 0.01
D

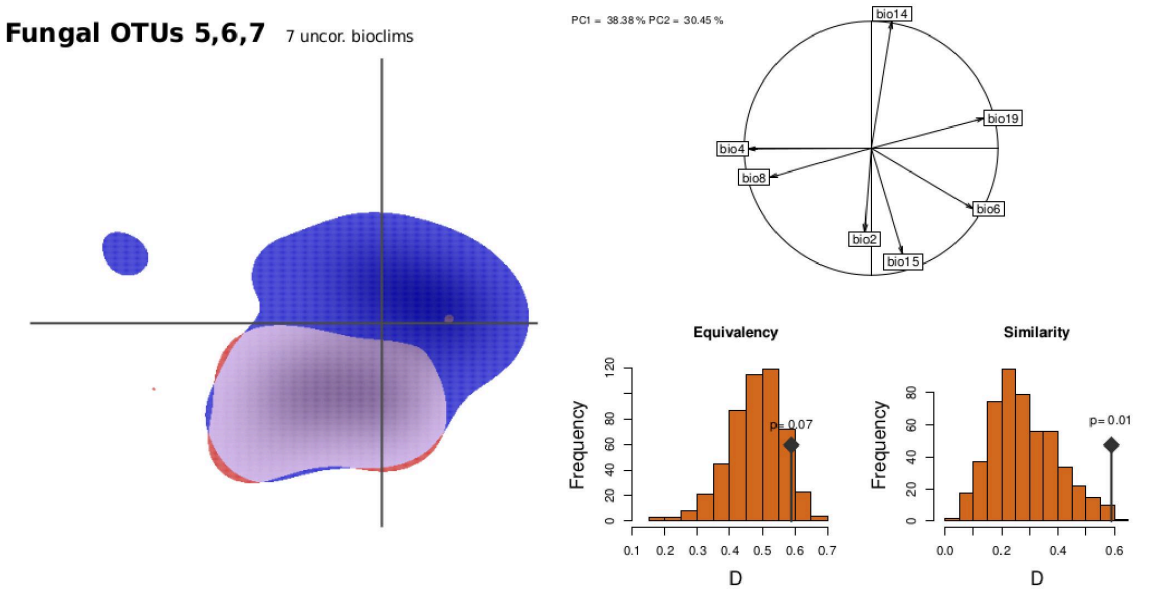

Figure S14. Left panel: Niche quantification and overlap along the two first PCA axes (based on the uncorrelated set of 7 bioclims). For each fungal OTU (indicated in figure header), the particular niche of the OTU is depicted in red, the niche for the remaining OTUfungus is depicted in blue, and their overlap is depicted in violet. Note that if there is no red extent plotted, the complete niche of the respective OTU falls within the overall niche of the remaining OTUs. Right panel: On the top, PCA loadings are shown for the first two PCA axes. On the bottom, histograms show the observed niche overlap score between the OTU's niche and the combined niche of the remaining OTUs calculated as Schoener's D (bars with a diamond). The orange bars show simulated overlaps (n=500 replications) on which tests for niche equivalency (left) and similarity (right) were calculated. Numbers above the bar show the significance based on these simulation runs. All niches were calculated using the algorithm implemented in the 'ecospat' R package with the following parameter set: n background-points = 5 000 (reduced in cases of too small niche extend), grid resolution = 500, low density values were not excluded.

APPENDIX 4

References

Broennimann, O. et al. 2012. Measuring ecological niche overlap from occurrence and spatial environmental data. – Global Ecol. Biogeogr. 21: 481-497.

Dal Grande, F. et al. 2017. Environment and host identity structure communities of green algal symbionts in lichens. – New Phytologist (in press)

Di Cola, V. et al. 2017. ecospat: an R package to support spatial analyses and modeling of species niches and distributions. – Ecography 40: 774-787.

Dormann, C. F. et al. 2013. Collinearity: a review of methods to deal with it and a simulation study evaluating their performance. – Ecography 36: 027-046.

Ezard, T. et al. 2014. Splits: SPecies' LImits by Threshold Statistics. R package version 1.0-19/r51. http://R-Forge.R-project.org/projects/splits/

Fujisawa, T. and Barraclough, T. G. 2013. Delimiting species using single-locus data and the generalized mixed yule coalescent approach: a revised method and evaluation on simulated data sets. – Syst. Biol. 62: 707-724.

Galpern, P. et al. 2014. MEMGENE: Spatial pattern detection in genetic distance data. - Methods Ecol. Evol. 5: 1116–1120.

Gruber, A. R. et al. 2008. The Vienna RNA Websuite. – Nucleic Acids Res. 36: W70-W74.

Hofacker, I. L. et al. 1994. Fast folding and the comparison of RNA secondary structures. – Monatsheft f. Chemie 125: 167-188

Katoh K. and Standley D. M. 2013. MAFFT multiple sequence alignment software version 7: Improvements in performance and usability. – Mol. Biol. Evol. 30: 772-780.

Leavitt, S. D. et al. 2015. Fungal specificity and selectivity for algae play a major role in determining lichen partnerships across diverse ecogeographic regions in the lichen-forming family *Parmeliaceae* (Ascomycota). – Mol. Ecol. 24: 3779–3797.

Lorenz, R. et al. 2011. ViennaRNA package 2.0 – Algorithms for Mol. Biol. 6: 26

Pons, J. et al. 2006. Sequence-based species delimitation for the DNA taxonomy of undescribed insects. – Syst. Biol. 55: 595-609.

Puillandre, N. et al. 2012. ABGD, Automatic Barcode Gap Discovery for primary species delimitation. – Mol. Ecol. 21: 1864–1877.

Qaio, H. et al. 2016. A cautionary note on the use of hypervolume kernel density estimators in ecological niche modelling. – Global Ecol. Biogeogr. 26: 1066-1070

R Development Core Team 2016. R: A Language and Environment for Statistical Computing. – Vienna, Austria. http://www.R-project.org

Rognes, T. et al. 2016. VSEARCH: a versatile open source tool for metagenomics. – PeerJ 4:e2584.

Schoener, T. W. 1968. The Anolis lizards of Bimini: resource partitioning in a complex fauna. – Ecology 49: 704-726.

Stamatakis, A. 2006. RAxML-VI-HPC: maximum likelihood-based phylogenetic analyses with thousands of taxa and mixed models. Bioinformatics 22: 2688-2690.

Stamatakis, A. et al. 2008. A rapid boostrap algorithm for the RAxML web servers. – Syst. Biol. 57: 758-771.

Zahradníková, M. et al. 2017. Molecular evidence of *Apatococcus*, including *A. fuscideae* sp. nov., as photobiont in the genus *Fuscidea.* – Protist 168: 425-438.

Zhang, J. et al. 2013. A general species delimitation method with applications to phylogenetic placements. Bioinformatics 29: 2869-2876.

Table S1. Overview of sampling locations, haplotype abundance, and OTU delimitation. The first spreadsheet gives a detailed listing of sampling locations, collector IDs, and additional geographic information (if available). The second spreadsheet has abundance data for all algal and fungal haplotypes for all 119 sampling locations, corresponding to the first spreadsheet. The third spreadsheet lists the OTU assignment of fungal and algal haplotypes based on ABGD and hierarchical clustering. The fourth spreadsheet gives the total number of sampling locations summarized for each OTU.

Sample location								
n	**Long**	**Lat**	**Alt**	**Country**	**date**	**Year**	**Collectors**	**Local geographic Information**
1	15.18	46.93	760	Austria	27.7.	2011	Sadowska-Des	Styria, Sporiroa-Ofen, near Mausegg and Sommereben
2	-3.07	47.6	20	France	1.8.	2011	Martin Grube	Bretagne, Morbiham, Carnac,Alignments de Kermanio, Route de Karlescan
3	2.53	48.38	80	France	18.8.	2013	Fernandez	Sables du Cul-du-Chien, Foret Domaniale des Trois Pignons 77123 Noisy- sur-Ecole.
4	6.58	43.4	155	France	22.7.	2013	Fernandez	Massif de Maures, 83120 Sainte-Maxime.
5	14.32	50.1	330	Czech Republic	7.11.	2011	J. Liska	Praha: Gorge Divoka Sarka (Nwoutskirts of Prague), chert rock,
6	13.99	49.04	580	Czech Republic	19.5.	2012	Jan Vondrak	South Bohemia, Husinec, rocky steep slope above left bank of river Blanice, below dam of Husinec water reservoir
7	14.61	48.75	785	Czech Republic	15.8.	2012	Palice Z.	South Bohemia, dist Cesky Krumlov, Kaplice, Slepcin hory hills.
8	18.34	59.34	23	Sweden	7.4.	2012	Wedin	Uppland, Boo par., Velamsund, E of lake Insjön, Mörbygärdet, SW-oriented open rocky outcrop in agricultural landscape.
9	18.33	59.35	24	Sweden	8.6.	2012	Wedin	Uppland, Boo par., Velamsund, open rocky mountain slopes NNE of Velamsund farm.
10	25.94	59.52	24	Estonia	31.7.	2008	Ave Suija/ Tiina Randlane	Lääne-Viru mk., Vihula vald, Vahakivi Ilumäe ligidal, Lahemaa rahvuspark, granite
11	25.16	60.2	10	Finland	7.8.	2011	Mohammad Sohrabi	Uusimaa, 13 km NEE Helsinki. Uutela, Seaside, pine forest
12	8.4	50.14	342	Germany	26.5.	2011	Sadowska-Des	Taunus, Eppstein, outcrops near Mendelson memorial/ close to Kaiser temple
13	7.54	49.56	500	Germany	17.6.	2011	Sadowska-Des, Volker John	Rheinland-Pfalz, Kusel, SchneeweiderHof,"Kiefernberg"
14	7.54	49.5	500	Germany	17.6.	2011	Sadowska-Des, Volker John	Rheinland-Pfalz, Kusel, SchneeweiderHof,"Kiefernberg"
15	7.14	49.6	400	Germany	17.6.	2011	Sadowska-Des, Volker John	Saarland, Lohfelden, "Elsenfels" S exposure/exposed rocks overlooking river valley
16	6.99	49.61	510	Germany	17.6.	2011	Sadowska-Des, Volker John	Saarland, Kahlenberg, "Mannfelsen" S exposure/exposed rocks in mixed forest with spruce and beech
17	6.54	49.5	300	Germany	17.6.	2011	Sadowska-Des, Volker John	Saarland, Orscholz, Saarschleife, below viewing point Cloef

18	11.25	50.67	453	Germany	25.6.	2011	Sadowska-Des	Tueringen, Bad Blankenburg, Griesbachfelsen
19	11.25	50.66	309	Germany	25.6.	2011	Sadowska-Des	Tueringen, Bad Blankenburg, Ingoklippefelsen
20	11.25	50.67	300	Germany	25.6.	2011	Sadowska-Des	Tueringen, Bad Blankenburg, Bindseil Felsen
21	11.02	51.74	403	Germany	13.8.	2011	Sadowska-Des	Bodetal, Rosstrappe
22	7.84	49.82	250	Germany	15.6.	2013	Sadowska-Des	Rotenfels, Bad Muenster am Stein Ebernburg
23	18.13	46.09	450	Hungary	30.1.	2010	Farkas, Lokos	Baranya district, Kovagoszolos, Mecsek Mts, Jakab-hegy, Babas-szerkovek
24	18.13	46.09	570	Hungary	7.5.	2011	Farkas, Lokos	Pest District, Perocseny, Borzsony Mts, Hollo-ko.
25	18.13	46.09	410	Hungary	30.10.	2010	Farkas, Lokos	Baranya district, Kovagoszolos, Mecsek Mts, Jakab-hegy, Babas-szerkovek
26	18.13	46.09	700	Hungary	7.5.	2011	Farkas, Lokos	Pest District, Kamence,Borzsony Mts, Nagy-Mana
27	18.13	46.09	670	Hungary	7.5.	2011	Farkas, Lokos	Pest District, Kamence,Borzsony Mts, Nagy-Mana
28	18.13	46.09	695	Hungary	7.5.	2011	Farkas, Lokos	Pest District, Kamence,Borzsony Mts, Nagy-Mana
29	18.91	47.74	495	Hungary	10.11.	2012	Farkas E., Lokos L.	Pest County, Domos. Pilis-Visegradi-hegyseg Mts, at NW side of Mt Keserus, on rigde
30	18.91	47.74	500	Hungary	10.11.	2012	Farkas E., Lokos L.	Pest County, Domos. Pilis-Visegradi-hegyseg Mts, at NW side of Mt Keserus, between valleys
31	9.45	41.05	100	Italy	30.4.	2012	Jan Vondrak	Sardinia: Olbia, San Pantaleo, exposed granite roks S of road between Cantone Saraghinu and San Pantalteo,
32	11.1	43.01	760	Italy	23.6.	2012	A. Guttova, L. Paoli, T.Pisani	Toccana- Maremma: Roccatederighi, the Hill topped by the ruins of the castle Sassoforte, NE exposed open rhyolit boulder
33	9.08	40.76	117	Italy	29.4.	2013	Sadowska-Des	Sardinien, from Berichida do Tempia
34	9.05	40.78	310	Italy	29.4.	2013	Sadowska-Des	Sardinia, Centrale di Caghinasas Entel
35	9.06	40.8	428	Italy	29.4.	2013	Sadowska-Des	Sardinia, Tempi direction
36	9.11	40.85	588	Italy	29.4.	2013	Sadowska-Des	Sardinia, dangerous steep slope, on the left side of the road
37	9.13	40.86	643	Italy	29.4.	2013	Sadowska-Des	Sardinia, Limbara Mt direction
38	9.13	40.86	844	Italy	30.4.	2013	Sadowska-Des	Sardinia, Limbara Mt direction
39	9.16	40.86	1117	Italy	30.4.	2013	Sadowska-Des	Sardinia, scattered small stones
40	9.17	40.85	1307	Italy	30.4.	2013	Sadowska-Des	Sardinia, Limbara Mt
41	9.3	40.81	280	Italy	28.4.	2013	Sadowska-Des	Sardinia, Berichida, Parking place
42	9.45	41.04	256	Italy	28.4.	2013	Sadowska-Des	Sardinia, from Olbia to Capo Testa
43	9.48	39.35	98	Italy	3.5.	2013	Sadowska-Des	Sardinia zjazd Conconiera Cannas, parking at Hotel Ristorante Sant' Angelo
44	9.47	39.96	899	Italy	28.4.	2013	Sadowska-Des	Sardinia, Villanova
45	-1.24	52.74	140	England	NA	2012	Chris Ellis, Brian Coppins	The Charnwood Forest SK51
46	-6.17	57.29	18	Scotland	24.9.	2012	Sadowska-Des	Cullin Hills, Slighan, Carbost, fence near building
47	-6.17	57.29	60	Scotland	24.9.	2012	Sadowska-Des	Cullin Hills, Slighan, Carbost, tourist path.

48	-6.17	57.29	120	Scotland	24.9.	2012	Sadowska-Des	Cullin Hills, Slighan, Carbost, tourist path.
49	8.09	58.7	1	Norway	7.6.	2009	Klepsland	AUST - AGDER, LELLESAND: Hellekilen/ UTM wgs84: MK 55114463 (map: 1511 II), pa strandberg, leg. Klepsland, Jon T./ No. JK 09-L139
50	8.09	58.7	2	Norway	7.6.	2009	Klepsland	AUST - AGDER, LELLESAND: Hellekilen/ UTM wgs84: MK 55114463 (map: 1511 II), pa strandberg, leg. Klepsland, Jon T./ No. JK 09-L140
51	11.38	60.06	110	Norway	11.5.	2008	Breili, Anders	HEDMARK, RINGSAKER: Brøttum sag, V for./ UTM wgs84: NN 83766447 (map:1817 II)/ Pa berg langs Mjøsa/ leg. Breili, Anders/ No.: L-3125/ Sørvendt, soleksponert
52	11.38	60.06	125	Norway	11.5.	2008	Breili, Anders	HEDMARK, RINGSAKER: Brøttum sag, V for./ UTM wgs84: NN 83766447 (map:1817 II)/ Pa berg langs Mjøsa/ leg. Breili, Anders/ No.: L-3125/ Sørvendt, soleksponert
53	11.38	60.06	111	Norway	11.5.	2008	Breili, Anders	NA
54	10.74	60.91	150	Norway	2.7.	2005	Breili, Anders	HEDMARK, RINGSAKER: Brøttumsberga/ UTM wgs84: NN 873 624 (map:1816I)/ Pa solvendi side av blokk I grov apen ur ovenfor rv. 213/ leg. Breili, Anders/ No. L-1322
55	10.74	60.91	151	Norway	2.7.	2005	Breili, Anders	NA
56	10.74	60.91	123	Norway	6.5.	2007	Breili, Anders	HEDMARK, RINGSAKER: Mjøsstranda S for Trettsvea/ UTM wgs84 :NN 887 618 (map: 1816 I)/ Pa konglomeratblokk langs Mjøsa/ leg. Breili Anders/ No.: L-2537
57	10.47	61.12	300	Norway	18.5.	2008	Breili, Anders	Oppland, Lillehammer: Svarverudberget/ UTMwgs84 : NN 7625 8949 (map 1817 II)/ Pa østvendt bergvegg/ leg. Breili, Anders/ No. L-3183
58	8.88	61.6	1185	Norway	24.6.	2008	Haugan	Oppland, VAGA: Russvassbue, UTM wgs84:(GPS) 32V MP 89012467 (map: 1618 III) Large boulder in low alpine mountain-side/ leg. Haugan R.,/ No. 8068
59	8.88	61.6	1186	Norway	24.6.	2008	Haugan	Oppland, VAGA: Russvassbue, UTM wgs84:(GPS) 32V MP 89012467 (map: 1618 III) Large boulder in low alpine mountain-side/ leg. Haugan R.,/ No. 8069
60	9.05	61.75	1300	Norway	25.3.	2005	Breili, Anders	Oppland, VAGA: Trollhø / UTM wgs84: NP 023 464 (map: 1618 I)/ Pa fylittblokk pa fjellrabbe. Fuglestein/ leg. Breili Anders/ No. L- 1100
61	6.32	61.67	2	Norway	8.4.	2009	Breili, Anders	SOGN OG FJORDANE, EID: Hamnest/ UTM wgs84: LP 2827 6659 9map:1218 IV)/ I fuktsig pa strandberg/ leg. Breili, Anders/ No. L- 3553
62	6.32	61.67	505	Norway	30.7.	2006	Anonby, J.E	Sogn Og Fjorfane, Gloppen, Hyen, W os Skogheim, Map 1218 III, Datum WGS84, UTM: 32V LP 2850 4245 F-0095
63	10.03	58.98	20	Norway	2.4.	2011	Rui, Timdal	Vestfold, Larvik / Stavern, near the Sailor's monument / UTM wgs84:(GPS) 32V NL 59603948/

								map:1812 IV / open hillside towards the sea / leg Rui, S. & Timdal E./ No.11831
64	11.03	58.98	20	Norway	2.4.	2011	Rui, Timdal	NA
65	12.03	58.98	20	Norway	2.4.	2011	Rui, Timdal	Vestfold, Larvik / Stavern, near the Sailor's monument / UTM wgs84:(GPS) 32V NL 59603948/ map:1812 IV / open hillside towards the sea / leg Rui, S. & Timdal E./ No.11832
66	13.03	58.98	20	Norway	2.4.	2011	Rui, Timdal	Vestfold, Larvik / Stavern, near the Sailor's monument / UTM wgs84:(GPS) 32V NL 59603948/ map:1812 IV / open hillside towards the sea / leg Rui, S. & Timdal E./ No.11834
67	7.83	59.62	1000	Norway	7.9.	2011	Johnsen J.I.	Telemark, Vinje,Wside of Kjelvatnet, Map 1414IV, Datum ED50. UTM:32V LM 981308, No F-0093
68	11.82	64.42	10	Norway	NA	NA	NA	NA
69	10.93	59.13	8	Norway	15.8.	2012	G.Singh, F Dal Grande	Asmaløy, Hvaler
70	10.94	59.14	8	Norway	15.8.	2012	G.Singh, F Dal Grande	Kjøkøya, Fredrikstad
71	10.95	59.23	2	Norway	14.8.	2012	G.Singh, F Dal Grande	Kjøkøya, Fredrikstad
72	15.63	50.83	600	Poland	23.6.	2011	Sadowska-Des	Zbojeckie Skaly, Karkonosze Mts
73	15.63	50.83	530	Poland	23.6.	2011	Sadowska-Des	Chojnik Hill, Karkonosze Mts
74	15.63	50.83	627	Poland	29.8.	2011	Sadowska-Des	Chojnik Castle, Karkonosze Mts
75	15.58	50.87	699	Poland	25.8.	2011	Sadowska-Des	Bobrowe skaly, Izery Mts
76	15.75	51.05	561	Poland	30.9.	2011	Sadowska-Des	Ostrzyca proboszczowicka, Kaczawskie Mts
77	15.9	50.58	563	Poland	30.9.	2011	Sadowska-Des	Bolczów, Rudawy Janowickie
78	15.76	50.87	383	Poland	12.9.	2011	J. Z. Sadowscy	Jelenia Góra, ul.Sudecka
79	16.01	50.69	681	Poland	NA	2011	Katarzyna Szczepanska	Sudety srodkowe, Kamienne Mts, srodkowe pasmo Gor Kruczych, Krucze Skaly, Rezerwat Krucza Skala,
80	30.57	39.09	1350	Turkey	8.7.	2011	Mahmet Candan	Eskisehir, Turkmen Dagi, Eskisehir -Afyon il siniri
81	34.82	40.6	1083	Turkey	14.1.	2007	K.Kinaliogl u	Corum:Canakci village
82	-5.3	40.22	1700	Spain	11.7.	2010	Mercedes Vivas Rebuelta	Sierra de Gredos (southern face) , from Chilla to Almanzor pear, Garganta de Chilla - Ávila, Subida al Sillao de la Peña Chilla
83	-5.16	40.22	1400	Spain	11.7.	2010	Mercedes Vivas Rebuelta	Sierra de Gredos (southern face) , from Chilla to Almanzor pear, Garganta de Chilla - Ávila, Subida al Sillao de la Peña Chilla
84	-5.28	40.22	1200	Spain	11.7.	2010	Mercedes Vivas Rebuelta	Sierra de Gredos (southern face) , from Chilla to Almanzor pear, Garganta de Chilla - Ávila, Subida al Sillao de la Peña Chilla
85	-5.28	40.22	1000	Spain	11.7.	2010	Mercedes Vivas Rebuelta	Sierra de Gredos (southern face) , from Chilla to Almanzor pear, Garganta de Chilla - Ávila, Subida al Sillao de la Peña Chilla
86	-5.28	40.18	900	Spain	11.7.	2010	Mercedes Vivas Rebuelta	Sierra de Gredos (southern face) , from Chilla to Almanzor pear, Garganta de Chilla - Ávila, Subida al Sillao de la Peña Chilla

87	-5.16	40.25	1720	Spain	16.7.	2010	Mercedes Vivas Rebuelta	Sierra de Gredos (southern face) ,from Nogal del Barranco to La Mira
88	-5.15	40.23	1380	Spain	16.7.	2010	Mercedes Vivas Rebuelta	Sierra de Gredos (southern face) ,from Nogal del Barranco to La Mira
89	-5.15	40.23	1140	Spain	14.7.	2010	Mercedes Vivas Rebuelta	Sierra de Gredos (southern face) ,from Nogal del Barranco to La Mira
90	-5.15	40.23	900	Spain	16.7.	2010	Mercedes Vivas Rebuelta	Sierra de Gredos (southern face) ,from Nogal del Barranco to La Mira
91	-5.23	40.23	1700	Spain	11.7.	2010	Mercedes Vivas Rebuelta	Sierra de Gredos (southern face) ,from Las Hiruelas to Carro de la Cagarruta
92	-5.24	40.23	1400	Spain	11.7.	2010	Mercedes Vivas Rebuelta	Sierra de Gredos (southern face) ,from Las Hiruelas to Carro de la Cagarruta
93	-5.23	40.22	1335	Spain	11.7.	2010	Mercedes Vivas Rebuelta	Sierra de Gredos (southern face) ,from Las Hiruelas to Carro de la Cagarruta
94	-5.22	40.2	1100	Spain	11.7.	2010	Mercedes Vivas Rebuelta	Sierra de Gredos (southern face) ,from Las Hiruelas to Carro de la Cagarruta
95	-5.07	39.76	550	Spain	22.1.	2012	Raquel Pino-Bodas	Toledo:Aldeanueva de Barbarrolla
96	-5.2	39.46	650	Spain	NA	2008	Mercedes Vivas Rebuelta	Estrecho de la Peña, pasado Alía. Cáceres, Spain
97	-3.65	41.12	1400	Spain	28.1.	2012	Mercedes Vivas Rebuelta	Acebeda y sabinar de Prádena, Segovia
98	-3.13	40.78	1376.5	Spain	6.6.	2012	Francesco Dal Grande	Guadalajara Province, near Valverde de los Arroyos (130 km ca. from Madrid)
99	-5.25	40.16	500	Spain	18.6.	2013	Sadowska-Des	Sierra de Gredos (southern face) , Puerto de Candeleda , from Las Hiruelas to Carro de la Cagarruta
100	-5.3	40.19	515	Spain	19.6.	2013	Sadowska-Des	Garganta de Chilla - Ávila, Finca el Casaron
101	-15.69	28.04	1170	Spain	18.12.	2013	T. Feuerer	Canary Islands, Gran Canaria, Agaete, Pinar de Tamadaba, start of circular road, Pinus canariensis forest.
102	8.5	46.31	NA	Switzerland	18.9.	2010	Olga Nadyeina	Canton of Tichino, Bosco Gurin, coniferous forest
103	8.53	46.36	1000	Switzerland	12.8.	2013	Christoph Scheidegger	Canton of Ticino, commune di Cevio. Val Calnegia E of Val Bavona, NW of Gerra. Big boulders on subalpine meadow.
104	31.01	47.72	79	Ukraine	2.10.	2006	Oleg Blum, Olga Nadyeina	Mykolaiv region. Vil. Trykraty. Rocks on the right bank of the South Bug river.
105	34.39	44.64	429	Ukraine	4.10.	2006	Oleg Blum, Olga Nadyeina	Crimea. Alushta region. Kastel' mountain.
106	37.08	47.3	NA	Ukraine	7.10.	2006	Oleg Blum, Olga Nadyeina	Donetzk region. Volodarsk district. National reserve \"Kamyani Mogily".
107	35.14	47.84	NA	Ukraine	8.10.	2006	Oleg Blum, Olga Nadyeina	Zaporizhia region. Zaporizhia city, Khortyttsja Island on Dniper river
108	18.11	48.34	528	Slovakia	27.7.	2011	Guttova A.	Tribec Mts. - Zobor Mt.: Nitra, the summit of the hill Zobor, the site Pyramida, quartzit cliffs and outcrops on S slopes
109	18.89	49.18	459	Slovakia	13.8.	2011	Guttova A	Mala Fatra Mts., Varin - Nezdubska Lucka, granitoid ridge with the ruins of the castle Stary hard above the meader of the

								river Vah
110	-8.59	37.32	890	Portugal	19.5.	2011	P.K. Divakar, A. Agudo y C. Ruibal	Algarve, Serra de Monchique, N266-3, Foia
111	-8.58	37.32	650	Portugal	19.5.	2011	P.K. Divakar, A. Agudo y C. Ruibal	Algarve, Serra de Monchique, Entre Foia y Monchique
112	-7.54	40.3	1300	Portugal	26.3.	2009	Mercedes Vivas Rebuelta	Serra da Estrela. Subida a Torre, pasada la desviación.
113	-17.08	32.75	1300	Portugal	15.3.	1997	Ch.Prinzten&B.Kanz	Madeira, Mountain ridge from Paul da Sierra tp Achadas de Cruz, Fonte do Bispo ca. 7 km NW of Rabacal, dense vegetation or Erica scoparia near the road
114	-6.99	40.86	972	Portugal	14.8.	2013	Fernandez	Alto Marofa, Figueira do Castel Rodrigo
115	22.26	42.65	1640	Serbia	24.6.	2011	Farkas, Lokos	SE Serbia, Pcinja District, Surdulica Municipality, Vardenik Mts near Lake Vlasina, Bilo, Ne of peak V. Streser
116	21.79	40.93	1705	Greece	15.7.	2010	Farkas, Lokos	Pella district, ca 9 km NW of Loutraki, Voras Mts, neat the Greek-Macedonia border
117	24.45	38.05	1370	Greece	26.9.	2005	H.Sipman, Th.Raus	W Aegean,Nomos Evvias,Ep. & Dim. Karistos: S Evvia, summit area of Mt Ochi
118	24.64	40.72	750	Greece	29.5.	2010	H.Sipman, Th.Raus	nom.Kavala:Thasos island,along road from Megalo Prinos to antennes on summit Toumba, halfway, S-facing rock outcrops on grazed mountain slope
119	24.7	40.7	1200	Greece	25.5.	2010	H.Sipman, Th.Raus	nom.Kavala:Thasos island,Mt. Ipsario, summit area

Haplotyle abandunces											
n	**1**	**2**	**3**	**4**	**5**	**6**	**7**	**8**	**9**	**10**	**11**
	12	**13**	**14**	**15**	**16**	**17**	**18**	**19**	**20**	**21**	**22**
HA01	0	0	15	0	0	0	0	0	0	0	0
	9	0	0	0	8	0	0	0	0	0	0
HA02	26	0	1	0	6	32	0	29	25	9	37
	0	25	1	12	0	0	29	15	11	17	17
HA03	0	0	0	0	0	0	0	0	0	0	0
	0	0	0	0	0	0	0	0	0	0	0
HA04	0	28	3	12	0	0	0	0	0	0	0
	0	0	0	0	0	26	0	0	0	0	4
HA05	0	0	0	0	2	0	0	0	0	10	0
	1	1	0	0	1	0	6	0	0	3	3
HA06	0	0	0	0	0	0	0	0	0	1	0
	1	0	0	0	0	0	0	0	0	0	0
HA07	0	0	0	0	0	0	0	0	0	0	0
	0	0	0	0	0	0	0	0	0	0	0
HA08	1	0	0	0	0	0	0	0	0	0	0
	0	0	0	0	0	0	0	0	0	0	0
HA09	0	0	0	0	0	0	0	0	0	0	0
	0	0	0	0	0	0	0	0	0	0	0
HA10	0	0	0	0	0	0	0	0	0	0	0
	0	0	0	0	0	0	0	0	0	0	0
HA11	0	0	0	0	0	0	0	0	0	0	0
	0	0	0	0	0	0	0	0	0	0	0
HA12	0	0	0	0	0	0	0	0	0	0	0
	0	0	0	0	0	0	0	0	0	0	0
HA13	0	0	0	0	0	0	0	0	0	0	0
	0	0	0	0	0	0	0	0	0	0	0
HA14	0	0	0	0	0	0	0	0	0	0	0
	0	0	0	0	0	0	0	0	0	1	0
HA15	0	0	0	0	0	0	2	0	0	0	0
	1	0	0	0	0	0	0	0	0	0	0
HA16	0	0	0	0	0	0	0	0	0	0	0
	1	0	0	0	0	0	0	0	0	0	0
HA17	0	0	0	0	0	0	0	0	0	0	0
	0	0	0	0	0	0	0	0	0	0	0
HA18	0	0	0	0	0	0	0	0	0	0	0
	0	0	0	0	0	0	0	0	0	0	0
HA19	0	0	0	0	1	0	0	0	0	0	0
	0	0	0	0	0	0	0	0	0	0	0
HA20	0	0	0	0	0	0	0	0	0	0	0
	0	0	0	0	0	0	0	0	0	0	0
HA21	0	0	0	0	0	0	0	0	0	0	0
	0	0	0	0	0	0	0	0	0	3	0
HA22	0	0	0	0	0	0	0	0	0	0	0
	0	0	0	0	0	0	2	0	0	0	0
n	**1**	**2**	**3**	**4**	**5**	**6**	**7**	**8**	**9**	**10**	**11**
	12	**13**	**14**	**15**	**16**	**17**	**18**	**19**	**20**	**21**	**22**
HA23	0	0	0	0	0	0	0	0	0	0	0
	0	0	0	0	0	0	1	0	0	0	0
HA24	0	0	0	0	0	0	0	0	0	1	0
	0	0	0	0	0	0	0	0	0	0	0
HA25	0	0	0	0	0	0	0	0	0	0	0
	0	0	0	0	0	0	0	0	0	2	0
HA26	0	0	0	0	0	0	0	0	0	0	0
	0	0	0	0	0	0	0	0	0	0	0
HA27	0	0	0	0	0	0	0	0	0	0	0
	0	0	0	0	0	0	0	0	0	0	0
HA28	0	0	0	0	0	0	0	0	0	0	0
	0	0	0	0	0	0	0	0	0	0	0
HA29	0	0	0	0	0	0	0	0	0	0	0
	0	0	0	0	0	0	0	0	0	0	0

HA30	0	1	0	0	0	0	0	0	0	0	0
	0	0	0	0	0	0	0	0	0	0	0
HA31	0	0	0	0	13	0	0	0	0	0	0
	0	0	0	0	0	0	0	0	0	0	0
HA32	0	0	0	0	1	0	0	0	0	0	0
	0	0	0	0	0	0	0	0	0	0	0
HA33	0	3	0	0	0	0	0	0	0	0	0
	0	0	0	0	0	0	0	0	0	0	0
HA34	0	0	0	0	0	0	0	0	0	0	0
	0	0	0	0	0	0	0	0	0	0	0
HA35	0	0	0	0	0	0	0	0	0	0	0
	0	0	0	0	0	0	0	0	0	0	0
HA36	0	0	0	0	0	0	0	0	0	0	0
	0	0	0	0	0	0	0	0	0	0	0
HA37	0	0	0	0	0	0	0	0	0	0	0
	0	0	0	0	0	0	0	0	0	0	0
HA38	0	0	0	0	0	0	0	0	0	0	0
	0	0	0	0	0	0	0	0	0	0	0
HA39	0	0	0	0	0	0	0	0	0	0	0
	0	0	0	0	0	0	0	0	0	0	0
HA40	0	0	0	0	0	0	0	0	0	0	0
	0	0	0	0	0	0	0	0	0	0	0
HA41	0	0	0	0	0	0	0	0	0	0	0
	0	0	0	0	0	0	0	0	0	0	0
HA42	0	0	0	0	0	0	33	0	0	0	0
	0	0	0	0	0	0	0	0	0	0	0
HF01	0	0	2	0	0	0	0	2	1	0	0
	0	0	0	2	0	0	0	0	0	0	6
HF02	0	29	4	2	0	0	0	0	0	0	0
	0	0	0	0	0	0	0	0	0	0	0
HF03	0	0	0	8	0	0	0	0	4	0	0
	0	0	0	0	0	0	0	0	0	0	0
n	**1**	**2**	**3**	**4**	**5**	**6**	**7**	**8**	**9**	**10**	**11**
	12	**13**	**14**	**15**	**16**	**17**	**18**	**19**	**20**	**21**	**22**
HF04	0	0	0	0	0	0	0	0	0	0	0
	0	0	0	0	0	0	0	0	0	0	0
HF05	0	0	0	0	0	0	0	0	0	0	0
	0	0	0	0	0	0	0	0	0	0	0
HF06	16	0	14	3	38	7	33	41	20	20	25
	5	20	1	0	1	23	26	2	1	22	24
HF07	0	0	0	0	0	0	0	0	0	0	0
	0	0	0	0	0	0	0	0	0	0	0
HF08	0	0	0	0	0	0	0	0	0	0	0
	0	0	0	0	0	0	0	0	0	0	0
HF09	0	0	0	0	0	0	0	0	0	0	0
	0	0	0	0	0	0	0	0	0	0	0
HF10	0	0	0	0	0	0	0	0	0	0	0
	0	0	0	0	0	0	0	0	0	0	0
HF11	0	0	0	0	0	0	0	0	0	0	0
	0	0	0	0	0	0	0	0	0	0	0
n	**23**	**24**	**25**	**26**	**27**	**28**	**29**	**30**	**31**	**32**	**33**
	34	**35**	**36**	**37**	**38**	**39**	**40**	**41**	**42**	**43**	**44**
HA01	0	0	0	0	0	0	0	0	0	0	0
	0	0	0	0	0	16	6	0	0	0	0
HA02	3	0	1	0	0	0	0	0	0	14	0
	0	0	0	0	0	2	12	0	0	0	0
HA03	0	0	0	0	0	0	0	0	0	0	0
	0	0	0	0	10	0	0	0	0	0	0
HA04	0	0	1	0	0	0	0	0	26	0	20
	20	15	19	20	5	0	0	13	14	20	14
HA05	0	0	0	0	0	0	0	0	0	0	0
	0	0	0	0	0	0	0	0	0	0	0
HA06	0	0	0	0	0	0	0	0	0	0	0
	0	0	0	0	0	0	0	0	0	0	0

HA07	0	0	0	0	0	0	0	0	0	0	0
	0	0	0	0	0	0	0	0	0	0	0
HA08	0	0	0	0	0	0	0	0	0	0	0
	0	0	0	0	0	0	0	0	0	0	0
HA09	0	0	0	0	0	0	0	0	0	0	0
	0	0	0	0	0	0	0	0	0	0	0
HA10	0	0	0	0	0	0	0	0	0	0	0
	0	0	0	0	0	0	0	0	0	0	0
HA11	0	0	0	0	0	0	0	0	0	0	0
	0	0	0	0	0	0	0	0	0	0	0
HA12	0	0	0	0	0	0	0	0	0	0	0
	0	0	0	0	0	0	0	0	0	0	0
HA13	0	0	0	0	0	0	0	0	0	0	0
	0	0	0	0	0	0	0	0	0	0	0
n	**23**	**24**	**25**	**26**	**27**	**28**	**29**	**30**	**31**	**32**	**33**
	34	**35**	**36**	**37**	**38**	**39**	**40**	**41**	**42**	**43**	**44**
HA14	0	0	0	0	0	0	0	0	0	0	0
	0	0	0	0	0	0	0	0	0	0	0
HA15	0	0	0	0	0	0	0	0	0	0	0
	0	0	0	0	0	0	0	0	0	0	0
HA16	0	0	0	0	0	0	0	0	0	0	0
	0	0	0	0	0	0	0	0	0	0	0
HA17	0	0	0	0	0	0	0	0	0	0	0
	0	0	0	0	0	0	0	0	0	0	0
HA18	0	0	0	0	0	0	0	0	0	0	0
	0	0	0	0	0	0	0	0	0	0	0
HA19	0	0	0	0	0	0	0	0	0	0	0
	0	0	0	0	0	0	0	0	0	0	0
HA20	0	0	0	0	0	0	0	0	0	0	0
	0	0	0	0	0	0	0	0	0	0	0
HA21	0	0	0	0	0	0	0	0	0	0	0
	0	0	0	0	0	0	0	0	0	0	0
HA22	0	0	0	0	0	0	0	0	0	0	0
	0	0	0	0	0	0	0	0	0	0	0
HA23	0	0	0	0	0	0	0	0	0	0	0
	0	0	0	0	0	0	0	0	0	0	0
HA24	0	1	0	2	1	2	34	39	0	0	0
	0	0	0	0	0	0	0	0	0	0	0
HA25	0	0	0	0	0	0	0	0	0	0	0
	0	0	0	0	0	0	0	0	0	0	0
HA26	0	0	0	0	0	0	0	0	0	0	0
	0	0	0	0	0	0	0	0	0	0	0
HA27	0	0	0	0	0	0	0	0	0	0	0
	0	0	0	0	0	0	0	0	0	0	0
HA28	0	0	0	0	0	0	0	0	0	0	0
	0	0	0	0	0	0	0	0	0	0	0
HA29	0	0	0	0	0	0	0	0	0	0	0
	0	0	0	0	0	0	0	0	0	0	0
HA30	0	0	0	0	0	0	0	0	0	0	0
	0	0	0	0	0	0	0	6	5	0	5
HA31	0	0	0	0	0	0	0	0	0	0	0
	0	0	0	0	0	0	0	0	0	0	0
HA32	0	0	0	0	0	0	0	0	0	0	0
	0	0	0	0	0	0	0	0	0	0	0
HA33	0	0	0	0	0	0	0	0	0	0	0
	0	0	0	0	0	0	0	0	0	0	0
HA34	0	0	0	0	0	0	0	0	0	0	0
	0	0	0	0	0	0	0	0	0	0	0
HA35	0	0	0	0	0	0	0	0	0	0	0
	0	0	0	0	0	0	0	0	0	0	0
HA36	0	0	0	0	0	0	0	0	0	0	0
	0	0	0	0	0	0	0	0	0	0	0

n	23 34	24 35	25 36	26 37	27 38	28 39	29 40	30 41	31 42	32 43	33 44
HA37	0 0	0 0	0 0	0 0	0 0	0 0	0 0	0 0	5 0	0 0	0 0
HA38	0 0	0 0	0 0	0 0	0 0	0 0	0 0	0 0	0 0	0 0	0 0
HA39	0 0	0 0	0 0	0 0	0 0	0 0	0 0	0 0	0 0	0 0	0 0
HA40	0 0	0 0	0 0	0 0	0 0	0 0	0 0	0 0	0 0	0 0	0 0
HA41	0 0	0 0	0 0	0 0	0 0	0 0	0 0	0 0	0 0	0 0	0 0
HA42	0 0	0 0	0 0	0 0	0 0	0 0	0 0	0 0	0 0	0 0	0 0
HF01	1 0	1 0	0 7	0 0	0 0	2 3	34 0	36 0	0 0	13 0	0 0
HF02	0 19	0 0	0 0	0 4	0 7	0 14	0 0	0 2	3 0	0 13	10 1
HF03	0 0	0 15	0 5	0 9	0 7	0 0	0 0	0 2	18 8	0 5	0 6
HF04	0 0	0 0	0 0	0 0	0 0	0 0	0 0	0 0	0 0	0 0	0 0
HF05	0 1	0 0	1 2	0 2	0 1	0 0	0 13	0 0	10 9	0 0	10 10
HF06	0 0	0 0	0 0	0 2	0 0	0 0	0 0	0 0	0 0	0 0	0 1
HF07	0 0	0 0	0 0	0 0	0 0	0 0	0 0	0 0	0 0	0 0	0 0
HF08	0 0	0 0	0 0	0 0	0 0	0 0	0 0	0 0	0 0	0 0	0 0
HF09	0 0	0 0	0 0	0 0	0 0	0 0	0 0	0 0	0 0	0 0	0 0
HF10	0 0	0 0	0 0	0 0	0 0	0 0	0 0	0 7	0 2	0 0	0 2
HF11	0 0	0 0	0 0	0 0	0 0	0 0	0 0	0 9	0 0	0 2	0 0
n	**45** **56**	**46** **57**	**47** **58**	**48** **59**	**49** **60**	**50** **61**	**51** **62**	**52** **63**	**53** **64**	**54** **65**	**55** **66**
HA01	11 0	0 0	0 0	0 0	0 0	0 0	0 0	0 0	0 0	0 0	0 0
HA02	0 0	0 0	0 0	0 0	1 0	1 0	0 0	0 1	0 0	0 1	0 0
HA03	0 0	0 0	0 0	0 0	0 0	0 0	0 0	0 0	0 0	0 0	0 0
HA04	0 0	0 0	0 0	0 0	0 0	0 0	0 0	0 0	0 0	0 0	0 0
n	**45** **56**	**46** **57**	**47** **58**	**48** **59**	**49** **60**	**50** **61**	**51** **62**	**52** **63**	**53** **64**	**54** **65**	**55** **66**
HA05	16 0	0 0	0 0	0 0	0 0	0 0	0 0	0 2	0 0	0 0	0 1
HA06	0 0	0 0	0 0	0 0	0 0	0 0	0 0	0 0	0 0	0 0	0 0
HA07	0 0	0 0	0 0	0 0	0 0	0 0	0 0	0 0	0 0	0 0	0 0
HA08	0 0	0 0	0 0	0 0	0 0	0 0	1 0	1 0	0 0	1 0	0 0
HA09	0 1	0 0	0 0	0 0	0 0	0 1	0 1	0 0	0 0	0 0	0 0
HA10	0 0	0 0	0 0	0 1	0 0	0 0	1 0	0 0	0 0	0 0	0 0
HA11	0 0	0 0	0 1	0 0	0 0	0 0	0 0	0 0	0 0	0 0	0 0
HA12	0 0	0 0	0 0	0 0	0 0	0 0	0 0	0 0	0 0	0 0	0 0

HA13	0	0	0	0	0	0	0	0	0	0	0
	0	0	0	0	0	0	0	0	0	0	0
HA14	0	0	0	0	0	0	0	0	0	0	0
	0	0	0	0	0	0	0	0	0	0	0
HA15	0	0	0	0	0	0	0	0	0	0	0
	0	0	0	0	0	0	0	0	0	0	0
HA16	0	0	0	0	0	0	0	0	0	0	0
	0	0	0	0	0	0	0	0	0	0	0
HA17	0	0	0	0	0	0	0	0	0	0	0
	0	0	0	0	1	0	0	0	0	0	0
HA18	0	0	0	0	0	0	0	1	0	0	0
	0	0	0	0	0	0	0	0	0	0	0
HA19	0	0	0	0	0	0	0	0	0	0	0
	0	0	0	0	0	0	0	0	0	0	0
HA20	0	0	0	0	0	0	0	0	0	0	0
	0	0	0	0	0	0	0	0	0	0	0
HA21	0	0	0	0	0	0	0	0	0	0	0
	0	0	0	0	0	0	0	0	0	0	0
HA22	0	0	0	0	0	0	0	0	0	0	0
	0	0	0	0	0	0	0	0	0	0	0
HA23	0	0	0	0	0	0	0	0	0	0	0
	0	0	0	0	0	0	0	0	0	0	0
HA24	0	0	0	0	0	0	0	0	0	0	0
	0	0	0	0	0	0	0	0	0	0	0
HA25	0	0	0	0	0	0	0	0	0	0	0
	0	0	0	0	0	0	0	0	0	0	0
HA26	0	0	0	0	0	0	0	0	0	0	0
	0	0	0	0	0	0	0	0	0	0	0
HA27	0	0	0	0	0	0	0	0	0	0	0
	0	0	0	0	0	0	0	0	0	0	0
n	**45**	**46**	**47**	**48**	**49**	**50**	**51**	**52**	**53**	**54**	**55**
	56	**57**	**58**	**59**	**60**	**61**	**62**	**63**	**64**	**65**	**66**
HA28	0	0	0	0	0	0	0	0	0	0	0
	0	0	0	0	0	0	0	0	0	0	0
HA29	0	0	0	0	0	0	0	0	0	0	0
	0	0	0	0	0	0	0	0	0	0	0
HA30	0	0	0	0	0	0	0	0	0	0	0
	0	0	0	0	0	0	0	0	0	0	0
HA31	0	0	0	0	0	0	0	0	0	0	0
	0	0	0	0	0	0	0	0	0	0	0
HA32	0	0	0	0	0	0	0	0	0	0	0
	0	0	0	0	0	0	0	0	0	0	0
HA33	0	0	0	0	0	0	0	0	0	0	0
	0	0	0	0	0	0	0	0	0	0	0
HA34	0	0	0	0	0	0	0	0	0	0	0
	0	0	0	0	0	0	0	0	0	0	0
HA35	0	0	0	0	0	0	0	0	0	0	0
	0	0	0	0	0	0	0	0	0	0	0
HA36	0	0	0	0	0	0	0	0	0	0	0
	0	0	0	0	0	0	0	0	0	0	0
HA37	0	0	0	0	0	0	0	0	0	0	0
	0	0	0	0	0	0	0	0	0	0	0
HA38	0	0	0	0	0	0	0	0	0	0	0
	0	0	0	0	0	0	0	0	0	0	0
HA39	0	0	0	0	0	0	0	0	0	0	0
	0	0	0	0	0	0	0	0	0	0	0
HA40	0	0	0	0	0	0	0	0	0	0	0
	0	0	0	0	0	0	0	0	0	0	0
HA41	0	25	30	10	0	0	0	0	0	0	0
	0	0	0	0	0	0	0	0	0	0	0
HA42	0	0	0	0	0	0	0	0	0	0	0
	0	0	0	0	0	0	0	0	0	0	0
HF01	0	0	0	0	0	0	0	0	0	0	0
	0	0	0	0	0	0	0	0	0	0	0

HF02	0	0	0	0	0	0	0	0	0	0	0
	0	0	0	0	0	0	0	0	0	0	0
HF03	0	0	0	0	0	0	1	2	0	0	0
	0	0	0	0	0	0	0	0	0	0	0
HF04	0	0	0	0	0	0	0	0	0	0	0
	0	0	0	0	0	0	0	0	0	0	0
HF05	0	0	0	0	0	0	0	0	0	0	0
	0	0	0	0	0	0	0	0	0	0	0
HF06	23	20	28	10	4	0	3	0	0	2	0
	2	1	2	0	3	2	1	2	0	0	1
HF07	0	0	0	0	0	0	0	0	0	0	0
	0	0	0	0	0	0	0	0	0	0	0
HF08	0	0	0	0	0	0	0	0	0	0	0
	0	0	0	0	0	0	0	0	0	0	0
n	**45**	**46**	**47**	**48**	**49**	**50**	**51**	**52**	**53**	**54**	**55**
	56	**57**	**58**	**59**	**60**	**61**	**62**	**63**	**64**	**65**	**66**
HF09	0	0	0	0	0	0	0	0	0	0	0
	0	0	0	0	0	0	0	0	0	0	0
HF10	0	0	0	0	0	0	0	0	0	0	0
	0	0	0	0	0	0	0	0	0	0	0
HF11	0	0	0	0	0	0	0	0	0	0	0
	0	0	0	0	0	0	0	0	0	0	0
n	**67**	**68**	**69**	**70**	**71**	**72**	**73**	**74**	**75**	**76**	**77**
	78	**79**	**80**	**81**	**82**	**83**	**84**	**85**	**86**	**87**	**88**
HA01	0	0	0	0	0	0	0	0	0	0	0
	0	0	0	0	7	0	2	8	6	0	0
HA02	0	0	10	24	27	3	0	9	28	8	5
	13	2	1	0	13	15	31	2	8	1	0
HA03	0	0	0	0	0	0	0	0	0	0	0
	0	0	0	0	0	0	0	0	0	0	0
HA04	0	0	0	0	0	0	0	0	0	0	0
	0	0	0	0	0	0	0	0	16	0	0
HA05	0	0	6	1	0	13	2	1	2	0	2
	1	2	0	0	0	0	0	0	0	0	0
HA06	0	0	0	0	0	2	2	0	0	0	0
	0	0	0	0	0	0	0	0	0	0	0
HA07	0	0	0	0	0	0	0	2	0	0	0
	0	0	0	0	0	0	0	0	0	0	0
HA08	0	0	0	0	0	0	0	0	0	0	0
	0	0	0	0	0	0	0	0	0	0	0
HA09	1	0	3	0	1	0	4	0	0	0	0
	0	0	0	0	0	0	0	0	0	0	0
HA10	0	0	0	0	0	0	0	0	0	0	0
	0	0	0	0	0	0	0	0	0	0	0
HA11	0	0	0	0	0	0	0	0	0	0	0
	0	0	0	0	0	0	0	0	0	0	0
HA12	0	0	0	0	0	0	0	0	2	0	0
	0	0	0	0	0	0	0	0	0	0	0
HA13	0	0	0	0	0	0	0	0	0	0	0
	0	0	0	1	0	0	0	0	0	0	0
HA14	0	0	0	0	0	0	4	0	1	0	0
	7	0	0	0	0	0	0	0	0	0	0
HA15	0	0	0	0	0	0	0	0	0	0	0
	0	0	0	0	0	0	0	0	0	0	0
HA16	0	0	0	0	0	0	0	0	0	0	0
	0	0	0	0	0	0	0	0	0	0	0
HA17	0	0	0	0	0	0	0	0	0	0	0
	0	0	0	0	0	0	0	0	0	0	0
HA18	0	0	0	0	0	0	0	0	0	0	0
	0	0	0	0	0	0	0	0	0	0	0
n	**67**	**68**	**69**	**70**	**71**	**72**	**73**	**74**	**75**	**76**	**77**
	78	**79**	**80**	**81**	**82**	**83**	**84**	**85**	**86**	**87**	**88**
HA19	0	0	0	0	0	0	0	0	1	0	0
	0	0	0	0	0	0	0	0	0	0	0

HA20	0	0	0	0	0	0	1	0	0	0	0
	0	0	0	0	0	0	0	0	0	0	0
HA21	0	0	0	0	0	1	0	0	0	0	0
	0	0	0	0	0	0	0	0	0	0	0
HA22	0	0	0	0	0	0	0	0	0	0	0
	0	0	0	0	0	0	0	0	0	0	0
HA23	0	0	0	0	0	0	0	0	0	0	0
	0	0	0	0	0	0	0	0	0	0	0
HA24	0	0	0	0	0	0	0	0	0	0	0
	0	0	0	0	0	0	0	0	0	0	0
HA25	0	0	0	0	0	0	0	0	0	0	0
	0	0	0	0	0	0	0	0	0	0	0
HA26	0	0	0	0	0	0	0	0	0	0	0
	0	0	0	0	0	0	0	0	0	0	0
HA27	0	0	0	0	0	0	0	0	0	0	0
	0	0	0	0	0	0	0	0	0	0	0
HA28	0	0	0	0	0	0	0	0	0	0	0
	0	0	0	0	0	0	0	0	0	0	0
HA29	0	0	0	0	0	0	0	0	0	0	0
	0	0	0	0	0	0	0	0	0	0	0
HA30	0	0	0	0	0	0	0	0	0	0	0
	0	0	0	0	0	0	0	0	0	0	0
HA31	0	0	0	0	0	0	0	0	0	0	0
	0	0	0	0	0	0	0	0	0	0	0
HA32	0	0	0	0	0	0	0	0	0	0	0
	0	0	0	0	0	0	0	0	0	0	0
HA33	0	0	0	0	0	0	0	0	0	0	0
	0	0	0	0	0	0	0	0	0	0	0
HA34	0	0	0	0	0	1	0	0	0	0	0
	0	0	0	0	0	0	0	0	0	0	0
HA35	0	0	0	0	0	0	0	0	0	0	0
	0	0	0	0	0	0	0	0	0	0	0
HA36	0	0	0	0	0	0	0	0	0	0	0
	0	0	0	0	0	0	0	0	0	0	0
HA37	0	0	0	0	0	0	0	0	0	0	0
	0	0	0	0	0	0	0	0	0	0	0
HA38	0	0	3	2	0	0	0	0	0	0	0
	0	0	0	0	0	0	0	0	0	0	0
HA39	0	0	2	1	1	0	0	0	0	0	0
	0	0	0	0	0	0	0	0	0	0	0
HA40	0	0	0	0	1	0	0	0	0	0	0
	0	0	0	0	0	0	0	0	0	0	0
HA41	0	0	0	0	0	0	0	0	0	0	0
	0	0	0	0	0	0	0	0	0	0	0
n	**67**	**68**	**69**	**70**	**71**	**72**	**73**	**74**	**75**	**76**	**77**
	78	**79**	**80**	**81**	**82**	**83**	**84**	**85**	**86**	**87**	**88**
HA42	0	0	0	0	0	0	0	0	0	0	0
	0	0	0	0	0	0	0	0	0	0	0
HF01	0	0	0	0	0	9	2	3	0	1	6
	0	0	0	0	28	41	37	7	24	0	0
HF02	0	0	0	0	0	0	0	0	0	0	0
	0	0	0	0	0	0	0	0	0	0	0
HF03	0	0	0	0	0	0	0	0	0	0	0
	0	0	0	0	0	0	0	0	0	0	0
HF04	0	0	0	0	0	0	0	0	0	0	0
	0	0	0	0	0	0	0	0	0	0	0
HF05	0	0	0	0	0	0	0	0	0	0	0
	0	0	0	0	0	0	0	2	11	0	0
HF06	1	0	25	30	30	10	12	8	25	11	0
	21	5	1	0	0	0	0	0	0	2	2
HF07	0	0	0	0	0	0	0	0	0	0	0
	0	0	0	0	0	0	0	0	0	0	0
HF08	0	0	0	0	0	0	0	0	0	0	0
	0	0	0	0	0	0	0	0	0	0	0

HF09	0	0	0	0	0	0	0	0	0	0	0
	0	0	0	0	0	0	0	0	0	0	0
HF10	0	0	0	0	0	0	0	0	0	0	0
	0	0	0	0	0	0	0	0	0	0	0
HF11	0	0	0	0	0	0	0	0	0	0	0
	0	0	0	0	0	0	0	0	0	0	0
n	**89**	**90**	**91**	**92**	**93**	**94**	**95**	**96**	**97**	**98**	**99**
	100	**101**	**102**	**103**	**104**	**105**	**106**	**107**	**108**	**109**	**110**
HA01	0	0	0	4	3	0	0	0	0	0	0
	0	0	0	0	0	0	0	0	0	8	0
HA02	10	11	10	19	0	4	0	0	19	60	0
	2	0	0	17	2	1	0	0	18	0	2
HA03	0	0	0	0	0	0	0	0	0	0	0
	0	0	0	0	0	0	0	0	0	0	0
HA04	0	0	0	0	0	0	29	19	0	0	17
	18	7	0	0	0	1	0	0	0	0	21
HA05	0	0	0	0	0	0	0	0	0	0	0
	0	0	0	0	1	0	0	0	0	0	0
HA06	0	0	0	0	0	0	0	0	0	0	0
	0	0	0	0	0	0	0	0	0	0	0
HA07	0	0	0	0	0	0	0	0	0	0	0
	0	0	0	0	0	0	0	0	0	0	0
HA08	0	0	0	0	0	0	0	0	0	0	0
	0	0	0	0	0	0	0	0	0	0	0
HA09	0	0	0	0	0	0	0	0	0	0	0
	0	0	0	0	0	0	0	0	0	0	0
n	**89**	**90**	**91**	**92**	**93**	**94**	**95**	**96**	**97**	**98**	**99**
	100	**101**	**102**	**103**	**104**	**105**	**106**	**107**	**108**	**109**	**110**
HA10	0	0	0	0	0	0	0	0	0	0	0
	0	0	0	0	0	0	0	0	0	0	0
HA11	0	0	0	0	0	0	0	0	0	0	0
	0	0	0	0	0	0	0	0	0	0	0
HA12	0	0	0	0	0	0	0	0	0	0	0
	0	0	0	0	0	0	0	0	0	0	0
HA13	0	0	0	0	0	0	0	0	0	0	0
	0	0	0	0	0	0	0	0	0	0	0
HA14	0	0	0	0	0	0	0	0	0	0	0
	0	0	0	0	0	0	0	0	2	0	0
HA15	0	0	0	0	0	0	0	0	0	0	0
	0	0	0	0	0	0	0	0	0	0	0
HA16	0	0	0	0	0	0	0	0	0	0	0
	0	0	0	0	0	0	0	0	0	0	0
HA17	0	0	0	0	0	0	0	0	0	0	0
	0	0	0	0	0	0	0	0	0	0	0
HA18	0	0	0	0	0	0	0	0	0	0	0
	0	0	0	0	0	0	0	0	0	0	0
HA19	0	0	0	0	0	0	0	0	0	0	0
	0	0	0	0	0	0	0	0	0	0	0
HA20	0	0	0	0	0	0	0	0	0	0	0
	0	0	0	0	0	0	0	0	0	0	0
HA21	0	0	0	0	0	0	0	0	0	0	0
	0	0	0	0	0	0	0	0	0	0	0
HA22	0	0	0	0	0	0	0	0	0	0	0
	0	0	0	0	0	0	0	0	0	0	0
HA23	0	0	0	0	0	0	0	0	0	0	0
	0	0	0	0	0	0	0	0	0	0	0
HA24	0	0	0	0	0	0	0	0	0	0	0
	0	0	0	0	0	0	0	0	0	0	0
HA25	0	0	0	0	0	0	0	0	0	0	0
	0	0	0	0	0	0	0	0	0	0	0
HA26	0	0	0	0	0	0	0	0	0	0	0
	0	0	0	0	4	0	0	0	15	0	0
HA27	0	0	0	0	0	0	0	0	0	0	0
	0	0	0	0	0	0	0	0	0	1	0

HA28	0	0	0	0	0	0	0	0	0	0	0
	0	0	0	0	0	1	0	0	0	0	0
HA29	0	0	0	0	0	0	0	0	0	0	0
	0	0	0	0	0	1	0	0	0	0	0
HA30	0	0	0	0	0	0	3	2	0	0	0
	0	21	0	0	0	0	0	0	0	0	0
HA31	0	0	0	0	0	0	0	0	0	0	0
	0	0	0	0	0	0	0	0	0	0	0
HA32	0	0	0	0	0	0	0	0	0	0	0
	0	0	0	0	0	0	0	0	0	0	0
n	89	90	91	92	93	94	95	96	97	98	99
	100	101	102	103	104	105	106	107	108	109	110
HA33	0	0	0	0	0	0	0	0	0	0	0
	0	0	0	0	0	0	0	0	0	0	0
HA34	0	0	0	0	0	0	0	0	0	0	0
	0	0	0	0	0	0	0	0	0	0	0
HA35	0	0	0	0	0	0	0	0	0	0	0
	0	0	0	0	0	0	0	0	0	0	0
HA36	0	0	0	0	0	0	0	0	0	0	0
	0	0	0	0	0	0	0	0	0	0	0
HA37	0	0	0	0	0	0	0	0	0	0	0
	0	0	0	0	0	0	0	0	0	0	0
HA38	0	0	0	0	0	0	0	0	0	0	0
	0	0	0	0	0	0	0	0	0	0	0
HA39	0	0	0	0	0	0	0	0	0	0	0
	0	0	0	0	0	0	0	0	0	0	0
HA40	0	0	0	0	0	0	0	0	0	0	0
	0	0	0	0	0	0	0	0	0	0	0
HA41	0	0	0	0	0	0	0	0	0	0	0
	0	0	0	0	0	0	0	0	0	0	0
HA42	0	0	0	0	0	0	0	0	0	0	0
	0	0	0	0	0	0	0	0	0	0	0
HF01	0	0	13	29	4	6	0	0	1	3	17
	0	0	0	12	0	0	0	0	21	0	8
HF02	0	0	0	0	0	0	33	1	0	0	0
	18	4	0	0	0	0	0	0	0	0	1
HF03	0	0	0	0	0	0	0	0	0	0	0
	0	1	0	0	0	0	0	0	0	0	13
HF04	0	0	0	0	0	0	0	0	0	0	0
	0	0	0	0	0	0	0	0	0	0	0
HF05	0	0	0	0	1	0	1	23	0	1	3
	2	0	0	0	0	0	0	0	0	0	1
HF06	10	11	0	0	0	0	1	0	17	55	0
	0	2	0	8	0	0	0	0	3	0	0
HF07	0	0	0	0	0	0	0	0	0	0	0
	0	2	0	0	0	0	0	0	0	0	0
HF08	0	0	0	0	0	0	0	0	0	0	0
	0	8	0	0	0	0	0	0	0	0	0
HF09	0	0	0	0	0	0	0	0	0	0	0
	0	4	0	0	0	0	0	0	0	0	0
HF10	0	0	0	0	0	0	0	0	0	0	0
	0	0	0	0	0	0	0	0	0	0	0
HF11	0	0	0	0	0	0	0	0	0	0	0
	0	0	0	0	0	0	0	0	0	0	0
n	**111**	**112**	**113**	**114**	**115**	**116**	**117**	**118**	**119**		
HA01	0	0	6	1	0	0	0	0	0		
HA02	0	15	0	12	3	0	0	7	6		
n	**111**	**112**	**113**	**114**	**115**	**116**	**117**	**118**	**119**		
HA03	0	0	0	0	0	0	0	0	0		
HA04	6	0	0	2	0	0	0	0	0		
HA05	0	0	0	0	0	0	0	0	0		
HA06	0	0	0	0	0	0	0	0	0		
HA07	0	0	0	0	0	0	0	0	0		
HA08	0	0	0	0	0	0	0	0	0		

HA09	0	0	0	0	0	0	1	0	0
HA10	0	0	0	0	0	0	0	2	0
HA11	0	0	0	0	0	0	0	0	0
HA12	0	0	0	0	0	0	0	0	0
HA13	0	0	0	0	0	0	0	0	0
HA14	0	0	0	0	0	0	0	0	0
HA15	0	0	0	0	0	0	0	0	0
HA16	0	0	0	0	0	0	0	0	0
HA17	0	0	0	0	0	0	0	0	0
HA18	0	0	0	0	0	0	0	0	0
HA19	0	0	0	0	0	0	0	0	0
HA20	0	0	0	0	0	0	0	0	0
HA21	0	0	0	0	0	0	0	0	0
HA22	0	0	0	0	0	0	0	0	0
HA23	0	0	0	0	0	0	0	0	0
HA24	0	0	0	0	0	0	0	0	0
HA25	0	0	0	0	0	0	0	0	0
HA26	0	0	0	0	0	0	0	0	0
HA27	0	0	0	0	0	0	0	0	0
HA28	0	0	0	0	0	0	0	0	0
HA29	0	0	0	0	0	0	0	0	0
HA30	0	0	0	0	0	0	0	0	0
HA31	0	0	0	0	0	0	0	0	0
HA32	0	0	0	0	0	0	0	0	0
HA33	0	0	0	0	0	0	0	0	0
HA34	0	0	0	0	0	0	0	0	0
HA35	0	0	0	0	0	0	2	0	0
HA36	0	0	0	0	0	0	1	0	0
HA37	0	0	0	0	0	0	0	0	0
HA38	0	0	0	0	0	0	0	0	0
HA39	0	0	0	0	0	0	0	0	0
HA40	0	0	0	0	0	0	0	0	0
HA41	0	0	0	0	0	0	0	0	0
HA42	0	0	0	0	0	0	0	0	0
HF01	0	3	0	5	0	0	0	0	0
HF02	0	1	0	6	0	0	0	0	0
HF03	1	0	0	1	0	0	0	0	0
HF04	0	1	0	0	0	0	0	0	0
n	**111**	**112**	**113**	**114**	**115**	**116**	**117**	**118**	**119**
HF05	1	1	0	0	0	0	0	0	0
HF06	0	15	15	8	1	1	9	6	5
HF07	0	0	0	0	0	0	0	0	0
HF08	0	0	0	0	0	0	0	0	0
HF09	0	0	0	0	0	0	0	0	0
HF10	0	0	0	0	0	0	0	0	0
HF11	0	0	0	0	0	0	0	0	0

OTU / hierarchical cluster delimitation of haplotypes

Haplotype ID	GenBank Accession#	ABGD	hier. Cluster
HA02	MG588097	OTU 1	CLU 1
HA13	MG588106	OTU 1	CLU 1
HA22	MG588117	OTU 1	CLU 1
HA24	MG588119	OTU 1	CLU 1
HA38	MG588133	OTU 1	CLU 1
HA42	MG588137	OTU 1	CLU 1
HA01	MG588107	OTU 2	CLU 2
HA15	MG588109	OTU 2	CLU 2
HA16	MG588110	OTU 2	CLU 2
HA05	MG588098	OTU 3	CLU 3
HA06	MG588099	OTU 3	CLU 3
HA07	MG588100	OTU 3	CLU 3
HA08	MG588101	OTU 3	CLU 3
HA12	MG588105	OTU 3	CLU 3
HA14	MG588108	OTU 3	CLU 3
HA18	MG588112	OTU 3	CLU 3
HA19	MG588113	OTU 3	CLU 3
HA20	MG588114	OTU 3	CLU 3
HA21	MG588115	OTU 3	CLU 3
HA23	MG588118	OTU 3	CLU 3
HA25	MG588120	OTU 3	CLU 3
HA26	MG588121	OTU 3	CLU 3
HA31	MG588126	OTU 3	CLU 3
HA32	MG588127	OTU 3	CLU 3
HA34	MG588129	OTU 3	CLU 3
HA03	MG588138	OTU 4	CLU 4
HA10	MG588103	OTU 4	CLU 4
HA11	MG588104	OTU 4	CLU 4
HA27	MG588122	OTU 4	CLU 4
HA35	MG588130	OTU 4	CLU 4
HA36	MG588131	OTU 4	CLU 4
HA09	MG588102	OTU 4	CLU 5
HA17	MG588111	OTU 4	CLU 5
HA41	MG588136	OTU 4	CLU 5
HA04	MG588116	OTU 5	CLU 6
HA28	MG588123	OTU 5	CLU 6
HA29	MG588124	OTU 5	CLU 6
HA30	MG588125	OTU 5	CLU 6

Haplotype ID	GenBank Accession#	ABGD	hier. Cluster
HA33	MG588128	OTU 5	CLU 6
HA37	MG588132	OTU 5	CLU 6
HA39	MG588134	OTU 6	CLU 7
HA40	MG588135	OTU 6	CLU 7

Haplotype ID	GenBank Accession#	ABGD	hier. Cluster
HF01	MG584157	OTU 1	CLU 1
HF06	MG584162	OTU 1	CLU 1
HF07	MG584163	OTU 1	CLU 1
HF08	MG584164	OTU 1	CLU 2
HF02	MG584158	OTU 2	CLU 3
HF03	MG584159	OTU 3	CLU 4
HF04	MG584160	OTU 3	CLU 5
HF05	MG584161	OTU 4	CLU 6
HF11	MG584167	OTU 5	CLU 7
HF10	MG584166	OTU 6	CLU 8
HF09	MG584165	OTU 7	CLU 9

OUT Summary

ALGAE				
		n Locations		
OTU 1		68		
OTU 2		16		
OTU 3		26		
OTU 4		18		
OTU 5		27		
OTU 6		3		not included in analyses
FUNGI				
OTU 1		88		
OTU 2		19		
OTU 3		18		
OTU 4		21		
OTU 5		1		merged for hypervolume analysis
OTU 6		3		
OTU 7		2		

Table S2 Description of the 12 bioclim variables that were used to model niche spaces and geographic distributions. Highlighting colors correspond to Fig. 2A/B in the main text.

Variable	Description	Analyzed / Interpreted as...	Least correlated Vars
Bio 1	**Annual Mean Temperature**	warm in cold&dry periods	
Bio 2	Mean Diurnal Range (Mean of monthly (max temp - min temp))	x	**+++**
Bio 3	Isothermality (BIO2/BIO7) (* 100)	x	
Bio 4	Temperature Seasonality (standard deviation *100)	x	**+++**
Bio 5	**Max Temperature of Warmest Month**	warm in warmer periods	
Bio 6	**Min Temperature of Coldest Month**	warm in cold&dry periods	**+++**
Bio 7	Temperature Annual Range (BIO5-BIO6)	x	
Bio 8	Mean Temperature of Wettest Quarter	x	**+++**
Bio 9	**Mean Temperature of Driest Quarter**	warm in cold&dry periods	
Bio 10	**Mean Temperature of Warmest Quarter**	warm in warmer periods	
Bio 11	**Mean Temperature of Coldest Quarter**	warm in cold&dry periods	
Bio 12	**Annual Precipitation**	more rain in cold&wet periods	
Bio 13	Precipitation of Wettest Month	x	
Bio 14	**Precipitation of Driest Month**	more rain in warm&dry periods	**+++**
Bio 15	Precipitation Seasonality (Coefficient of Variation)	x	**+++**
Bio 16	**Precipitation of Wettest Quarter**	more rain in cold&wet periods	
Bio 17	**Precipitation of Driest Quarter**	more rain in warm&dry periods	
Bio 18	**Precipitation of Warmest Quarter**	more rain in warm&dry periods	
Bio 19	**Precipitation of Coldest Quarter**	more rain in cold&wet periods	**+++**

Additionally analyzed to correct for autocorrelation see Suppl. Material Figure S7.

OUT alga 1			
Model	**Parameter**	**AICc**	**delta.AICc**
1	L_0.5	2147.403	74.305
2	LQ_0.5	2086.883	13.785
3	H_0.5	2584.774	511.676
4	LQH_0.5	2958.864	885.766
5	LQHP_0.5	NA	NA
6	LQHPT_0.5	NA	NA
7	L_1	2154.282	81.184
8	LQ_1	2087.256	14.158
9	H_1	2221.451	148.353
10	LQH_1	2123.400	50.302
11	LQHP_1	2148.930	75.832
12	LQHPT_1	2286.315	213.217
13	L_1.5	2161.652	88.554
14	LQ_1.5	2098.859	25.761
15	H_1.5	2274.573	201.475
16	LQH_1.5	2082.576	9.478
17	**LQHP_1.5**	**2073.098**	**0.000**
18	LQHPT_1.5	2087.920	14.822
19	L_2	2167.586	94.488
20	LQ_2	2100.637	27.539
21	H_2	2159.760	86.662
22	LQH_2	2085.103	12.005
23	LQHP_2	2090.640	17.542
24	LQHPT_2	2090.331	17.233
25	L_2.5	2174.485	101.387
26	LQ_2.5	2101.401	28.303
27	H_2.5	2149.436	76.338
28	LQH_2.5	2094.236	21.138
29	LQHP_2.5	2089.320	16.222
30	LQHPT_2.5	2089.804	16.706
31	L_3	2182.648	109.550
32	LQ_3	2108.115	35.017
33	H_3	2158.525	85.427
34	LQH_3	2088.943	15.844
35	LQHP_3	2094.430	21.332
36	LQHPT_3	2100.335	27.237
37	L_3.5	2193.173	120.075
38	LQ_3.5	2112.676	39.578
39	H_3.5	2146.098	73.000
40	LQH_3.5	2087.544	14.446
41	LQHP_3.5	2099.227	26.129
42	LQHPT_3.5	2099.717	26.619
43	L_4	2192.357	119.259
44	LQ_4	2107.766	34.668
45	H_4	2144.231	71.132
46	LQH_4	2099.591	26.493
47	LQHP_4	2107.631	34.532
48	LQHPT_4	2105.095	31.997

Table S3 Model AICc values for the suite of 48 MaxEnt models run for all parameter combinations. The parameter sets with the lowest AICc were chosen for the final models. Parameter sets comprise varying classes of response curves (L: linear, LQ: linear and quadratic, LQH: linear quadratic hinge, H: hinge, and LQHP: linear quadratic hinge product) and regularization multipliers (ranging from 0.5 – 4). Parameter sets chosen for further analysis are highlighted in grey.

OUT alga 2			
Model	**Parameter**	**AICc**	**delta.AICc**
1	**L_0.5**	**495.312**	**0.000**
2	LQ_0.5	506.360	11.048
3	H_0.5	NA	NA
4	LQH_0.5	NA	NA
5	LQHP_0.5	NA	NA
6	LQHPT_0.5	NA	NA
7	L_1	520.002	24.690
8	LQ_1	530.026	34.714
9	H_1	NA	NA
10	LQH_1	NA	NA
11	LQHP_1	NA	NA
12	LQHPT_1	NA	NA
13	L_1.5	519.724	24.412
14	LQ_1.5	509.203	13.891
15	H_1.5	NA	NA
16	LQH_1.5	NA	NA
17	LQHP_1.5	NA	NA
18	LQHPT_1.5	NA	NA
19	L_2	525.042	29.730
20	LQ_2	506.889	11.578
21	H_2	609.118	113.806
22	LQH_2	920.919	425.607
23	LQHP_2	NA	NA
24	LQHPT_2	925.013	429.701
25	L_2.5	522.379	27.067
26	LQ_2.5	511.409	16.097
27	H_2.5	541.486	46.174
28	LQH_2.5	520.514	25.202
29	LQHP_2.5	538.426	43.114
30	LQHPT_2.5	554.404	59.093
31	L_3	524.289	28.978
32	LQ_3	503.207	7.895
33	H_3	570.905	75.593
34	LQH_3	525.072	29.761
35	LQHP_3	536.177	40.865
36	LQHPT_3	536.177	40.865
37	L_3.5	523.272	27.960
38	LQ_3.5	510.301	14.989
39	H_3.5	522.989	27.677
40	LQH_3.5	520.923	25.611
41	LQHP_3.5	527.472	32.160
42	LQHPT_3.5	527.472	32.160
43	L_4	523.442	28.130
44	LQ_4	513.782	18.470
45	H_4	521.641	26.329
46	LQH_4	525.725	30.413
47	LQHP_4	532.298	36.986
48	LQHPT_4	532.298	36.986

OUT alga 3			
Model	**Parameters**	**AICc**	**delta.AICc**
1	L_0.5	803.788	21.342
2	LQ_0.5	836.214	53.769
3	H_0.5	NA	NA
4	LQH_0.5	1284.357	501.911
5	LQHP_0.5	1079.332	296.886
6	LQHPT_0.5	NA	NA
7	L_1	800.471	18.025
8	LQ_1	802.353	19.907
9	H_1	NA	NA
10	LQH_1	801.098	18.652
11	LQHP_1	799.037	16.591
12	LQHPT_1	NA	NA
13	L_1.5	799.042	16.596
14	LQ_1.5	785.010	2.564
15	H_1.5	841.543	59.098
16	LQH_1.5	785.006	2.560
17	LQHP_1.5	802.842	20.396
18	LQHPT_1.5	872.427	89.982
19	L_2	800.624	18.178
20	**LQ_2**	**782.446**	**0.000**
21	H_2	809.718	27.272
22	LQH_2	784.840	2.394
23	LQHP_2	793.814	11.368
24	LQHPT_2	801.455	19.009
25	L_2.5	802.492	20.046
26	LQ_2.5	783.486	1.041
27	H_2.5	835.251	52.805
28	LQH_2.5	783.492	1.046
29	LQHP_2.5	785.549	3.103
30	LQHPT_2.5	785.548	3.102
31	L_3	804.617	22.171
32	LQ_3	784.674	2.228
33	H_3	810.109	27.663
34	LQH_3	784.679	2.233
35	LQHP_3	788.150	5.704
36	LQHPT_3	788.150	5.704
37	L_3.5	806.966	24.521
38	LQ_3.5	785.975	3.529
39	H_3.5	843.773	61.327
40	LQH_3.5	785.975	3.529
41	LQHP_3.5	790.939	8.494
42	LQHPT_3.5	790.938	8.493
43	L_4	809.508	27.062
44	LQ_4	783.843	1.397
45	H_4	836.880	54.434
46	LQH_4	783.843	1.397
47	LQHP_4	793.865	11.419
48	LQHPT_4	793.865	11.419

OUT algal 4			
Model	**Parameter**	**AICc**	**delta.AICc**
1	**L_0.5**	**541.117**	**0.000**
2	LQ_0.5	556.526	15.409
3	H_0.5	NA	NA
4	LQH_0.5	NA	NA
5	LQHP_0.5	NA	NA
6	LQHPT_0.5	NA	NA
7	L_1	545.341	4.224
8	LQ_1	562.264	21.147
9	H_1	NA	NA
10	LQH_1	NA	NA
11	LQHP_1	NA	NA
12	LQHPT_1	NA	NA
13	L_1.5	547.886	6.769
14	LQ_1.5	545.525	4.408
15	H_1.5	599.224	58.106
16	LQH_1.5	1033.478	492.361
17	LQHP_1.5	626.437	85.320
18	LQHPT_1.5	762.313	221.196
19	L_2	543.405	2.288
20	LQ_2	551.383	10.266
21	H_2	549.329	8.212
22	LQH_2	555.107	13.990
23	LQHP_2	549.331	8.214
24	LQHPT_2	549.332	8.215
25	L_2.5	545.155	4.038
26	LQ_2.5	549.018	7.901
27	H_2.5	559.272	18.155
28	LQH_2.5	566.776	25.659
29	LQHP_2.5	559.241	18.124
30	LQHPT_2.5	553.150	12.033
31	L_3	547.682	6.565
32	LQ_3	543.654	2.536
33	H_3	561.678	20.561
34	LQH_3	561.857	20.740
35	LQHP_3	561.678	20.561
36	LQHPT_3	555.620	14.502
37	L_3.5	551.384	10.267
38	LQ_3.5	544.872	3.755
39	H_3.5	553.040	11.923
40	LQH_3.5	557.972	16.855
41	LQHP_3.5	553.040	11.923
42	LQHPT_3.5	553.020	11.903
43	L_4	557.036	15.919
44	LQ_4	546.443	5.326
45	H_4	547.157	6.039
46	LQH_4	550.541	9.424
47	LQHP_4	547.157	6.039
48	LQHPT_4	547.157	6.039

OUT alga 5			
Model	**Parameter**	**AICc**	**delta.AICc**
1	L_0.5	810.494	17.094
2	LQ_0.5	804.378	10.978
3	H_0.5	NA	NA
4	LQH_0.5	NA	NA
5	LQHP_0.5	NA	NA
6	LQHPT_0.5	NA	NA
7	L_1	815.185	21.785
8	LQ_1	795.586	2.186
9	H_1	NA	NA
10	LQH_1	916.697	123.297
11	LQHP_1	1382.734	589.334
12	LQHPT_1	NA	NA
13	L_1.5	815.788	22.388
14	**LQ_1.5**	**793.400**	**0.000**
15	H_1.5	1046.119	252.719
16	LQH_1.5	830.661	37.261
17	LQHP_1.5	973.753	180.353
18	LQHPT_1.5	971.814	178.413
19	L_2	820.036	26.636
20	LQ_2	799.560	6.160
21	H_2	881.903	88.503
22	LQH_2	817.317	23.917
23	LQHP_2	834.316	40.916
24	LQHPT_2	861.991	68.591
25	L_2.5	822.988	29.588
26	LQ_2.5	804.702	11.302
27	H_2.5	858.514	65.114
28	LQH_2.5	827.881	34.480
29	LQHP_2.5	835.842	42.442
30	LQHPT_2.5	846.165	52.764
31	L_3	824.748	31.348
32	LQ_3	810.303	16.902
33	H_3	845.086	51.686
34	LQH_3	822.678	29.278
35	LQHP_3	812.720	19.320
36	LQHPT_3	812.780	19.380
37	L_3.5	823.950	30.550
38	LQ_3.5	812.217	18.817
39	H_3.5	846.984	53.584
40	LQH_3.5	826.718	33.318
41	LQHP_3.5	814.166	20.766
42	LQHPT_3.5	814.269	20.868
43	L_4	826.023	32.623
44	LQ_4	824.376	30.976
45	H_4	858.152	64.752
46	LQH_4	809.259	15.859
47	LQHP_4	826.022	32.622
48	LQHPT_4	821.917	28.517

OUT fungus 1			
Model	**Parameter**	**AICc**	**delta.AICc**
1	L_0.5	2755.330	23.014
2	**LQ_0.5**	**2732.316**	**0.000**
3	H_0.5	NA	NA
4	LQH_0.5	NA	NA
5	LQHP_0.5	NA	NA
6	LQHPT_0.5	NA	NA
7	L_1	2753.887	21.571
8	LQ_1	2740.446	8.130
9	H_1	3012.604	280.288
10	LQH_1	2903.981	171.665
11	LQHP_1	3055.703	323.387
12	LQHPT_1	3081.299	348.983
13	L_1.5	2767.666	35.350
14	LQ_1.5	2734.044	1.729
15	H_1.5	2811.465	79.149
16	LQH_1.5	2782.596	50.280
17	LQHP_1.5	2857.478	125.162
18	LQHPT_1.5	2842.489	110.173
19	L_2	2770.676	38.360
20	LQ_2	2736.240	3.924
21	H_2	2784.464	52.149
22	LQH_2	2743.907	11.591
23	LQHP_2	2779.116	46.800
24	LQHPT_2	2766.829	34.513
25	L_2.5	2775.623	43.308
26	LQ_2.5	2741.294	8.978
27	H_2.5	2792.738	60.422
28	LQH_2.5	2747.261	14.945
29	LQHP_2.5	2759.195	26.880
30	LQHPT_2.5	2773.011	40.695
31	L_3	2782.519	50.203
32	LQ_3	2745.189	12.873
33	H_3	2798.361	66.045
34	LQH_3	2756.824	24.508
35	LQHP_3	2752.443	20.127
36	LQHPT_3	2760.844	28.528
37	L_3.5	2789.387	57.071
38	LQ_3.5	2755.893	23.577
39	H_3.5	2806.345	74.029
40	LQH_3.5	2755.062	22.746
41	LQHP_3.5	2758.585	26.269
42	LQHPT_3.5	2763.228	30.912
43	L_4	2798.609	66.293
44	LQ_4	2753.438	21.122
45	H_4	2814.091	81.775
46	LQH_4	2753.626	21.310
47	LQHP_4	2761.147	28.831
48	LQHPT_4	2766.993	34.677

OUT fungus 2			
Model	**Parameter**	**AICc**	**delta.AICc**
1	L_0.5	542.107	10.456
2	**LQ_0.5**	**531.651**	**0.000**
3	H_0.5	NA	NA
4	LQH_0.5	NA	NA
5	LQHP_0.5	NA	NA
6	LQHPT_0.5	NA	NA
7	L_1	552.048	20.396
8	LQ_1	539.329	7.677
9	H_1	NA	NA
10	LQH_1	NA	NA
11	LQHP_1	NA	NA
12	LQHPT_1	NA	NA
13	L_1.5	563.032	31.381
14	LQ_1.5	539.365	7.714
15	H_1.5	614.214	82.563
16	LQH_1.5	815.099	283.447
17	LQHP_1.5	649.796	118.145
18	LQHPT_1.5	NA	NA
19	L_2	566.984	35.333
20	LQ_2	551.496	19.844
21	H_2	583.663	52.012
22	LQH_2	709.767	178.116
23	LQHP_2	717.251	185.600
24	LQHPT_2	713.657	182.006
25	L_2.5	572.263	40.611
26	LQ_2.5	566.160	34.509
27	H_2.5	631.079	99.428
28	LQH_2.5	604.308	72.657
29	LQHP_2.5	573.071	41.420
30	LQHPT_2.5	565.071	33.420
31	L_3	578.191	46.539
32	LQ_3	562.033	30.381
33	H_3	639.835	108.184
34	LQH_3	583.594	51.942
35	LQHP_3	578.973	47.322
36	LQHPT_3	578.871	47.220
37	L_3.5	576.904	45.252
38	LQ_3.5	567.037	35.386
39	H_3.5	683.549	151.897
40	LQH_3.5	574.262	42.611
41	LQHP_3.5	585.230	53.578
42	LQHPT_3.5	577.567	45.916
43	L_4	577.760	46.109
44	LQ_4	572.120	40.469
45	H_4	619.859	88.207
46	LQH_4	589.867	58.216
47	LQHP_4	577.893	46.242
48	LQHPT_4	577.875	46.224

OUT fungus 3			
Model	**Parameter**	**AICc**	**delta.AICc**
1	L_0.5	529.664	10.573
2	LQ_0.5	540.674	21.584
3	H_0.5	NA	NA
4	LQH_0.5	NA	NA
5	LQHP_0.5	NA	NA
6	LQHPT_0.5	NA	NA
7	L_1	533.207	14.117
8	**LQ_1**	**519.091**	**0.000**
9	H_1	NA	NA
10	LQH_1	NA	NA
11	LQHP_1	740.622	221.532
12	LQHPT_1	NA	NA
13	L_1.5	532.982	13.891
14	LQ_1.5	521.528	2.438
15	H_1.5	757.769	238.679
16	LQH_1.5	NA	NA
17	LQHP_1.5	543.931	24.840
18	LQHPT_1.5	741.960	222.869
19	L_2	537.555	18.465
20	LQ_2	524.538	5.447
21	H_2	545.640	26.549
22	LQH_2	544.840	25.750
23	LQHP_2	551.967	32.877
24	LQHPT_2	597.220	78.129
25	L_2.5	542.763	23.673
26	LQ_2.5	523.401	4.311
27	H_2.5	553.431	34.340
28	LQH_2.5	540.210	21.119
29	LQHP_2.5	581.589	62.499
30	LQHPT_2.5	656.972	137.881
31	L_3	543.700	24.609
32	LQ_3	527.191	8.101
33	H_3	576.901	57.810
34	LQH_3	547.091	28.000
35	LQHP_3	591.504	72.413
36	LQHPT_3	667.291	148.200
37	L_3.5	548.906	29.816
38	LQ_3.5	531.495	12.404
39	H_3.5	571.389	52.298
40	LQH_3.5	545.767	26.676
41	LQHP_3.5	581.620	62.530
42	LQHPT_3.5	577.777	58.687
43	L_4	555.152	36.061
44	LQ_4	536.323	17.233
45	H_4	561.695	42.604
46	LQH_4	543.830	24.740
47	LQHP_4	567.020	47.930
48	LQHPT_4	592.616	73.526

OUT fungus 4			
Model	**Parameter**	**AICc**	**delta.AICc**
1	L_0.5	598.903	10.171
2	LQ_0.5	602.501	13.769
3	H_0.5	NA	NA
4	LQH_0.5	NA	NA
5	LQHP_0.5	NA	NA
6	LQHPT_0.5	NA	NA
7	L_1	607.935	19.202
8	LQ_1	593.338	4.606
9	H_1	719.634	130.901
10	LQH_1	NA	NA
11	LQHP_1	NA	NA
12	LQHPT_1	NA	NA
13	L_1.5	622.593	33.860
14	**LQ_1.5**	**588.732**	**0.000**
15	H_1.5	644.725	55.993
16	LQH_1.5	657.717	68.985
17	LQHP_1.5	640.462	51.729
18	LQHPT_1.5	729.288	140.555
19	L_2	630.677	41.944
20	LQ_2	599.562	10.830
21	H_2	627.070	38.338
22	LQH_2	592.161	3.429
23	LQHP_2	613.999	25.267
24	LQHPT_2	623.003	34.271
25	L_2.5	634.234	45.502
26	LQ_2.5	602.255	13.523
27	H_2.5	612.688	23.955
28	LQH_2.5	593.829	5.097
29	LQHP_2.5	608.011	19.278
30	LQHPT_2.5	602.511	13.779
31	L_3	638.207	49.475
32	LQ_3	605.540	16.808
33	H_3	610.504	21.771
34	LQH_3	605.051	16.318
35	LQHP_3	639.933	51.201
36	LQHPT_3	639.728	50.996
37	L_3.5	642.603	53.870
38	LQ_3.5	609.008	20.276
39	H_3.5	623.573	34.841
40	LQH_3.5	612.575	23.843
41	LQHP_3.5	650.071	61.339
42	LQHPT_3.5	633.516	44.784
43	L_4	647.387	58.655
44	LQ_4	612.612	23.879
45	H_4	629.159	40.427
46	LQH_4	610.660	21.927
47	LQHP_4	628.435	39.702
48	LQHPT_4	628.498	39.766

OUT fungus 5-7			
Model	**Parameter**	**AICc**	**delta.AICc**
1	L_0.5	NA	NA
2	LQ_0.5	NA	NA
3	H_0.5	NA	NA
4	LQH_0.5	NA	NA
5	LQHP_0.5	NA	NA
6	LQHPT_0.5	NA	NA
7	L_1	NA	NA
8	LQ_1	NA	NA
9	H_1	NA	NA
10	LQH_1	NA	NA
11	LQHP_1	NA	NA
12	LQHPT_1	NA	NA
13	L_1.5	NA	NA
14	LQ_1.5	NA	NA
15	H_1.5	NA	NA
16	LQH_1.5	NA	NA
17	LQHP_1.5	NA	NA
18	LQHPT_1.5	NA	NA
19	L_2	166.699	14.353
20	LQ_2	NA	NA
21	H_2	NA	NA
22	LQH_2	NA	NA
23	LQHP_2	NA	NA
24	LQHPT_2	NA	NA
25	L_2.5	168.772	16.426
26	LQ_2.5	NA	NA
27	H_2.5	NA	NA
28	LQH_2.5	NA	NA
29	LQHP_2.5	173.586	21.239
30	LQHPT_2.5	173.586	21.239
31	L_3	171.279	18.933
32	LQ_3	166.753	14.407
33	H_3	NA	NA
34	LQH_3	166.753	14.407
35	LQHP_3	154.394	2.048
36	LQHPT_3	154.394	2.048
37	**L_3.5**	**152.346**	**0.000**
38	LQ_3.5	169.063	16.716
39	H_3.5	182.031	29.685
40	LQH_3.5	169.063	16.716
41	LQHP_3.5	154.981	2.635
42	LQHPT_3.5	154.981	2.635
43	L_4	153.128	0.782
44	LQ_4	171.668	19.321
45	H_4	163.511	11.164
46	LQH_4	171.668	19.321
47	LQHP_4	155.543	3.197
48	LQHPT_4	155.543	3.197